NANYANG TECHNOLOGICAL UNIVERSITY

MECHANISTIC INSIGHTS INTO THE CONNECTION BETWEEN POLLUTION AND ACNE VULGARIS

TAN YONG QUAN ALVIN

Interdisciplinary Graduate Programme

NTU HEALTHTECH

2023

MECHANISTIC INSIGHTS INTO THE CONNECTION BETWEEN POLLUTION AND ACNE VULGARIS

TAN YONG QUAN ALVIN

Interdisciplinary Graduate Programme

NTU HEALTHTECH

A thesis submitted to the Nanyang Technological University in partial fulfilment of the requirement for the degree of Doctor of Philosophy

2023

Statement of Originality

I hereby certify that the work embodied in this thesis is the result of original research, is free of plagiarised materials, and has not been submitted for a higher degree to any other University or Institution.

23/08/2023

. . . . . .
Date

. . . . . .
[TAN YONG QUAN ALVIN]

Supervisor Declaration Statement

I have reviewed the content and presentation style of this thesis and declare it is free of plagiarism and of sufficient grammatical clarity to be examined. To the best of my knowledge, the research and writing are those of the candidate except as acknowledged in the Author Attribution Statement. I confirm that the investigations were conducted in accord with the ethics policies and integrity standards of Nanyang Technological University and that the research data are presented honestly and without prejudice.

23/08/2023

. . . . . .

Date

. . . . . .

[MAURICE VAN STEENSEL]

Authorship Attribution Statement

*(A) This thesis **does not** contain any materials from papers published in peer-reviewed journals or from papers accepted at conferences in which I am listed as an author.

23/08/2023

. . . . . .
Date

. . . . . .
[TAN YONG QUAN ALVIN]

Acknowledgements

First of all, I would like to express my sincere gratitude to Nanyang Technological University of Singapore and the Interdisciplinary Graduate Programme for the opportunity to embark on this journey. I would like to thank my supervisor Maurice van Steensel for the constant support and guidance throughout this project. Without his excellent mentorship and understanding, I would not have made it this far. I would also like to thank my Thesis Advisory Committee Members, Professor Ng Kee Woei and Assistant Professor Navin Kumar Verma for the support and guidance in every meeting. Special thanks to fellow PhD student Daniel Law whom provided constant encouragement and was always willing and enthusiastic to assist in any way he could throughout the research project. I am deeply grateful to my wife, Jessica Lim for her unwavering support and belief in me. I wish to thank my loving and supportive parents for indulging their son in this journey. I would also like to thank my supportive friends whom encouraged and push me along throughout this whole journey. Many thanks to the students and staff of MvS lab for creating such an encouraging and supportive environment. Last but not least, I would like to thank God for His favour and wisdom throughout this journey.

Table of Contents

Summary 9

Introduction 10

Literature Review 13

1. Acne vulgaris 13
   1.1. Epidemiology of acne vulgaris 14
      1.1.1. Pubescent acne 14
      1.1.2. Adult acne 15
      1.1.3. Acne burden 16
2. The pathogenesis of acne vulgaris 18
   2.1. Comedogenesis 18
   2.2. Comedo-swtich hypothesis 20
   LRIG1+ sebaceous progenitors contribute to acne pathogenesis 21
      2.2.1. Cutibacterium acnes virulence factors and inflammation 21
      2.2.2. Androgen 23
      2.2.3. Growth hormones 24
      2.2.4. Neuropeptides (NP) 24
      2.2.5. Retinoids 25
      2.2.6. GWAS candidate genes associated with acne 26
         2.2.6.1. WNT signaling 27
      2.2.7. Pollutants 29
         2.2.7.1. Aryl hydrocarbon receptor (AHR) 30
3. Management for acne vulgaris 32
   3.1. Topical therapies 33
      3.1.1. Antimicrobials 33
      3.1.2. Retinoids 33
      3.1.3. Antibiotics 34
   3.2. Systemic therapies 35
      3.2.1. Systemic antibiotics 35
      3.2.2. Hormonal agents 35
      3.2.3. Isotretinoin 36

Hypothesis 37

Research Methods 39

1. Cell culture 39
2. Evaluation of sebaceous glands markers 40
3. Cytotoxicity evaluation of 2,3,7,8-Tetrachlorodibenzo-p-dioxin (TCDD) and Benzo[a]pyrene (B[a]P) 40
4. Evaluation of Aryl hydrocarbon receptor (AHR) activation by B[a]P and TCDD 41
5. Evaluation of the effects of B[a]P and TCDD on 1008-HFSE2 human primary sebocyte progenitors and sebaceous gland organoids 41
4. Cell culture optimization to evaluate DNA damage and cellular senescence 42
5. Evaluation of AHR antagonist CH223191 and BAY-218 on the inhibition of AHR activation, DNA damage and cellular senescence 43
6. Polymerase Chain Reaction (RT-PCR and qPCR) analysis 43

7. Immunohistochemistry (IHC) 44

8. Immunocytochemistry (ICC) 45

9. Western Blot analysis 45

10. RNAseq analysis 46

***Results* 48**

1. Human primary sebocyte progenitors are able to generate lipid-filled human sebaceous gland organoids that resembles structurally to *in vivo* sebaceous glands 48

2. TCDD and B[a]P are non-cytotoxic pollutants that activate AHR in 1008-HFSE2 human primary sebocyte progenitors 51

3. TCDD and B[a]P perturb development and maintenance of 1008-HFSE2 derived hSGOs 59

4. Inhibition of TCDD/B[a]P-induced AHR activation does not rescue the perturbation of the development and maintenance of hSGOs 67

5. TCDD and B[a]P induces DNA damage in 1008-HFSE2 primary human sebocytes but does not lead to cellular senescence 75

6. B[a]P and TCDD induce a comedo-like switch behavior in sebocyte progenitors 86

***Discussion* 99**

***Conclusion* 109**

***References* 110**

***Appendix* 126**

***Supplementary Materials* 129**

Summary

Acne vulgaris is a complex chronic disease that heavily impacts on the quality of life of patients. The need to elucidate the mechanisms of acne pathogenesis is driven by the growing impact in global skin disease burden and the lack of new acne therapy over decades. The comedo-switch hypothesis is being recognized to be the key factor in driving acne as it highlights comedogenesis as the major process needed for acne development. However, the exact mechanism has yet to be elucidated. Pollutants were recently proposed to be associated with acne exacerbation, and insights unto alteration of cellular development of keratinocytes and sebocytes via aryl hydrocarbon receptor (AHR) activation suggest a possible role of AHR in acne development. Therefore, this study hypothesized that AHR signaling can initiate comedogenesis by influencing the behavior of human primary sebocyte progenitors. This is represented in a human sebaceous gland organoid (hSGO) as these recapitulate what happens during sebaceous development and growth. As demonstrated in this study, the exposure to AHR ligands, benzo[a]pyrene (B[a]P) and 2,3,7,8-tetrachlorodibenzodioxin (TCDD) can activate AHR signaling in 2D and 3D cultured sebocytes. However, pollutant exposure perturbing the development and maintenance of hSGOs was not a consequence of AHR signaling. RNAseq analysis of exposed samples revealed a change in differentiation behavior of sebocyte progenitors towards terminal differentiation of keratinocytes through the upregulation of genes involved in keratinization and cornification. This suggests that B[a]P and TCDD can drive comedo-switch in sebocyte progenitors.

Introduction

Acne vulgaris is one of the most prevalent skin diseases, affecting 9.5% of the global population[1,2]. Acne can affect up to 95% of adolescents without significant gender bias in various communities around the world, but its incidence is highest in developed nations[3–5]. Although majority of the patients developed mild-to-moderate forms of acne, 10% of them develops severe disease[3,5]. Acne can regress past adolescence but its incidence in adults (>25 years old) remains significant[6]. Acne is a debilitating disease as it is associated with severe psychological and socioeconomic factors[7] that influences the quality of life of patients. Individuals with severe disease develops irreversible scarring, which can lead to low self-esteem, mental health issues and reduced ability to secure gainful employment[8–10]. The United States alone reported an annual cost of 12 billion dollars associated with acne including direct medical costs and loss productivity costs[11].

Although acne is regarded as a multifactorial disease[7], comedogenesis or the 'comedo-swtich' being the key event that drives acne development is well established[12]. The comedo-switch hypothesis proposes that endogenous and/or exogenous influence on stem cells/progenitors that reside in the junctional zone of the hair follicle, which maintains both the infundibulum and sebaceous glands, drives commitment towards infundibular fate. This switch towards infundibular fate results in the formation of comdeone while sebaceous glands atrophied[13]. It is of interest to understand the biomolecular mechanisms driving comedogenesis to develop novel treatments that specifically targets the key process in acne other than alleviating symptoms or preventing remission of disease which are commanded by current treatments such as antimicrobials and retinoids.

Although acne studies have primarily focused on the role of *C.acnes* and inflammation, advances on genetic association studies and environmental influences such as pollutants highlight potential novel mechanisms driving comedogenesis in acne[14–17]. Genetic predisposition to acne has been well established through familial and twin-based studies[18–21], the development of acne-like lesions in rare monogenic disorders[22] and genome-wide association studies on severe acne[17,23]. However, the effect of environmental influence on acne is less ventured with only a recent review proposing the association between pollution and acne[16,24].

The role of pollutants in acne has been shown to influence sebum production, potentiate inflammation via oxidative stress[25,26] and the involvement of aryl hydrocarbon receptor (AHR)[27,28]. Additional studies have also shown that pollutants can alter sebaceous gland differentiation and lipogenesis through AHR in immortalized sebocytes (SZ95)[29,30]. Although the association of pollutants and acne is supported by the effects of AHR on lipogenesis and sebocyte differentiation, the role of pollutants in comedogenesis is not explored. Further investigations on the influence of pollutant on comedogenesis (if any) could reveal a new biological mechanism on disease pathogenesis, possibly a novel therapeutic target.

Therefore, this study aims to gather mechanistic insights of pollutants in acne pathogenesis. To understand how pollutants may influence comedogenesis, a commonly studied polycyclic aromatic hydrocarbon (PAH) pollutant known as benzo[a]pyrene (B[a]P) and a known chloracne agent and environmental pollutant, 2,3,7,8-tetrachlorodibenzodioxin (TCDD) were used. Populations living in urban

environments are easily exposed to B[a]P as it is produced from incomplete burning of fuels including daily household cooking. Whereas TCDD serves as a control compound for B[a]P since it has been shown to be a potential comedogenic agent[31]. The effect of these pollutants on sebaceous gland biology and its role in comedogenesis were assessed using a human primary sebocyte progenitor cell line (1008-HFSE2) that was used to generate human sebaceous gland organoids (hSGOs). As most studies on these pollutants were modelled on 2D keratinocytes and isolated immortalized sebocytes such as SZ95 and SEB-1[27,29,32], we believe that our human primary sebocyte progenitors and organoids can model *in vivo* sebaceous glands. Therefore, any effect observed in this study might be translatable to *in vivo* applications.

Literature Review

The skin is the largest organ in the human body that forms the protective barrier that prevents external stimuli such as harmful chemicals and bacteria from entering the body. It is made up of three distinct layers: epidermis, dermis, and hypodermis, that holds a variety of appendages such as hair follicles, sebaceous glands, apocrine glands, sweat glands, lymphatic and blood vessels. The skin is susceptible to the development of different disorders through genetic and environmental influences, causing debilitating consequences that have an impact on the quality of living for affected individuals. And acne vulgaris is one of the most prevalent skin diseases that has a growing impact on global disease burden. This literature review primarily discusses the impact of acne vulgaris globally and the current knowledge of acne pathology including the genetic and environmental factors of acne.

1. Acne vulgaris

Acne is a pilosebaceous (hair follicle and sebaceous glands) disease where the sebaceous follicle develops lesions (inflammatory/noninflammatory) on the face, the upper chest, and the back of patients. Acne severity can be determined based on the number and type of lesions (comedonal, papulopustular, nodular, nodulocystic) present, and subsequently clinically graded as mild, moderate or severe[33]. However, this is just one of several grading systems available for determining acne severity. The type of treatments used also differs between acne severity where topical retinoids, antimicrobials and oral antibiotics are used to treat mild-to-moderate acne while a combination of both oral isotretinoin and high-dose oral antibiotics are used to treat severe forms of acne[34]. As acne is one of the most prevalent skin diseases that has a growing impact on burden globally, understanding disease progression may lead to new mechanistic insights driving novel drug development.

1.1. Epidemiology of acne vulgaris

Global analysis of skin disease places acne as the 8th most prevalent disease affecting 9.4% of the global population[1,35]. A systematic review on the epidemiology of acne globally has reported strong association between several factors such as family history, age, lifestyle, and diet with acne severity. The rate of acne prevalence can range from 20% to over 95% depending on the type of studies including age group (Figure 1A, C, D and Figure 2A) and geographic populations[36]. Although most acne prevalence studies have been conducted in the US and UK, recent studies have also been done in Asia[37–40] and other communities[41–44] around the world (Figure 1B). It has been well established that acne is associated with puberty (Figure 1C and D) and the prevalence of adult acne is rising.

1.1.1. Pubescent acne

The development of acne often correlates with puberty, where testosterone is the key androgen that modulates the increase in sebum production[9]. Following this trend, acne prevalence increases with age where higher prevalence were observed in teenagers aged 10-19 years old (Figure 1D) and lower prevalence in pre-pubertal children aged ≤10 years old[9,45] (Figure 1C). Community studies conducted in China, Germany, Egypt, Taiwan, and regional studies in South Asia and Western Europe reported increased prevalence of acne across the age of 10-19 years old[5,45–47]. Although acne prevalence between males and females have been shown to not have any significant differences[3–5], there have been reports of higher prevalence in females at younger ages of 11-13 years old than males[1,48]. This could be attributed to an earlier onset of puberty in females compared to males. Acne severity has been reviewed to be higher in older teenagers especially in males compared to females[36].

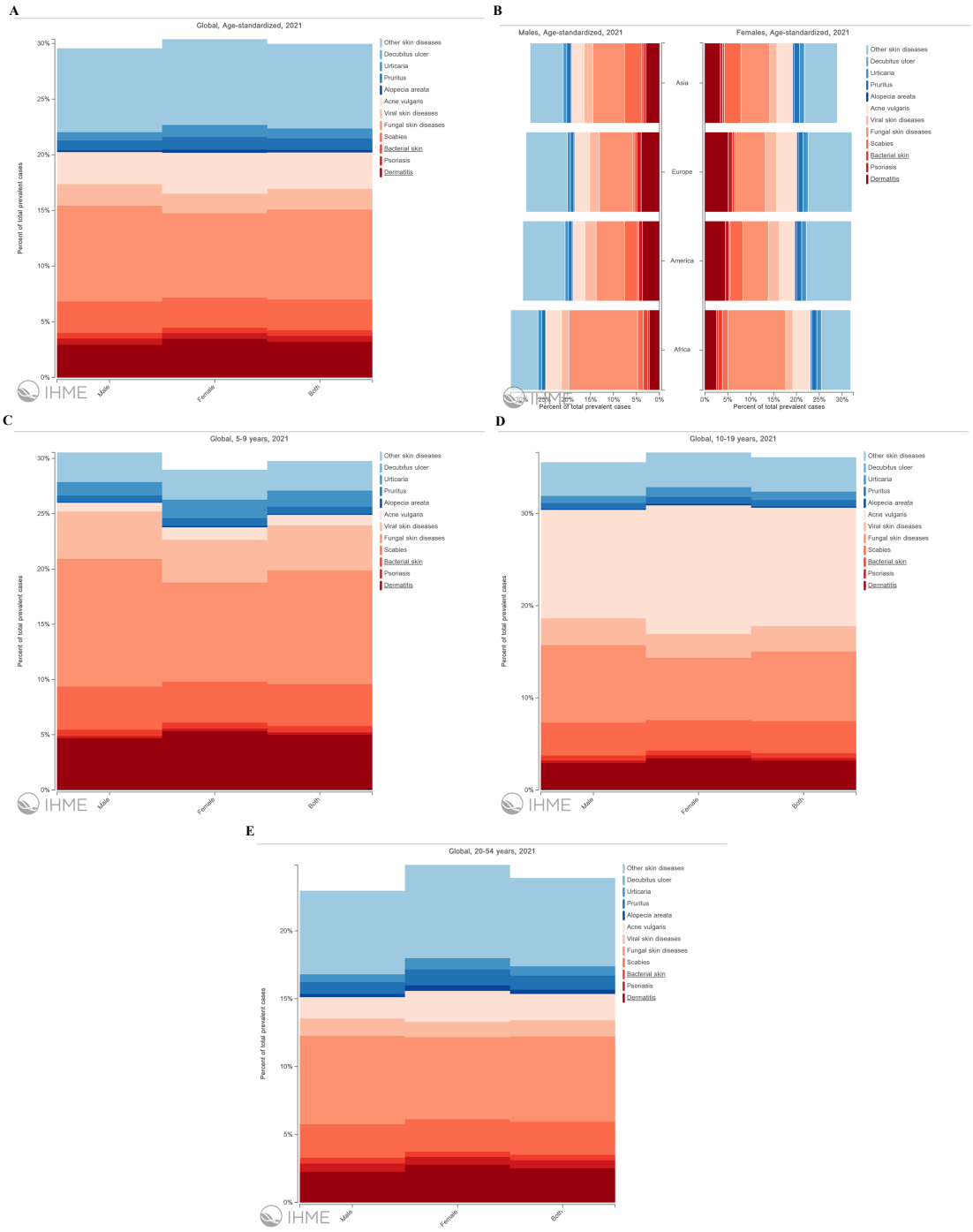

Figure 1. Global Burden of Diseases (GBD) data visualizations of global acne prevalence in 2021. Global acne prevalence is observed in both genders across age-standardized group **(A)** and from the four world regions **(B).** Lower acne prevalence was observed between ages 5-9 years old **(C)** while higher acne prevalence was observed between ages 10-19 years old, in both genders **(D).** The prevalence of acne was observed in adults between ages 20-54 years old **(E)**, suggesting persistence of acne into adulthood. The data used and the figures were generated from the VizHub tool by the Institute for Health Metrics and Evaluation (IHME).

1.1.2. Adult acne

Although acne is predominantly known as an adolescent skin disease, persistence of acne into adulthood remains significant[6] (Figure 1E). The reported incidence of adult acne is higher in females, but it might be due to

ascertainment bias.[49–52]. Skroza *et al* reported that among 1,167 acne patients, 85% were adult females and 15% were adult males, whereby the majority of both genders were reported to have mild acne[50]. Collier *et al* reported higher prevalence of adult acne in females across various age group from 20-29 years old and up to 50 years and older[51]. Goulden *et al* reported higher incidence of facial acne in 12% of adult females and 3% in adult males among 749 participants aged 25 years and older[52]. There is no clear indication whether the increased in incidence of adult acne is due to the ease of access to disease information and therefore leading to seek medical care. However, these studies have shown that majority of adult acne is persistent due to precedence of adolescent acne[6,49,51].

1.1.3. Acne burden

The World Health Organization (WHO) has defined quality of life (QoL) as 'an individual's perception of their position in life in the context of the culture and value systems in which they live and in relation to their goals, expectations, and standards and concerns[53]. Adolescents undergoing physical development as they adopt their social personality are easily affected by the visible changes cause by acne. This is further amplified as media shaped the social standards of beautification in body image and appearance. This impact has shown to cause emotional instability, significant psychosocial and mental burden including depression and suicide.

The period between acne development, onset of treatment and/or acne relapse were identified as risk factors for scarring[54,55]. Various studies have supported

the association of treatment onset and acne duration, whereby initial treatment focus on minimizing inflammatory lesions would reduce the likelihood of physical and psychosocial scarring[56,57]. An evaluation on the risk factors and clinical characteristics of scarring, scarring prevalence and burden illustrated the impact of scarring on acne patients from Brazil, France, and the US. Scars are seen as a source of anxiety, frustration and embarrassment, and results from a multinational survey showed that society perceived negatively towards facial acne scars[58]. Bullying and teasing[59] and appearance-related distress[60,61] has also been identified in a review on acne impacts. The impact of acne on appearance (especially in females) has been associated with self-consciousness of appearance and has been suggested to be the foundation of other negative consequences of acne[61].

As acne can persist into adulthood even with treatment, acne as a chronic disease can prolong its impacts leading to significant psychiatric comorbidities. Adults with acne have been reported to possess a degree of emotional impact to that of psoriasis patients and a greater degree of emotional impairment compared to adolescents due to the chronic nature of the disease[62]. Moreover, economic consequences can be driven by the psychosocial impact of acne on interpersonal relationships, productivity, and employment opportunities. Acne patients in the UK experienced higher unemployment rates than acne-free adults of those aged 18-30 years old[8]. Another study reported that among 30 acne patients, 14% had experienced limited opportunities, 17% with functional difficulty and 45% encountered interpersonal difficulties at work[63]. Patients are also willing to pay to alleviate acne symptoms, further contributing to the

economic burden. Such intangible cost was reported to be $12 billion in the US in 2004[11]. The psychosocial and economic impact that acne patients must bear emphasize the need for better acne management practices and availability of more affordable preventive treatment options.

Epidemiological studies provided insights into acne prevalence and incidence in adult acne despite the challenges by a diversified acne grading system, self-reported vs clinician-reported outcomes and varying sample size and population. However, there is corroboration among these studies on the rising acne prevalence and incidence of adult acne globally, supporting the growing impact of acne on disease burden.

2. The pathogenesis of acne vulgaris

Acne vulgaris is a pilosebaceous (hair follicle and sebaceous glands) disease that is regarded to be an interplay of factors that drive disease progression. However, recent reviews and studies present a new paradigm highlighting comedogenesis to be the key driving process of acne development. Moreover, genetic-wide association studies (GWAS) and recent review on pollution provided a link to support the association between various signaling pathways and acne pathogenesis. Although acne studies were revolved on the role of *Cutibacterium* acnes and inflammation, the pathological evidence of *C. acnes* on acne development has not been demonstrated.

2.1. Comedogenesis

The development of acne lesions is probably the key process in driving acne pathogenesis although the mechanisms driving comedogenesis are not yet fully

understood. Acne lesions can be categorized into inflammatory and noninflammatory lesions. Noninflammatory lesions are either open (blackheads) or closed comedones (whiteheads) and can developed into inflammatory lesions that consists of papules, pustules, or nodules[64]. The development of such lesions results from infundibular hyperkeratinization where abnormal differentiation of follicular keratinocytes causes obstruction in the pilosebaceous unit (Figure 2). Together with elevated sebum levels that accumulates in the comedone, creates a conducive environment for *C. acnes* to thrive, and contributes to inflammation[15]. Isotretinoin is currently the most effective treatment for acne as it targets comedonal acne, indicative of how crucial comedogenesis is in acne pathogenesis.

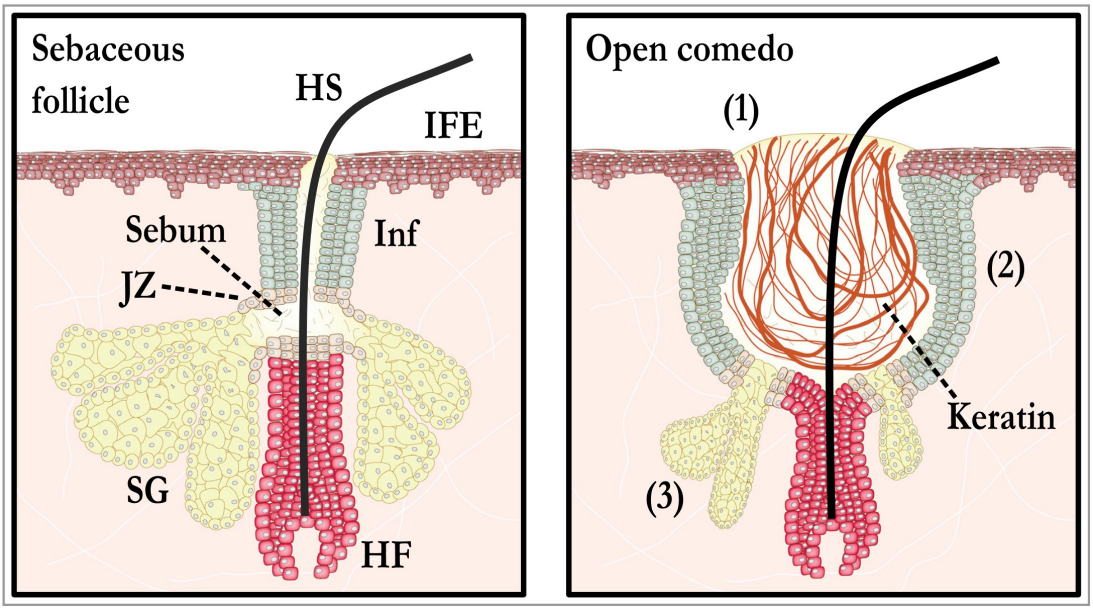

Figure 2. A normal sebaceous follicle (left) versus a non-inflammatory acne lesion of a sebaceous follicle (right), also known as an open comedo. A healthy sebaceous follicles consist of the hair follicle (HF), multilobular sebaceous glands (SG) and a normal infundibulum (Inf). Cells residing in the junctional zone (JZ) give rise to the Inf and SG. The main feature in an acne lesion is the development of a comedo, which consists of sebum and keratin (1), hyperplasia and abnormal hyperkeratinzation of the Inf (2). Atrophied SG iwas also observed n acne lesions (3). Additional structures in the figure include the hair shaft (HS) and interfollicular epidermis (IFE). *This illustration is taken from Clayton, R. W., et al (2019). Homeostasis of the sebaceous gland and mechanisms of acne pathogenesis. British Journal of Dermatology. https://doi.org/10.1111/bjd.17981*

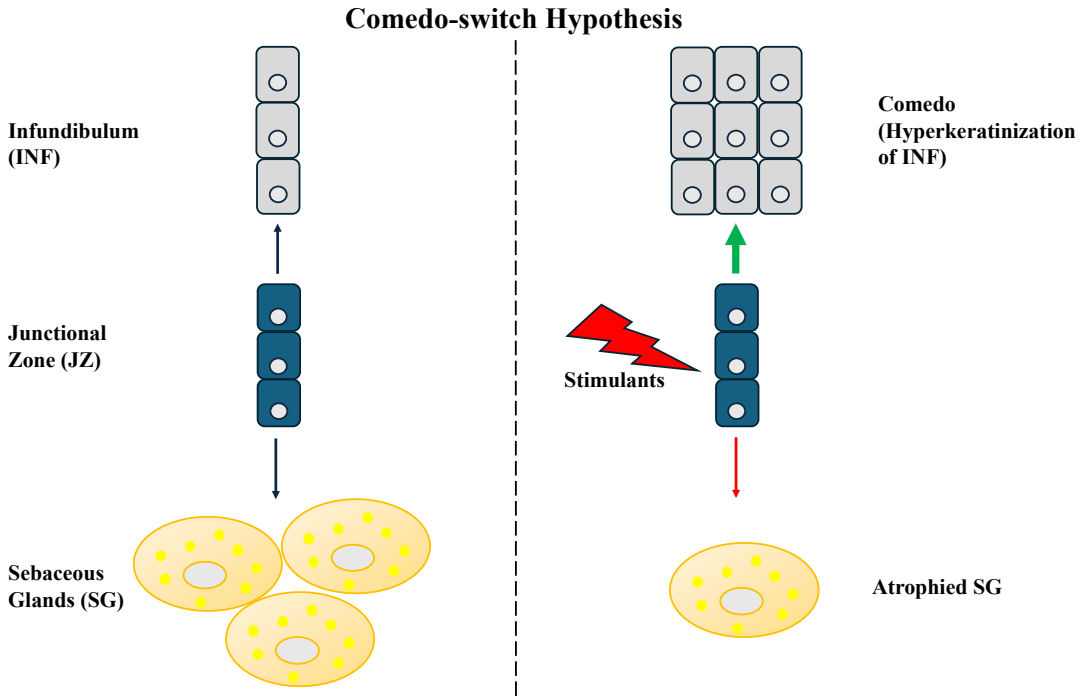

Figure 3. The comedo-switch hypothesis. Left: Progenitor cells the reside within the junctional zone (JZ) contribute to both the infundibulum (INF) and the sebaceous gland (SG). Right: A comedogenic stimulus acts on cells in the JZ, causing a switch in lineage determination that favours the infundibulum, resulting in the histopathology of acne lesions.

2.2. Comedo-switch hypothesis

The comedo-switch hypothesis (Figure 3) was first described by Saurat in 2015 where he highlights that the initial biological events of comedogenesis is driven by the abnormal behavior of LRIG1+ sebaceous progenitors[13]. The perceptive nature of this paradigm highlighted comedogenesis as the key process to the beginning of acne formation. Comedogenesis is described as the process of alterations to the infundibulum at the junction of sebaceous gland duct, where hyperproliferation of keratinocytes and defective separation of ductal corneocytes can result in comedones[65]. Xenobiotic comedogens such as 2,3,7,8-tetrachlorodibenzodioxin (TCDD) has been demonstrated to be involved in comedo formation[31,66], while retinol deficiency in a rare genetic disorder causes severe acne[67,68]. Although *C. acnes* and hyperseborrhea which can generate comedogenic lipids has been implicated to induce comedogenesis[69], evidence that support this are limited.

2.3.LRIG1+ sebaceous progenitors contribute to acne pathogenesis

Studies have shown through lineage tracing that LRIG1+ cells contributed to both the infundibulum, sebaceous duct and sebaceous glands[70–73]. Since LRIG1+ cells can contribute to different lineages in the pilosebaceous unit, Saurat proposed that LRIG1+ sebaceous progenitors to be the target population for comedogenesis. Therefore, it is likely that comedogenic agents target this population of cells, resulting in a comedo-switch towards infundibulum, initiating acne development.

As LRIG1+ cells reside in the junctional zone, modifying factors such as *Cutibacterium* acnes, androgens, growth hormones, neuropeptides and retinoids can affect these cells[67,74]. Aside from these modifying factors, the genetic architecture of acne and pollution association studies have highlighted some signaling pathways that could potentially alter sebaceous progenitors' behavior and induce comedogenesis. Although the genetic basis of acne is well-established, the focus will be on the recent GWAS analysis. Interested readers can refer to a review by Commons *et al.* for a more in-depth understanding on acne genetics[75].

2.3.1. Cutibacterium acnes virulence factors and inflammation

Cutibacterium acnes is a commensal bacterium that has been described to be an opportunistic pathogen in acne vulgaris[76]. Majority of acne studies focused on the relationship between *C. acnes* and inflammation while recent studies have suggested that the equilibrium between *C. acnes* phylotypes (IA, IB, II, III) and skin microbiota may contribute to the onset of disease. Moreover, phylotype IA of *C. acnes* has been associated with inflammatory acne[77]. However, there are currently no evidence to support the role of *C. acnes* in

comdeogenesis. Readers may refer to the review published by Dreno *et al.* on the current updates on the role of *C. acnes* and ace vulgaris[76].

The association of *C. acnes* to acne pathogenesis is primarily based on its virulence factors such as CAMP factors, porphyrins and hyaluronate lyase. CAMP factors are secretory proteins that function as membrane pore-forming toxins which can induce degradation of host tissue. It is expressed across all *C. acnes* strains which can be cytotoxic to keratinocytes and macrophages and induce skin inflammation[78]. *In vitro* evidence has shown that CAMP1 may be a virulence factor as it can interact directly with toll-like receptor 2 (TLR2) and amplify inflammatory responses[79]. Interestingly, proteomic analysis in the sebaceous follicle of both acne and healthy skin identified CAMP1 and adhesins to be the most abundant proteins of *C. acnes*[80]. These findings have provided insights into the relationship between CAMP factors and inflammation. However, such studies remained exploratory and is unable to establish the relationship between *C. acnes* strains with acne.

C. acnes also produces porphyrins that exhibit absorbance properties in both visible and ultraviolet (UV) light. These properties can result in the generation of singlet oxygen under UV exposure which may enhance cytotoxic substrate production such as squalene peroxide (proinflammatory) via oxidation[81]. Additionally, porphyrins can induce expression of inflammatory mediators such interleukin (IL)-8 and prostaglandin E2 in keratinocytes[82]. Interestingly, higher levels of porphyrins were detected in *C. acnes* phylotype IA1 isolated from acne patients compared phylotype II strains[83]. Therefore, the increased

production of porphyrins by phylotype IA1 may contribute to further inflammatory acne.

Hyaluronate lyase (HYL) were reported to have different alleles based on the phylotypes of *C. acnes*[84]. Further investigation into the genotypic and phenotypic nature of HYL including a *hyl* knockout model of *C. acnes* revealed two distinct variants that function in either complete (HYL-IB/II) or incomplete hyaluronic acid degradation (HYL-IA)[85]. HYL together with other enzymes that are involved in the degradation of ECM components such as proteins, hyaluronic acid and glycosaminoglycans, may suggest tissue remodeling and possibly spreading of inflammation during acne.

2.3.2. Androgen

The most well-studied mechanism involved in sebaceous gland homeostasis is androgens and the androgen receptor (AR)[86]. Androgen is a sex steroid hormone that is known to contribute to the development of male/female characteristics[87] where testosterone is the major circulating androgen in the body. Testosterone is metabolized by 5α-reductase to its more potent form, 5α-dihydrotestoerone (5α-DHT) where both can bind to AR with the latter having a higher affinity[88]. It has been shown that human sebaceous glands is a site of androgen metabolism and expresses AR in both basal and early differentiating sebocytes[89,90]. Sebaceous glands were also reported to be an androgen target tissue where castration prevented sebum production and testosterone replacement can rescue this condition[91]. *In vitro* evidence has shown that androgens can promote the proliferation of human sebocytes and upregulate

lipogenic enzymes in rodents while low levels or non-functional AR repressed sebocyte differentiation[92–97]. These findings support the mechanistic role of androgens in sebaceous gland homeostasis and how it can contribute to acne development.

2.3.3. Growth hormones

Growth hormones such as insulin-like growth factor-1 (IGF-1) has been shown to modulate sebum production in sebaceous glands. IGF-1 can enhance sebum production in human sebocytes and its serum level was highest during peak sebum production in adolescents with acne[98,99]. Moreover, IGF-1 expression in human sebocytes was shown to be strongest in maturing sebocytes, suggesting a role of IGF-1 in lipogenesis[100]. This was evident in SEB-1 immortalized human sebocyte, where IGF-1 induced sterol response element-binding protein-1 (SREBP-1) through the activation of PI3K/Akt and MAPK/ERK-signal transduction pathway to increase lipogenesis[101]. Therefore, the role of IGF-1 in lipogenesis of sebaceous glands may contribute to acne pathogenesis as sebum production was increased in acne patients.

2.3.4. Neuropeptides (NP)

NP are signaling proteins found in the neurons of the central and peripheral nervous system. Interestingly, human sebaceous glands were found to express these functional receptors for NP, notably for corticotropin-releasing hormone (CRH), melanocortins (MC), cannabinoid, neuropeptide Y, vasointestinal polypeptide, and calcitonin gene-related peptide[102]. CRH is known to modulate neuroendocrine and behavioral responses to stress where both CRH and its functional receptors (CRH-R1/2) are abundant in sebaceous glands and can

induce sebum production and synthesis of IL-6 and IL-8[103,104]. MC receptors (MC-1R/5R) was found in human sebocytes where MC-5R has been associated to be a sebaceous gland differentiation marker[105,106]. MC peptides such as α-melanocyte-stimulating hormone have been proposed to promote anti-inflammatory actions as its receptor, MC-1R have been shown to be upregulated in sebocytes as a response to increased proinflammatory signals in acne lesions[105,107].

Cannabinoid receptors (CB1 and CB2) are expressed in human sebaceous glands where enhanced lipid production and cell death via CB2-mediated signaling was reported[108,109]. Vasointestinal peptide that can be induced by stress have been shown to promote proliferation and differentiation of sebaceous glands[102]. Additionally, ectopeptidases that degrade vasointestinal peptide is highly expressed in human sebocytes and the inhibition of these enzymes can suppress proliferation but also induce terminal differentiation of SZ95 sebocytes[110]. The presence of innervations within the pilosebaceous unit may play a role in sebaceous glands differentiation and in acne pathogenesis.

2.3.5. Retinoids

Retinoids are commonly used as a topical treatment effective in managing the symptoms of acne. While their mechanisms are unknown, its effect on sebaceous glands results in shrinkage of sebaceous gland and reduced sebum production[111–114]. Retinoids bind to retinoic acid receptors (RAR) and retinoid X receptors (RXR) to elicit its effects. These are ligand-activated nuclear receptors that have been found in human sebaceous glands[115]. It has been

shown that isotretinoin, all-trans-retinoic acid (ATRA) and 13-cis-retinoic acid can activate RARs and suppress the proliferation and lipogenesis of human sebocytes[116–119]. However, low doses of retinoids have been shown to stimulate sebocytes. Sebocytes cultured in vitamin-A free media have reduced proliferation and lipogenesis compared to those cultured with lose doses of isotretinoin[120]. Moreover, retinol deficiency caused by a rare genetic disorder (Retinal dystrophy, iris coloboma and comedogenic acne syndrome) causes severe acne, suggesting that retinol deficiency may be involved in acne development[75]. Therefore, these findings support the role of retinoids in sebaceous gland differentiation and acne pathogenesis as evident by the effectiveness of retinoid treatment[67].

2.3.6. GWAS candidate genes associated with acne

GWAS on acne population has been performed in four geographical locations including China, Australia, Northern Europe, and North America[17,21,121,122]. Majority of these studies focuses on Caucasian patients with one cohort on Han Chinese patients. Each GWAS reported new susceptibility loci that did not overlap with each study, indicating genetic heterogeneity between and among ethnicities. Identified susceptibility risk loci in these GWAS proposed biological pathways involved in cell fate, tissue patterning/remodeling, and inflammation to be associated with acne development[22].

The Han Chinese GWAS reported two susceptibility loci found on chromosome 1q24.2 (rs7531806 and rs1060573) for DNA-binding protein 2 (DDB2), and another on chromosome 11p11.2 (rs7531806) for L-selectin

(SELL). These genes are implicated in androgen metabolism and inflammation, respectively[121]. A smaller GWAS on European Americans reported two SNPs on chromosome 8q24 (closest to c-MYC) but without genome-wide significance[122]. c-MYC is a proliferative marker and a proto-oncogene that was implicated in the proliferation and differentiation of LRIG1 sebaceous progenitors[74,92,123].

An initial GWAS conducted in the UK identified three novel susceptibility risk loci on chromosome 11q13.1, 5q11.2 and 1q4.1, which contain genes that encode for ovo-like transcriptional repressor 1 (OVOL1), follistatin (FST) and transforming growth factor beta-2 (TGFβ2). These genes are reported to be involved in the TGFβ signaling pathway which has been shown to modulate lipogenesis, wound healing, scarring and tissue remodeling[17,124]. A follow-up study reported an additional 12 susceptibility risk loci with implicated genes. Candidate genes identified through meta-analysis were reported to be involved in hair follicle development and morphogenesis. Among candidate genes, two genes are associated with WNT signaling: a WNT mediator, leucine rich repeat containing G protein-coupled receptor 6 (LGR6), and a WNT ligand, WNT10A. These reported gene candidates have been implicated in the maintenance of hair follicle and sebaceous glands[125], suggesting a role of WNT signaling in acne pathogenesis.

2.3.6.1. WNT signaling

WNT signaling has been established as an important pathway for embryonic development and tissue homeostasis[126]. The canonical WNT signaling pathway describes the binding of WNT ligands to frizzled

receptor, which induces downstream release and translocation of transcription factor, β-catenin into the nucleus. Within the nucleus, β-catenin can bind with other transcription factors to drive WNT target gene expression involved in skin morphogenesis and homeostasis, including the hair follicle and sebaceous glands[126–128].

The effects of WNT signaling on sebaceous gland were mostly studied using genetic knockout mouse models. Impaired β-catenin/Lef1 function in mouse skin induced the enlargement of sebaceous glands and sebaceous tumors[129–132]. As previously discussed, GWAS on severe acne population reported WNT10A as a potential target gene associated with acne, although its loss-of-function allele is reported to be protective[17,23]. A Wnt10A-deficient transgenic mouse model was shown to have truncated hair follicles and enlarged sebaceous glands[133]. Another recent study has shown that WNT signaling is important in cell fate specification and tissue patterning in LRIG1 cells. The loss of WNT signaling induced the expansion of both the infundibulum and sebaceous glands while constitutive WNT signaling resulted in comedo-like cyst with atrophied sebaceous glands in mice[72]. This phenomenon would also explain the histological observation of 'more comedones, smaller sebaceous glands' in acne[65]. Therefore, perturbations to WNT activity within the pilosebaceous unit, especially on sebaceous progenitors may contribute to acne pathogenesis through altering cell fate and tissue patterning of Lrig1+ progenitors.

2.3.7. Pollutants

The impact of pollutants on skin homeostasis and diseases have been of increasing importance due to increasing evidence showing the correlation between pollutants and skin problems[134]. However, the role of pollutants on acne pathogenesis is not well explored due to the lack of understanding. A recent review by Krutmann *et al.* proposed a pathophysiological link between acne prevalence and high ambient pollution levels according to three epidemiological studies conducted[24]. These studies have shown that high ambient levels of air pollutants such as particulate matter ($PM_{2.5/10}$), nitrogen dioxide (NO_2) were associated with an increased in outpatient visits for acne vulgaris while sulfur dioxide (SO_2) and ozone (O_3) were associated with decreased in outpatient visits. The effects of these pollutants were also contrasting whereby $PM_{2.5/10}$ and NO_2 were associated with increased sebum secretion and increased in both inflammatory and noninflammatory lesions, while SO_2 and O_3 had the opposite effect[135]. Moreover, pollutants including polycyclic aromatic hydrocarbons have been recognized as an inflammatory mediator as it can generate reactive oxygen species (ROS) to induce oxidative stress, thus contributing to inflammation in acne[136]. Therefore, these observations support a potential link between pollutants and acne pathogenesis although more research is needed to clarify the role of pollutants in acne pathogenesis.

The most prominent case of association between pollutant and acne pathogenesis is the case study of dioxin poisoning of Victor Yushchenko. The former president ingested a dioxin compound known as TCDD and he was observed to have extremely dry skin with facial edema and numerous nodular

lesions[66]. Upon histological inspection of his skin biopsy, it was revealed that the sebaceous follicle developed comedo-like cyst structure with the loss of sebaceous glands[31]. This phenotype observed was also known as Chloracne. Chloracne has a long history since its discovery from industrial incidents since the 1970s and further received more attention with additional case studies that included Yushchenko's case[137–139]. It was later discovered that dioxins such as TCDD could induce chloracne, inducing comedo-like structures observed in acne vulgaris[137–139]. It is important to note that the general population can be exposed to low levels of dioxins and dioxin-like compounds primarily through food consumption[140]. Moreover, TCDD is an organic environmental pollutant that is a by-product of organic synthesis and fuel combustion. It is also classified as a human carcinogen. TCDD is also a comedogenic agent and ligand of AHR. It can trigger the AHR signaling pathway, which has been associated with chloracne[31]. The role of AHR modulating skin homeostasis and inflammatory diseases is well reviewed by Furue *et al*[141,142]. However, the focus will be on the association of AHR to acne pathogenesis.

2.3.7.1. Aryl hydrocarbon receptor (AHR)

AHR is a xenobiotic-response receptor that binds to both endogenous and exogenous ligands such as pollutants (dioxins and polycyclic aromatic hydrocarbons). It primarily regulates the expression of cytochrome P450 family genes which are involved in the redox system[143]. It also functions through a non-genomic pathway whereby it may be associated with other transcriptional regulators such as nuclear factor kappa light chain enhancer of activated B cells (NFkB), estrogen receptor α (ERα) and β-catenin. The association with these other transcription factors in the non-genomic

pathway can elicit increase intracellular calcium concentrations and promote activity of Src and focal adhesion kinases with functional consequences for cellular functional properties (adhesion and migration) or other pathways such as mitogen-activated protein kinase pathway[144].

The role of AHR in acne pathogenesis is primarily associated with the effects of TCDD in chloracne[31,66]. *In vitro* experiments reported that AHR activation via TCDD in keratinocytes have been reported to induce epidermal differentiation in human stem cells by promoting keratinocyte differentiation with eventual depletion of the epidermal stem cells[145,146]. Moreover, TCDD exposure in immortalized sebocytes such as SZ95 and SEB-1 resulted in the transcriptional downregulation of sebaceous gland differentiation markers epithelial membrane antigen (EMA) and KRT7 while upregulating keratinocyte differentiation marker, KRT10[30,32]. Furthermore, AHR activation via TCDD modulates the expression of interleukin (IL)-8 and tumor necrosis factor alpha (TNF-α) in SZ95 sebocytes[147]. The induction of epidermal differentiation by TCDD may contribute to interfollicular epidermal hyperkeratinization, which result in the formation of comedones observed in acne.

Aside from TCDD, another pollutant known as benzo[a]pyrene (B[a]P) has been used to study the effects of AHR. B[a]P is a polycyclic aromatic hydrocarbon and is a common air pollutant produced via incomplete combustion of fuels and in daily household cooking[148]. AHR activation via B[a]P exposure in SZ95 sebocytes resulted in reduced lipogenesis and

induced IL-6 production[29]. Furthermore, silencing of AHR resulted in the induction of lipogenesis and increased expression of early differentiation marker, KRT7 and reduced expression of late differentiation marker, EMA and expression of CYP1A1 and keratinocyte differentiation marker, KRT10 was downregulated[149]. Although the role of B[a]P in AHR activation may modulate sebaceous differentiation and lipogenesis, its role in comedogenesis is unclear.

Overall, AHR activation via TCDD or B[a]P in keratinocytes and sebocytes seem to modulate cellular differentiation, lipogenesis as well as inflammatory functions. Although there is a strong support for the association of comedogenesis and AHR activation via TCDD, the lack of evidence from AHR activation via B[a]P prompted the need to further evaluate whether AHR activation is involved in comedogenesis.

3. Management for acne vulgaris

Acne being one of the most prevalent skin diseases does not possess a universal guideline for managing acne. Multiple grading systems exist for scoring acne severity and yet not one is accepted universally[150]. Even the most widely used treatments have not seen any changes or improvements in the past couple of decades. The lack of a universal guideline system has impeded the progress for quality clinical research. Despite the lack of a "gold standard" for the management of acne, the use of mainstream treatments based on acne severity is consistently advised by dermatologist globally (Table 1).

3.1. Topical therapies

Many topical therapies used for acne treatment are available through prescriptions or over the counter. The type of therapy used can be influence by several factors such as patient preference and age, acne site and disease severity. Topical therapies are often used for mild acne and can include either monotherapy or combinations of multiple topical agents for initial control and maintenance.

3.1.1. Antimicrobials

Benzoyl peroxide (BP) is one of the most commonly use topical agents for its bactericidal effect through free radicals and it is mildly comedolytic[151]. BP in combination with other therapies such as antibiotics can enhance efficacy and may reduce resistance development[152]. It can be found as creams, gels, topical washes, as well as leave on or wash-off agents. Treatment concentrations of BP can range from 2.5-10% as it can cause skin irritation depending on the concentration used and BP possess bleaching properties as well. The efficacy of BP can be influenced by total contact time and formulation. Patients are advised to use lower concentrations as it is more tolerable for sensitive skin.

3.1.2. Retinoids

Retinoids are vitamin A derivatives that are effective against microcomedones. It has been shown to act on follicular keratinocytes to prevent keratinocyte expansion and excessive cornification resulting in follicular blockage[153]. There are three active agents of retinoids: tretinoin (0.025-0.1%), adapalene (0.1-0.3%) and tazarotene (0.05-0.1%). The formulation for retinoids is mostly cream or lotion based. As retinoids can cause skin irritation, dryness and erythema, small amounts of topical application are recommended. Retinoids are the foundation for topical therapy and are commonly prescribed for

comedonal acne. It can also be used with other agents in combination preparations to treat all acne variants.

3.1.3. Antibiotics

Topical antibiotics are used for their anti-inflammatory and antibacterial effects[154]. However, it is not recommended to use antibiotics for monotherapy given the concern of antibiotic resistance. Antibiotics are mostly used in combination with other agents such as BP and retinoids to reduce the risk of resistance development. Topical erythromycin (2%) and clindamycin (1%) have shown to reduce inflammatory lesions[155], with the former having less efficacy over time[154]. Although there is a study that reported diarrhea as a side effect from the use of topical clindamycin, the risk is low, and the tolerability of these antibiotics is excellent.

Table 1. Acne treatment options that are currently available and utilised for acne disease management.

Treatment Options	Types of treatment	Mode of Action	Side Effects
Topical Treatments	Antimicrobials • 2.5-10% Benzoyl Peroxide	• Comedolytic • Bactericidal via free radicals	• Skin irritation • Bleaching properties
	Retinoids • 0.0025-0.1% Tretinonin • 0.1-0.3% Adapalene • 0.05-0.1% Tazarotene	• Targets keratinocites • Prevent keratinocyte expansion • Prevent cornification	• Skin irritation • Dryness • Erythema
	Antibiotics • 2% Erythromycin • 1% Clindamycin	• Reduce inflammatory lesions	• Risk of antibiotic resistance
Systemic Treatments	Antibiotics • Tetracycline classes • Macrolide classes • Trimethoprim/sulfamethoxazole (TMP/SMX) • Amoxicillin • Cephalexin	• Anti-inflammatory effects • Reduce inflammatory lesions	• Pregnant women should not use Tetracyclines • Gastrointestinal upset • Dizziness • Pigment changes • Risk of antibiotic resistance
	Hormonal agents • Combination oral contraceptives (COC)	• Antiandrogenic properties • Reduce inflammatory and comedonal lesions	• Hyperkalemia • Menstrual irregularities • Feminization of a male fetus.
	Isotretinonin (13-cis-retinoic acid)	• Reduce inflammatory and comedonal lesions • Improve acne scarring	• Dry skin, nose, and mouth • Erythemal changes • Eye irritation • Musculoskeletal discomfort

3.2.Systemic therapies

Topical therapies are usually effective for the control and maintenance of mild acne. However, if acne persists or develops into moderate or severe acne, additional therapies in combination with topical applications are required.

3.2.1. Systemic antibiotics

Systemic antibiotics are often considered when acne is severe not just in the facial region but includes the chest, back and shoulders[34]. The list of systemic antibiotics includes tetracycline classes (tetracycline, doxycycline, minocycline), macrolide classes (erythromycin, azithromycin), trimethoprim/sulfamethoxazole (TMP/SMX), amoxicillin, and cephalexin. The tetracycline and macrolide classes of antibiotics are commonly used for the treatment of acne. The mode of mechanism for these classes is to inhibit protein synthesis with some anti-inflammatory effects, including inhibition of cytokines and matrix metalloproteinase[156,157]. Side effects from the use of antibiotics are usually rare. The use of tetracyclines is advised against pregnant women and the side effects include gastrointestinal upset (doxycycline and macrolides), dizziness and pigment changes (minocycline). Although antibiotics have been reported to be effective in reducing inflammatory lesions, using antibiotics as a monotherapy is not practiced due to increasing incidence of drug resistance. Therefore, a combinational therapy with non-antibiotic topical agent with oral antibiotics is advised[34].

3.2.2. Hormonal agents

The use of hormonal agents provides an additional line of effective treatment for women regardless of androgen excess[158]. Combination oral contraceptives (COC) which contains both an estrogen and a progestin component have been

effective for acne treatment[64]. The US Food and Drug Administration (FDA) have approved 4 COCs (ethinyl estradiol/drospirenone/levomefolate, ethinyl estradiol/drospirenone, ethinyl estradiol/norethindrone acetate/ferrous fumarate, and ethinyl estradiol/norgestimate) for the treatment of acne. The main mechanism of COCs is their antiandrogenic properties where they reduce androgen production and 5α-reductase activity[159,160]. Clinical trials have reported that COCs can reduce both inflammatory and comedonal lesions[161–164]. However, such improvements require at least 3 to 6 months of therapy. In addition to COC, spironolactone which is also an oral antiandrogen drug can be administered to improve acne. However, its side effects include hyperkalemia, menstrual irregularities, and feminization of a male fetus.

3.2.3. Isotretinoin

13-cis retinoic acid or isotretinoin is a potent oral retinoid that is used to treat severe acne when other therapies are not effective, and scarring is evident over the course of treatment. It is considered to be the most effective drug as it can improve severe acne by reducing inflammatory and comedonal leisons, improves acne scarring and is anti-inflammatory[165]. Isotretinoin efficacy has also been reported in a 10-year study that patients given a cumulative dose of isotretinoin have a lower rate of recurrence of acne[165]. Although the efficacy of isotretinoin is high, treatment must be monitored carefully due to its adverse effects. The common and less severe adverse effects include dry skin, nose, and mouth, erythemal changes, eye irritation and musculoskeletal discomfort. The other more severe but rarer adverse effects (usually based on individuals' reaction to drug) include infections, fever, Stevens-Johnson Syndrome (SJS)

and others[166]. Isotretinoin is also known to be teratogenic and therefore not recommended for use by pregnant women.

The choice of treatments based on the severity of acne and their increased efficacy in combination with other therapies have shown to improve acne. However, most of these therapies focus on its anti-inflammatory and antibacterial effects with only a handful that targets specifically to comedonal lesions. Although side effects are often unavoidable, the unchanging therapy options for more than several decades emphasize the need to further unravel the mechanisms of acne pathogenesis to enable development of new treatments, especially against comedogenesis.

Hypothesis

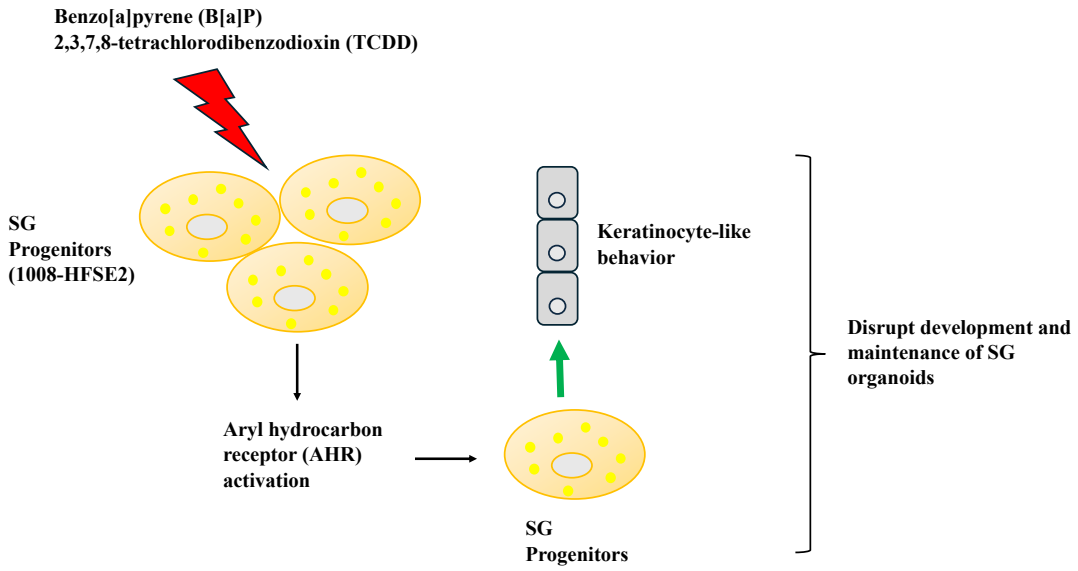

Figure 4. AHR activation through exposure to pollutants may result in a comedo-switch of SG progenitors (1008-HFSE2, resulting in the disruption of development and maintenance of SG organoids.

The role of AHR in cellular differentiation observed in keratinocytes and sebocytes suggest a potential role of AHR as a comedogenic pathway in acne pathogenesis. Although AHR activation can trigger epidermal differentiation in human keratinocytes which may contribute to interfollicular hyperkeratinization, the key process of

comedo-switching lies in sebaceous progenitors residing in the junctional zone, whereas most studies on pollutants are focus on kerationcytes[27,145,167]. Evidence of AHR activation in immortalized sebocytes (mainly SZ95) have shown modulation of sebaceous differentiation, lipogenesis, and inflammatory cytokine production[147,149]. However, there is a lack of evidence suggesting that AHR activation in sebocytes can induce a comedo-switch which involve a change in the cell fate of sebaceous progenitors.

Therefore, we hypothesize that pollution can induce comedogenesis through AHR activation. This study aims to unravel the role of pollutants and AHR signaling in sebaceous progenitors using a human primary sebocyte progenitor cell line to generate human sebaceous gland organoids. We think that TCDD/B[a]P-induced AHR activation can trigger a comedo-switch in sebaceous progenitors. The use of human sebaceous gland organoids would allow us to study if pollutant induced AHR activation will disrupt the development and maintenance of human sebaceous gland organoids by altering its differentiation program towards keratinocyte-like differentiation.

Research Methods

1. Cell culture

Human primary sebocyte cell line, 1008-HFSE2 was previously derived from human facial skin tissue obtained by an external Clinical Research Organisation with IRB approval. The use of this cell line for research was declared and approved by the A*STAR Human Biomedical Research Office for the usage of non-identifiable cell line in accordance with the Human Biomedical Research Act. These human primary sebocyte progenitors were co-cultured with inactivated mouse fibroblast feeders (3T3J2) in CCMY media [3:1 DMEM (Gibco) and Ham's F12 GlutaMAX (Gibco), 10% (v/v) FBS (Hyclone), 10nM cholera toxin (Sigma), 1ug/mL hydrocortisone (Sigma), 200ng/mL epidermal growth factor (EGF; PeproTech) and 10uM Y-27632 (Torcis)], maintained at 37°C with 5% CO_2. Inactivated mouse fibroblast feeders were generated using 1mg/mL mitomycin C added to MEF media [DMEM, 10% (v/v) FBS, 1% (v/v) Penicillin/Streptomycin (P/S; Gibco) and 2mM L-glutamine (Gibco)]. 3D sebaceous glands organoids were generated from 1008-HFSE2 human primary sebocyte progenitors, harvested using 0.125% Trypsin-EDTA (Gibco). Feeders were removed using mouse feeder removal beads and passed through a LS MACs column as per manufacturer's protocol (Miltenyi). Feeder-free 1008-HFSE2 human primary sebocyte progenitors were seeded into 40-50% (v/v) Matrigel (Corning) to develop sebaceous glands organoids. The organoids were culture in serum free CCMY supplemented with 200ng/mL insulin-like growth factor-1 (IGF-1; R&D Systems) at 37°C with 5% CO_2 for 14 days.

2. Evaluation of sebaceous glands markers

Sebaceous glands markers: keratins (*KRT*) 7/10/14, epithelial membrane antigen (*MUC1*), peroxisome proliferator activated receptor gamma (*PPARγ*), stearoyl-CoA desaturase 1 (*SCD1*), fatty acid synthase (*FASN*) and leucine rich repeats and immunoglobulin like domain 1 (*LRIG1*) were analyzed using polymerase chain reaction (PCR) of cDNA generated from RNA harvested from 1008-HFSE2 human primary sebocyte progenitors. Additional genes such as proliferative marker *MKI67*, *WNT10A*, ovo-like transcriptional repressor 1 (*OVOL1*), leucine rich repeat containing G protein-coupled receptor 6 (*LGR6*), transforming growth factor beta 2 (*TGFβ2*), laminin subunit gamma-2 (*LAMC2*), semaphorin 4B (*SEMA4B*) and follistatin (*FST*) was evaluated. Immunohistochemistry (IHC) and immunocytochemistry (ICC) was performed on 1008-HFSE2 human primary sebocyte progenitors and human sebaceous gland organoids. IHC analysis was used to detect FASN, SCD1, PPARγ, MUC1, KRT10/14 in human skin tissues, and ICC analysis was used in 2D and 3D cell culture to detect FASN, SCD1, PPARγ, MUC1, KRT10/14, MKI67, integrin alpha 6 (ITGA6/CD49f) and LipidTOX staining of neutral lipids.

3. Cytotoxicity evaluation of 2,3,7,8-tetrachlorodibenzo-p-dioxin (TCDD) and benzo[a]pyrene (B[a]P)

Cell viability assay was conducted in a 96-well plate format and 1008-HFSE2 human primary sebocyte progenitors were exposed to 10/50/100/200/400nM/1µM B[a]P and 1/5/10/20/30nM TCDD for 24/48/72/96 hours. Cell viability was assessed using 2uM calcein AM (Invitrogen) to detect LIVE cells and Hoechst 33342 (Invitrogen) to stain for nuclei. The absorbance reading of calcein AM (Ex:

494nM, Em: 517nM) and Hoechst 33342 (Ex: 360nM, Em: 460nM) was performed on the VarioSkan plate reader (Thermofisher). Further cell viability evaluation was conducted in human sebaceous gland organoids after acute (day1-3 and day7-9 of organoid growth) and chronic (day1-8 and day7-14 of organoid growth) exposures to 10/50/100/200/400nM B[a]P and 1/5/10/20/30nM TCDD. Multiple regions of interest (ROIs) images were used to quantify the percentage of calcein AM positive cells over total nuclei. Statistical analysis was performed using One-way ANOVA with Tukey for multiple comparisons across 3 technical replicates.

4. Evaluation of aryl hydrocarbon receptor (AHR) activation by B[a]P and TCDD

Transcriptional analysis of AHR target genes: aryl hydrocarbon receptor repressor (*AHRR*) and cytochrome P450 family 1, subfamily A, polypeptide 1 (*CYP1A1*) was performed after 1008-HFSE2 human primary sebocyte progenitors were exposed to 10/50/100/200/400nM B[a]P and 1/5/10/20/30nM TCDD for 24/48/72/96 hours. Further western blot (WB) and ICC analysis of AHR protein was conducted after 72 hours of exposure to 10nM TCDD and 400nM B[a]P. Additional transcriptional analysis of *AHRR* and *CYP1A1*, and WB analysis of AHR protein was performed after 1/2/4/6 hours of exposure to 400nM B[a]P and 10nM TCDD.

5. Evaluation of the effects of B[a]P and TCDD on 1008-HFSE2 human primary sebocyte progenitors and human sebaceous gland organoids

Transcriptomic analysis of sebaceous glands markers: *FASN, SCD1, PPARγ, LRIG1* and *c-MYC* was assessed after 24/48/72/96 hours of exposure to

10/50/100/200/400nM B[a]P and 1/5/10/20/30nM TCDD. ICC analysis of FASN, SCD1 and PPARγ was also performed after 72 hours of exposure to 10nM TCDD and 400nM B[a]P. Acute (day1-3 and day7-9 of organoid growth) and chronic (day1-8 and day7-14 of organoid growth] exposure to 400nM B[a]P and 10nM TCDD was performed on human sebaceous gland organoids. The organoids were stained with CD49f, LipidTOX, phalloidin and DAPI. Quantitative analysis on the size (volume) and number of organoids was performed on an imaging software, IMARIS (v9.2). Further transcriptomic analysis of day7-9 acute exposed organoid samples was performed to evaluate gene expression of FASN, *SCD1, PPARγ, LRIG1, c-MYC, MSH2, MSH6, RAD51,* cyclin dependent kinase inhibitor 1A (*CDKN1A/P21)* and lamin B1 (*LMNB1*). Statistical analysis was performed using One-way ANOVA with Tukey for multiple comparisons across 3 technical replicates.

4. Cell culture optimization to evaluate DNA damage and cellular senescence

2D cell culture optimization of 1008-HFSE2 human primary sebocyte progenitors to study DNA damage and cellular senescence was evaluated with 5/10uM Y-27632 titration CCMY assay and sebocyte progenitor growth in serum free CCMY with and without supplementation with IGF-1. The cell culture optimization was also performed with exposure to 250μM of hydrogen peroxide (H_2O_2) as a positive control for DNA damage and cellular senescence. Transcriptomic analysis was performed on samples from Y titration CCMY assay to evaluate gene expression *MSH2, MSH6, RAD51, CDKN1A and LMNB1* and transcriptomic analysis was performed on samples from serum free CCMY with/without IGF-1, to evaluate

gene expression of *FASN, SCD1, PPARγ, LRIG1, c-MYC, MSH2, MSH6, RAD51, CDKN1A and LMNB1*. Statistical analysis was performed using One-way ANOVA with Tukey for multiple comparisons across 3 technical replicates.

5. Evaluation of AHR antagonist CH223191 and BAY-218 on the inhibition of AHR activation, DNA damage and cellular senescence

1008-HFSE2 human primary sebocyte progenitors were exposed to 250μM H_2O_2, 400nM/1μM B[a]P and 10nM TCDD supplemented with 30/60nM CH223191 or 40nM BAY-218. Transcriptional analysis of *c-MYC, CYP1A1, MSH2, MSH6, RAD51, LMNB1* and *CDKN1A* was performed. Additional analysis of *FASN, SCD1, PPARg* and *LRIG1* was performed for samples that were supplemented with 60nM CH223191. ICC analysis of MKI67 and co-localization of γH2AX and 53BP1 proteins was performed for all treated samples. WB analysis of AHR, MSH2, MSH6, LMNB1 and p21 was performed for samples that were supplemented with 30/60nM CH223191. Human sebaceous gland organoids were chronically (day 1-8 and day7-14 of organoid growth) exposed to 250μM H_2O_2, 400nM/1μM B[a]P and 10nM TCDD supplemented with 30/60nM CH223191. The organoids were stained with CD49f, LipidTOX, phalloidin and DAPI. Quantitative analysis of the size (volume) and number of organoids was performed on an imaging software, IMARIS (v9.2). Statistical analysis was performed using One-way ANOVA with Tukey for multiple comparisons across 3 technical replicates.

6. Polymerase Chain Reaction (RT-PCR and qPCR) analysis

RNA was extracted from 1008-HFSE2 human primary sebocyte progenitors following manufacturer's protocol from RNeasy mini kit (Qiagen). Human sebaceous gland organoids were harvested in ice-cold cell recovery solution

(Corning) with incubation at 4°C for 15 minutes. Organoids were centrifuged down at 500g for 7 minutes at 4°C. Cold PBS wash of organoid pellet was performed 3 times with the same centrifuge settings. Organoid pellet was resuspended in lysis buffer. All samples were kept in -80°C and RNA was extracted according to manufacturer's protocol. Total cDNA was generated from 1ug of total RNA using qScript cDNA SuperMix (Quantabio). Total cDNA was used in RT-PCR and qPCR analysis. qPCR analysis was performed in QuantStudio Pro 6 (Applied Biosystems). The primer sequences used in both RT-PCR and qPCR analysis are listed in Appendix, Table 1.

7. Immunohistochemistry (IHC)

Human abdominal tissue sections of 6um were deparaffinized in the following reagents: xylene (2x5 minutes), 100% ethanol (2x3 minutes), 95% ethanol (1x3 minutes) and then 80% ethanol (1x3 minutes). Citrate buffer (ph6.0) was used to perform heat-induced antigen retrieval using a pressure cooker for 2 hours. Slides were cooled down at room temperature for 20 minutes. Blocking buffer (0.5% PBS-Tween 20 and 5% normal goat serum) was used to block sections for an hour at room temperature. Primary antibodies were incubated at 4°C overnight, and secondary antibodies were incubated at room temperature for an hour. Sections were washed with 0.5% PBST (3x5minutes) after primary and secondary antibody incubation. Sections were mounted using VECTASHIELD Plus antifade mounting medium (Vector Laboratories). Images were captured using confocal laser scanning microscope, FV3000RS (Olympus). The primary and secondary antibodies, and chemical stains used for IHC are listed in Appendix, Table 2.

8. Immunocytochemistry (ICC)

1008-HFSE2 human primary sebocyte progenitors were seeded into an 8-well chamber slide (Ibidi). Cells were fixed with 4% paraformaldehyde (PFA) for 10 minutes followed by a single PBS wash. Cells were permeabilized in 0.5% PBS-Triton-X100 for 10 minutes followed by incubation with blocking buffer (10% (v/v) bovine albumin serum/goat/donkey serum) at room temperature for an hour. Primary antibodies were incubated overnight at 4°C and secondary antibodies were incubated for 2 hours at room temperature. Cells were washed with 0.05% PBS-Triton-X100 (3x5minutes) after primary and secondary antibody incubation. Sebaceous gland organoids grown in 8-well chamber slide were fixed in 8% PFA for an hour, followed by a single PBS wash. Organoids were blocked in 10% BSA for an hour in room temperature. Primary antibodies were incubated at 4°C overnight and secondary antibodies were incubated for 2 hours at room temperature. Organoids were washed with PBS (3x10minutes) after primary and secondary antibody incubation. Chamber slides were mounted with VECTASHIELD Plus antifade mounting medium. Images were captured using confocal laser scanning microscope, FV3000RS (Olympus). The primary and secondary antibodies, and chemical stains used for ICC are listed in Appendix, Table 2.

9. Western Blot analysis

1008-HFSE2 primary sebocytes were harvested in cold lysis buffer (25mM HEPES, 25mM $MgCl_2$, 300nM NaCl, 0.1mM EDTA, 20% Glycerol) supplemented with Complete Mini, EDTA-free proteinase inhibitors (Merck) and PhosSTOP phosphatase inhibitors (Roche) and whole cell lysate was generated

through sonication in a Biorupter Pico (Diagenode) with the following settings: speed: M, on/off 30 second intervals, total of 10 minutes and sonication repeated twice. Protein lysate was spun down at 17,000g at 4°C for 10 minutes and supernatant was transferred to a new 1.5mL micro-centrifuge tube. Protein quantification was analysed using DC protein assay (Biorad) according to manufacturer's protocol. Protein lysates were added with 2x Laemmli buffer (Biorad) and boiled at 99°C for 5 minutes. 25-50ug of total proteins were loaded to each well and Chameleon Duo pre-stained protein ladder (LI-COR) was loaded at the first and last well of the gel. Gel was run at 120V for 50-60 minutes and proteins were transferred to PVDF membrane using Trans-Blot Turbo transfer system (Biorad). Membrane was blocked with Intercept Blocking Buffer [Tris-buffered saline (TBS); LI-COR] for an hour at room temperature. Primary antibody incubation was performed in TBS-Tween 20 (TBST) at 4°C overnight. Secondary antibody incubation was performed in TBST supplemented with 0.01-0.02% SDS, for an hour in the dark at room temperature. Membrane was washed with TBST (4x5minutes) at room temperature after primary and secondary antibody incubation. Membrane was rinsed in TBST with 0.01% SDS wash buffer and imaging was done on the LI-COR Odyssey CLx imaging system. The primary and secondary antibodies used for WB are listed in Appendix, Table 1.

10. RNAseq analysis

RNAseq analysis for 1008-HFSE2 human primary sebocyte progenitors exposed to DMSO, 1μM B[a]P and 10nM TCDD for 72 hours was provided as a service by NovogeneAIT. A total of 9 samples (3 treatments, 3 bio replicates) were used to perform sequencing with NovaSeq PE150 at 60M reads (18G) of raw data per

sample. Quality assurance of samples, directional mRNA library preparations (poly A enrichment), data quality, differentiation expression gene analysis, quantitative and bioinformatic analysis across databases (Gene Ontology and REACTOME) with gene set enrichment analysis, were performed by NovogeneAIT.

Results

1. Human primary sebocyte progenitors are able to generate lipid-filled human sebaceous gland organoids that resembles structurally to *in vivo* sebaceous glands

To translate the findings of pollutant exposure *in vitro*, the primary sebocyte progenitor cell line used must be validated. Sebaceous gland markers for sebocyte progenitors and differentiated cells have been published[168] and were used as a guideline to identify sebocytes both *in vitro* and *in vivo.* RT-PCR analysis was performed for sebocyte progenitor markers: keratin 7 and 14 (*KRT7/14*), leucine rich repeats and immunoglobin like domain 1 (*LRIG1*) and *MKI67* proliferative marker, and sebocyte differentiation markers: epithelial membrane antigen 1 (*MUC1*), *KRT10*, peroxisome proliferator activated receptor gamma (*PPARγ*), stearoyl-CoA 1 (*SCD1*) and fatty acid synthase (*FASN*). The results showed that sebaceous glands markers were expressed in the 1008-HFSE2 human primary sebocyte progenitor cell line (Figure 1A). Furthermore, markers such as *WNT10A*, laminin subunit gamma-2 (*LAMC2*), transforming growth factor beta-2 (*TGFß2*), ovo-like transcriptional repressor 1 (*OVOL1*), follistatin (*FST*) and semaphorin 4B (*SEMA4B*) that were reported to be involved in pilosebaceous morphogenesis in GWAS studies[17,23], were also expressed (Figure 1A).

Immunofluorescence (IF) analysis of FASN, SCD1, PPARγ, MUC1, KRT10 and 14 was performed in *in vitro* human primary sebocyte progenitor cell line, human sebaceous glands organoids and in abdominal human skin tissue that contained sebaceous glands (Figure 1B-D). Additional *in vitro* analysis of lipid content in sebocyte progenitors using LipidTOX neutral lipid stain and proliferative marker

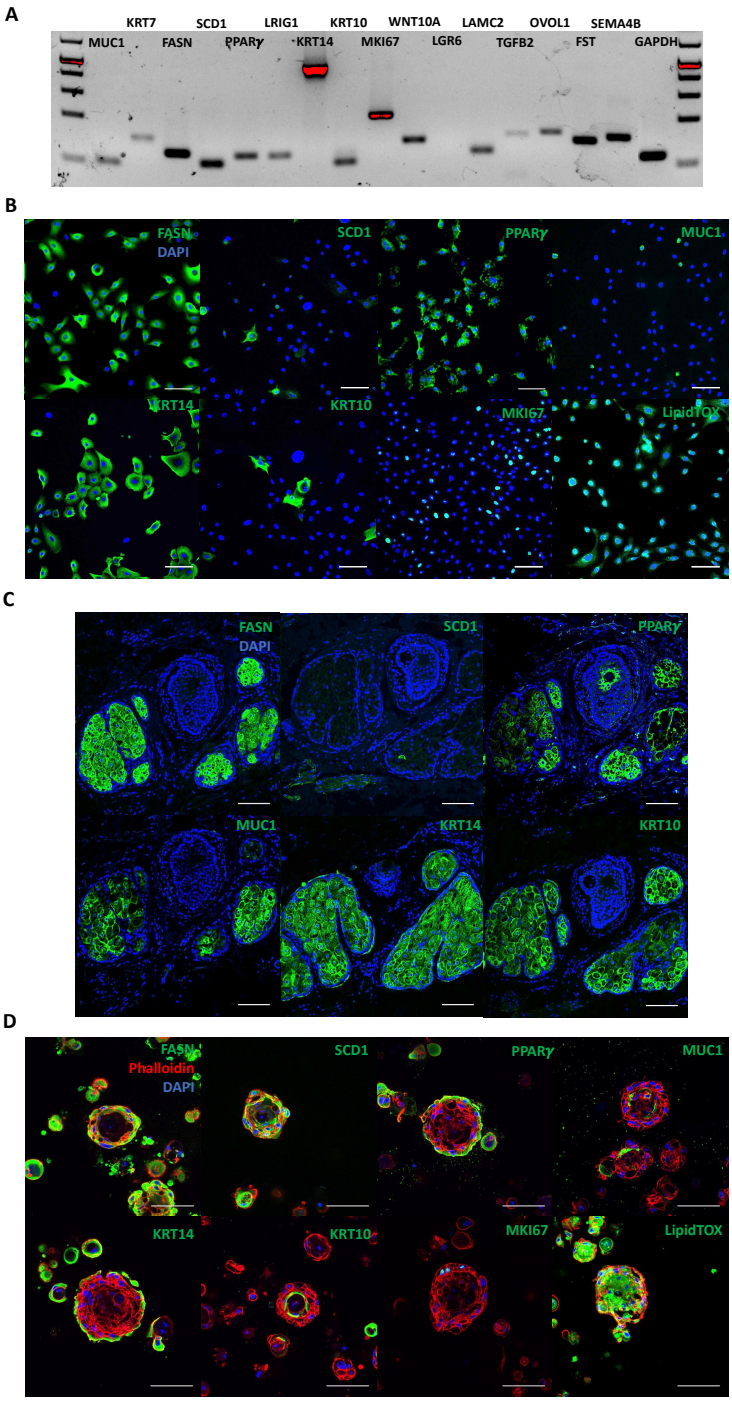

Figure 1: *In vitro* platform derived from 1008-HFSE2 human primary sebocyte progenitors are similar to *in vivo* sebaceous glands . RT-PCR analysis **(A)** of MUC1, KRT7, FASN, SCD1, PPARγ, LRIG1, KRT14, KRT10, MKI67, WNT10A, LGR6, LAMC2, TGFB2, OVOL1, FST, SEMA4B and, GAPDH. *In vitro* immunofluorescence analysis **(B)** for FASN, SCD1, PPARγ, MUC1, KRT10/14, MKI67 and LipidTOX staining of neutral lipids. Immunohistochemistry analysis **(C)** of human abdominal skin tissue for FASN, SCD1, PPARγ, MUC1 and KRT10/14. *In vitro i*mmunofluorescence analysis **(D)** of day 14 human sebaceous gland organoids for FASN, SCD1, PPARγ, MUC1, KRT10/14, MKI67 and LipidTOX staining of neutral lipids. Scale bar: 100um. *MUC1: Epithelial membrane antigen; KRT7/10/14: Keratin 7/10/14 ; FASN: Fatty acid synthase; SCD1: Stearoyl-CoA 1; PPARγ : Peroxisome proliferator activated receptor gamma; LRIG1: Leucine rich repeats and immunoglobin like domain 1; LGR6: Leucine rich repeat containing G protein-coupled receptor 6; LAMC2: Laminin subunit gamma-2; TGFB2: Transforming growth factor beta-2; OVOL1: Ovo like transcriptional repressor 1; FST: Follistatin; SEMA4B: Semaphorin 4B; GAPDH: Glyceraldehyde 3-phosphate dehydrogenase.*

MKI67 was also performed (Figure 1B). 1008-HFSE2 human primary sebocyte progenitors were mostly positive for FASN, PPARγ, KRT14, MKI67 and LipidTOX while few cells were positive for SCD1, MUC1 and KRT10 (Figure 1B). In human skin tissue, SCD1 staining was not detected while FASN, MUC1, KRT10 and PPARγ were positive in the differentiated layer of sebaceous glands while KRT14 was positive throughout the sebaceous glands. In contrast, human sebaceous gland organoids derived from human primary sebocyte progenitor cell line showed positive FASN and SCD1 staining throughout the organoids while PPARγ was positive in the peripheral layer of the organoids (Figure 1D). KRT14 was positive in the peripheral layer while MUC1 and KRT10 were found in the differentiated layer of sebaceous gland organoids (Figure 1D). Furthermore, proliferative marker MKI67 was positive only in the peripheral layer and LipidTOX staining was positive throughout the sebaceous gland organoids (Figure 1D). Although the sebocyte differentiation makers FASN, SCD1 and PPARγ were expressed in organoids compartments that slightly differ to *in vivo* sebaceous glands, the presence of these markers including a proliferative peripheral layer and lipid-filled organizational structure, the structural morphology of the sebaceous gland organoids is comparable to *in vivo* human sebaceous glands. Therefore, 1008-HFSE2 human primary sebocyte progenitor cell line and its derived human sebaceous gland organoid (hSGO) platform can be used to evaluate the effects of pollutants on sebaceous glands and their influence on acne pathogenesis.

2. TCDD and B[a]P are non-cytotoxic pollutants that activate AHR in 1008-HFSE2 human primary sebocyte progenitors

To determine the effects of pollutants B[a]P and TCDD in *in vitro* cell culture systems, their cytotoxicity was evaluated on 1008-HFSE2 human primary sebocyte progenitor cell line and hSGOs (Figure 2 and 3). The highest concentration tested in the cytotoxic evaluation of TCDD and B[a]P in various pollutant studies was 10nM and 2uM, respectively[27,30–32,169]. Therefore, our cytotoxicity evaluation was performed by testing a range of concentrations for TCDD (1/5/10/20/30nM) and B[a]P (10/50/100/200/400nM) over 96 hours (Figure 2) with acute and chronic exposures in hSGOs (Figure 3).

The 2D cytotoxic evaluation measured the mean %LIVE cells over 96 hours at every 24 hours interval (Figure 2). The mean %LIVE cells values after 24 hours of exposure are as follows: CCMY (85.20% ±2.564), DMSO (91.60% ±4.270), 1/5/10/20/30nM TCDD (83.87% ±4.897/87.73% ±14.26/90.48% ±14.10/81.68% ±7.338/85.89% ±3.217), and 10/50/100/200/400nM B[a]P (86.90% ±4.444/74.56% ±10.95/84.05% ±1.998/82.13% ±2.910/79.27% ±4.963). The mean %LIVE cells values after 48 hours of exposure are as follows: CCMY (60.96% ±7.387), DMSO (69.91% ±1.367), 1/5/10/20/30nM TCDD (64.08% ±0.293/56.92% ±4.491/60.04%±6.300/59.97% ±1.119/66.84% ±4.291), and 10/50/100/200/400nM B[a]P (64.28% ±2.468/61.13% ±6.181/68.47%±1.519/60.54% ±6.023/55.83% ±2.570). The mean %LIVE cells after 72 hours of exposure are as follows: CCMY (97.88% ±4.357), DMSO (105.7% ±5.205), 1/5/10/20/30nM TCDD (90.39% ±2.919/82.55% ±3.816/90.48% ±5.801/88.83% ±2.143/81.85% ±6.974), and

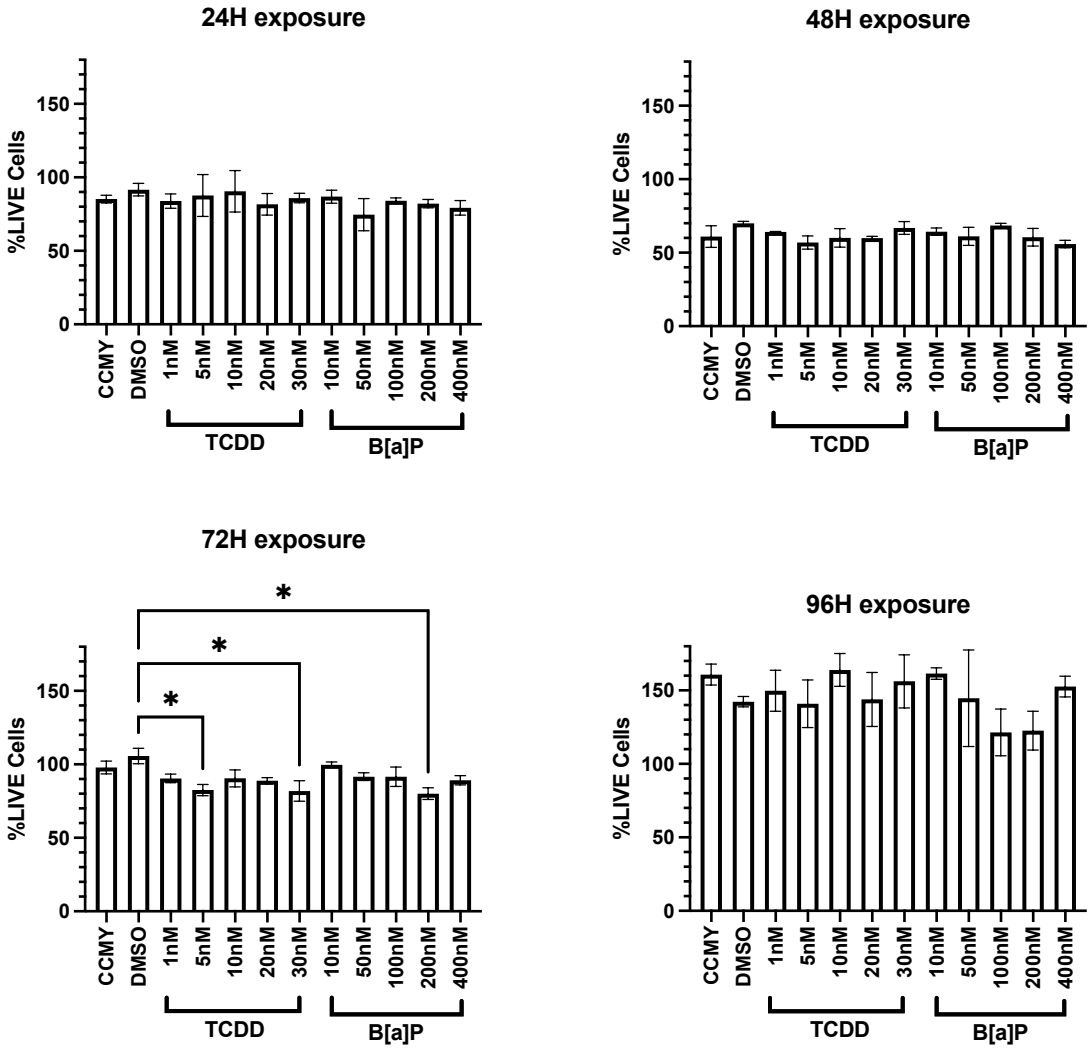

Figure 2. TCDD and B[a]P are not cytotoxic in 2D cell culture. 1008-HFSE2 human primary sebocyte progenitors were exposed to 0.1% DMSO (Control), 10/50/100/200/400nM B[a]P and 1/5/10/20/30nM TCDD for 24/48/72/96H. Untreated control (CCMY) was included in this assay. Calcein AM absorbance readings was normalized to DAPI. One-Way ANOVA statistical analysis using Tukey multiple comparison test was applied to compare the means of TCDD/B[a]P treated samples to DMSO sample (3 technical replicates/sample) . *DMSO: Dimethyl sulfoxide; B[a]P: Benzo[a]pyrene; TCDD: 2,3,7,8-Tetrachlorodibenzodioxin.*

10/50/200/400nM B[a]P (99.68% ±1.919/91.64% ±2.629/91.57% ±6.575/80.06% ±4.009/89.13% ±3.129). The mean %LIVE cells after 96 hours of exposure are as follows: CCMY (160.8%, ±7.074), DMSO (142.3% ±3.463), 1/5/10/20/30nM

TCDD (149.8% ±13.93/140.9% ±16.20/163.9% ±11.11/143.9% ±18.38/156.2% ±18.07), and 10/50/200/400nM B[a]P (161.5% ±3.898/144.6% ±32.88/121.4% ±15.94/122.6% ±13.18/152.6% ±7.099). Overall, the mean %LIVE cells of exposed sebocyte progenitors (Figure 2) were not statistically different (except for 5 and 30nM TCDD, and 200nM B[a]P after 72 hours of exposure) when compared to DMSO and CCMY control across the exposure durations. Despite the slight significance shown in 72 hours of exposure to 5nM TCDD and 200nM B[a]P, their respective higher concentrations (10/20nM TCDD and 400nM B[a]P) during the same exposure period showed otherwise, suggesting that the significance observed may be random.

The hSGOs cytotoxic evaluation also measured the mean %LIVE cells after D1-3/D7-9 acute and D1-8/D7-14 chronic exposures (Figure 3). The mean %LIVE cells after D1-3 acute exposure are as follows: DMSO (77.29% ±2.084), 1/5/10/20/30nM TCDD (83.97% ±2.441/89.17% ±2.786/88.62% ±1.763/89.46% ±1.658/85.14% ±1.795), 10/50/100/200/400nM B[a]P (83.72% ±2.074/85.87% ±2.248/80.22% ±3.565/85.13% ±2.474/84.51% ±2.365), and 4uM puromycin (17.74% ±4.225). The mean %LIVE cells after D7-9 acute exposure are as follows: DMSO (87.45% ±2.290), 1/5/10/20/30nM TCDD (83.67% ±3.183/84.16% ±4.106/82.35% ±3.817/88.11% ±2.914/84.21% ±3.044), 10/50/100/200/400nM B[a]P (89.58% ±3.601/85.85% ±3.219/91.20% ±1.907/88.79% ±2.764/83.01% ±3.095), and 4uM puromycin (40.36% ±5.402). The mean %LIVE cells after D1-8 chronic exposure are as follows: DMSO (90.06% ±3.003), 1/5/10/20/30nM TCDD (94.37% ±2.017/77.78% ±1.428/85.44%

±2.734/89.48% ±3.741/95.75% ±1.845), 10/50/200/400nM B[a]P (97.50% ±2.500/96.98% ±1.417/76.24% ±4.258/96.52% ±1.196/81.50% ±2.612), and

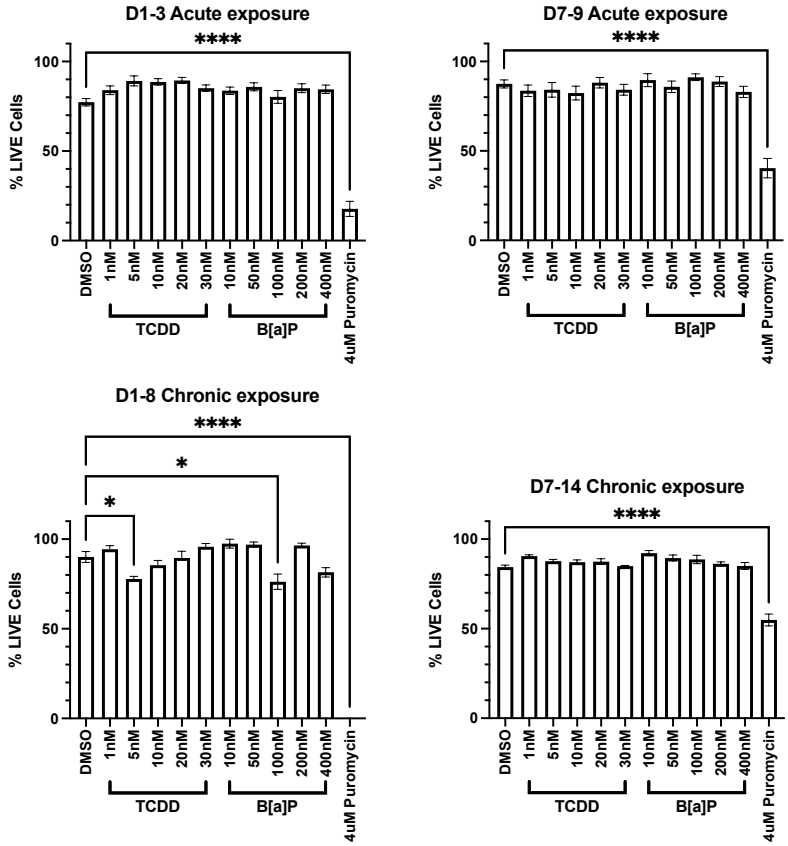

Figure 3. TCDD and B[a]P are not cytotoxic in 3D organoid culture. 1008-HFSE2 sebocyte progenitors and human sebaceous gland organoids (hSGOs) was exposed to 0.1% DMSO (Control), 10/50/100/200/400nM B[a]P and 1/5/10/20/30nM TCDD during D1-3 and D7-9 (acute exposure), D1-8 and D7-14 (chronic exposure) during organoid growth. 4uM puromycin was used as a cytotoxic control. One-Way ANOVA statistical analysis using Tukey multiple comparison test was applied to compare the means of TCDD/B[a]P treated samples to DMSO treated sample (3 technical replicates/sample) (****: P<0.0001 Statistical significance represents how different the treated groups are compared to puromycin sample. *DMSO: Dimethyl sulfoxide; B[a]P: Benzo[a]pyrene; TCDD: 2,3,7,8-Tetrachlorodibenzodioxin..*

4uM puromycin (0.00% ±0.000). The mean %LIVE cells after D7-14 chronic exposure are as follows: DMSO (84.41% ±1.082), 1/5/10/20/30nM TCDD (90.48% ±0.7892/87.68% ±1.042/87.15% ±1.230/87.44% ±1.604/84.92% ±0.392), 10/50/200/400nM B[a]P (92.18% ±1.494/89.46% ±1.691/88.65% ±2.364/86.19% ±1.137/85.00% ±1.946), and 4uM puromycin (54.84% ±3.317). Overall, the mean %LIVE cells of exposed hSGOs (Figure 3) were not statistically different

(except for 5nM TCDD, and 100nM B[a]P after D1-8 chronic exposure) when compared to DMSO and was significantly different when compared to 4uM puromycin control across the different exposure durations. Despite the slight significance shown in D1-8 chronic exposure to 5nM TCDD and 100nM B[a]P, their respective higher concentrations (10/20/30nM TCDD and 200/400nM B[a]P) during the same exposure period showed otherwise, suggesting that the significance observed may be random or due to chance. The results suggests that the tested range of concentrations of TCDD and B[a]P was not cytotoxic to sebocyte progenitors and hSGOs.

TCDD and B[a]P are known AHR agonists[170]. The evaluation of AHR pathway activation by TCDD and B[a]P was analyzed through transcriptomic analysis of downstream targets, AHRR and CYP1A1 (Figure 4A and B, Figure 5). The same range of concentrations of TCDD and B[a]P and exposure durations (Figure 2) was used. AHRR and CYP1A1 expression was upregulated across all tested TCDD concentrations (1/5/10/20/30nM) as early as 24 hours and persisted over 96 hours of exposure (Figure 4A). The upregulation of AHRR was observed in 100/200/400nM B[a]P and peaked at 48 hours whereas CYP1A1 expression was

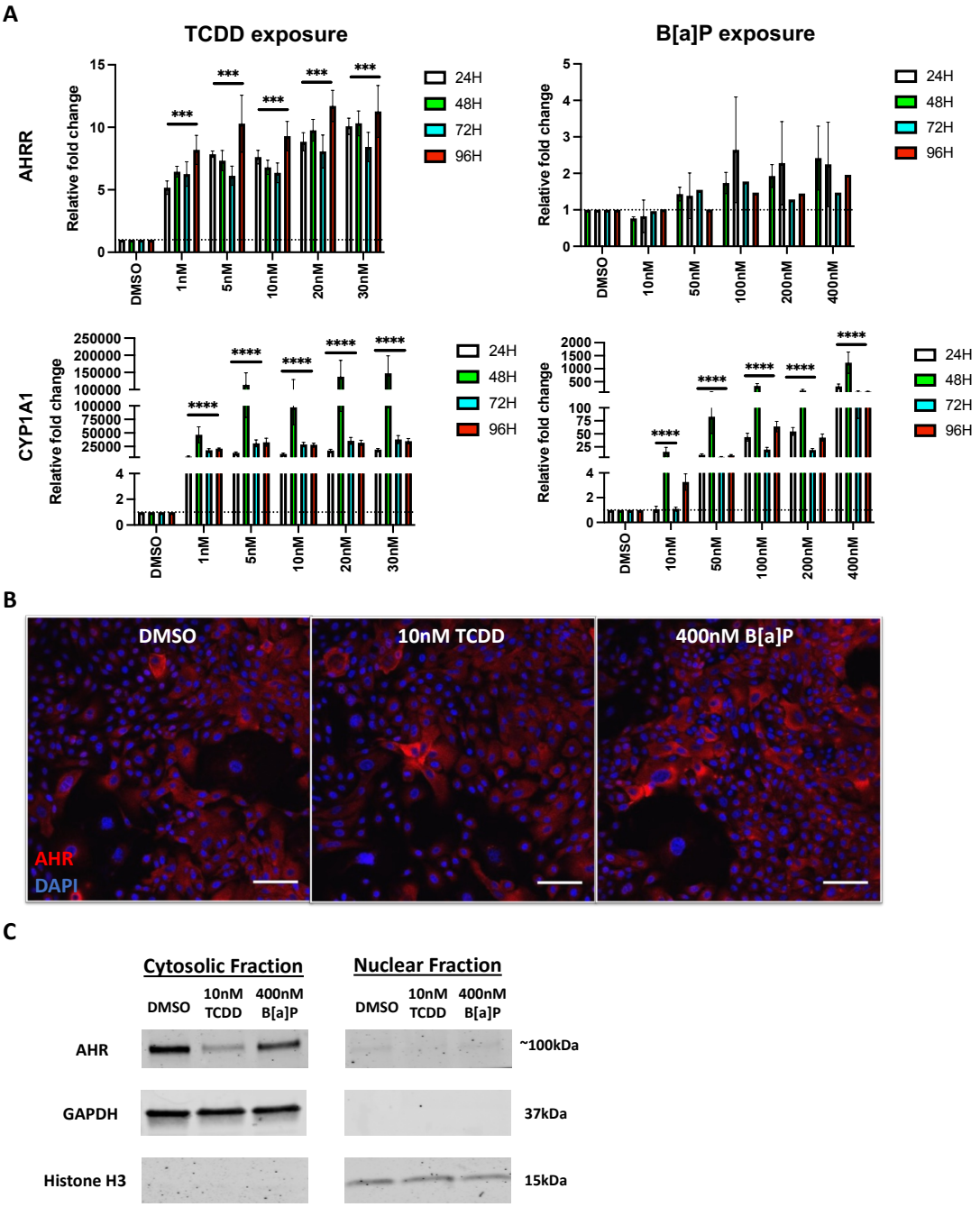

Figure 4. Gene expression analysis showed AhR signaling activation through upregulation of *AHRR* and *CYP1A1* upon exposure to TCDD and B[a]P (A). 1008-HFSE2 human primary sebocyte progenitors were exposed to 0.1% DMSO (Control), 1/5/10/20/30nM TCDD and 10/50/100/200/400nM B[a]P for 24/48/72/96 hours. Relative fold change of gene expression was normalized to endogenous *GAPDH* expression and calculated based on $2^{-\Delta\Delta CT}$. Two-Way ANOVA statistical analysis using Tukey multiple comparison test was applied to compare the mean relative fold change across treated groups (3 technical replicates/group) [*: <0.05, **:<0.01, ***:<0.001, ****:<0.0001]. Immunofluorescence staining images **(B)** of AHR protein (Red) in the cytosol and western blot analysis **(C)** of AHR protein (~100kDa) after sebocyte progenitors were exposed to 0.1% DMSO (Control), 10nM TCDD and 400nM B[a]P for 72 hours. Scale bar: 100um. *AHR: Aryl hydrocarbon receptor; AHRR: Aryl hydrocarbon receptor repressor; CYP1A1: Cytochrome P450, family 1, subfamily A, polypeptide 1; DMSO: Dimethyl sulfoxide; B[a]P: Benzo[a]pyrene; TCDD: 2,3,7,8-Tetrachlorodibenzodioxin.*

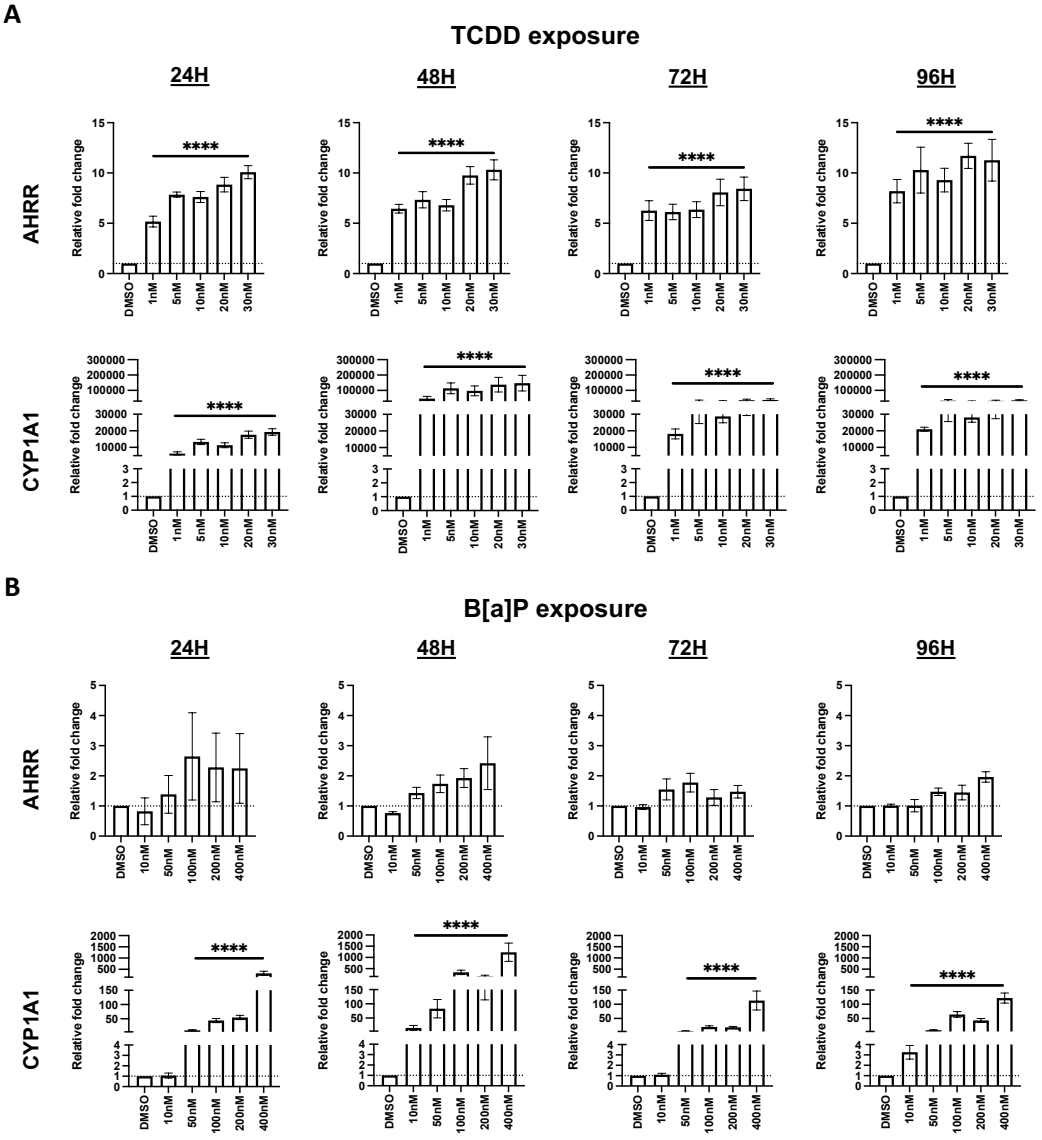

Figure 5. Activation of AhR signaling pathway through upregulation of *AHRR* and *CYP1A1* upon exposure to TCDD (A) and B[a]P (B). Individual time-point analysis of *AHRR* and *CYP1A1* after primary sebocyte progenitors were exposed to 0.1% DMSO (Control), 10/50/100/200/400nM B[a]P and 1/5/10/20/30nM TCDD. Relative fold change of *AHRR* and *CYP1A1* expression was normalized to endogenous GAPDH expression and calculated based on $2^{-\Delta\Delta CT}$. One-Way ANOVA using Tukey statistical analysis was applied to compare the relative fold change across treated samples (3 technical replicates/sample) [*: <0.05, **:<0.01, ***:<0.001, ****:<0.0001]. Statistical significance represents how different the treated samples are compared to DMSO sample. *AhR: Aryl hydrocarbon; AhRR: Aryl hydrocarbon receptor repressor; CYP1A1: Cytochrome P450, family 1, subfamily A, polypeptide 1; DMSO: Dimethyl sulfoxide; B[a]P: Benzo[a]pyrene; TCDD: 2,3,7,8-Tetrachlorodibenzodioxin.*

upregulated in 50/100/200/400nM B[a]P as early as 24 hours and persisted over 96 hours of exposure (Figure 4A). However, neither a dose- nor time-dependent responses were observed for both TCDD and B[a]P in AHRR and CYP1A1 expression (Figure 5B).

Additional analysis was performed to identify the activation of AHR signaling through the translocation of AHR protein from the cytosol into the nucleus[144] upon binding to TCDD and B[a]P (Figure 4C and D). IF analysis after 72 hours of exposure to 10nM TCDD and 400nM B[a]P showed absence of AHR staining in the nucleus and positive AHR staining in the cytoplasm (Figure 4C). WB analysis of AHR protein in the cytosolic and nuclear fractions after 72 hours of exposure to 10nM TCDD and 400nM B[a]P demonstrated absence of AHR protein in the nuclear fraction while there was a decreased in AHR protein in the cytosolic fraction (Figure 4D). To corroborate the absence of AHR protein in the nucleus, short time-point exposure of 10nM TCDD and 400nM B[a]P was performed (Supplementary Figure 2). AHRR and CYP1A1 expression was upregulated in both 10nM TCDD and 400nM B[a]P across 1/2/4/6 hours of exposure (Supplementary Figure 2B) indicative of activation of AHR signaling. Interestingly, a time-dependent decrease of AHR protein in the cytosolic fraction was observed while AHR protein was not detected in the nuclear fraction even though Histone H3 was observed in the nuclear fraction only (Supplementary Figure 2A). The nuclear absence and cytosolic reduction of AHR protein upon pollutant exposure could be due to the nature of AHR signaling pathway. It has been reported that the nucleocytoplasmic shuttling (export) of AHR protein is required to induce expressional changes after activation, of which follows the rapid degradation of the receptor protein upon export[171,172]. This would explain the absence of nuclear AHR together with a decrease in cytosolic AHR. Therefore, we

conclude that the upregulation of AHR signaling target genes, AHRR and CYP1A1, along with the reduction of AHR protein observed in the cytosol suggests that these two pollutants activate the AHR signaling pathway.

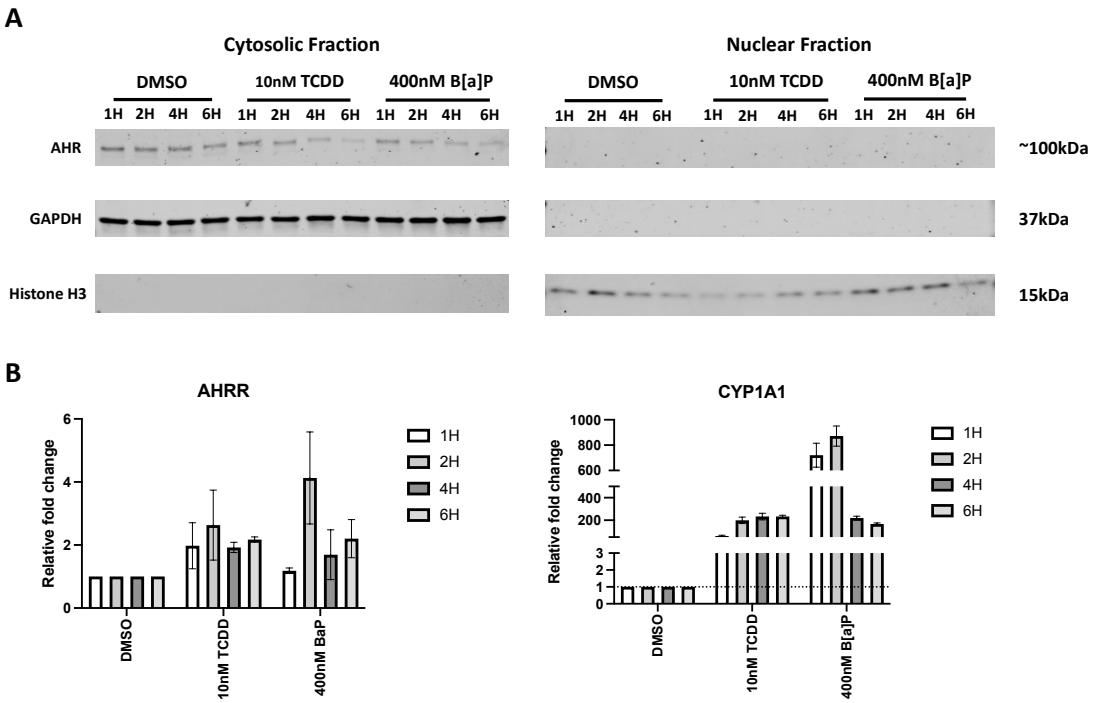

Figure 6. Loss of cytosolic AHR protein coincide with AhR signaling pathway activation in a time-dependent manner. Western blot analysis of cytosolic and nuclear AHR protein after 1/2/4/6 hours exposure of a single-dose of 10nM TCDD and 400nM B[a]P **(A)**. GAPDH and Histone H3 were used as loading controls for cytosolic and nuclear fraction, respectively. qPCR analysis of AhR signaling target genes *AHRR* and *CYP1A1* after 1/2/4/6 hours exposure of a single-dose of 10nM TCDD and 400nM B[a]P **(B).** Relative fold change of gene expression was normalized to endogenous *GAPDH* and calculated based on $2^{-\Delta\Delta CT}$. One-Way ANOVA using Tukey statistical analysis was applied to compare the relative fold change across treated samples (3 technical replicates/group). *AHR: Aryl hydrocarbon receptor; AHRR: Aryl hydrocarbon receptor repressor; CYP1A1: Cytochrome P450, family 1, subfamily A, polypeptide 1; DMSO: Dimethyl sulfoxide; B[a]P: Benzo[a]pyrene; TCDD: 2,3,7,8-Tetrachlorodibenzodioxin.*

3. TCDD and B[a]P perturb development and maintenance of 1008-HFSE2 derived hSGOs

Since both pollutants were evaluated to be non-cytotoxic and were shown to activate the AHR signaling pathway, the effects of AHR signaling pathway activation on the proliferation and differentiation of sebocyte progenitors could be evaluated (Figure 7, 8 and 9). Sebocyte progenitors were exposed to concentrations

of 1/5/10/20/30nM TCDD and 10/50/100/200/400nM B[a]P over 24/48/72/96 hours, and sebocyte differentiation-related markers such as *FASN, SCD1, PPARγ, LRIG1,* in addition to the proliferative marker *c-MYC* were screened for any expressional changes.

Exposure to TCDD resulted in *FASN* and *SCD1* expression peaked at 48 hours of exposure and were normalized afterwards across all concentrations (Figure 7). However, this upregulation was not statistically significant (Supplementary Figure 3A). Although *FASN* and *SCD1* expression was upregulated after 48 hours of exposure in 100nM and 400nM B[a]P (Figure 7), it was not statistically significant (Figure 8B). Moreover, there is no distinct pattern of influence by B[a]P on *FASN* and *SCD1* expression. TCDD exposure resulted in upregulation of *PPARγ* expression only within the first 48 hours of exposure in all concentrations except 1nM (Figure 7), but these changes were not significant (Supplementary Figure 8A). Although *PPARγ* expression was upregulated after 72-96 hours of exposure in across all B[a]P concentrations except 10nM (Figure 7B), it was not statistically significant (Supplementary Figure 8B). There was also no discernable dose or time-dependent influence by TCDD and B[a]P in the transcriptomic analysis. Additional IF analysis on FASN, SCD1 and PPARγ showed no observable changes after 72 hours of exposure to 10nM TCDD and 400nM B[a]P (Figure 9). *LRIG1* expression was significantly upregulated after 48-96 hours of exposure to all TCDD concentrations (Figure 7 and 8A). Although there was a slight increase in *LRIG1* expression across all tested B[a]P concentrations after 48 hours of exposure (Figure 7), these changes were not significant (Figure 8B). Lastly, no significant changes to *c-MYC* expression were observed in all TCDD and B[a]P

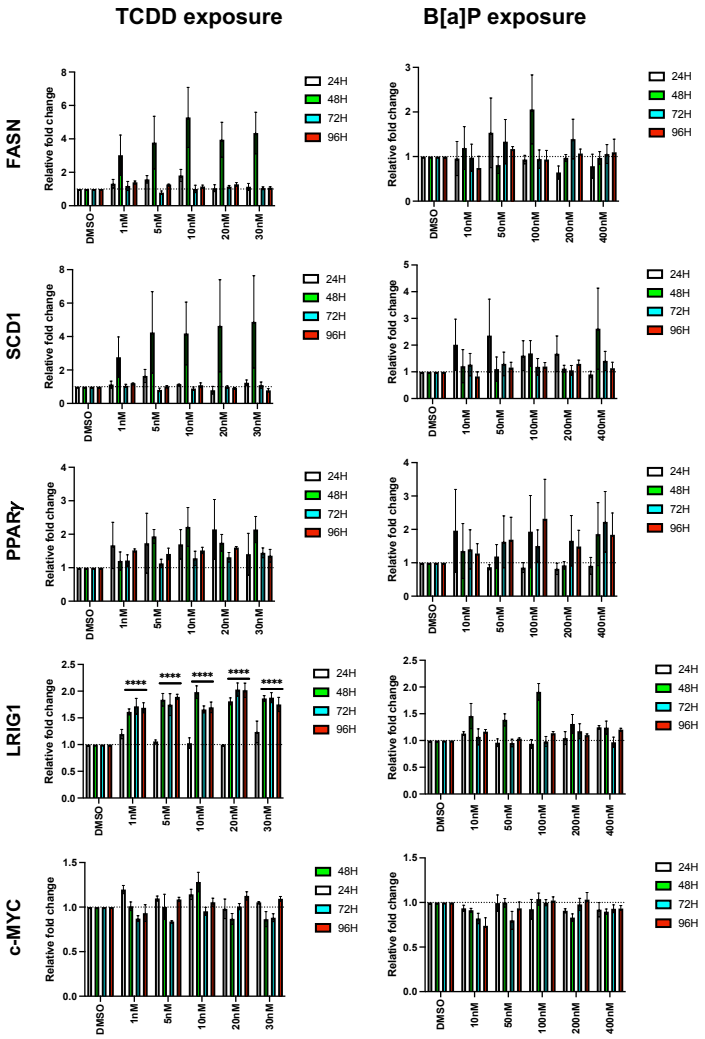

Figure 7. Gene expression analysis showed no changes to the proliferation and differentiation capacity of sebocyte progenitors after exposure to TCDD and B[a]P. 1008-HFSE2 human primary sebocytes were exposed to 0.1% DMSO (Control), 10/50/100/200/ 400nM B[a]P and 1/5/10/20/30nM TCDD for 24/48/72/96H. qPCR analysis on gene expression of sebaceous gland markers *FASN, SCD1 PPARγ, LRIG1* and proliferative marker, *c-MYC* upon exposure to TCDD and B[a]P. Relative fold change of gene expression was normalized to endogenous *GAPDH* expression and calculated based on $2^{-\Delta\Delta CT}$. Two-Way ANOVA statistical analysis using Tukey multiple comparison test was applied to compare the mean relative fold change across treated groups (3 technical replicates/group) [*: <0.05, **:<0.01, ***:<0.001, ****:<0.0001]. *FASN: Fatty acid synthase; SCD1: Stearoyl-CoA 1; PPARγ: Peroxisome proliferator activated receptor gamma; LRIG1: Leucine rich repeats and immunoglobin like domain 1; GAPDH: Glyceraldehyde 3-phosphate dehydrogenase; DMSO: Dimethyl sulfoxide; B[a]P: Benzo[a]pyrene; TCDD: 2,3,7,8-Tetrachlorodibenzodioxin.*

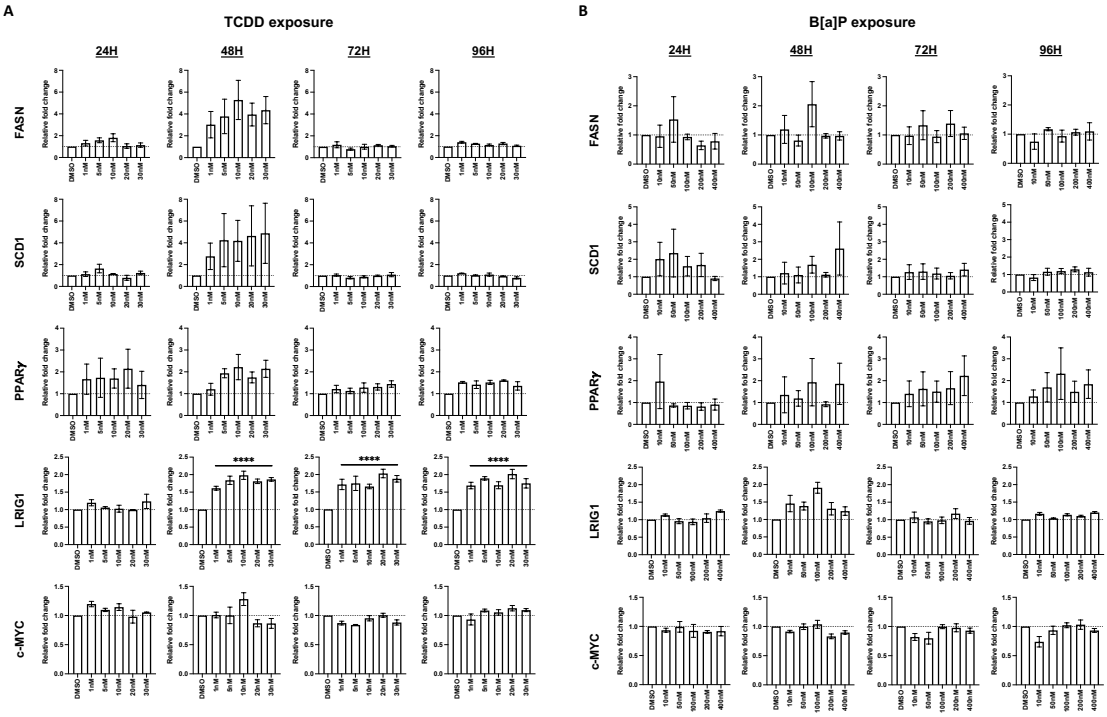

Figure 8. Proliferation and differentiation capacity of sebocyte progenitors were not affected after exposure to TCDD and B[a]P. 1008-HFSE2 human primary sebocytes were exposed to 0.1% DMSO (Control), 10/50/100/200/400nM B[a]P and 1/5/10/20/30nM TCDD for 24/48/72/96H. qPCR analysis of sebaceous gland markers *FASN, SCD1, PPARγ, LRIG1* and proliferative marker, *c-MYC* upon exposure to TCDD **(A)** and B[a]P **(B).** Relative fold change of gene expression was normalized to endogenous *GAPDH* and calculated based on $2^{-\Delta\Delta CT}$. One-Way ANOVA statistical analysis using Tukey multiple comparison test was applied to compare the mean relative fold change across 3 samples (3 technical replicates/group) [*: <0.05, **:<0.01, ***:<0.001, ****:<0.0001]. Statistical significance represents how different the treated samples are compared to DMSO sample. *FASN: Fatty acid synthase; SCD1: Stearoyl-CoA 1; PPARγ: Peroxisome proliferator activated receptor gamma; LRIG1: Leucine rich repeats and immunglobin like domain 1; GAPDH: Glyceraldehyde 3-phosphate dehydrogenase; DMSO: Dimethyl sulfoxide; B[a]P: Benzo[a]pyrene; TCDD: 2,3,7,8-Tetrachlorodibenzodioxin.*

concentrations across all exposure durations (Figure 7 and 8), suggesting no influence on the proliferation of sebocyte progenitors. Although there were some transcriptomic changes in sebocyte differentiation markers, those remain non-significant due to the lack of any discernable pattern of influence after exposure to B[a]P. TCDD exposure seem to influence sebocyte differentiation markers *FASN*, *SCD1* and *PPARγ* even though it is statistically non-significant. It has been reported that TCDD can alter *in vitro* sebocyte differentiation[32] and although insignificant, the transcriptomic changes observed in TCDD exposure might be consistent with this reported influence on sebocyte differentiation.

To further evaluate the role AHR signaling pathway and effects of pollutant exposure on sebocyte progenitors, hSGOs were exposed to acute (D1-3/7-9) and chronic (D1-8/7-14) treatments of 10nM TCDD and 400nM B[a]P, respectively

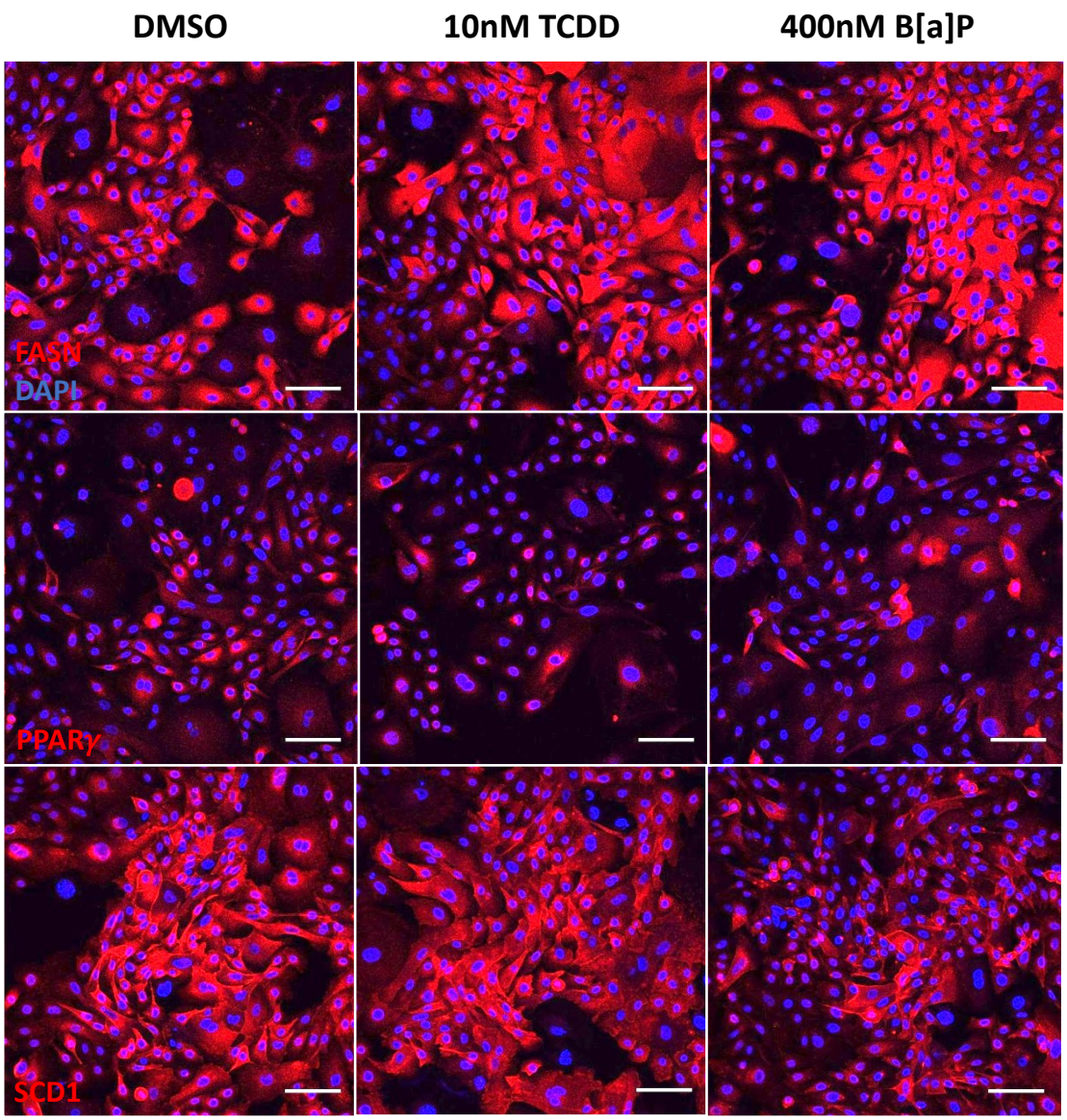

Figure 9. Immunofluorescence analysis showed no effect on sebocyte differentiation after exposure to TCDD and B[a]P. 1008-HFSE2 human primary sebocyte progenitors were exposed to 0.1% DMSO (Control), 10nM TCDD and 400nM B[a]P for 72 hours. IF staining of sebaceous glands differentiation markers FASN, SCD1, PPARγ (all in Red). Scale bar: 100um. *FASN: Fatty acid synthase; SCD1: Stearoyl-CoA 1; PPARγ: Peroxisome proliferator activated receptor gamma; DMSO: Dimethyl sulfoxide; B[a]P: Benzo[a]pyrene; TCDD: 2,3,7,8-Tetrachlorodibenzodioxin.*

during their developmental growth (day 0-7) and maintenance (homeostasis) phases (day 7-14) (Figure 10). Both acute and chronic exposure of 10nM TCDD and 400nM B[a]P during the developmental growth phase of hSGOs resulted in significant decreases in both the size and number of hSGOs (Figure 10A and C).

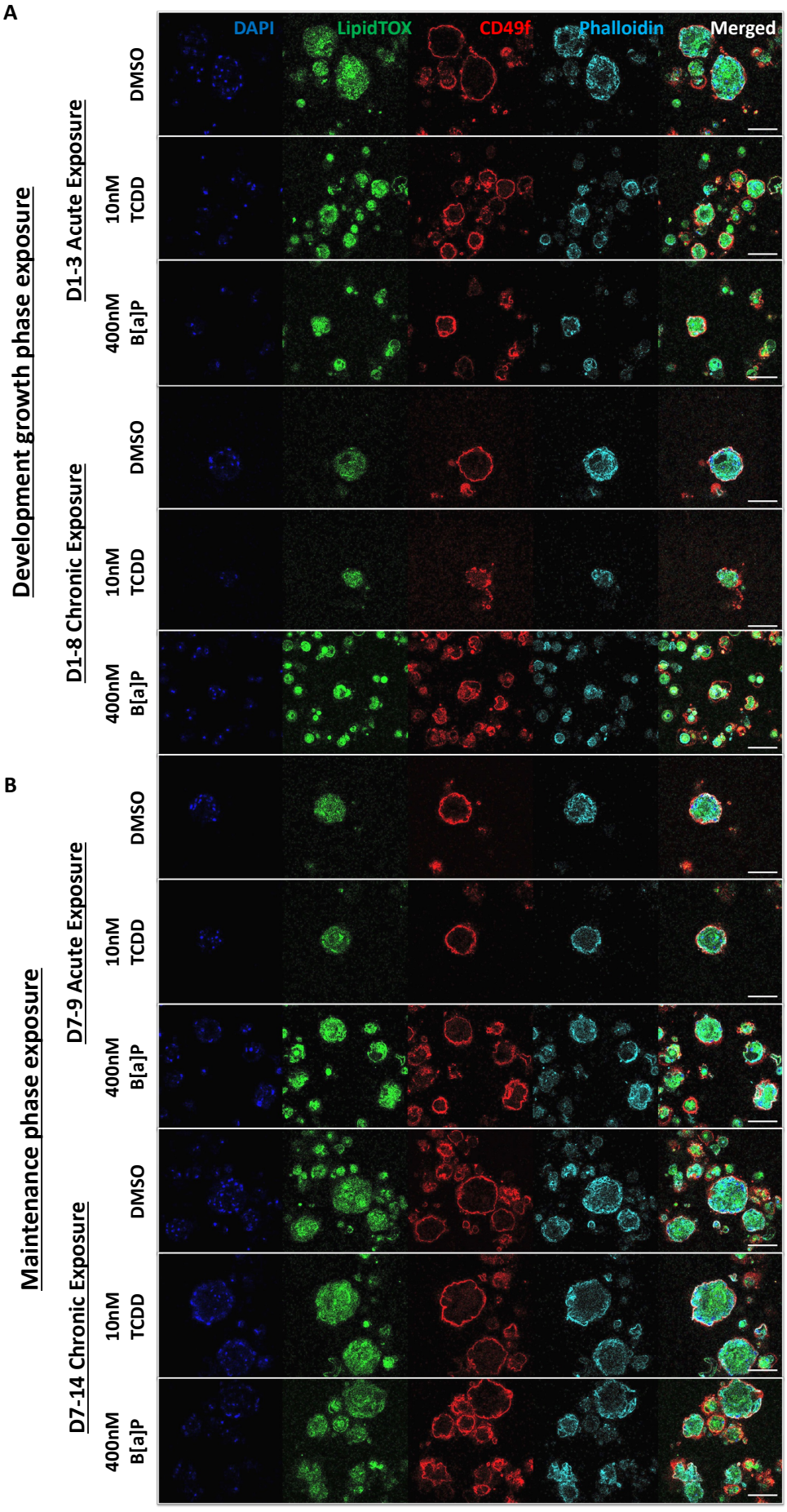
A
Development growth phase exposure
D1-8 Chronic Exposure
D1-3 Acute Exposure
400nM B[a]P
10nM TCDD
DMSO
400nM B[a]P
10nM TCDD
DMSO
DAPI
LipidTOX
CD49f
Phalloidin
Merged
B
Maintenance phase exposure
D7-14 Chronic Exposure
D7-9 Acute Exposure
400nM B[a]P
10nM TCDD
DMSO
400nM B[a]P
10nM TCDD
DMSO

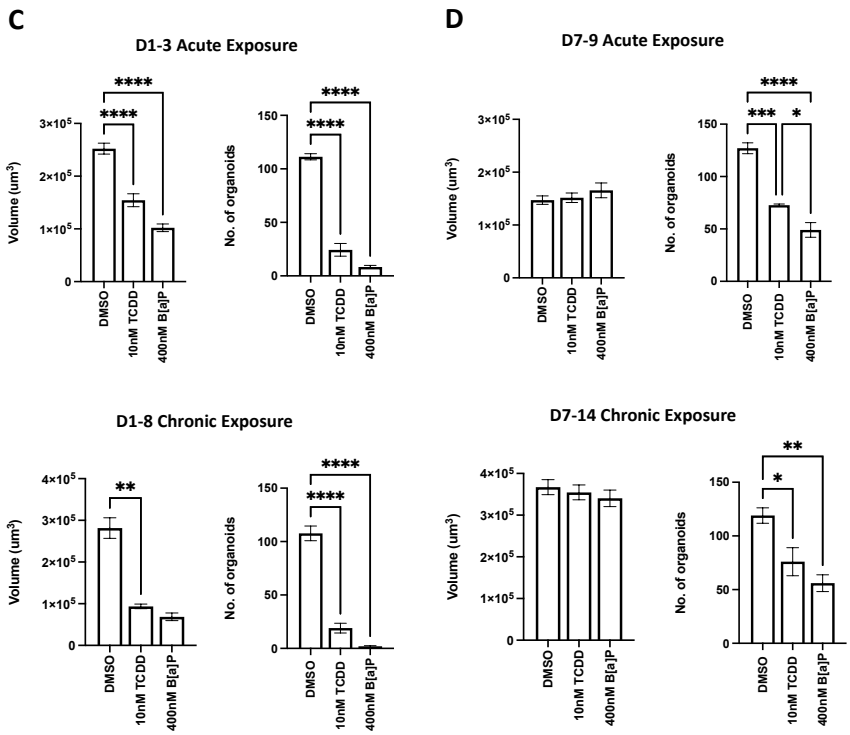

Figure 10. Quantitative image analysis showed perturbation to the development and maintenance of 1008-HFSE2-derived human sebaceous gland organoids upon exposure to TCDD and B[a]P. Human sebaceous gland organoids were acutely (D1-3/7-9) or chronically (D1-8/7-14) exposed to 0.1% DMSO (Control), 10nM TCDD and 400nM B[a]P during developmental growth phase **(A)** and maintenance phase **(B)**. Immunofluorescence z-stack images **(A and B)** were taken at day 14 of organoid growth for all exposures, and the size (volume) and number of organoids were quantified **(C and D)**. One-Way ANOVA statistical analysis using Tukey multiple comparison test was applied to compare the means across treated groups (3 biological replicates/group) [*: <0.05, **:<0.01, ***:<0.001, ****:<0.0001]. Scale bar: 100um. *DMSO: Dimethyl sulfoxide; B[a]P: Benzo[a]pyrene; TCDD: 2,3,7,8-Tetrachlorodibenzodioxin.*

Interestingly, acute, and chronic exposure to10nM TCDD and 400nM B[a]P during the maintenance phase resulted in a significant reduction of the number of hSGOs, but their size remained comparable to the DMSO control (Figure 10B and D). This suggests that TCDD and B[a]P may affect sebocyte progenitors' ability to develop into an organoid during the developmental phase, whilst they perturb maintenance of hSGOs, even though 2D transcriptomic analysis revealed non-significant influence on proliferation (*c-MYC*), differentiation (*PPARγ*) and lipogenesis (*FASN* and *SCD1*) markers (Figure 7).

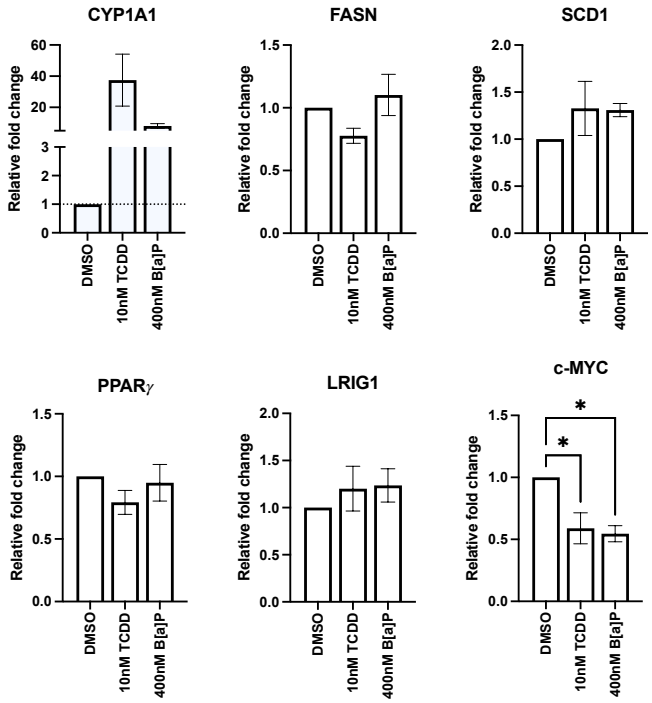

Figure 11. Gene expression analysis of acute exposed organoids showed downregulation in proliferation with no influence on sebocyte differentiation. 1008-HFSE2-derived human sebaceous gland organoids were acutely (D7-9) exposed to 0.1% DMSO (Control), 10nM TCDD and 400nM of B[a]P**.** qPCR analysis on gene expression of sebaceous gland markers (*FASN, SCD1 PPARγ, LRIG1*) and proliferative marker (*c-MYC*). Relative fold change of gene expression was normalized to endogenous *GAPDH* expression and calculated based on $2^{-\Delta\Delta CT}$. One-Way ANOVA statistical analysis using Tukey multiple comparison test was applied to compare the mean relative fold change across treated samples (3 technical replicates/sample) [*: <0.05]. *FASN: Fatty acid synthase; SCD1: Stearoyl-CoA 1; PPARγ : Peroxisome proliferator activated receptor gamma; LRIG1: Leucine rich repeats and immunoglobin like domain 1; GAPDH: Glyceraldehyde 3-phosphate dehydrogenase, DMSO: Dimethyl sulfoxide; B[a]P: Benzo[a]pyrene; TCDD: 2,3,7,8-Tetrachlorodibenzodioxin.*

To understand the phenotype observed in the maintenance of hSGOs (Figure 6D), transcriptomic analysis of *CYP1A1*, *FASN*, *SCD1*, *PPARγ*, *LRIG1* and *c-MYC* was performed on D7-9 acute exposed samples (Figure 11). *CYP1A1* expression was upregulated in both TCDD and B[a]P exposed organoids and a significant decreased in *c-MYC* expression (Figure 11) which was not observed in 2D transcriptomic analysis (Figure 7). *FASN, SCD1* and *PPARγ* showed no significant difference in their expression levels (Figure 11). This finding suggests that TCDD and B[a]P exposure may modulate the proliferation but not differentiation of

sebocyte progenitors. The decrease in proliferative sebocyte progenitors alone is not sufficient to explain the loss of maintenance of hSGOs as sebocytes progenitors are still capable of differentiating into mature sebocytes contributing to the growth and maintenance of organoids. Thus, the size of organoid is unchanged. Therefore, aside from the decreased proliferative capacity of sebocyte progenitors, the involvement of another molecular pathway may have driven the loss of organoids.

4. Inhibition of TCDD/B[a]P-induced AHR activation does not rescue the perturbation of the development and maintenance of hSGOs

As AHR activation was observed from acute D7-9 exposed organoids, it highlights the possibility that both TCDD's and B[a]P's influence on hSGOs development and maintenance could be modulated through AHR activation. To evaluate if AHR signaling pathway activation by TCDD and B[a]P causes the phenotype observed, AHR antagonists, CH223191 and BAY-218 (competitive inhibitors) were co-exposed with DMSO, 10nM TCDD and 400nM B[a]P. The inclusion of 1μM B[a]P serves as a control to AHR inhibition efficacy, as the EC_{50} of B[a]P to AHR is 617nM[173] and we expect that AHR antagonists at their IC_{50} should effectively compete against 400nM B[a]P for AHR.

The initial effect of 30nM CH223191 and 40nM BAY-218 was able to effectively downregulate *CYP1A1* expression compared to 400nM/1μM B[a]P control but was not observed for TCDD (Figure 12B). It is worth noting that CH223191 appeared to be more effective than BAY-218 in AHR inhibition when comparing *CYP1A1* expression after co-exposure with 400nM and 1μM B[a]P, respectively (Figure

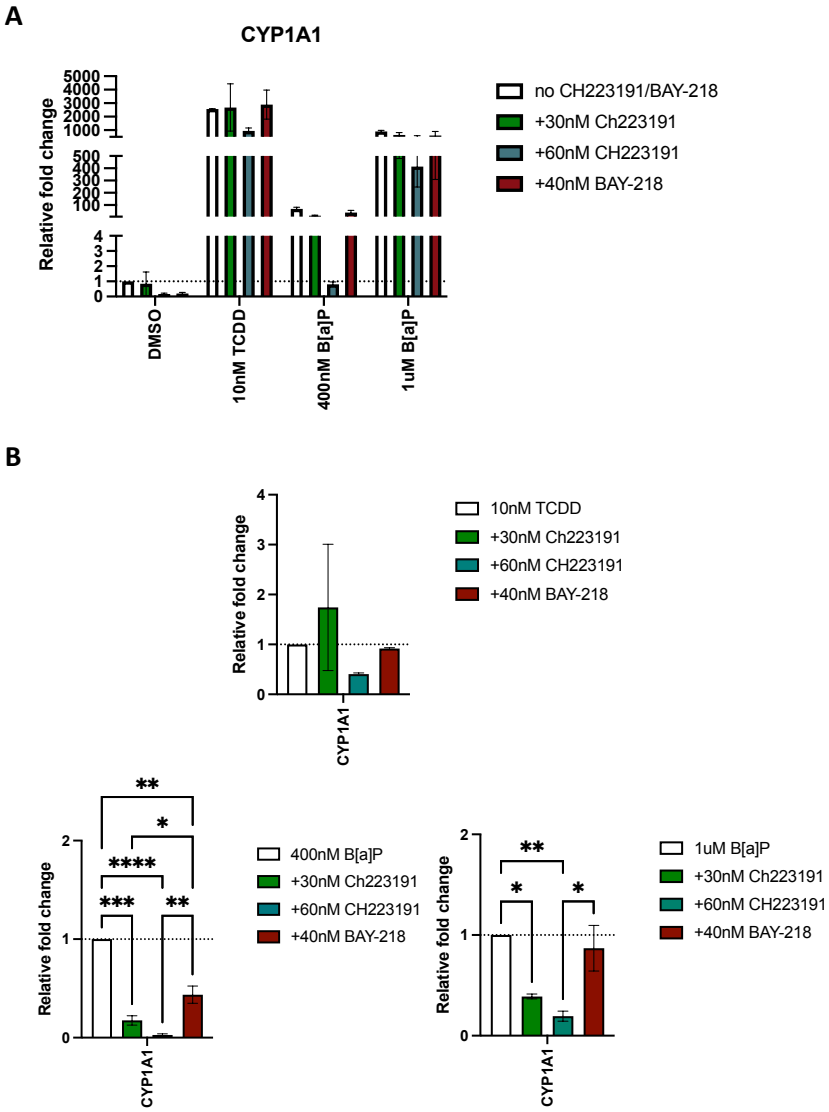

Figure 12. Gene expression analysis showed 60nM CH223191 can inhibit AhR signaling activation by repressing *CYP1A1* expression after co-exposure with TCDD and B[a]P. 1008-HFSE2 human primary sebocytes were exposed to 0.1% DMSO (Control), 400nM/1uM B[a]P and 10nM TCDD, with each exposure supplemented with 30/60nM CH223191 or 40nM BAY-218 for 72 hours. *CYP1A1* expression of all exposed samples were compared to 0.1% DMSO (Control) **(A)**, and the efficacy of each AhR antagonist to repress *CYP1A1* expression when co-exposed to 400nM/1uM B[a]P/10nM TCDD was analyzed **(B)**. Relative fold change of gene expression was normalized to endogenous *GAPDH* expression and calculated based on $2^{-\Delta\Delta CT}$. One-Way ANOVA statistical analysis using Tukey multiple comparison test was applied to compare the mean relative fold change across 4 sampels (3 technical replicates/group) [*: <0.05, **:<0.01, ***:<0.001, ****:<0.0001]. *CYP1A1: Cytochrome P450, family 1, subfamily A, polypeptide 1; DMSO: Dimethyl sulfoxide; B[a]P: Benzo[a]pyrene; TCDD: 2,3,7,8-Tetrachlorodibenzodioxin.*

12B). Although both AHR antagonist suppressed *CYP1A1* expression, the levels in B[a]P exposed samples were still significantly higher compared to DMSO control (Figure 12A). As CH223191 is more effective than BAY-218, the concentration of

CH223191 was doubled to 60nM, and *CYP1A1* expression was further downregulated in B[a]P exposed samples when compared to 30nM CH223191 (Figure 12B). Furthermore, *CYP1A1* expression was observed to be downregulated in 10nM TCDD exposed samples when treated with 60nM CH223191 (Figure 12B). Most importantly, *CYP1A1* expression levels in 400nM B[a]P exposed samples treated with 60nM CH223191 were significantly downregulated to levels similar to DMSO control (Figure 12A). These results suggest that 60nM CH223191 can suppress AHR activation induced by 400nM B[a]P, allowing us to elucidate if AHR activation is involved in the organoid phenotype observed.

The next step would to be perform AHR inhibition in hSGOs exposed to B[a]P and TCDD, to evaluate if a rescue of the loss of organoids could be achieved (Figure 10). hSGOs were chronically (D1-8/D7-14) co-exposed to 10nM TCDD, 400nM B[a]P or 1μM B[a]P supplemented with 30nM/60nM CH223191 (Figure 13 and 14). As per previous observations (Figure 10), B[a]P chronic exposure during the developmental phase saw a decrease in both the size and number of hSGOs (Figure 13B and 14B), whereas a loss of organoids only was observed in the maintenance phase (Figure 13C and 14C). TCDD chronic exposure only caused the loss of organoids in both developmental and maintenance phase (Figure 13 and 14). The addition of 30/60nM CH223191 to 400nM B[a]P exposed organoids still resulted in the decreased in the size and number of hSGOs (Figure 13B-C and 14B-C). As 30nM and 60nM CH223191 was unable to completely supress AHR activation in TCDD and 1μM B[a]P exposed organoids, it is expected that no changes would be observed. Interestingly, a non-significant decreased in the size of organoids was observed in both chronic D1-8 and D7-14 samples co-exposed to 10nM TCDD

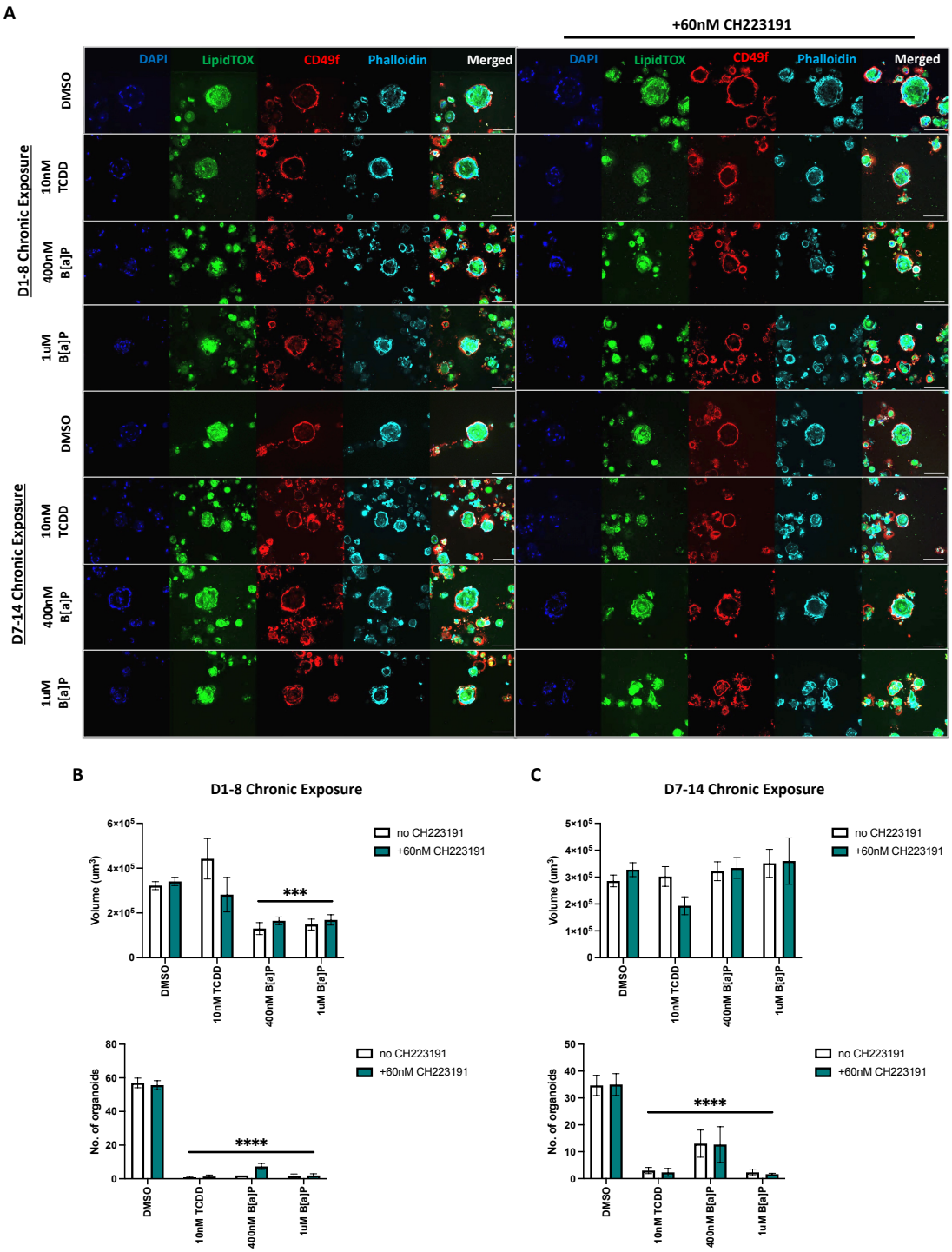

Figure 13. Quantitative image analysis revealed that AhR signaling pathway inhibition by 60nM CH223191 did not rescue the perturbation of development and maintenance of organoids caused by 400nM B[a]P exposure. Human sebaceous gland organoids were chronically (D1-8/7-14) exposed to 0.1% DMSO (Control), 400nM/1uM B[a]P and 10nM TCDD, with each exposure supplemented with 60nM CH223191 (AhR antagonist). Immunofluorescence z-stack images **(A)** were taken at day 14 of organoid growth for all exposures and the size (volume) and number of organoids were quantified **(B and C)**. Two-Way ANOVA statistical analysis using Tukey multiple comparison test was applied to compare the means across treated groups (3 biological replicates/group) [*: <0.05, **:<0.01, ***:<0.001, ****:<0.0001]. Statistical significance represents how different the treated groups are compared to DMSO sample. Scale bar: 100um. *DMSO: Dimethyl sulfoxide; B[a]P: Benzo[a]pyrene; TCDD: 2,3,7,8-Tetrachlorodibenzodioxin.*

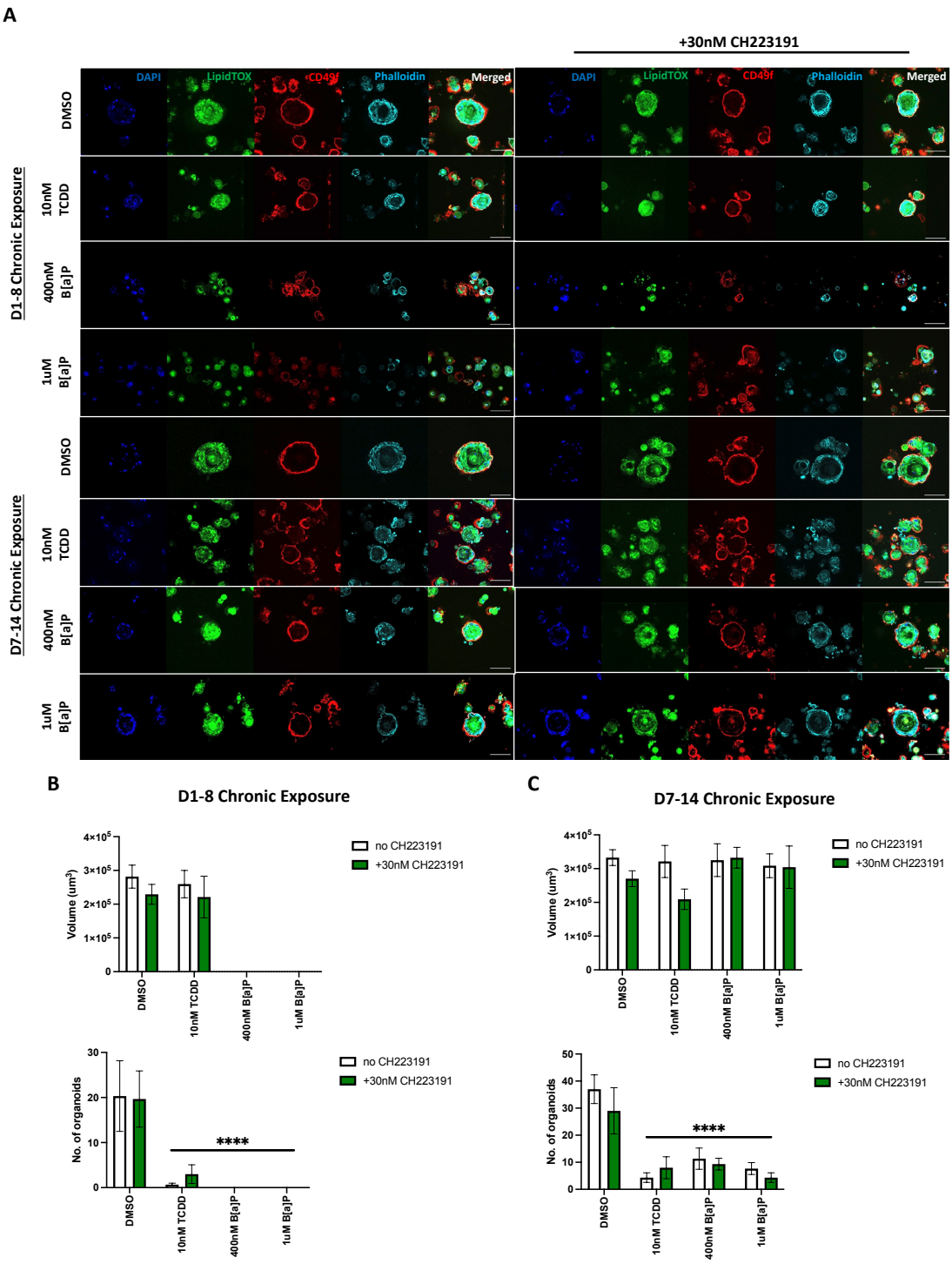

Figure 14. Quantitative image analysis showed that AhR signaling inhibition by 30nM CH223191 does not rescue the perturbation of development and maintenance of organoids caused by TCDD and B[a]P exposure. Human sebaceous gland organoids were chronically (D1-8/7-14) exposed to 0.1% DMSO (Control), 250uM H_2O_2, 400nM/1uM B[a]P and 10nM TCDD, with each exposure supplemented with 30nM CH223191 (AhR antagonist). Immunofluorescence z-stack images **(A)** were taken at day 14 of organoid growth for all exposures, and the size (volume) and number of organoids were quantified **(B and C)**. Two-Way ANOVA statistical analysis using Tukey multiple comparison test was applied to compare the means across treated groups (3 biological replicates/group) [*: <0.05, **:<0.01, ***:<0.001, ****:<0.0001]. Statistical significance represents how different the treated groups are compared to DMSO sample. Scale bar: 100um. *DMSO: Dimethyl sulfoxide; B[a]P: Benzo[a]pyrene; TCDD: 2,3,7,8-Tetrachlorodibenzodioxin.*

with 30/60nM CH223191 as compared to 10nM TCDD only exposed samples. This effect might be due to CH223191 however, this observation was not seen in DMSO control and B[a]P samples suggesting that it might be due to chance.

Further transcriptional analysis of proliferative marker, *c-MYC*, showed that its expression level in samples co-exposed to TCDD/B[a]P with 60nM CH223191 is still significantly downregulated (Figure 15A) compared to its TCDD/B[a]P only. controls. Similar effect was also observed in samples co-exposed to TCDD/B[a]P with 30nM CH223191 or 40nM BAY-218 (Supplementary Figure 1). The proliferative capacity of sebocyte progenitors was further evaluated by the %MKI67+ nuclei staining (Figure 16A) where exposure to both TCDD and B[a]P resulted in significant reduction of MKI67+ sebocyte progenitors (Figure 15B and 16B). This reduction in MKI67+ sebocyte progenitors was still observed in co-exposure to TCDD/B[a]P with 30/60nM CH223191 and 40nM BAY-218 (Figure 15B and 16B). Transcriptional analysis of sebaceous-related markers (*FASN*, *SCD1, PPARγ* and *LRIG1*) did not yield any significant expression difference even with AHR antagonists (Figure 15C). On a side note, 60nM CH223191 seem to slightly downregulate *c-MYC* expression (non-significant) in DMSO control but does not induce any significant changes to other gene expression (Figure 15A and C). These results suggest that the loss of hSGOs and the declined proliferative capacity of sebocytes progenitors is not modulated by AHR signalling pathway activation by TCDD and B[a]P. As the effects observed from both TCDD and B[a]P exposure are similar, both pollutants might trigger similar pathway/biological process, other than those directly associated with the AHR signalling pathway.

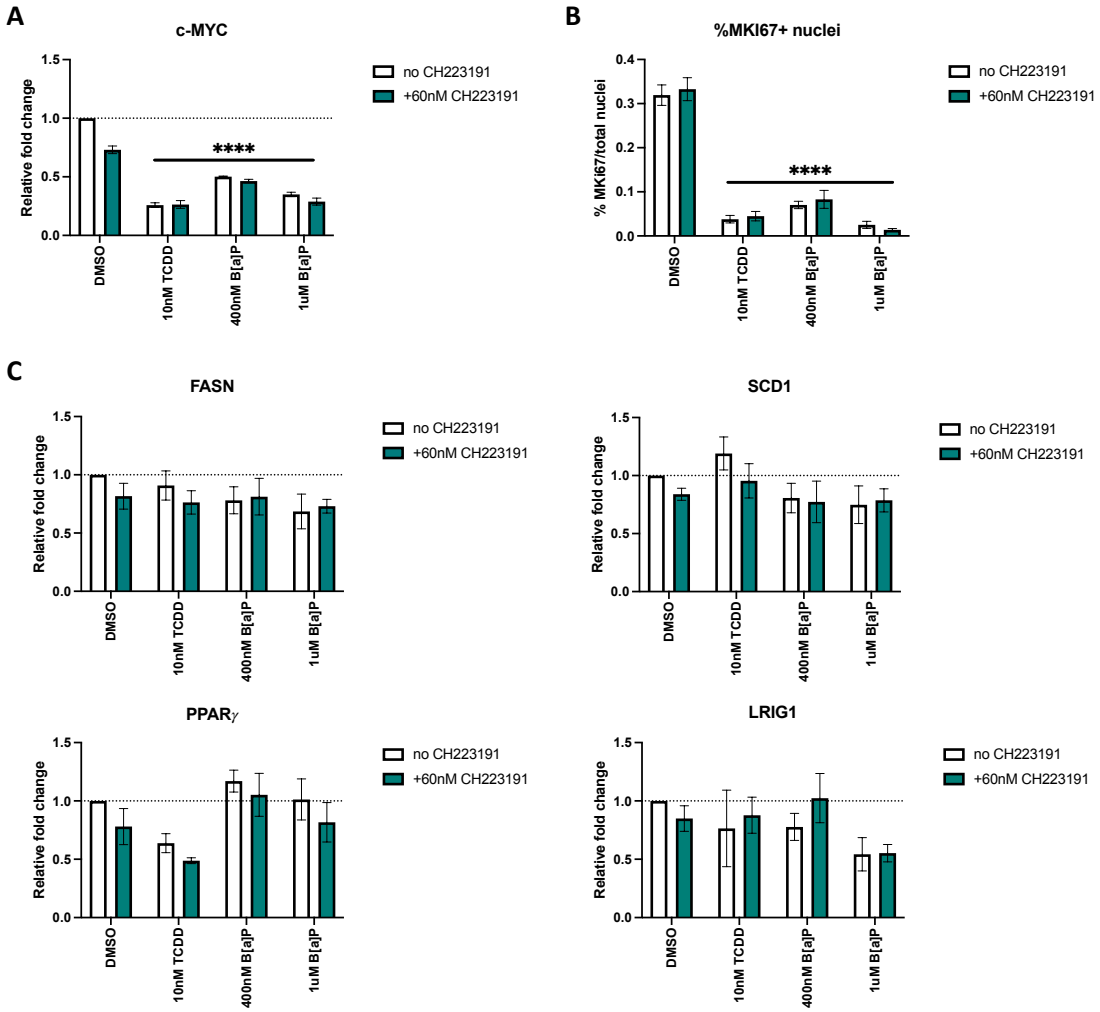

Figure 15. qPCR analysis showed no rescue of the proliferation capacity of sebocyte progenitors after AhR signaling pathway inhibition by 60nM CH223191 in 400nM B[a]P exposed samples. Sebocyte progenitors were exposed to 0.1% DMSO (Control), 400nM/1uM B[a]P and 10nM TCDD, with each exposure supplemented with 60nM CH223191 (AhR antagonist), for 72 hours. Proliferation capacity was measured by the relative fold change on *c-MYC* expression **(A)** and percentage of MKI67+ nuclei of exposed samples compared to DMSO control **(B).** There were no changes to the relative fold change of *FASN, SCD1, PPARγ* and *LRIG1* expression **(C).** Two-Way ANOVA statistical analysis using Tukey multiple comparison test was applied to compare the mean relative fold change across 4 groups (3 technical replicates/group) [*: <0.05, **:<0.01, ***:<0.001, ****:<0.0001]. Statistical significance represents how different the treated groups are compared to DMSO sample. *FASN: Fatty acid synthase; SCD1: Stearoyl-CoA 1; PPARγ: Peroxisome proliferator activated receptor gamma; LRIG1: Leucine rich repeats and immunoglobin like domain 1; GAPDH: Glyceraldehyde 3-phosphate dehydrogenase; DMSO: Dimethyl sulfoxide; B[a]P: Benzo[a]pyrene; TCDD: 2,3,7,8-Tetrachlorodibenzodioxin.*

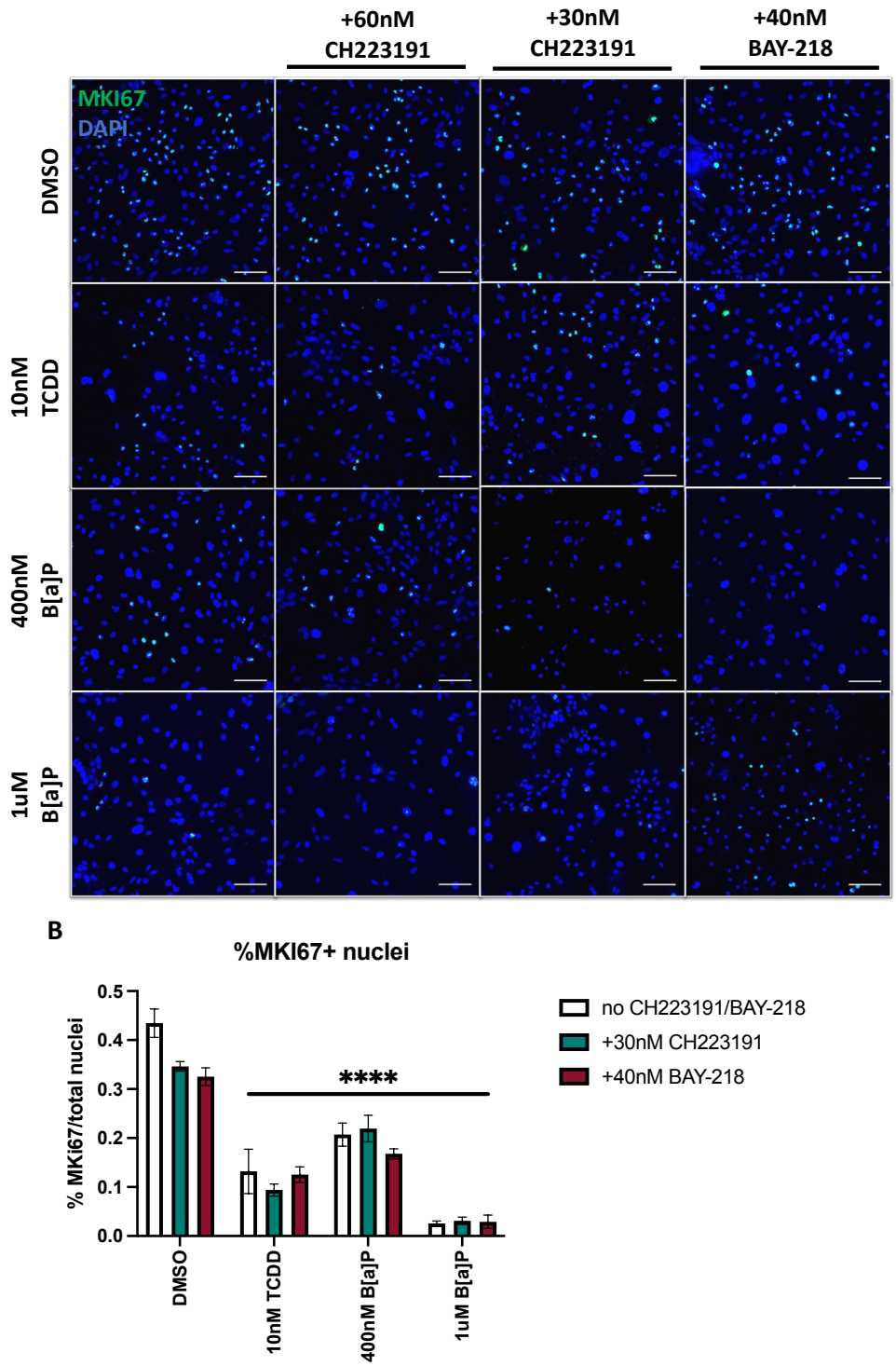

Figure 16. AhR signaling pathway inhibition by 30nM CH223191 and 40nM BAY-218 do not rescue the loss of proliferation of sebocyte progenitors. 1008-HFSE2 human primary sebocytes were exposed to 0.1% DMSO (Control), 400nM/1uM B[a]P and 10nM TCDD, with each exposure supplemented with 30/60nM CH223191 and 40nM BAY-218 for 72 hours. Proliferative capacity of sebocyte progenitors was measured using IF staining of MKI67 (Green) **(A)** and calculating the percentage of MKI67+ nuclei **(B)**. Two-Way ANOVA statistical analysis using Tukey multiple comparison test was applied to compare the means across treated groups (3 biological replicates/group) [*: <0.05, **:<0.01, ***:<0.001, ****:<0.0001]. Statistical significance represents how different the treated groups are compared to DMSO sample. *DMSO: Dimethyl sulfoxide; B[a]P: Benzo[a]pyrene; TCDD: 2,3,7,8-Tetrachlorodibenzodioxin.*

5. TCDD and B[a]P induces DNA damage in 1008-HFSE2 primary human sebocytes but does not lead to cellular senescence

As AHR signaling has been shown previously via AHR inhibition that it does not modulate the phenotypes observed in hSGOs, there is likely an alternate molecular process triggered by both TCDD and B[a]P. A recent article reported that B[a]P can repress DNA repair and trigger DNA damage-induced cellular senescence[174] whereas TCDD has been reported to influence DNA double-strand break repair and DNA damage[175,176]. It would be of interest to evaluate whether TCDD and B[a]P can result in DNA-damage induced cellular senescence, which may influence the reduction in proliferation of sebocyte progenitors (Figure 13) and loss of hSGOs (Figure 10).

Using the same D7-9 acute exposed organoids samples used in Figure 17, transcriptional analysis of mismatch repair genes Mut S homolog 2 and 6 (*MSH2 and 6*), homologous recombination DNA repair protein RAD51 homolog 1 (*RAD51*), senescence markers lamin B1 (*LMNB1*) and cyclin-dependent kinase inhibitor 1 (*CDKN1A/P21*) was performed (Figure 17). *MSH2* and *RAD51* expression levels were observed to be slightly downregulated in both TCDD and B[a]P exposed organoids. The downregulation of *LMNB1* expression was statistically significant and *CDKN1A* expression was upregulated in both TCDD and B[a]P exposed organoids, suggesting possible senescence of sebocyte progenitors/hSGOs. However, a positive control for DNA damage-induced cellular senescence was lacking in this experiment to corroborate the effects of both TCDD and B[a]P in this area.

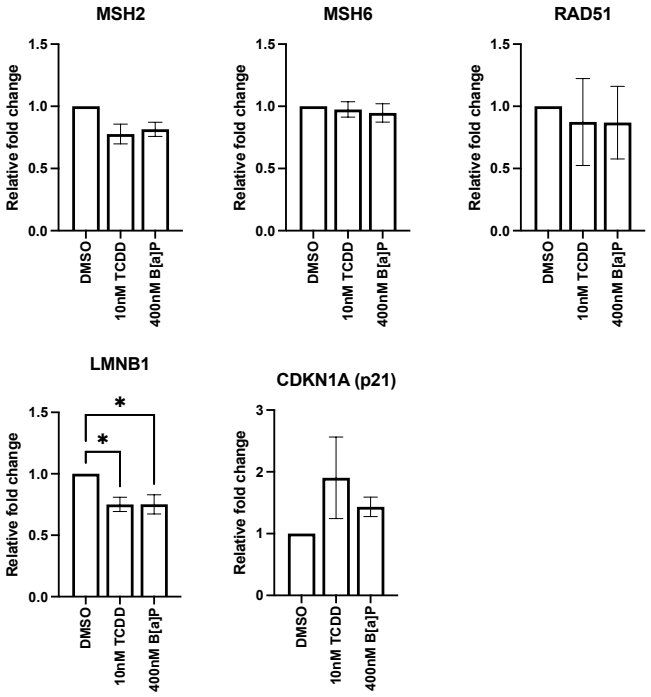

Figure 17. Gene expression analysis of acute exposed organoids showed downregulation in LMNB1 with possible effect on DNA repair and cellular senescence. 1008-HFSE2-derived human sebaceous gland organoids were acutely (D7-9) exposed to 0.1% DMSO (Control), 10nM TCDD and 400nM of B[a]P**.** qPCR analysis on gene expression of DNA repair genes (*MSH2/6, RAD51*) and senescence makers (*LMNB1, CDKN1A*) **(B).** Relative fold change of gene expression was normalized to endogenous *GAPDH* expression and calculated based on $2^{-\Delta\Delta CT}$. One-Way ANOVA statistical analysis using Tukey multiple comparison test was applied to compare the mean relative fold change across 3 samples (3 technical replicates/group) [*: <0.05]. *MSH2: DNA mismatch repair protein MutS homolog 2/6; RAD51: DNA repair protein RAD51 homolog 1; LMNB1: Lamin B1; CDKN1A: Cyclin dependent kinase inhibitor 1A; GAPDH: Glyceraldehyde 3-phosphate dehydrogenase, DMSO: Dimethyl sulfoxide; B[a]P: Benzo[a]pyrene; TCDD: 2,3,7,8-Tetrachlorodibenzodioxin.*

Hydrogen peroxide (H_2O_2) is often used as a positive control for DNA damage-induced cellular senescence. However, the optimization of 2D culture media conditions was required as the effect of H_2O_2 to induce loss of *LMNB1* expression and increase in CDKN1A expression was not observed in sebaceous progenitors cultured in CCMY media (Supplementary Figure 2). Therefore, the effect of H_2O_2 was evaluated on 3 culture media conditions; CCMY, serum-free CCMY (CCMY SF) and CCMY SF supplemented with IGF-1 (Figure 18).

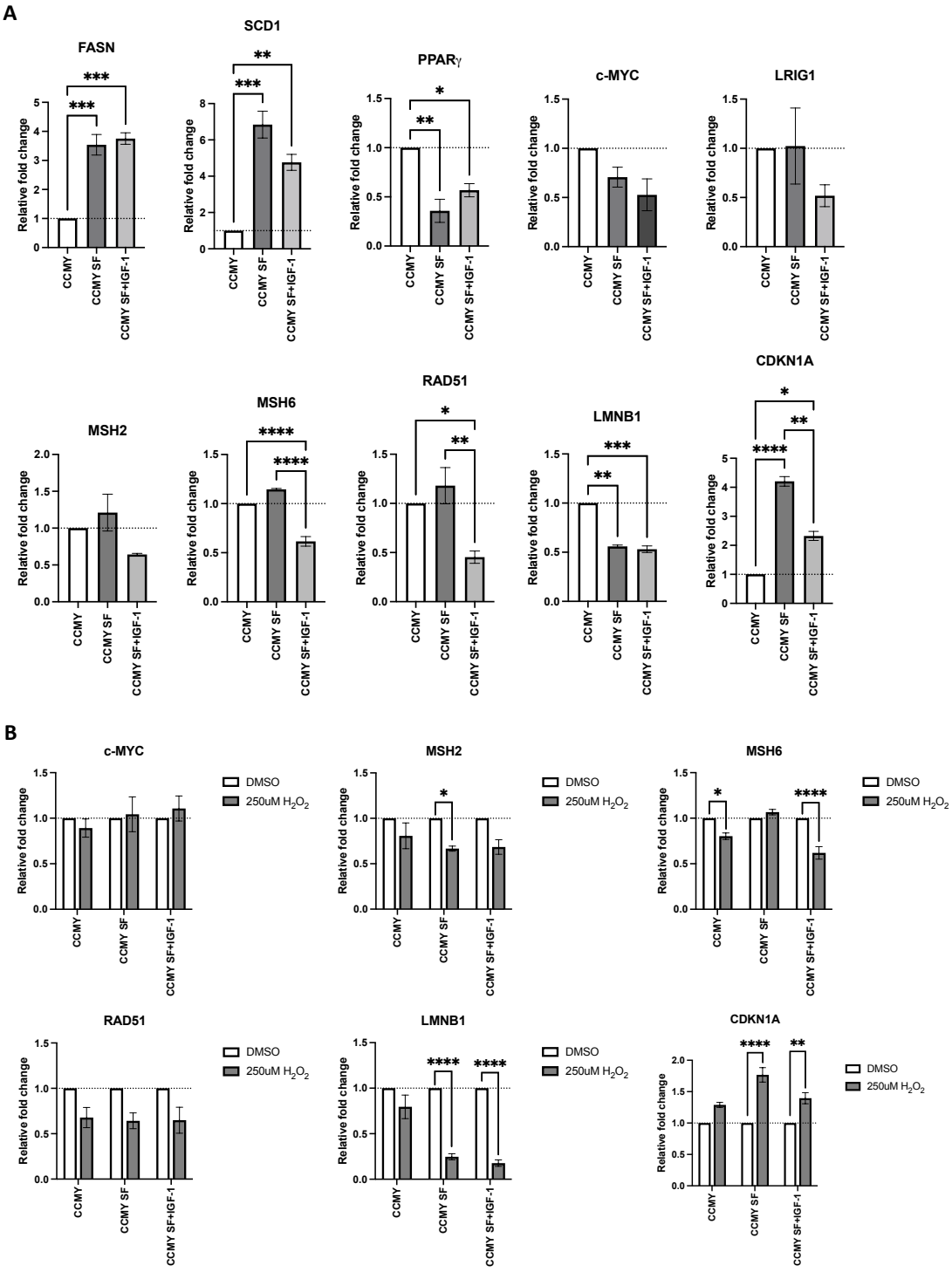

Figure 18. CCMY SF supplemented with IGF-1 is a promising media replacement to CCMY to study DNA damage-induced cellular senescence. Sebaceous gland markers (*FASN, SCD1, PPARγ, LRIG1*), proliferative marker (*c-MYC*), DNA repair genes (*MSH2/6, RAD51*), cellular senescence markers (*LMNB1, CDKN1A*) were analyzed in 1008-HFSE2 human primary sebocytes cultured in CCMY, CCMY SF and CCMY SF+IF-1 media conditions **(A).** *c-MYC, MSH2, MSH6, RAD51, LMNB1, CDKN1A* were analyzed in 1008-HFSE2 cultured in the three media conditions and exposed to 0.1% DMSO (Control) and 250uM H_2O_2 for 72 hours **(B)**. Relative fold change of gene expression was normalized to endogenous GAPDH and calculated based on $2^{-\Delta\Delta CT}$ One-Way ANOVA statistical analysis using Tukey multiple comparison test was applied to compare the mean relative fold change across treated groups (3 technical replicates/group) [*: <0.05, **:<0.01, ***:<0.001, ****:<0.0001]. *FASN: Fatty acid synthase; SCD1: Stearoyl-CoA 1; PPARγ: Peroxisome proliferator activated receptor gamma; LRIG1: Leucine rich repeats and immunglobin like domain 1; MSH2: DNA mismatch repair protein MutS homolog 2/6; RAD51: DNA repair protein RAD51 homolog 1; LMNB1: Lamin B1; CDKN1A: Cyclin dependent kinase inhibitor 1A; GAPDH: Glyceraldehyde 3-phosphate dehydrogenase; DMSO: Dimethyl sulfoxide; B[a]P: Benzo[a]pyrene; TCDD: 2,3,7,8-Tetrachlorodibenzodioxin.*

The switching of culture media from CCMY to CCMY SF and CCMY SF+IGF-1 seem to influence lipogenesis of sebocyte progenitors as *FASN* and *SCD1* were significantly upregulated and *PPARγ* was significantly downregulated, while *c-MYC* and *LRIG1* showed no significant expression changes (Figure 18A). As hSGO culture system uses CCMY SF+IGF-1 as its culture media, this increased in lipogenesis might be required for the development of hSGOs. It is also worth noting that switching of culture media condition to CCMY SF+IGF-1 resulted in decreased expression of DNA repair genes (*MSH2, MSH6, RAD51*) and the senescence marker, LMNB1 together with upregulation of CDKN1A (Figure 18A). The effects of 250μM H_2O_2 treatment has minimal impact on sebocyte progenitors cultured in CCMY but induced the downregulation of *LMNB1* expression and upregulated *CDKN1A* expression in sebocyte progenitors cultured in CCMY SF and CCMY SF+IGF-1 (Figure 18B). Furthermore, H_2O_2 treatment on sebocyte progenitors cultured in CCMY SF+IGF-1 showed downregulation of *MSH2*, *MSH6* and *RAD51* DNA repair genes (Figure 18B). This result suggests that H_2O_2 treatment of sebocyte progentiors cultured in CCMY SF+IGF-1in 2D can be used to study the effects of DNA damage and cellular senescence

Additional analysis on the effects of H_2O_2 on hSGO development and maintenance was performed (Figure 19) where a single exposure of 250μM H_2O_2 in the developmental and maintenance phase resulted in reduced number, but not size, of hSGOs (Supplementary Figure 19B). Transcriptional analysis on *CYP1A1*, sebaceous-related markers (*FASN, SCD1, PPARγ* and *LRIG1*) showed little to no expression changes by H_2O_2 (Figure 19D). Proliferation of sebocyte progenitors was affected by H_2O_2 as downregulation of *c-MYC*

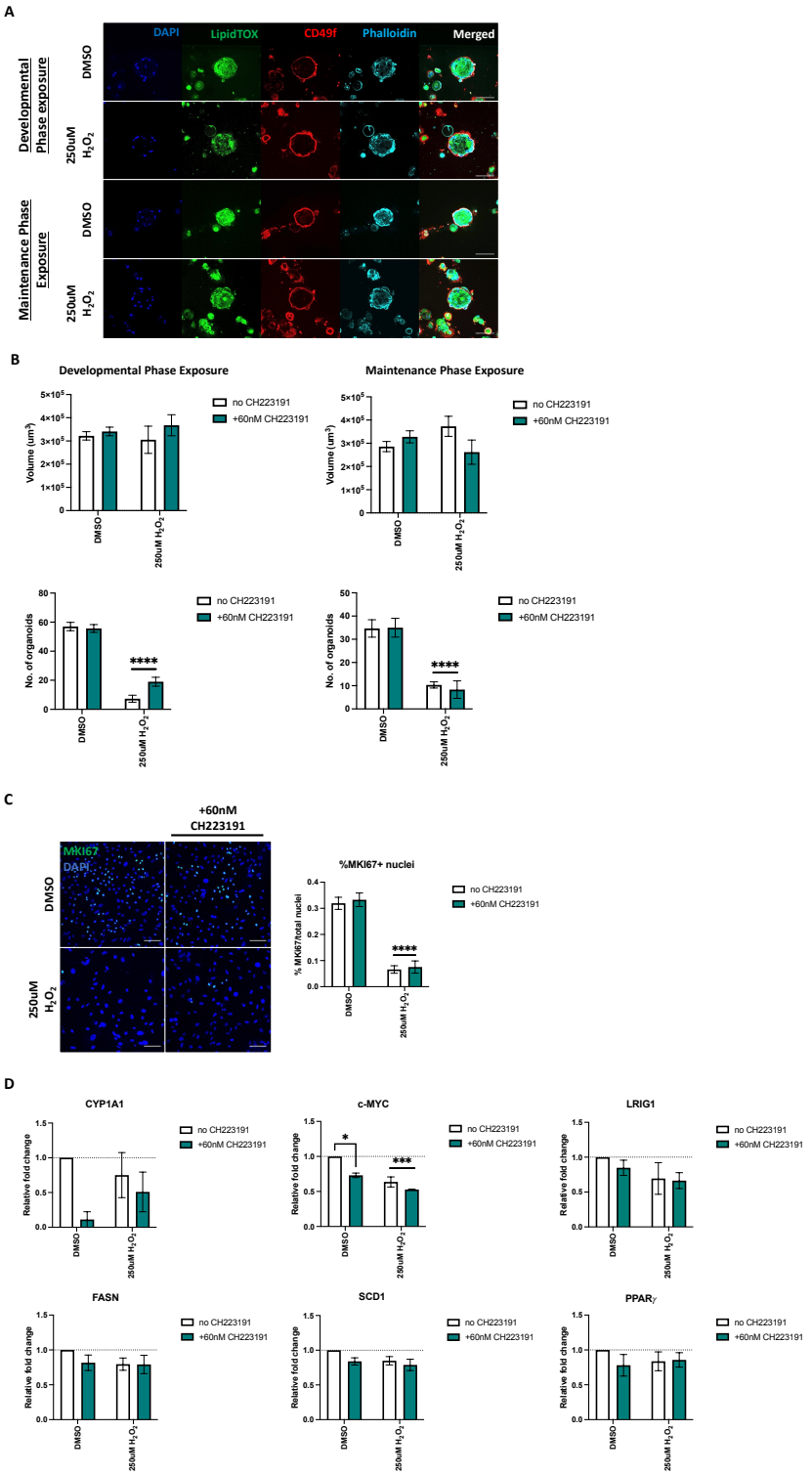

Figure 19. Treatment with H_2O_2 can perturb the maintenance of human sebaceous glands organoids and proliferation capacity of sebocyte progenitors. All H_2O_2 experiments only had a one-time exposure at 250uM concentration. Immunofluorescence images and quantitative analysis of H_2O_2 exposure at day 1 and day 7 of hSGOs with 60nM CH223191 chronic treatment (D1-8/D7-14) **(A and B).** Two-Way ANOVA statistical analysis using Tukey multiple comparison test was applied to compare the means across treated groups (3 biological replicates/group). Percentage of MKI67+ nuclei was calculated after 72 hours of 60nM CH223191 treatment with a single H_2O_2 exposure **(C).** Two-Way ANOVA statistical analysis using Tukey multiple comparison test was applied to compare the means across treated groups (3 biological replicates/group). Gene expression analysis on *CYP1A1, c-MYC, LRIG1, FASN, SCD1* and *PPARγ* was evaluated **(D)**. Relative fold change of gene expression was normalized to endogenous *GAPDH* and calculated based on $2^{-\Delta\Delta CT}$. Two-Way ANOVA statistical analysis using Tukey multiple comparison test was applied to compare the mean relative fold change across groups (3 technical replicates/group) [*: <0.05, **:<0.01, ***:<0.001, ****:<0.0001]. Statistical significance represents how different treated group is compared to DMSO sample. *CYP1A1: Cytochrome P450, family 1, subfamily A, polypeptide 1; FASN: Fatty acid synthase; SCD1: Stearoyl-CoA 1; PPARγ: Peroxisome proliferator activated receptor gamma; LRIG1: Leucine rich repeats and immunoglobin like domain 1; GAPDH: Glyceraldehyde 3-phosphate dehydrogenase; DMSO: Dimethyl sulfoxide; B[a]P: Benzo[a]pyrene; TCDD: 2,3,7,8-Tetrachlorodibenzodioxin.*

expression and the reduction in %MKI67+ nuclei were observed (Figure 19C and D). Therefore, the role of TCDD and B[a]P in DNA damage and cellular senescence was performed in CCMY SF+IGF-1 culture media.

As H_2O_2 was able to trigger DNA damage-induce cellular senescence on sebocyte progenitors, the role of TCDD and B[a]P on DNA damage and cellular senescence was evaluated (Figure 20-23). The experiments included AHR antagonist (both 30/60nM CH223191 and 40nM BAY-218) treatment to exclude the involvement of AHR signalling pathway as AHR has been implicated in aging process by promoting cellular senescence through age-related remodelling of the immune system and oxidative stress[177]. *MSH2*, *MSH6* and *RAD51* gene expression levels was observed to be downregulated in 10nM TCDD, 400nM/1μM B[a]P and 250μM H_2O_2 exposed samples (Figure 20A) while no expressional differences of these genes were observed in samples that were co-exposed with AHR antagonists compared to TCDD/B[a]P/H_2O_2 only samples (Figure 20A and 21A).

Although the transcriptional analysis showed a slight downregulation of *MSH2* and *MSH6*, WB analysis showed that MSH2 protein levels were slightly increased in 400nM B[a]P co-exposed with 60nM CH223191 (Figure 20B). However, this may be due to uneven loading of protein as GAPDH protein levels seems to be slightly higher. MSH6 protein levels were slightly increased in 400nM and 1μM B[a]P exposed samples and similar MSH6 protein levels were also observed in B[a]P samples co-exposed with 60nM CH223191 (Figure 20B). It has been reported that B[a]P and BPDE (a metabolized form of B[a]P) treated samples resulted in the

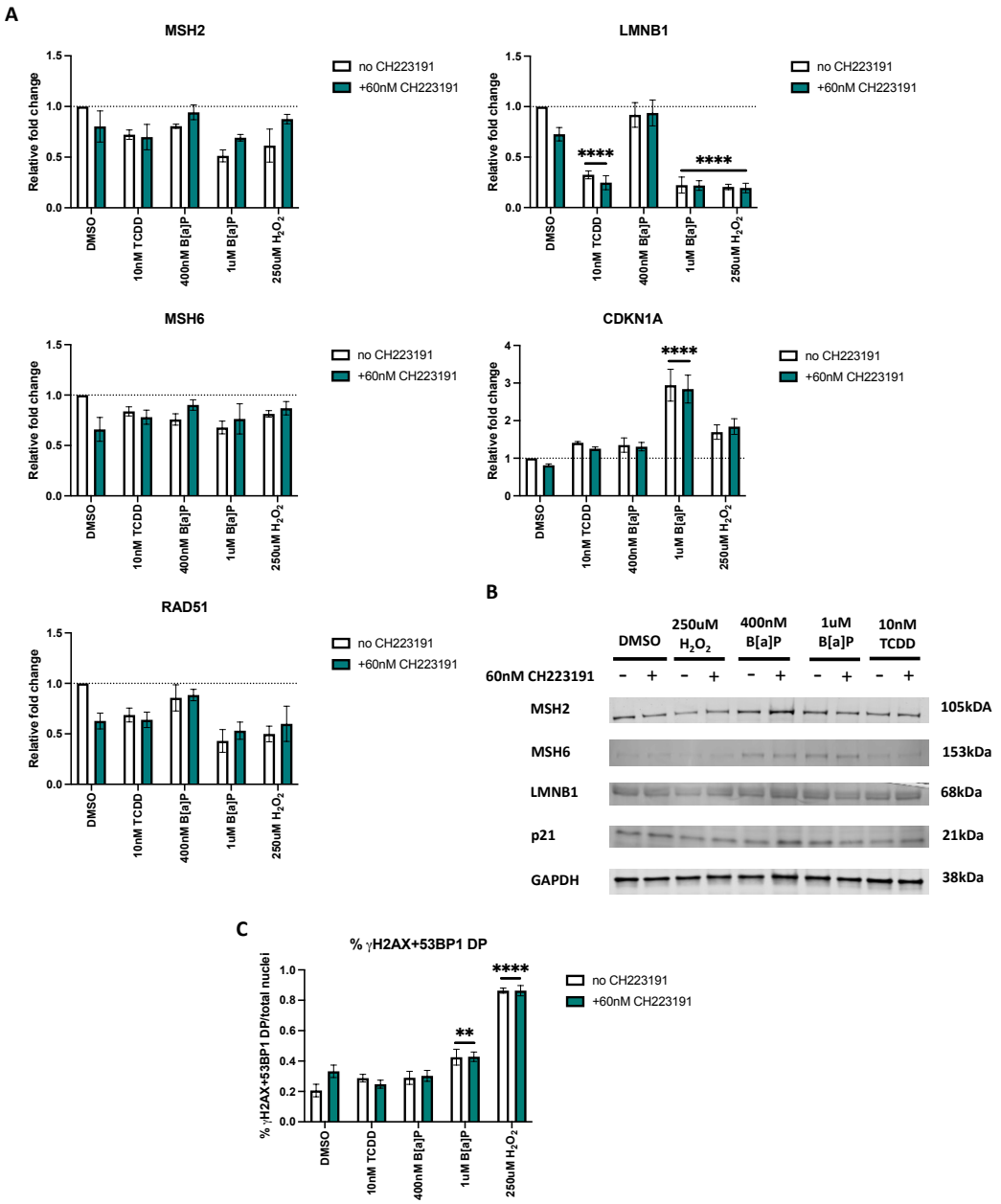

Figure 20. TCDD and B[a]P do not trigger DNA damage-induced cellular senescence. Sebocyte progenitors were exposed to 0.1% DMSO (Control), 400nM/1uM B[a]P and 10nM TCDD, with each exposure supplemented with 60nM CH223191 (AhR antagonist), for 72 hours. Relative fold change analysis on *MSH2, MSH6, RAD51, LMNB1* and *CDKN1A* expression suggests possible senescence **(A).** Two-Way ANOVA statistical analysis using Tukey multiple comparison test was applied to compare the mean relative fold change across treated groups (3 technical replicates/group) [*: <0.05, **:<0.01, ***:<0.001, ****:<0.0001]. WB analysis of MSH2, MSH6, LMNB1 and P21 revealed no significant changes to all protein levels compared to DMSO **(B).** Quantitative analysis on the co-localization of DNA damage markers γH2AX and 53BP1 showed accumulation of both markers in nuclei for 1uM B[a]P and H_2O_2 samples **(C).** Two-Way ANOVA statistical analysis using Tukey multiple comparison test was applied to compare the means across treated groups (3 biological replicates/group) [*: <0.05, **:<0.01, ***:<0.001, ****:<0.0001]. Statistical significance represents how different the treated groups are compared to DMSO sample. *MSH2: DNA mismatch repair protein MutS homolog 2/6; RAD51: DNA repair protein RAD51 homolog 1; LMNB1: Lamin B1; CDKN1A: Cyclin dependent kinase inhibitor 1A; GAPDH: Glyceraldehyde 3-phosphate dehydrogenase; γH2AX: Phosphorylated H2A histone family member X; 53BP1: p53-binding protein 1; DMSO: Dimethyl sulfoxide; B[a]P: Benzo[a]pyrene; TCDD: 2,3,7,8-Tetrachlorodibenzodioxin.*

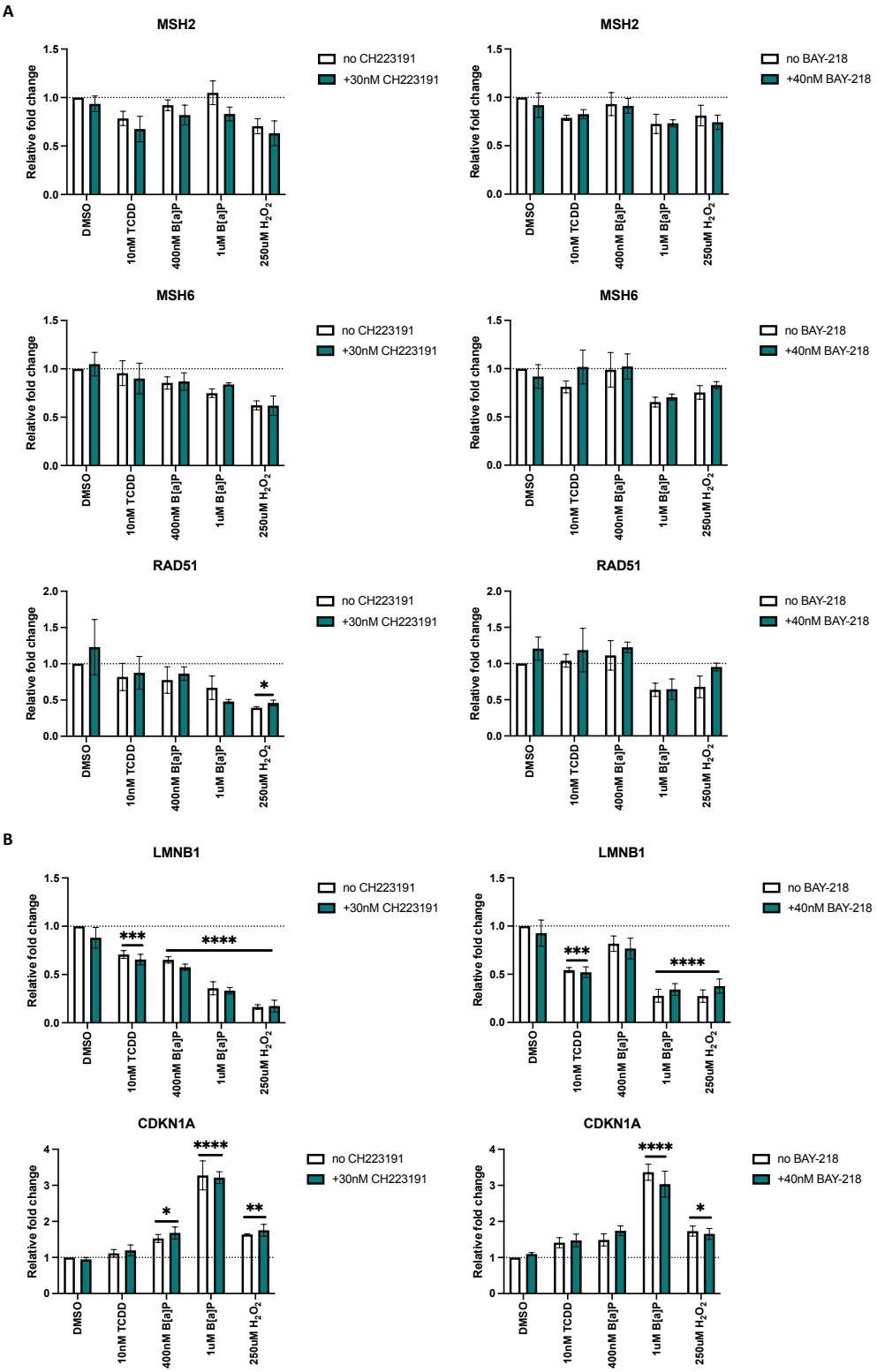

Figure 21. TCDD and B[a]P influence expression of senescence markers, *LMNB1* and *CDKN1A*. DNA repair genes (*MSH2/6, RAD51*) **(A)** and cellular senescence markers (*LMNB1, CDKN1A*) **(B)** were analyzed in 1008-HFSE2 human primary sebocytes exposed to 0.1% DMSO (Control), 250uM H_2O_2, 400nM/1uM B[a]P and 10nM TCDD, with each exposure supplemented with 30nM CH223191or 40nM BAY-218 for 72 hours. Relative fold change of gene expression was normalized to endogenous *GAPDH* and calculated based on 2^-▵▵CT. Two-Way ANOVA statistical analysis using Tukey multiple comparison test was applied to compare the mean relative fold change across groups (3 technical replicates/group) [*: <0.05, **:<0.01, ***:<0.001, ****:<0.0001]. Statistical significance represents how different treated group is compared to DMSO sample. *MSH2: DNA mismatch repair protein MutS homolog 2/6; RAD51: DNA repair protein RAD51 homolog 1; LMNB1: Lamin B1; CDKN1A: Cyclin dependent kinase inhibitor 1A; GAPDH: Glyceraldehyde 3-phosphate dehydrogenase; DMSO: Dimethyl sulfoxide; B[a]P: Benzo[a]pyrene; TCDD: 2,3,7,8-Tetrachlorodibenzodioxin.*

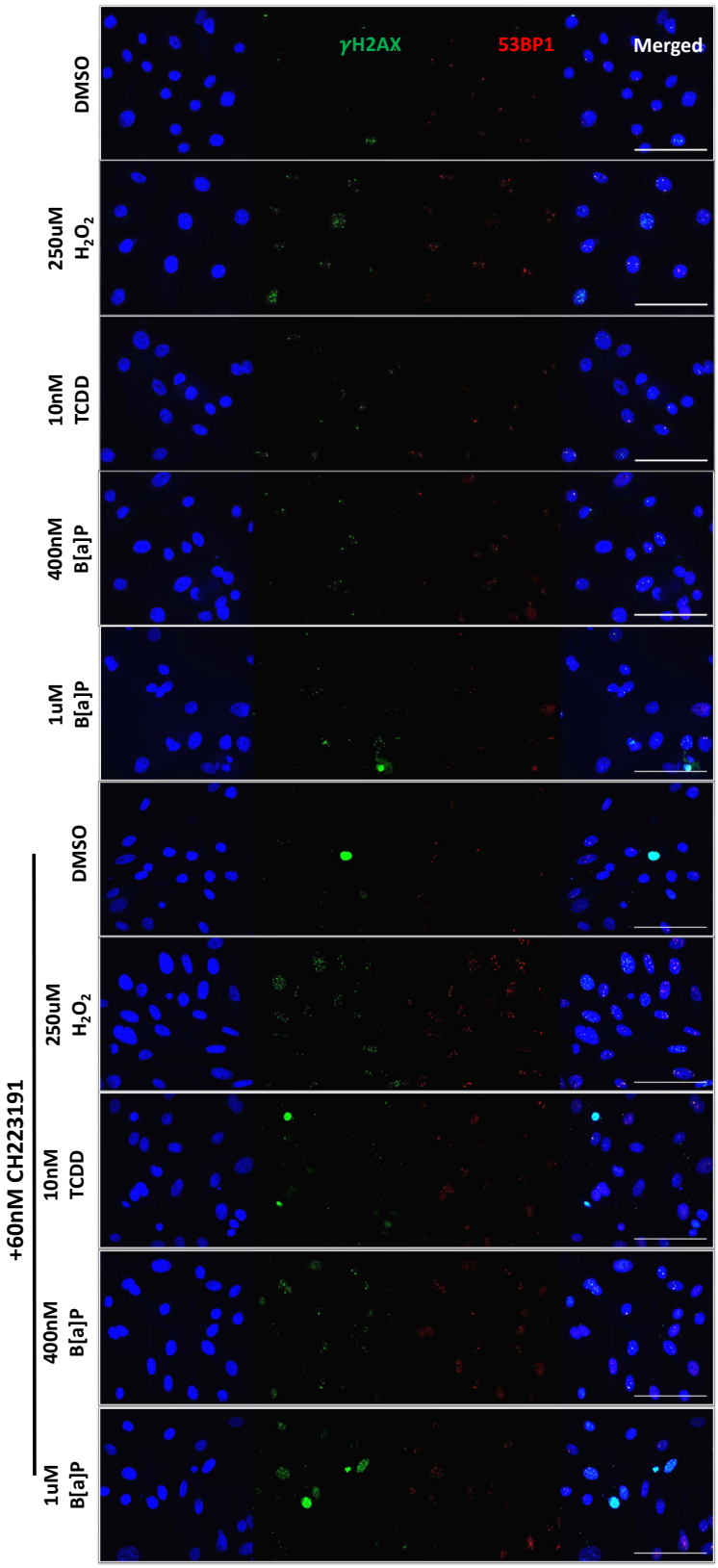

Figure 22 . Accumulation of γH2AX and 53BP1 in sebocyte progenitor nuclei after exposure to TCDD, B[a]P and H_2O_2. 1008-HFSE2 human primary sebocytes were exposed to 0.1% DMSO (Control), 250uM H_2O_2, 400nM/1uM B[a]P and 10nM TCDD, with each exposure supplemented with 60nM CH223191 (AhR antagonist) for 72 hours. Sebocytes were analyzed for DNA damage through staining of γH2AX (Green) and 53BP1 (Red). The percentage of co-localized γH2AX/53BP1 over total nuclei was calculated. Scale bar = 100uM *γH2AX: Phosphorylated H2A histone family member X; 53BP1: p53-binding protein 1; DMSO: Dimethyl sulfoxide; B[a]P: Benzo[a]pyrene; TCDD: 2,3,7,8-Tetrachlorodibenzodioxin.*

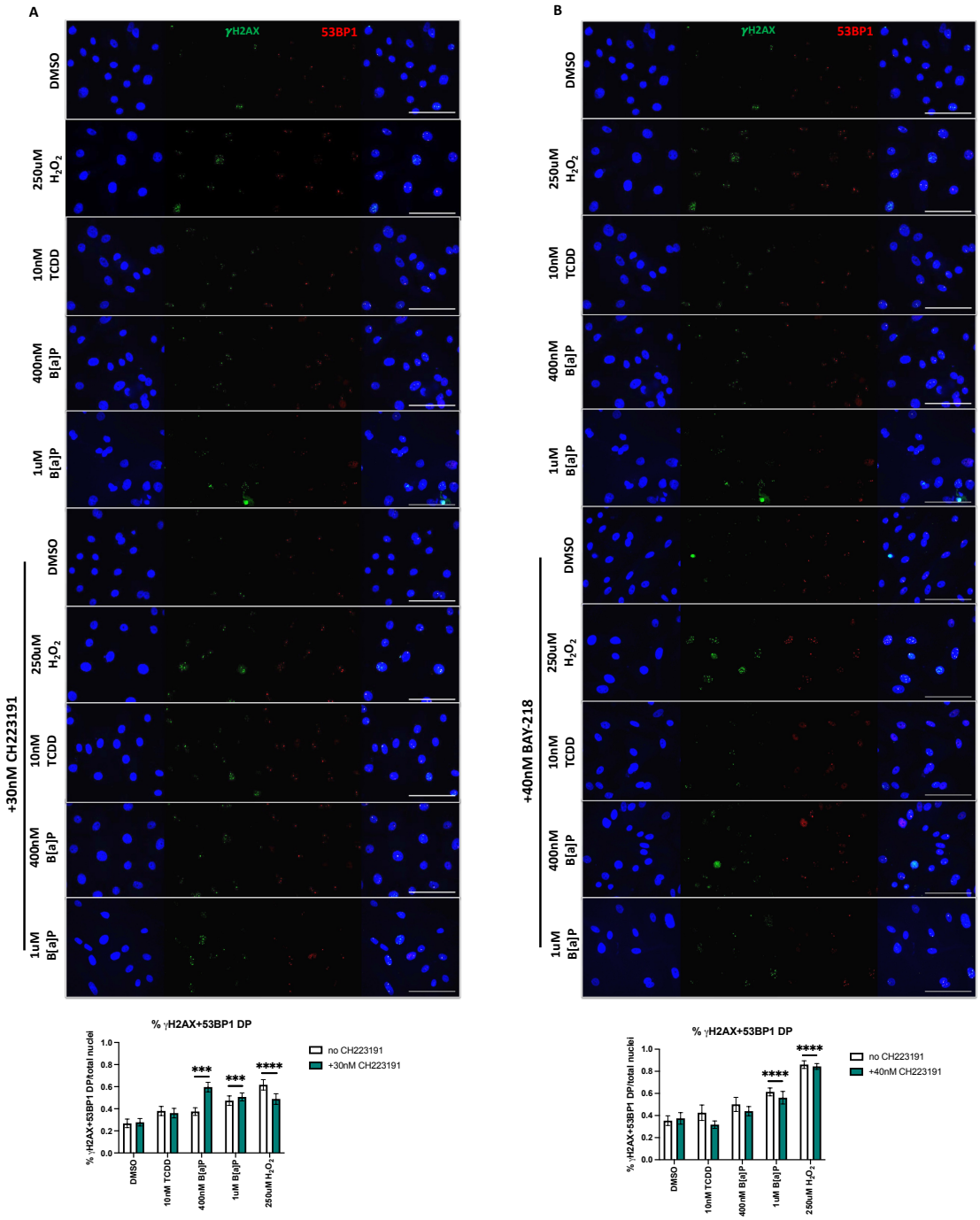

Figure 23. Accumulation of γH2AX and 53BP1 in sebocyte progenitor nuclei after exposure to TCDD, B[a]P and H_2O_2. Immunofluorescence images and quantitative analysis of co-localization of γH2AX and 53BP1 upon co-exposure to B[a]P/TCDD with 30nM CH223191 **(A)** or 40nM BAY-218 **(B)**, for 72 hours. Sebocytes were analyzed for DNA damage by staining γH2AX (Green) and 53BP1 (Red). The percentage of co-localized γH2AX/53BP1 over total nuclei was calculated. Two-Way ANOVA statistical analysis using Tukey multiple comparison test was applied to compare the means across groups (3 biological replicates/group)[*: <0.05, **:<0.01, ***:<0.001, ****:<0.0001]. Statistical significance represents how different treated group is compared to DMSO sample. *γH2AX: Phosphorylated H2A histone family member X; 53BP1: p53-binding protein 1; DMSO: Dimethyl sulfoxide; B[a]P: Benzo[a]pyrene; TCDD: 2,3,7,8-Tetrachlorodibenzodioxin.*

decreased in both gene and protein expression of MSH2 and MSH6[178], however this is not reflected in our observations. The observed increase in MSH6 protein levels suggests that the DNA repair mechanism may be activated upon exposure to B[a]P.

The presence of γH2AX and 53BP1 co-localisation (Figure 20C, 22 and 23) can indicate genomic instability resulting from DNA damage response[179]. Quantitative analysis of the co-localisation of γH2AX and 53BP1 demonstrated a slight increase in the %γH2AX+53BP1 co-localisation in 10nM TCDD and 400nM B[a]P exposed samples while 1μM B[a]P and 250μM H_2O_2 exposed samples were observed to have higher %γH2AX+53BP1 co-localisation (Figure 20C and 23). No difference was observed for %γH2AX+53BP1 co-localisation in samples that were co-exposed with AHR antagonists compared to their respective controls (Figure 20C and 23). Therefore, these findings suggests that B[a]P can induce DNA damage but its role in repressing DNA repair pathway remains inconclusive. Although TCDD can induce DNA damage, it does not influence the DNA repair pathway.

Transcriptional (Figure 20A and 21B) and WB analysis (Figure 20B) of senescence markers, LMNB1 and CDKN1A/p21 was performed to evaluate if cellular senescence is triggered after DNA damage by B[a]P and TCDD. *LMNB1* expression was observed to be downregulated after exposure to 10nM TCDD, 1μM B[a]P and 250μM H_2O_2 including co-exposure with AHR antagonists (Figure 20A and 21B). Moreover, 10nM TCDD, 400nM B[a]P and 250μM H_2O_2 samples induced slight increase in *CDKN1A* expression while 1μM B[a]P exposure resulted in a significant upregulation of *CDKN1A* expression (Figure 20A and 21B).

In contrast with the decreased mRNA expression levels of *LMNB1* and increased mRNA expression levels of *CDKN1A*, protein levels of LMNB1 and p21 showed

no changes in 10nM TCDD, 400nM/1µM B[a]P samples, whereas 250µM H_2O_2 samples showed a slight decreased in LMNB1 and p21 protein compared to DMSO control (Figure 20B). Co-exposed samples with 60nM CH223191 showed no changes to protein levels of LMNB1 and p21 compared to their respective controls (Figure 20B). These data suggests that even though TCDD and B[a]P can induce DNA damage response in sebocyte progenitors, this response does not lead to cellular senescence. However, the induction of DNA damage by 10nM TCDD and 400nM B[a]P is not sufficient to explain the organoid phenotype observed as the impact of both concentrations on DNA damage and senescence seems minimal as compared to the response elicited by H_2O_2. Therefore, employing RNAseq and bioinformatic analysis should provide insights on the role of TCDD and B[a]P beyond these tested pathways.

6. B[a]P and TCDD induce a comedo-like switch behavior in sebocyte progenitors

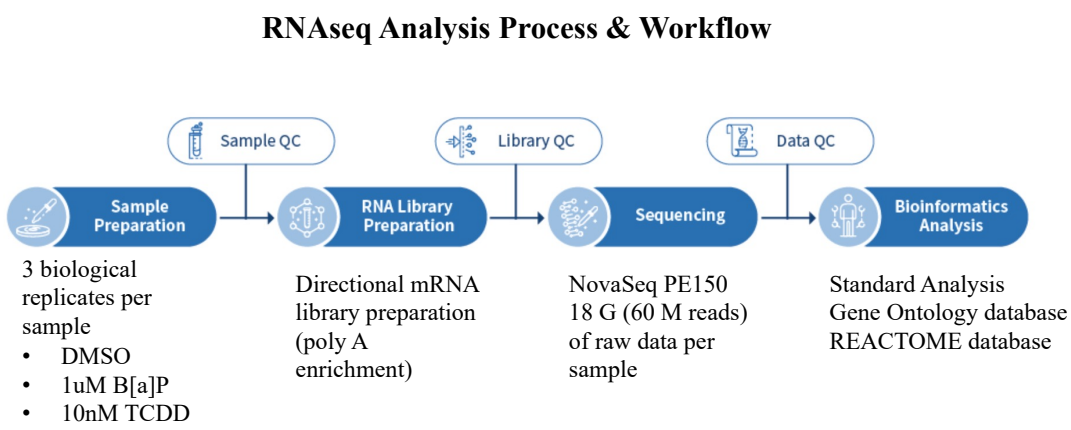

Figure 24. RNAseq sequencing strategy, process and workflow.

To further elucidate the biological processes/pathways that B[a]P and TCDD act on, RNAseq analysis of sebocyte progenitors exposed to DMSO, 1µM B[a]P and 10nM TCDD was performed (Figure 24).

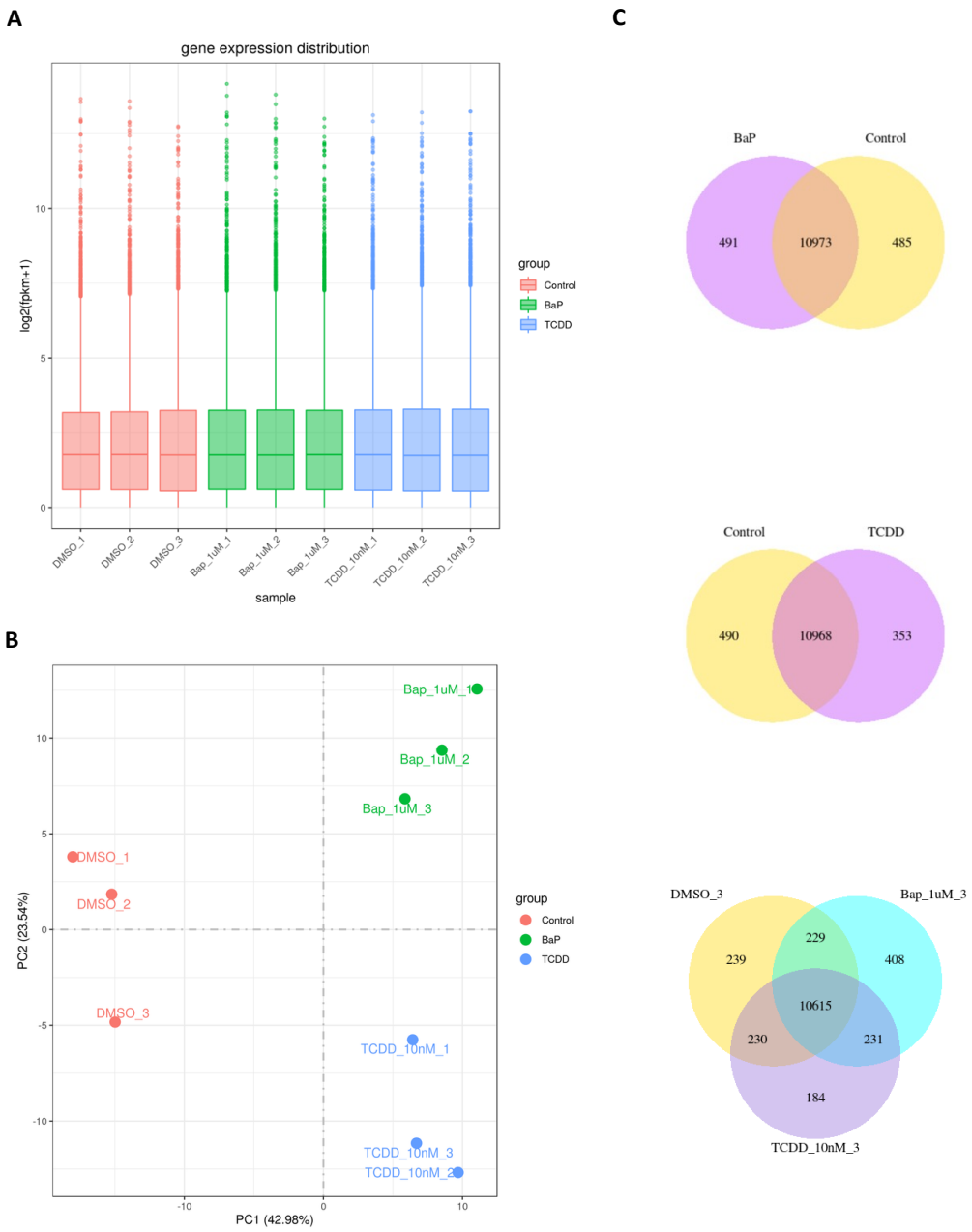

Figure 25. Gene expression analysis of RNAseq data performed on 1008-HFSE2 human primary sebocyte progenitors showed seperated grouping amongst DMSO, 1uM B[a]P and 10nM TCDD samples. The distribution of gene expression levels and FPKM among different samples are displayed by boxplots **(A)**. Principal component analysis (PCA) of showed intergroup differences among DMSO, B[a]P and TCDD samples **(B)**. The co-expression venn diagram shows the number of genes that are uniquely expressed within each group and sample where the overlapping regions represents the number of genes that are co-expressed in two or more groups/samples **(C)**.

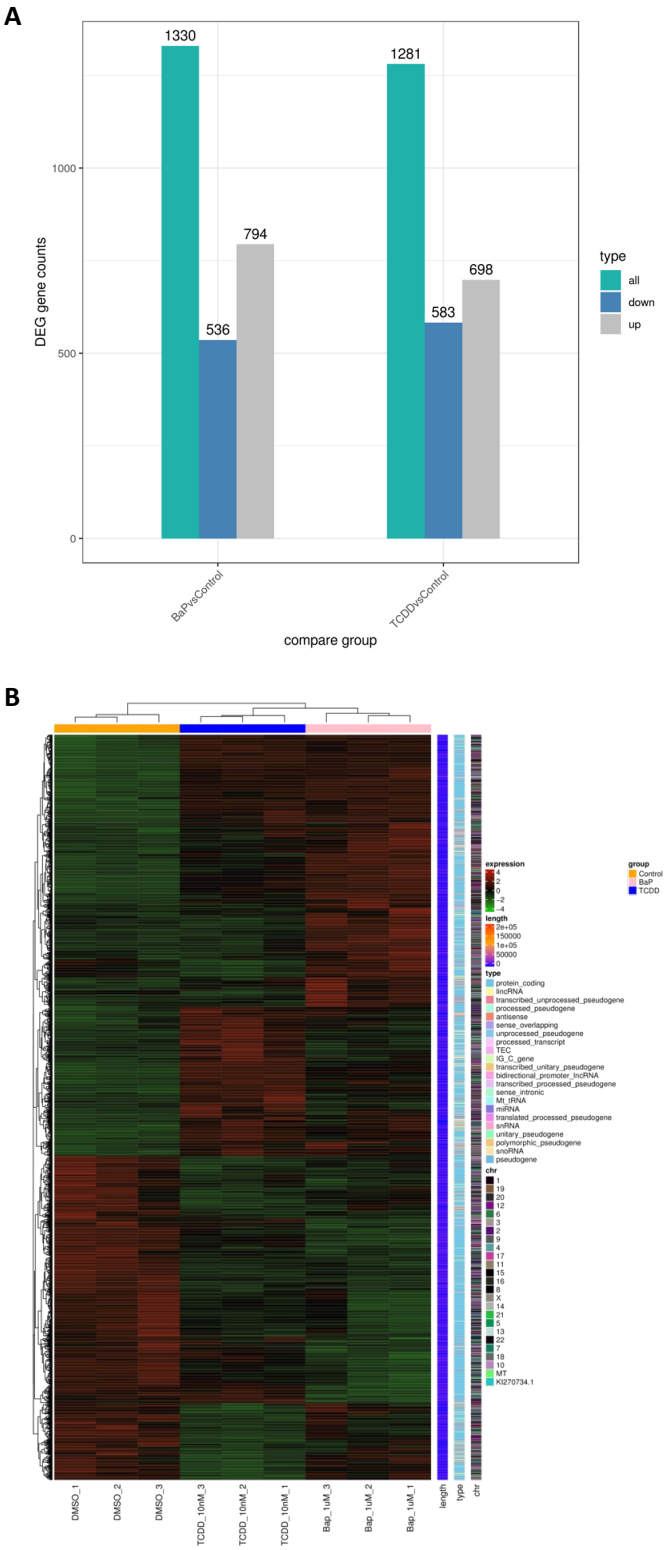

Figure 26. Differential expression genes (DEGs) analysis showing the number of DEGs that are up/downregulated with clustering to identify expression pattern in comparison groups. The number of DEG for each comparison combination is shown in a histogram **(A)**. Cluster analysis was performed using hierarchical clustering to cluster the FKPM values of genes and homogenized the row (Z-score). The genes or samples with similar expression patterns in the heat map will be clustered **(B)**. Comparisons in the heat map can only be compared horizontally but not vertically.

The RNAseq results highlighted gene expression distribution and the similarities and differences among sample groupings (Figure 25). The distribution of gene expression levels for each biological replicates was presented in a boxplot (Figure 25A) while principal component analysis (PCA) showed that DMSO, 1μM B[a]P and 10nM TCDD are tightly clustered among replicates, and the groupings are well separated (Figure 25B). This shows that the groups are distinct from one another. When the B[a]P and TCDD groups were compared to the DMSO (control) group, 491 and 490 genes were uniquely expressed in B[a]P and TCDD respectively, where B[a]P and TCDD shared 231 genes according to a single biological replicate comparison (Figure 25C).

Clustering of differential expression genes (DEGs) showed that B[a]PvsControl grouping have 794 and 536 gene that were upregulated (red) and downregulated (green), respectively, while TCDDvsControl grouping have 698 and 583 genes, that were upregulated (red) and downregulated, respectively (Figure 26). These results suggest that both B[a]P and TCDD samples are significantly different from DMSO control, and the DEGs shared between B[a]P and TCDD may potentially be driving the organoid phenotype observed.

To validate our qPCR results of sebaceous glands markers (Figure 15), DNA repair and senescence markers (Figure 20), expressional changes of these markers was extracted from the RNAseq analysis (Figure 27). RNAseq analysis of sebaceous gland differentiation markers (FASN, SCD, PPARγ, LRIG1) showed little to no changes in expression (Figure 27) which corroborated with our qPCR analysis of these genes (Figure 15). However, RNAseq analysis of MYC did not show any

observable changes in expression (Figure 27) when compared to our qPCR analysis (Figure 15). RNAseq analysis of DNA repair markers (MSH2, MSH6, RAD51) showed little to no changes in their expression levels (Figure 27) which corroborated with our qPCR analysis (Figure 20). RNAseq analysis showed a slight downregulation of LMNB1 expression while CDKN1A expression showed a slight upregulation in the 1µM B[a]P treated group (Figure 27). These results corroborated with what was observed in our qPCR results for LMNB1 and CDKN1A genes (Figure 20). Additionally, AhR signaling activation genes CYP1A1 was observed to be upregulated in the TCDD and B[a]P treated groups which corroborated with our qPCR analysis of these genes (Figure 12).

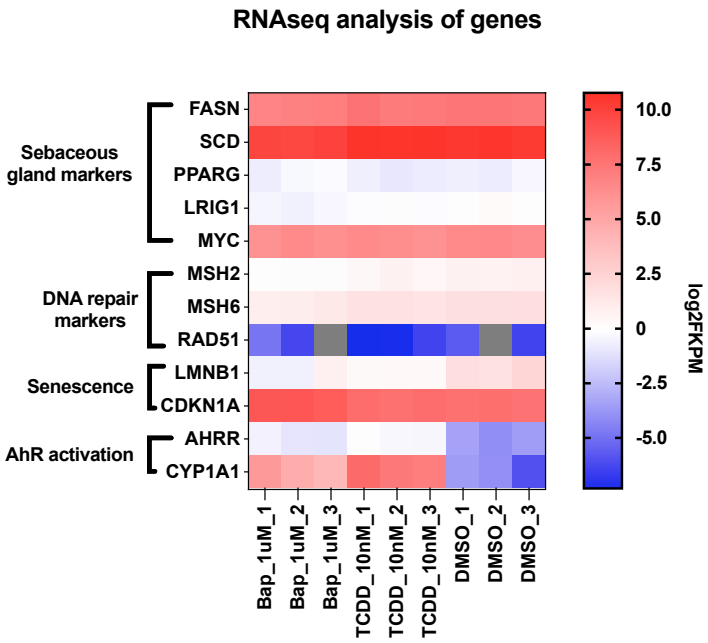

Figure 27. Heatmap of Differential expression genes (DEGs) of FASN, SCD, PPARG, LRIG1, MYC (Sebecaous markers), MSH2, MSH6, RAD51 (DNA repair markers), LMNB1, CDKN1A (Senescence markers), AHRR and CYP1A1 (AhR signaling markers) from B[a]P, TCDD and DMSO groups. Heatmap generated based on log2FKPM values as shown within the scale. Grey box represents no expression in sample.

To further evaluate the processes or pathways that B[a]P and TCDD can influence in sebocyte progenitors, significant DEGs (Supplementary Table 1 and 2) were

analyzed using gene ontology (GO) database to elucidate the type of biological processes upregulated or downregulated (Figure 28 and Supplementary Figure 3).

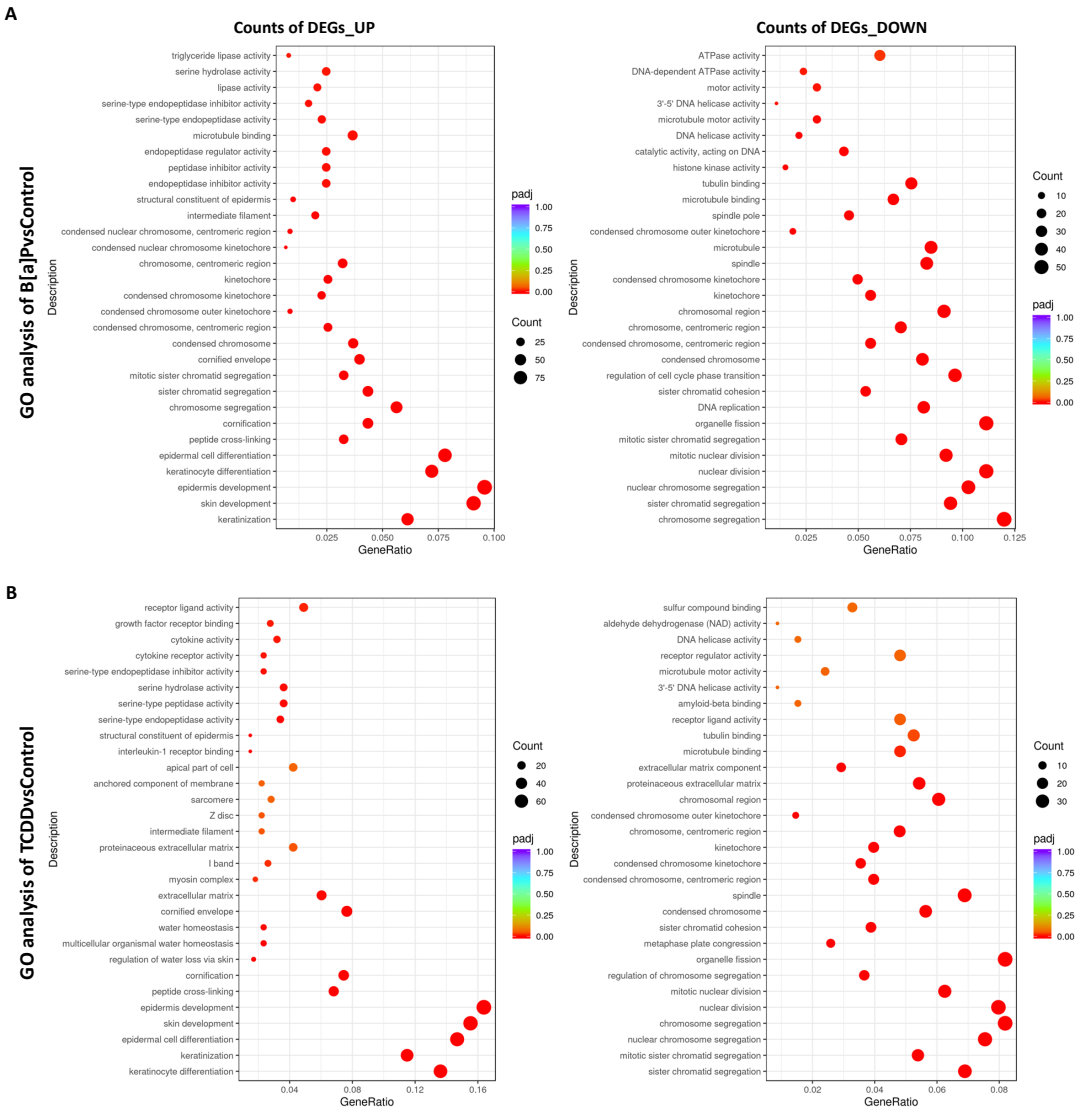

Figure 28. Gene ontology (GO) analysis showing the top 20 processes altered in sample groupings of B[a]PvsControl (A) and TCDDvsControl (B). Dot plot analysis displaying the count of DEGs involved in various processes that are significantly upregulated and downregulated in B[a]PvsControl and TCDDvsControl.

The dot plots displayed the top 20 processes that are significantly upregulated and downregulated in B[a]PvsControl and TCDDvsControl groups (Figure 28A and B). It revealed several biological processes that were upregulated in both groups. These biological processes include skin development, epidermis development, epidermal differentiation, keratinocyte differentiation, keratinization, and cornification. Similarly, B[a]PvsControl and TCDDvsControl groups also shared

similar downregulated biological processes that are involved in DNA and chromosomal functions. It is interesting that sebocyte progenitors committed to differentiate into lipid-producing cells developing into sebaceous gland organoids, upon exposure to B[a]P or TCDD are driving the expression of genes involved in terminal keratinocyte differentiation including keratinization and cornification. This is further supported by significant enrichment of keratinocyte differentiation (P value$<1^{-20}$) and keratinization (P value $<1^{-20}$) biological processes in B[a]PvsControl and TCDDvsControl (Figure 29).

The number of DEGs in B[a]PvsControl and TCDDvsControl that were enriched in keratinocytes differentiation were 72 and 64 respectively; in keratinization 62 and 54 respectively; in cornification 44 in both (Figure 30 and 31). The DEGs involved in these biological processes overlap with each other indicating the importance of the function of these genes in keratinocyte differentiation. Moreover, gene set enrichment analysis (GSEA) of DEGs highlighted positive enrichment in keratinocyte differentiation, keratinization, and cornification (Figure 32A). This suggests that sebocyte progenitors, upon exposure to B[a]P and TCDD, may initiate a 'behavioural switch' towards keratinocyte differentiation. When DEGs of B[a]P and TCDD were analyzed using REACTOME pathway database, it emerged that DEGs were highly enriched in pathways involved in keratinization and formation of cornified envelope (Figure 29). This is further supported by GSEA plots that showed positive enrichment of these pathways (Figure 33A).

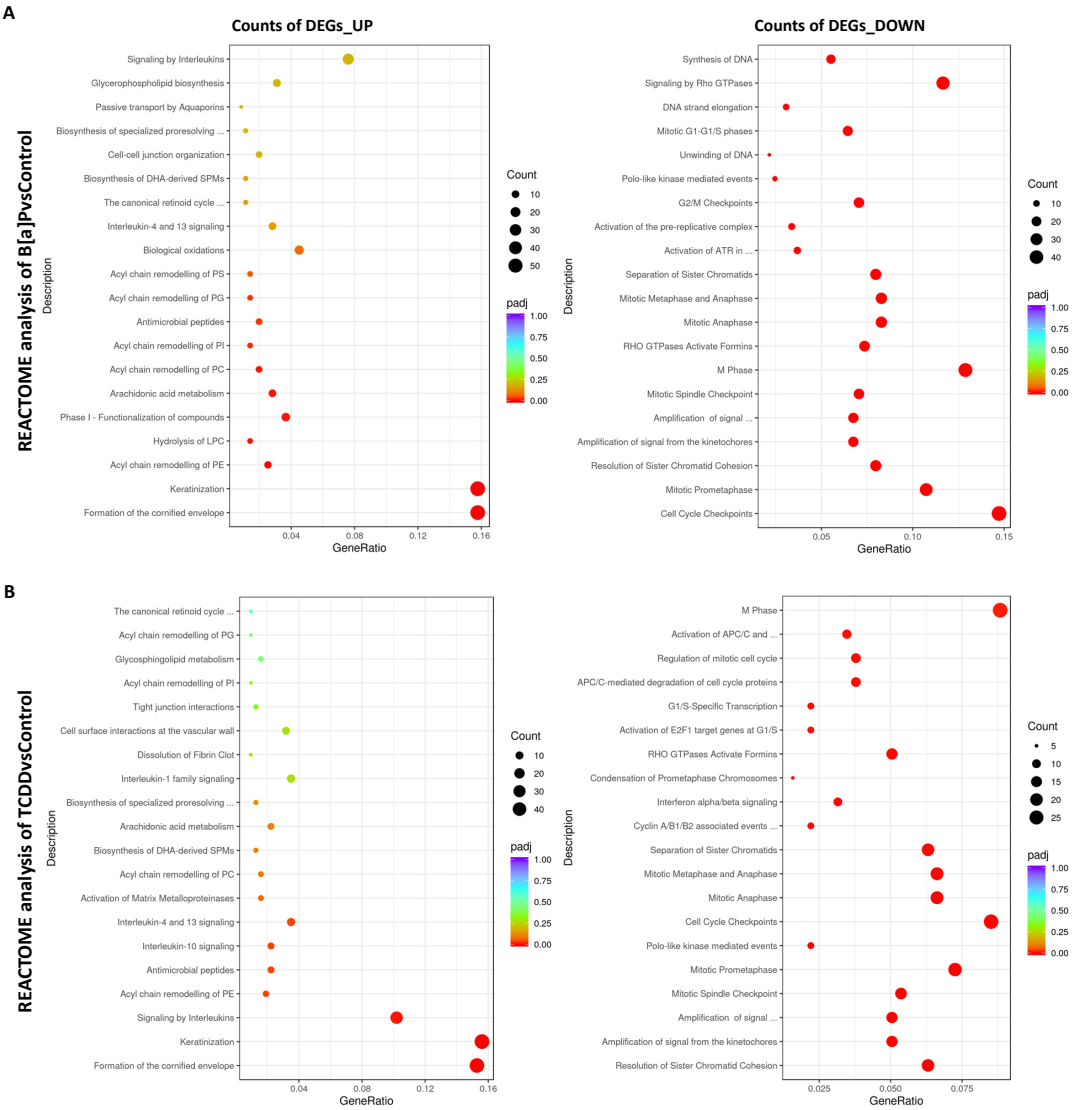

Figure 29. REACTOME analysis showing the top 20 pathways altered in sample groupings of B[a]PvsControl (A) and TCDDvsControl (B). Dot plot analysis displaying the count of DEGs involved in various processes that are significantly upregulated and downregulated in B[a]PvsControl and TCDDvsControl.

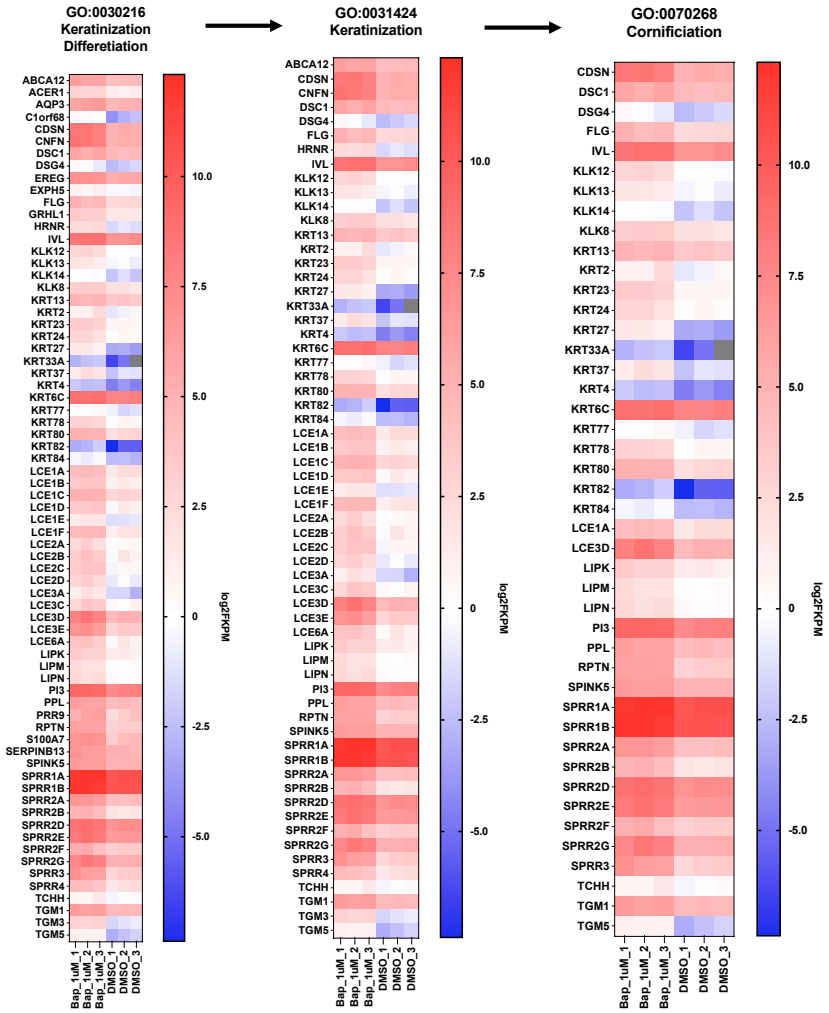

Figure 30. Gene ontology of differential expression genes (DEGs) from B[a]PvsControl revealed 'behavioral switch' of sebocyte progenitors toward keratinocyte terminal differentiation. Heatmap of DEGs significantly enriched in biological process of keratinocyte differentiation (GO:0030216) following keratinization (GO:0031421) and cornification (GO:0070268). Results are obtained from enrichment analysis of DEGs with Gene Ontology knowledgebase. Heatmap generated based on log2FKPM values as shown within the scale. Grey box represents no expression in sample.

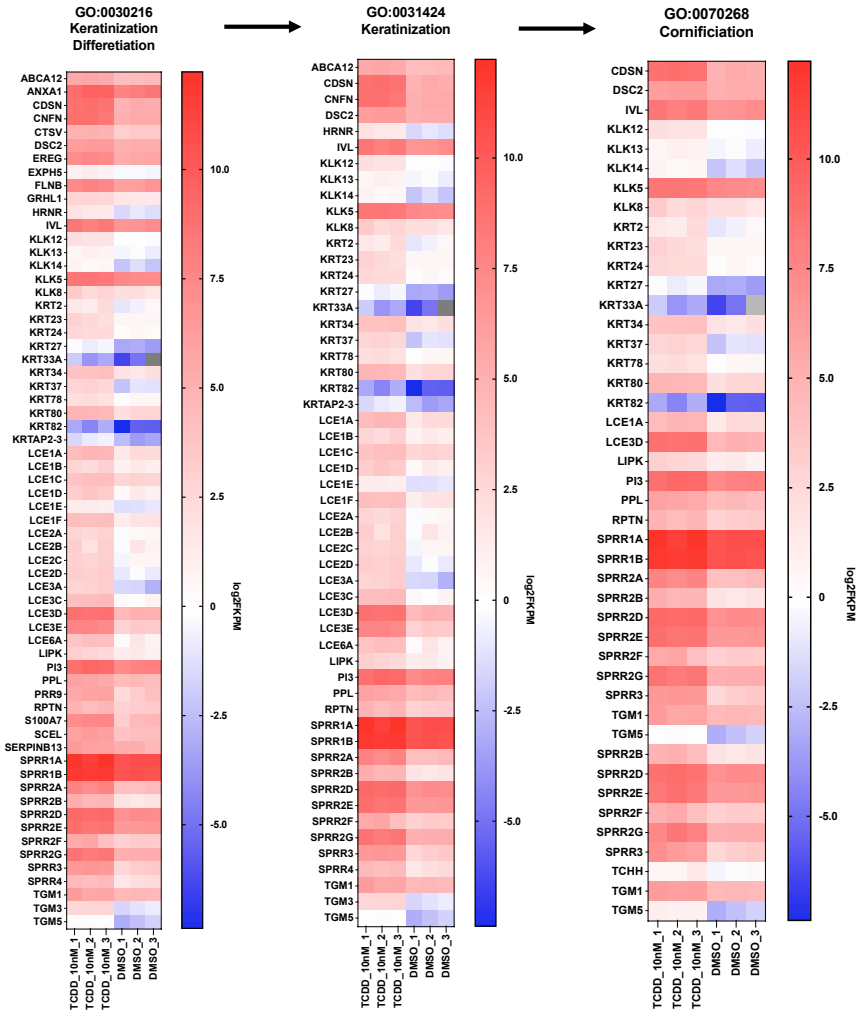

Figure 31. Gene ontology of differential expression genes (DEGs) from TCDDvsControl revealed 'behavioral switch' of sebocyte progenitors toward keratinocyte terminal differentiation. Heatmap of DEGs significantly enriched in biological process of keratinocyte differentiation (GO:0030216) following keratinization (GO:0031421) and cornification (GO:0070268). Results are obtained from enrichment analysis of DEGs with Gene Ontology knowledgebase. Heatmap generated based on log2FKPM values as shown within the scale. Grey box represents no expression in sample.

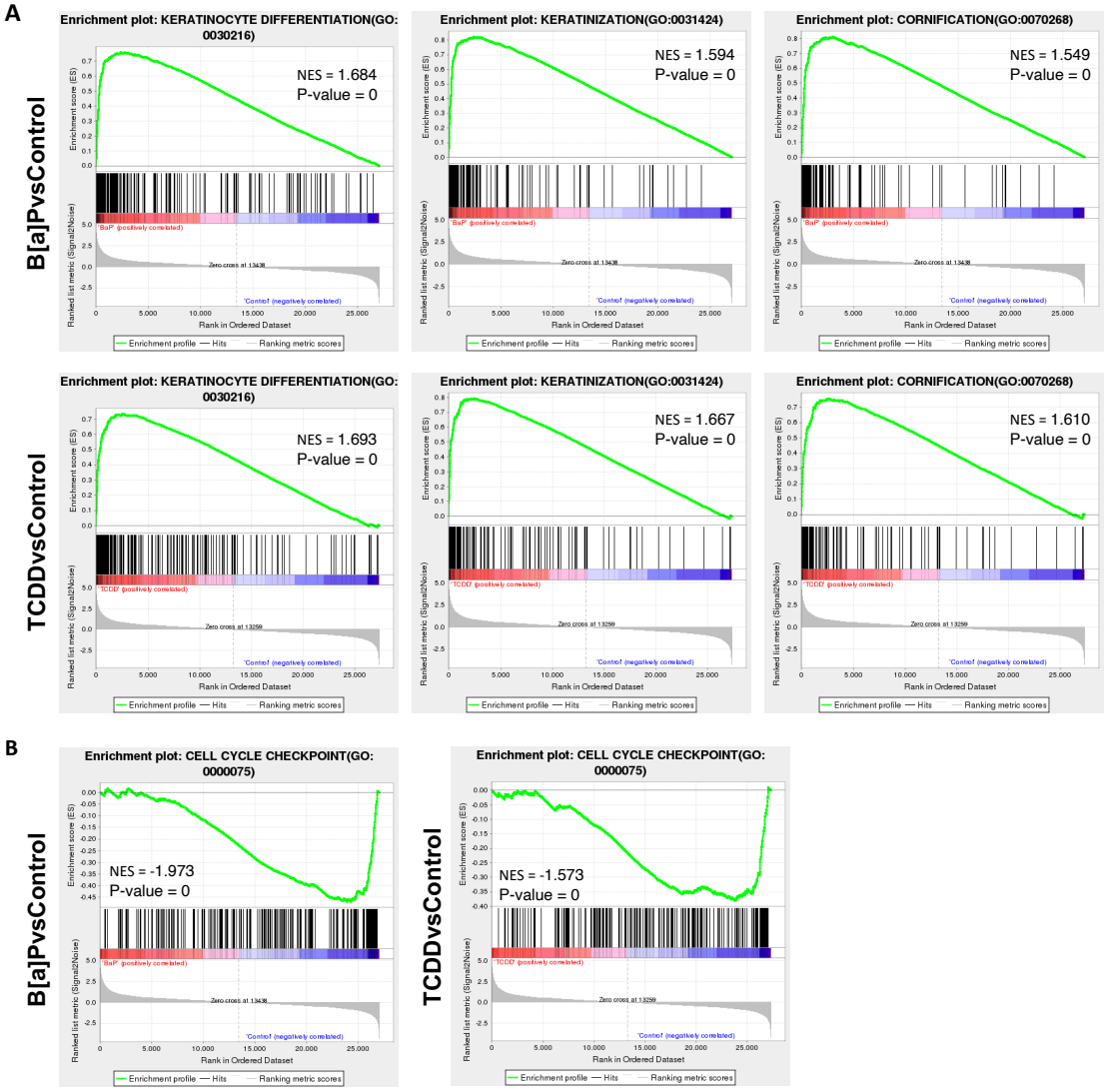

Figure 32. Gene Set Enrichment Analysis (GSEA) showed enrichment in biological processes supporting 'behavioural switch' in sebocyte progenitors exposed to B[a]P and TCDD. GSEA plots of B[a]PvsControl and TCDDvsControl showing positively enriched processes **(A)** and negatively enriched process **(B).** Positive normalized enrichment score (NES) showed DEGs upregulated in keratinocyte differentiation, keratinization and cornification and negative NES showed DEGs downregulated in cell cycle checkpoint in B[a]P and TCDD exposed samples.

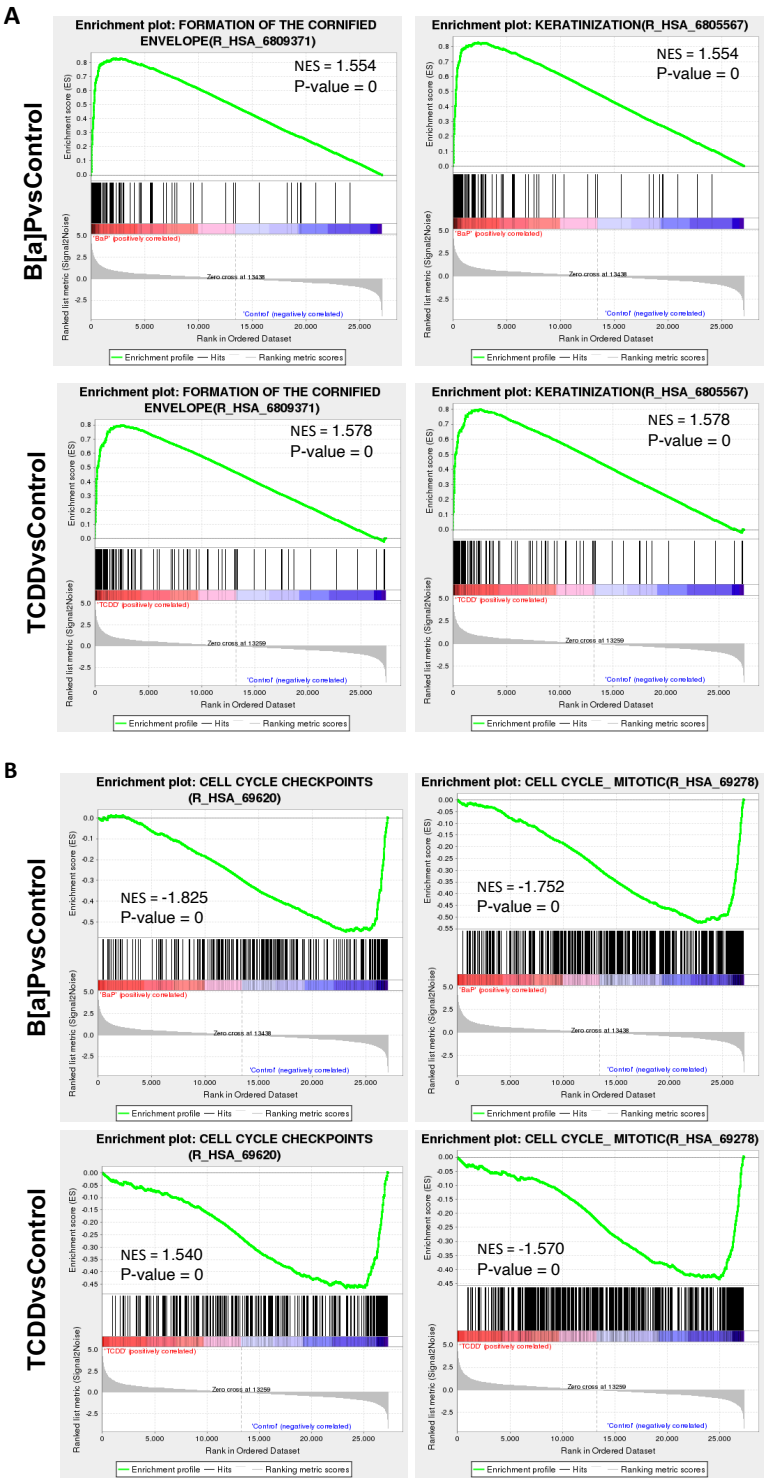

Figure 33. Gene Set Enrichment Analysis (GSEA) showed enrichment in biological pathway supporting 'behavioural switch' in sebocyte progenitors exposed to B[a]P and TCDD. GSEA plots of B[a]PvsControl and TCDDvsControl showing positive enrichment pathways **(A)** and negative enrichment pathways **(B).** Positive normalized enrichment score (NES) showed DEGs upregulated in the formation of the cornified envelope and keratinization, and negative NES showed DEGs downregulated in cell cycle checkpoints and mitotic cell cycle in B[a]P and TCDD exposed samples.

The enrichment in keratinocyte differentiation, keratinization, and formation of cornified envelope support the idea of B[a]P and TCDD exposure inducing a 'behavioural switch' in sebocyte progenitors. This suggestive 'behavioural switch' could also explain the loss of organoids during the maintenance phase whereby sebocyte progenitors that undergo this 'behavioural switch' will start expressing genes involved in keratinization, driving itself towards keratinocyte terminal differentiation. This depletes the progenitor pool leading to the eventual loss of organoids. This effect is more prominent during the developmental phase as sebocyte progenitors have yet to begin the development of organoids, thus the lack of both size and number. Moreover, this suggestive 'behavioural switch' towards keratinocyte terminal differentiation may have driven the consequences of DEGs negatively enriched in cell cycle related pathways instead of being an effect from B[a]P and TCDD (Figure 32B and 33B). Therefore, this analysis suggests the potential role of B[a]P and TCDD inducing a comedo-like switch in sebocyte progenitors.

Discussion

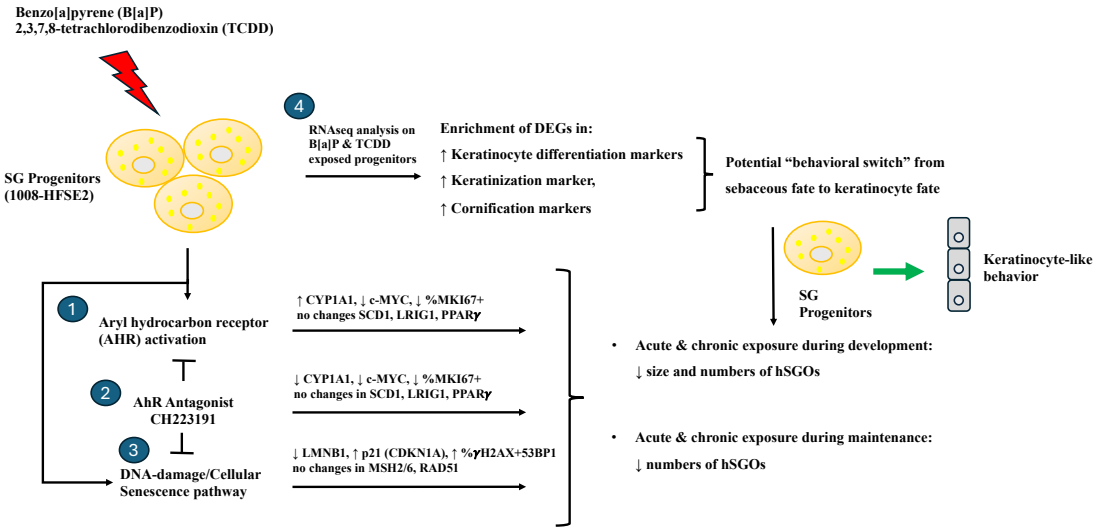

Figure 1. Illustration of the findings of this study. 1) 1008-HFSE2 SG progenitors exposed to B[a]P and TCDD triggers AHR activation with increased expression of CYP1A1, decreased proliferative capacity of progenitors via decreased in c-MYC expression and reduction in MKI67+ progenitors. This resulted in perturbed development and maintenance of hSGOs. 2) As AHR activation was thought to be the mechanistic process that drives hSGOs phenotype, inhibition of AHR activation through AHR antagonist (CH223191) should in theory rescue the phenotype. However, that was not the case even though CYP1A1 expression was decreased, indicating inhibition of AHR, the phenotype of hSGOs remains. 3) We explored DNA-damage and cellular senescence pathway as TCDD and B[a]P has been implicated as potential factors in affecting this pathway. Exposure to TCDD and B[a]P resulted in reduction of LMNB1 expression and increased p21 (CDKN1A) expression, while DNA damage markers MSH2/6, RAD51 showed no expression changes. Increased in %γH2AX+53BP1 suggests potential DNA damage induction. However, it remains inconclusive if DNA-damage and cellular senescence may play a role in hSGO phenotype observed. 4) In an effort to make sense of the data we have generated, RNAseq analysis of progenitors exposed to TCDD and B[a]P was performed. Data from RNAseq analysis corroborated with our own data and revealed a potential behavioral "switch" of cell fate in sebaceous progenitors to a keratinocyte-like behavior. This is supported by enrichment of DEGs in the biological processes of keratinocyte differentiation, keratinzation and cornification which represents keratinocyte cycle behavior in the epidermis. This suggestive "behavioral switch" could explain the loss of hSGOs after exposure to B[a]P and TCDD as progenitors are unable to maintain the hSGOs due to a cell fate switch.

Figure 1 above illustrates our findings in this study where it has tried to provide a mechanistic basis for the observed connection between pollution and acne, by examining the effects of known pollutants in cell culture systems that are relevant to acne pathogenesis. Our investigations have shown that B[a]P and TCDD may play a role in triggering a comedo-switch effect on sebaceous progenitors. Although AHR signaling pathway was thought to be the mechanistic driver of this switch, our data suggests otherwise leading to the exploration of other plausible mechanisms that could provide us an answer. This led us to look into the possibility of DNA damage and cellular senescence as a novel mechanism for acne pathogenesis as it has been reported that exposure to TCDD and B[a]P resulted in DNA damage and cellular senescence[174,176]. However, our experimental data is insufficient to suggest that cellular senescence may have caused the hSGOs phenotype observed and that cellular

senescence may play a role in acne pathogenesis. To make sense of our data and the phenotype observed, we performed RNAseq analysis of sebaceous progenitors exposed to TCDD and B[a]P. The data obtained from RNAseq analysis provided insights suggesting a potential role of TCDD and B[a]P in inducing a "behavioral switch" of sebaceous fate to keratinocyte fate by upregulating genes involved in keratinocyte terminal differentiation, keratinization and cornification process which are involved in development of epidermis[180]. This alteration of cell fate may explain the phenotype observed in exposed hSGOs even though the expression of sebaceous markers were not attenuated from the RNAseq data. Although the molecular pathway that is driving this "behavioral switch" remains elusive, our data provided new mechanistic insights that suggests a potential role of pollutants (in this case TCDD and B[a]P) in inducing comedo-switching in sebaceous progenitors. Further work needs to be done to ascertain this hypothesis.

An organoid is described to be a self-organized 3D tissue cell-based *in vitro* model that recapitulates aspects of complex structure and function of *in vivo* tissue[181]. These organoids can be derived from either pluripotent or tissue-specific resident stem or progenitor cells from healthy or diseased tissues, and are more accessible to manipulation and in-depth biological studies compared to animal models[182]. Our hSGOs are derived from primary sebocyte progenitors that were previously obtained from healthy facial skin tissue and maintained in a cell culture system void of genetic manipulation of the sebaceous progenitors. Embedding these progenitors into a Matrigel system with specific culture media components resulted in individual cells self-organizing (through proliferation and differentiation) into a hSGO that structurally resembles *in vivo* sebaceous glands. Human sebaceous glands are holocrine glands

within the dermis of the skin that produces lipid (sebum). It is structurally made-up of lipid-producing sebocytes (that are positive for differentiation markers such as FASN, SCD1, PPARγ) surrounded by a peripheral layer of proliferative progenitors (that are also marked by KRT14 and CD49f/ITGA6) that differentiates into sebocytes[183]. Our sebaceous gland organoids consisted of a peripheral layer of proliferative progenitors surrounding lipid-producing sebocytes that are positive for differentiation markers (Figure 1D and 10A). Therefore, these sebocyte progenitors can self-organized into lipid-producing hSGOs that structurally resembles *in vivo* sebaceous glands and can be used to study the effects of pollutants on sebaceous progenitors in relation to acne pathogenesis.

Even though the use of our 3D sebaceous gland organoid model system to study the effects of pollutants may have shed some insights into the effects of pollutants on organoid development and maintenance, there are still limitations to using organoids for disease modelling. Our organoid model lacked the heterogeneity of cell types and appendages (hair follicles, sweat glands, dermis, vascular structures etc.) to model a real human skin. The lack of such appendages may not fully encapsulate the dynamic effects of pollutants in relation to acne pathogenesis. The use of a skin organoid that include appendages such as a complete epidermis and hair follicle structure would make a more compelling model[184] to study acne pathogenesis. This would allow a comprehensive investigation into the effects of pollutants not only on the sebaceous glands, but how it would influence other compartments and what dynamics could be involved in the cross-talks between these different compartments. Although skin organoid is in continuous development to provide a more accurate model system for disease modelling and translational research, it still lacks inter-tissue communication, a

vasculature system, neural networks and immune clusters[185]. However, the use of skin organoids in future work for understanding acne pathogenesis and the comedo-switch mechanism may present a more complete picture of how pollutants may a role in these areas.

B[a]P is a common air pollutant that arises from any sources of incomplete combustion of fuels including cigarette smoke and daily household cooking, whereas TCDD is a dioxin that is produced from organic synthesis or fuel combustion and both pollutants are carcinogenic for humans. Our initial idea was to utilize particulate matter 2.5 ($PM_{2.5}$) as a pollutant to study the effects of AHR signaling pathway on human primary sebocyte progenitors and on the development and maintenance of hSGOs. However, $PM_{2.5}$ is a mixture of organic and inorganic compounds[186] that could elicit various effects including AHR activation[167], making it difficult to deconvolute the effects cause by AHR activation. Therefore, we decided to utilize TCDD and B[a]P, where B[a]P can be found in $PM_{2.5}$[187], and both are also known AHR ligands that can activate the AHR signaling pathway[170]. Although previous studies have shown that B[a]P and TCDD in various concentrations were not cytotoxic, the models that these compounds were tested on were either immortalized/primary keratinocytes or immortalized sebocytes[29,30,32,32,145–147,149]. As our study model uses human primary sebocyte progenitors and organoids derived from those, the cytotoxic effects of B[a]P and TCDD on our model needs to be ruled out (Figure 2 and 3) to ensure that any phenotype observed is specific to the action of the compounds of interests.

As demonstrated in this study, B[a]P and TCDD are not cytotoxic to primary sebocyte progenitors and can activate the AHR signaling pathway (Figure 4). Although no

discernable transcriptional changes were observed for the proliferation and differentiation of sebocyte progenitors in 2D cell culture (Figure 7 and 8), perturbations to the development and maintenance of hSGOs was reported (Figure 10). Transcriptional analysis of organoids did not reveal any significant expression changes to sebocyte differentiation markers but the proliferation of sebocyte progenitors was repressed by the downregulation of *c-MYC* expression (Figure 11). This suggests that AHR activation through TCDD and B[a]P may not modulate differentiation and lipogenesis in sebocytes although articles supporting this effect were reported[29,32,149]. These results also indicate that AHR activation, either through direct AHR transcriptional regulation or indirect influence associated with other transcriptional regulators[141], interferes with sebocyte progenitors from forming and maintaining organoids.

However, this notion was dismissed when AHR inhibition by CH223191 did not rescue the phenotype observed (Figure 13 and 14) even though AHR activation was clearly suppressed (Figure 12). The limitation of pharmacological inhibition of AHR activation lies with not being able to completely rule out the involvement of AHR as the use of genetic knockdown or knockout of AHR would have been ideal to demonstrate whether AHR is crucial for the phenotype observed in hSGOs. Nevertheless, suppressing AHR activation did not rescue the phenotype and thus we suspect there might be an alternate pathway other than AHR signaling causing the phenotype observed. As TCDD and B[a]P has been implicated in influencing DNA repair pathway resulting in DNA damage-induced cellular senescence[174–176], this presents a plausible alternate process that may drive the organoid phenotype we observed.

The idea of cellular senescence driving acne pathogenesis has not been explored and presents an exciting avenue as it might be a potential novel mechanism for acne pathogenesis and the use of anti-aging agents for acne treatment if validated. Moreover, AHR has also been implicated in the aging process by promoting cellular senescence through age-related remodelling of the immune system and oxidative stress[177], therefore AHR antagonists were used in the evaluation of DNA damage and cellular senescence by B[a]P and TCDD. Transcriptional analysis saw a slight reduction in DNA repair genes and significant changes to senescence markers (Figure 20A and 21). However, the impact of both pollutants on DNA damage-induced cellular senescence remains inconclusive due to the lack of evident loss of senescence marker, LMNB1 and proteins in the DNA repair pathway even though DNA damage was observed (Figure 20B-C, 22 and 23). Although DNA damage-induced cellular senescence was a potential mechanism driving organoid phenotype, it remains inconclusive due to the lack of evidence supporting it.

RNAseq analysis provided mechanistic insights on the effects of TCDD and B[a]P exposure to sebocyte progenitors. RNAseq analysis revealed significant transcriptomic changes in sebocyte progenitors which allowed the identification of possible biological processes that might be involved in the organoid phenotype we observed. Enrichment analysis in both GO and REACTOME highlighted two of the most enriched biological processes: keratinization and cornification/formation of the cornified envelope. These biological processes are involved in terminal differentiation of keratinocytes into corneocytes to form part of the cornified layer known as the stratum corneum. It involves in the cross-linking of proteins such as involucrin, loricrin and filaggrin with

keratin intermediate filaments and other cornified envelope proteins via transglutaminase family of enzymes to form an insoluble and tough structure known as the cornified envelope[188]. It forms the protective barrier of skin to prevent harmful external stimuli from entering the body. A deeper look into the DEGs revealed upregulation of genes that function in the process of keratinization and cornification (Figure 29 and 30). Genes expressing keratin intermediate filaments (KIF) proteins (KRT2/4/6C/13/23/24/27/33A/34/37/80/82/84) binds to cell-cell adhesion complexes such as desmosomes (DCS1/2, DSG4) to maintain the cytoskeletal integrity of keratinocytes[189]. KIF then cross-linked with filaggrin (FLG) to organize into bundles which stabilizes the keratin network, allowing the collapse and flattening of cells that contributes to the structure of corneocytes[188,190]. Together with periplakin (PPL), involucrin (IVL), small proline rich proteins (SPRR1A/B/C/D/E/F/2A/B/D/E/F/G/3/4/5), cornified envelope proteins (TCHH, PI3, RPTN, CDSN), transglutaminase family of enzymes (TGM1/3/5) and late cornified envelope gene cluster (LCE1A/B/C/D/E/F/2A/B/C/D/3A/C/D/E/6A) to form the components that construct the cornified envelope[188,190]. Moreover, genes such as SPINK5 (encodes lymho-epithelial Kazal-type related inhibitor 1) and KLK8/12/13/14 (serine proteases) involved in the desquamation processes of skin[191] were also upregulated, as were genes expressing keratinocyte lipases (LIKP/M/N) which are predicted to be involved in skin surface lipid metabolism[180]. Collectively, these upregulated genes represent the whole process of cornification from initiation to desquamation[190].

The enrichment of keratinization/cornification biological processes suggests a potential ‘behavioural switch’ of sebocyte progenitors from their normal differentiation, which may explain the loss of organoids (although not the reduction in

size) observed after exposure of B[a]P and TCDD during the maintenance phase. As hSGOs were considered developed and mature by the time of exposure, this potential 'switching' causes progenitors in affected organoids to stop maintenance (proliferation and differentiation of sebocytes), committing towards terminal keratinocyte differentiation which depletes the progenitor pool and eventually led to the loss of organoids. Similarly, early 'switching' of sebocyte progenitors towards terminal keratinocyte differentiation at the developmental phase can perturb the early development of hSGOs, resulting in both reduction in size and number of organoids formed. Although the expression of differentiation markers (*FASN, SCD1, PPARγ*) of hSGOs were not significantly altered (Figure 15 and 27), the upregulation of genes involved in terminal differentiation of keratinocytes (Figure 29 and 30) may suggest a 'switch' in commitment of sebocyte progenitors towards keratinization. This potential 'switch' would also explain the declined proliferative capacity of sebocyte progenitors as terminally differentiated cells would cease proliferation activity even though MYC expression was not attenuated from the RNAseq data (Figure 27). Therefore, it is likely that both B[a]P and TCDD may have a role in driving cell fate 'switch' from sebocytes to keratinocytes.

Several publications support the role of TCDD as a comedogenic agent but not for B[a]P. One publication reported a sebocyte 'switch' to keratinocyte after exposure to TCDD[32], while a dioxin case study reported how TCDD exposure in a patient saw the loss of sebaceous glands and comedo-like cyst formation in the hair follicle[31], suggesting a clear mechanistic connection between AHR signaling and comedogenesis. Moreover, Lrig1 sebaceous progenitors seem to be the target population that drives the formation of comedo-like cyst structures in a murine

model[31], supporting a role of TCDD inducing a comedo-like switch behavior in Lrig1 cells. Furthermore, TCDD has also been reported to accelerate epidermal barrier formation and increased gene expression of human epidermal differentiation complex in human epidermal keratinocytes[192]. Therefore, this study further supported the role of TCDD in driving a 'switch' of sebocyte progenitors towards a keratinocyte fate while for the first time demonstrating that B[a]P may also induce this 'switch'. Although AHR signaling as per our data does not seem to be involved with this 'switch' in the case of B[a]P, the molecular pathway that may flip this 'switch' remain elusive.

One pathway that could potentially modulate this comedo-switch would be the WNT signaling pathway. Our recent study in a transgenic mouse model have shown that aberrant Wnt signaling in the Lrig1 compartment of the mouse pilosebaceous unit resulted in atrophied sebaceous glands and formation of a comedo-like cyst structure[72]. This is informative and crucial because driving Wnt signaling in the Lrig1 compartment causes comedo-like lesions and a departure from sebaceous identity which corroborates with Saurat's comedo-switch hypothesis. Although RNAseq results revealed WNT ligands such as WNT3A/5B and WNT6/7A were downregulated in B[a]P and TCDD respectively and both WNT4 and WNT10A were downregulated in both groups (Supplementary Table 1 and 2), there is no clear indication that WNT signaling is affected. Perhaps future research into the WNT signaling pathway using our hSGO model might further elucidate the role of WNT signaling in comedogenesis in acne pathogenesis.

Future work into elucidating the mechanisms of acne pathogenesis or this "behavioural switch" in our model system (or future skin organoid model) should utilise techniques such as single-cell transcriptomics (scRNAseq) and spatial transcriptomic analysis[193–195]. ScRNAseq and spatial transcriptomics are powerful tools to dissect disease pathophysiology at high resolution by assessing cell-to-cell variation. A recent study employed these techniques to analyse early papules taken from six patients with active acne and reported of gene changes associated with early-stage acne-skin[196]. The study looked at cellular dynamics across seven different cell types and identified alterations in 49 signaling pathways including pathways that govern proinflammatory responses and keratinization processes. The use of scRNAseq and spatial transcriptomics to assess the effects of pollutants on sebaceous or skin organoids could potentially further support the 'behavioural switch' of sebaceous progenitors and have the potential to uncover additional signaling pathways and molecular targets that may be explore as potential new treatments options.

Conclusion

The comedo-switch hypothesis for acne proposed a cell fate 'switch' of 'stem cells'/progenitors that reside in the junctional zone of the hair follicle, driving towards infundibulum cell fate (keratinocytes) instead of sebaceous gland fate (sebocytes). In this study, we caught a glimpse of such 'switching' of sebocyte progenitors towards keratinocytes from the exposure to B[a]P and TCDD. Moreover, both B[a]P and TCDD may drive comedogenesis by upregulating genes involved in terminal differentiation of keratinocytes towards keratinization although proliferation was not affected. This may explain the higher incidence of acne outpatient visits and exacerbation of acne symptoms in populations living in high pollution urban environments[24]. Although an indicative molecular pathway was not elucidated in this 'switching' process, this study supported the role of TCDD in comedogenesis and presented for the first-time that B[a]P may play a potential role in the comedo-switch of sebocyte progenitors. This highlights the importance of this key process in acne pathogenesis and further research in this area to unravel the molecular pathway that drives the comedo-switch process would advance development of new treatments.

References

1. Hay RJ, Johns NE, Williams HC, et al. The global burden of skin disease in 2010: An analysis of the prevalence and impact of skin conditions. *J Invest Dermatol*. 2014;134(6):1527-1534. doi:10.1038/jid.2013.446

2. Tan JKL, Bhate K. A global perspective on the epidemiology of acne. *Br J Dermatol*. 2015;172(S1):3-12. doi:https://doi.org/10.1111/bjd.13462

3. Cunliffe WJ, Gould DJ. Prevalence of facial acne vulgaris in late adolescence and in adults. *Br Med J*. 1979;1(6171):1109-1110. doi:10.1136/bmj.1.6171.1109

4. Tan HH, Tan AWH, Barkham T, Yan XY, Zhu M. Community-based study of acne vulgaris in adolescents in Singapore. *Br J Dermatol*. 2007;157(3):547-551. doi:https://doi.org/10.1111/j.1365-2133.2007.08087.x

5. Shen Y, Wang T, Zhou C, et al. Prevalence of acne vulgaris in Chinese adolescents and adults: A community-based study of 17,345 subjects in six cities. *Acta Derm Venereol*. 2012;92(1):40-44. doi:10.2340/00015555-1164

6. Goulden V, Stables GI, Cunliffe WJ. Prevalence of facial acne in adults. *J Am Acad Dermatol*. 1999;41(4):577-580. doi:10.1016/S0190-9622(99)80056-5

7. Williams HC, Dellavalle RP, Garner S. Acne vulgaris. *The Lancet*. 2012;379(9813):361-372. doi:10.1016/S0140-6736(11)60321-8

8. Cunliffe WJ. Acne and unemployment. *Br J Dermatol*. 1986;115(3):386-386. doi:https://doi.org/10.1111/j.1365-2133.1986.tb05757.x

9. Bhate K, Williams HC. Epidemiology of acne vulgaris. *Br J Dermatol*. 2013;168(3):474-485. doi:https://doi.org/10.1111/bjd.12149

10. Smithard A, Glazebrook C, Williams HC. Acne prevalence, knowledge about acne and psychological morbidity in mid-adolescence: a community-based study. *Br J Dermatol*. 2001;145(2):274-279. doi:https://doi.org/10.1046/j.1365-2133.2001.04346.x

11. Bickers DR, Lim HW, Margolis D, et al. The burden of skin diseases: 2004: A joint project of the American Academy of Dermatology Association and the Society for Investigative Dermatology. *J Am Acad Dermatol*. 2006;55(3):490-500. doi:10.1016/j.jaad.2006.05.048

12. Common JEA, Barker JN, van Steensel MAM. What does acne genetics teach us about disease pathogenesis? *Br J Dermatol*. 2019;181(4):665-676. doi:10.1111/bjd.17721

13. Saurat JH. Strategic Targets in Acne: The Comedone Switch in Question. *Dermatology*. 2015;231(2):105-111. doi:10.1159/000382031

14. Zouboulis CC, Eady A, Philpott M, et al. What is the pathogenesis of acne? *Exp Dermatol*. 2005;14(2):143-143. doi:https://doi.org/10.1111/j.0906-6705.2005.0285a.x

15. Dréno B. What is new in the pathophysiology of acne, an overview. *J Eur Acad Dermatol Venereol*. 2017;31(S5):8-12. doi:https://doi.org/10.1111/jdv.14374

16. Dréno B, Bettoli V, Araviiskaia E, Sanchez Viera M, Bouloc A. The influence of exposome on acne. *J Eur Acad Dermatol Venereol*. 2018;32(5):812-819. doi:10.1111/jdv.14820

17. Navarini AA, Simpson MA, Weale M, et al. Genome-wide association study identifies three novel susceptibility loci for severe Acne vulgaris. *Nat Commun*. 2014;5(1):4020. doi:10.1038/ncomms5020

18. Lichtenberger R, Simpson MA, Smith C, Barker J, Navarini AA. Genetic architecture of acne vulgaris. *J Eur Acad Dermatol Venereol*. 2017;31(12):1978-1990. doi:https://doi.org/10.1111/jdv.14385

19. Hecht H. Hereditary trends in acne vulgaris. Prevention of acne. *Dermatologica*. 1960;121:297-307. doi:10.1159/000255280

20. Friedman GD. Twin studies of disease heritability based on medical records: application to acne vulgaris. *Acta Genet Med Gemellol (Roma)*. 1984;33(3):487-495. doi:10.1017/s0001566000005948

21. Mina-Vargas A, Colodro-Conde L, Grasby K, et al. Heritability and GWAS Analyses of Acne in Australian Adolescent Twins. *Twin Res Hum Genet*. 2017;20(6):541-549. doi:10.1017/thg.2017.58

22. Common J e. a., Barker J n., van Steensel M a. m. What does acne genetics teach us about disease pathogenesis? *Br J Dermatol*. 2019;181(4):665-676. doi:10.1111/bjd.17721

23. Petridis C, Navarini AA, Dand N, et al. Genome-wide meta-analysis implicates mediators of hair follicle development and morphogenesis in risk for severe acne. *Nat Commun*. 2018;9(1):5075. doi:10.1038/s41467-018-07459-5

24. Krutmann J, Moyal D, Liu W, et al. Pollution and acne: is there a link? *Clin Cosmet Investig Dermatol*. 2017;10:199-204. doi:10.2147/CCID.S131323

25. Al-Shobaili HA, Alzolibani AA, Al Robaee AA, Meki AMA, Rasheed Z. Biochemical Markers of Oxidative and Nitrosative Stress in Acne Vulgaris: Correlation With Disease Activity. *J Clin Lab Anal*. 2013;27(1):45-52. doi:10.1002/jcla.21560

26. Kardeh S, Moein SA, Namazi MR, Kardeh B. Evidence for the Important Role of Oxidative Stress in the Pathogenesis of Acne. *Galen Med J*. 2019;8(0):1291. doi:10.31661/gmj.v8i0.1291

27. Tsuji G, Takahara M, Uchi H, et al. An environmental contaminant, benzo(a)pyrene, induces oxidative stress-mediated interleukin-8 production in human keratinocytes via the aryl hydrocarbon receptor signaling pathway. *J Dermatol Sci*. 2011;62(1):42-49. doi:10.1016/j.jdermsci.2010.10.017

28. Fabbrocini G, Kaya G, Silverio PC, et al. Aryl Hydrocarbon Receptor Activation in Acne Vulgaris Skin: A Case Series from the Region of Naples, Italy. *Dermatology*. 2015;231(4):334-338. doi:10.1159/000439402

29. Hu T, Pan Z, Yu Q, et al. Benzo(a)pyrene induces interleukin (IL)-6 production and reduces lipid synthesis in human SZ95 sebocytes via the aryl hydrocarbon receptor signaling pathway. *Environ Toxicol Pharmacol*. 2016;43:54-60. doi:10.1016/j.etap.2016.02.011

30. Bock KW. 2,3,7,8-Tetrachlorodibenzo-p-dioxin (TCDD)-mediated deregulation of myeloid and sebaceous gland stem/progenitor cell homeostasis. *Arch Toxicol*. 2017;91(6):2295-2301. doi:10.1007/s00204-017-1965-2

31. Fontao F, Barnes L, Kaya G, Saurat JH, Sorg O. From the Cover: High Susceptibility of Lrig1 Sebaceous Stem Cells to TCDD in Mice. *Toxicol Sci*. 2017;160(2):230-243. doi:10.1093/toxsci/kfx179

32. Ju Q, Fimmel S, Hinz N, Stahlmann R, Xia L, Zouboulis CC. 2,3,7,8-Tetrachlorodibenzo-p-dioxin alters sebaceous gland cell differentiation in vitro. *Exp Dermatol*. 2011;20(4):320-325. doi:10.1111/j.1600-0625.2010.01204.x

33. Tuchayi SM, Makrantonaki E, Ganceviciene R, Dessinioti C, Feldman SR, Zouboulis CC. Acne vulgaris. *Nat Rev Dis Primer*. 2015;1(1):1-20. doi:10.1038/nrdp.2015.29

34. Kraft J, Freiman A. Management of acne. *CMAJ*. 2011;183(7):E430-E435. doi:10.1503/cmaj.090374

35. Vos T, Flaxman AD, Naghavi M, et al. Years lived with disability (YLDs) for 1160 sequelae of 289 diseases and injuries 1990–2010: a systematic analysis for the Global Burden of Disease Study 2010. *The Lancet*. 2012;380(9859):2163-2196. doi:10.1016/S0140-6736(12)61729-2

36. Heng AHS, Chew FT. Systematic review of the epidemiology of acne vulgaris. *Sci Rep*. 2020;10(1):5754. doi:10.1038/s41598-020-62715-3

37. Tan HH, Tan AWH, Barkham T, Yan XY, Zhu M. Community-based study of acne vulgaris in adolescents in Singapore. *Br J Dermatol*. 2007;157(3):547-551. doi:10.1111/j.1365-2133.2007.08087.x

38. Shen Y, Wang T, Zhou C, et al. Prevalence of acne vulgaris in Chinese adolescents and adults: A community-based study of 17,345 subjects in six cities. *Acta Derm Venereol*. 2012;92(1):40-44. doi:10.2340/00015555-1164

39. Yeung CK, Teo LynnHY, Lei HX, Chan HHL. A Community-based Epidemiological Study of Acne Vulgaris in Hong Kong Adolescents. doi:10.1080/00015550252948121

40. Muthupalaniappen di L, Tan HC, Puah JWD, et al. Acne prevalence, severity and risk factos among medical students in Malaysia. Accessed December 31, 2020. http://www.seu-roma.it/riviste/clinica_terapeutica/apps/autos.php?id=1339

41. Yahya H. Acne vulgaris in Nigerian adolescents – prevalence, severity, beliefs, perceptions, and practices - Yahya - 2009 - International Journal of Dermatology - Wiley Online Library. Accessed December 31, 2020. https://onlinelibrary.wiley.com/doi/full/10.1111/j.1365-4632.2009.03922.x

42. Aksu AEK, Metintas S, Saracoglu ZN, et al. Acne: prevalence and relationship with dietary habits in Eskisehir, Turkey. *J Eur Acad Dermatol Venereol*. 2012;26(12):1503-1509. doi:https://doi.org/10.1111/j.1468-3083.2011.04329.x

43. Alanazi MS, Hammad SM, Mohamed AE. Prevalence and psychological impact of Acne vulgaris among female secondary school students in Arar city, Saudi Arabia, in 2018. *Electron Physician*. 2018;10(8):7224-7229. doi:10.19082/7224

44. Freyre EA, Rebaza RM, Sami DA, Lozada CP. The prevalence of facial acne in Peruvian adolescents and its relation to their ethnicity - Journal of Adolescent Health. Accessed December 31, 2020. https://www.jahonline.org/article/S1054-139X(97)00277-2/fulltext

45. Lynn DD, Umari T, Dunnick CA, Dellavalle RP. The epidemiology of acne vulgaris in late adolescence. *Adolesc Health Med Ther*. 2016;7:13-25. doi:10.2147/AHMT.S55832

46. Augustin M, Herberger K, Hintzen S, Heigel H, Franzke N, Schäfer I. Prevalence of skin lesions and need for treatment in a cohort of 90 880 workers. *Br J Dermatol*. 2011;165(4):865-873. doi:10.1111/j.1365-2133.2011.10436.x

47. Abdel-Hafez K, Abdel-Aty MA, Hofny ERM. Prevalence of skin diseases in rural areas of Assiut Governorate, Upper Egypt. *Int J Dermatol*. 2003;42(11):887-892. doi:10.1046/j.1365-4362.2003.01936.x

48. A COMPREHENSIVE REVIEW ON ACNE, ITS PATHOGENESIS, TREATMENT, IN-VITRO AND IN-VIVO MODELS FOR INDUCTION AND EVALUATION METHODS | INTERNATIONAL JOURNAL OF PHARMACEUTICAL SCIENCES AND RESEARCH. June 30, 2019. Accessed July 11, 2023. https://ijpsr.com/bft-article/a-comprehensive-review-on-acne-its-pathogenesis-treatment-in-vitro-and-in-vivo-models-for-induction-and-evaluation-methods/

49. Rocha MA, Bagatin E. Adult-onset acne: prevalence, impact, and management challenges. *Clin Cosmet Investig Dermatol*. 2018;11:59-69. doi:10.2147/CCID.S137794

50. Skroza N, Tolino E, Mambrin A, et al. Adult Acne Versus Adolescent Acne. *J Clin Aesthetic Dermatol*. 2018;11(1):21-25.

51. Collier CN, Harper JC, Cantrell WC, Wang W, Foster KW, Elewski BE. The prevalence of acne in adults 20 years and older. *J Am Acad Dermatol*. 2008;58(1):56-59. doi:10.1016/j.jaad.2007.06.045

52. Goulden V, Clark SM, Cunliffe WJ. Post-adolescent acne: a review of clinical features. *Br J Dermatol*. 1997;136(1):66-70. doi:https://doi.org/10.1046/j.1365-2133.1997.d01-1144.x

53. Power M, Quinn K, Schmidt S, WHOQOL-OLD Group. Development of the WHOQOL-Old Module. *Qual Life Res*. 2005;14(10):2197-2214. doi:10.1007/s11136-005-7380-9

54. Evaluation of the prevalence, risk factors, clinical characteristics, and burden of acne scars among active acne patients in Brazil, France, and the USA. *J Am Acad Dermatol*. 2017;76(6):AB132. doi:10.1016/j.jaad.2017.04.518

55. Tan J, Kang S, Leyden J. Prevalence and Risk Factors of Acne Scarring Among Patients Consulting Dermatologists in the US. *J Drugs Dermatol*. 2017;16(2):97-102.

56. LAYTON AM, HENDERSON CA, CUNLIFFE WJ. A clinical evaluation of acne scarring and its incidence. *Clin Exp Dermatol*. 1994;19(4):303-308. doi:10.1111/j.1365-2230.1994.tb01200.x

57. Tan JKL, Tang J, Fung K, et al. Development and Validation of a Scale for Acne Scar Severity (SCAR-S) of the Face and Trunk. *J Cutan Med Surg*. 2010;14(4):156-160. doi:10.2310/7750.2010.09037

58. Dréno B, Tan J, Kang S, et al. How People with Facial Acne Scars are Perceived in Society: an Online Survey. *Dermatol Ther*. 2016;6(2):207-218. doi:10.1007/s13555-016-0113-x

59. McCabe RE, Antony MM, Summerfeldt LJ, Liss A, Swinson RP. Preliminary Examination of the Relationship Between Anxiety Disorders in Adults and Self-Reported History of Teasing or Bullying Experiences. *Cogn Behav Ther*. 2003;32(4):187-193. doi:10.1080/16506070310005051

60. Smith H, Layton AM, Thiboutot D, et al. Identifying the Impacts of Acne and the Use of Questionnaires to Detect These Impacts: A Systematic Literature Review. *Am J Clin Dermatol*. 2021;22(2):159-171. doi:10.1007/s40257-020-00564-6

61. Magin P, Adams J, Heading G, Pond D, Smith W. Psychological sequelae of acne vulgaris: results of a qualitative study. *Can Fam Physician*. 2006;52(8):978-979.

62. Lasek RJ, Chren MM. Acne Vulgaris and the Quality of Life of Adult Dermatology Patients. *Arch Dermatol*. 1998;134(4):454-458. doi:10.1001/archderm.134.4.454

63. Jowett S, Ryan T. Skin disease and handicap: An analysis of the impact of skin conditions. *Soc Sci Med*. 1985;20(4):425-429. doi:10.1016/0277-9536(85)90021-8

64. Zaenglein AL, Pathy AL, Schlosser BJ, et al. Guidelines of care for the management of acne vulgaris. *J Am Acad Dermatol*. 2016;74(5):945-973.e33. doi:10.1016/j.jaad.2015.12.037

65. Cunliffe WJ, Holland DB, Jeremy A. Comedone formation: Etiology, clinical presentation, and treatment. *Clin Dermatol*. 2004;22(5):367-374. doi:10.1016/j.clindermatol.2004.03.011

66. Saurat JH, Kaya G, Saxer-Sekulic N, et al. The Cutaneous Lesions of Dioxin Exposure: Lessons from the Poisoning of Victor Yushchenko. *Toxicol Sci*. 2012;125(1):310-317. doi:10.1093/toxsci/kfr223

67. Everts HB. Endogenous retinoids in the hair follicle and sebaceous gland. *Biochim Biophys Acta BBA - Mol Cell Biol Lipids*. 2012;1821(1):222-229. doi:10.1016/j.bbalip.2011.08.017

68. Rollman O, Vahlquist A. Vitamin A in skin and serum--studies of acne vulgaris, atopic dermatitis, ichthyosis vulgaris and lichen planus. *Br J Dermatol*. 1985;113(4):405-413. doi:10.1111/j.1365-2133.1985.tb02354.x

69. Contassot E, French LE. New Insights into Acne Pathogenesis: Propionibacterium Acnes Activates the Inflammasome. *J Invest Dermatol*. 2014;134(2):310-313. doi:10.1038/jid.2013.505

70. Frances D, Niemann C. Stem cell dynamics in sebaceous gland morphogenesis in mouse skin. *Dev Biol*. 2012;363(1):138-146. doi:10.1016/j.ydbio.2011.12.028

71. Clayton RW, Göbel K, Niessen CM, Paus R, Steensel MAM van, Lim X. Homeostasis of the sebaceous gland and mechanisms of acne pathogenesis. *Br J Dermatol*. 2019;181(4):677-690. doi:https://doi.org/10.1111/bjd.17981

72. W S, Ayq T, Mam van S, X L. Aberrant Wnt Signaling Induces Comedo-Like Changes in the Murine Upper Hair Follicle. *J Invest Dermatol*. 2022;142(10). doi:10.1016/j.jid.2021.11.034

73. Niemann C, Horsley V. Development and homeostasis of the sebaceous gland. *Semin Cell Dev Biol*. 2012;23(8):928-936. doi:10.1016/j.semcdb.2012.08.010

74. Jensen KB, Collins CA, Nascimento E, et al. Lrig1 Expression Defines a Distinct Multipotent Stem Cell Population in Mammalian Epidermis. *Cell Stem Cell*. 2009;4(5):427-439. doi:10.1016/j.stem.2009.04.014

75. Common JEA, Barker JN, Steensel MAM van. What does acne genetics teach us about disease pathogenesis? *Br J Dermatol*. 2019;181(4):665-676. doi:https://doi.org/10.1111/bjd.17721

76. Dréno B, Pécastaings S, Corvec S, Veraldi S, Khammari A, Roques C. Cutibacterium acnes (Propionibacterium acnes) and acne vulgaris: a brief look at the latest updates. *J Eur Acad Dermatol Venereol*. 2018;32(S2):5-14. doi:10.1111/jdv.15043

77. McDowell A, Barnard E, Nagy I, et al. An Expanded Multilocus Sequence Typing Scheme for Propionibacterium acnes: Investigation of 'Pathogenic', 'Commensal' and Antibiotic Resistant Strains. *PLOS ONE*. 2012;7(7):e41480. doi:10.1371/journal.pone.0041480

78. Beylot C, Auffret N, Poli F, et al. Propionibacterium acnes: an update on its role in the pathogenesis of acne. *J Eur Acad Dermatol Venereol*. 2014;28(3):271-278. doi:10.1111/jdv.12224

79. Lheure C, Grange PA, Ollagnier G, et al. TLR-2 Recognizes Propionibacterium acnes CAMP Factor 1 from Highly Inflammatory Strains. *PLOS ONE*. 2016;11(11):e0167237. doi:10.1371/journal.pone.0167237

80. Bek-Thomsen M, Lomholt HB, Scavenius C, Enghild JJ, Brüggemann H. Proteome Analysis of Human Sebaceous Follicle Infundibula Extracted from Healthy and Acne-Affected Skin. *PLOS ONE*. 2014;9(9):e107908. doi:10.1371/journal.pone.0107908

81. Oyewole AO, Birch-Machin MA. Sebum, inflammasomes and the skin: current concepts and future perspective. *Exp Dermatol*. 2015;24(9):651-654. doi:10.1111/exd.12774

82. Shu M, Kuo S, Wang Y, et al. Porphyrin metabolisms in human skin commensal Propionibacterium acnes bacteria: potential application to monitor human radiation risk. *Curr Med Chem*. 2013;20(4):562-568. doi:10.2174/0929867311320040007

83. Johnson T, Kang D, Barnard E, Li H. Strain-Level Differences in Porphyrin Production and Regulation in Propionibacterium acnes Elucidate Disease Associations. *mSphere*. 2016;1(1):e00023-15. doi:10.1128/mSphere.00023-15

84. Scholz CFP, Brüggemann H, Lomholt HB, Tettelin H, Kilian M. Genome stability of Propionibacterium acnes: a comprehensive study of indels and homopolymeric tracts. *Sci Rep*. 2016;6(1):20662. doi:10.1038/srep20662

85. Nazipi S, Stødkilde K, Scavenius C, Brüggemann H. The Skin Bacterium Propionibacterium acnes Employs Two Variants of Hyaluronate Lyase with Distinct Properties. *Microorganisms*. 2017;5(3):57. doi:10.3390/microorganisms5030057

86. Lai JJ, Chang P, Lai KP, Chen L, Chang C. The Role of Androgen and Androgen Receptor in the Skin-Related Disorders. *Arch Dermatol Res*. 2012;304(7):499-510. doi:10.1007/s00403-012-1265-x

87. Breehl L, Caban O. Physiology, Puberty. In: *StatPearls*. StatPearls Publishing; 2023. Accessed July 17, 2023. http://www.ncbi.nlm.nih.gov/books/NBK534827/

88. Chen W, Zouboulis CC, Fritsch M, et al. Evidence of heterogeneity and quantitative differences of the type 1 5alpha-reductase expression in cultured human skin cells--evidence of its presence in melanocytes. *J Invest Dermatol*. 1998;110(1):84-89. doi:10.1046/j.1523-1747.1998.00080.x

89. Fritsch M, Orfanos CE, Zouboulis CC. Sebocytes are the key regulators of androgen homeostasis in human skin. *J Invest Dermatol*. 2001;116(5):793-800. doi:10.1046/j.1523-1747.2001.01312.x

90. Choudhry R, Hodgins MB, Kwast THV der, Brinkmann AO, Boersma WJA. Localization of androgen receptors in human skin by immunohistochemistry: implications for the hormonal regulation of hair growth, sebaceous glands and sweat glands. *J Endocrinol*. 1992;133(3):467-NP. doi:10.1677/joe.0.1330467

91. Pochi PE, Strauss JS. Endocrinologic control of the development and activity of the human sebaceous gland. *J Invest Dermatol*. 1974;62(3):191-201. doi:10.1111/1523-1747.ep12676783

92. Cottle DL, Kretzschmar K, Schweiger PJ, et al. c-MYC-Induced Sebaceous Gland Differentiation Is Controlled by an Androgen Receptor/p53 Axis. *Cell Rep*. 2013;3(2):427-441. doi:10.1016/j.celrep.2013.01.013

93. Akamatsu Hirohiko, Zouboulis CC, Orfanos CE. Control of Human Sebocyte Proliferation In Vitro by Testosterone and 5-Alpha-Dihydrotestosterone Is Dependent on the Localization of the Sebaceous Glands. *J Invest Dermatol*. 1992;99(4):509-511. doi:10.1111/1523-1747.ep12616181

94. Fujie T, Shikiji T, Uchida N, Urano Y, Nagae H, Arase S. Culture of cells derived from the human sebaceous gland under serum-free conditions without a biological feeder layer or specific matrices. *Arch Dermatol Res*. 1996;288(11):703-708. doi:10.1007/BF02505281

95. Ebling FJ, Ebling E, Skinner J. THE INFLUENCE OF PITUITARY HORMONES ON THE RESPONSE OF THE SEBACEOUS GLANDS OF THE MALE RAT TO TESTOSTERONE. *J Endocrinol*. 1969;45(2):245-256. doi:10.1677/joe.0.0450245

96. Petersen MJ, Zone JJ, Krueger GG. Development of a nude mouse model to study human sebaceous gland physiology and pathophysiology. *J Clin Invest*. 1984;74(4):1358-1365. doi:10.1172/JCI111546

97. Rosignoli C, Nicolas JC, Jomard a, Michel S. Involvement of the SREBP pathway in the mode of action of androgens in sebaceous glands in vivo. *Exp Dermatol*. 2003;12(4):480-489. doi:10.1034/j.1600-0625.2003.00014.x

98. Makrantonaki E, Vogel K, Fimmel S, Oeff M, Seltmann H, Zouboulis CC. Interplay of IGF-I and 17beta-estradiol at age-specific levels in human sebocytes and fibroblasts in vitro. *Exp Gerontol*. 2008;43(10):939-946. doi:10.1016/j.exger.2008.07.005

99. Deplewski D, Rosenfield RL. Growth hormone and insulin-like growth factors have different effects on sebaceous cell growth and differentiation. *Endocrinology*. 1999;140(9):4089-4094. doi:10.1210/endo.140.9.6957

100. Rudman SM, Philpott MP, Thomas GA, Kealey T. The role of IGF-I in human skin and its appendages: morphogen as well as mitogen? *J Invest Dermatol*. 1997;109(6):770-777. doi:10.1111/1523-1747.ep12340934

101. Smith TM, Gilliland K, Clawson GA, Thiboutot D. IGF-1 Induces SREBP-1 Expression and Lipogenesis in SEB-1 Sebocytes via Activation of the Phosphoinositide 3-Kinase / Akt Pathway. 2008;128:1286-1293. doi:10.1038/sj.jid.5701155

102. Makrantonaki E, Ganceviciene R, Zouboulis CC. An update on the role of the sebaceous gland in the pathogenesis of acne. *Dermatoendocrinol*. 2011;3(1):41-49. doi:10.4161/derm.3.1.13900

103. Zouboulis CC, Seltmann H, Hiroi N, et al. Corticotropin-releasing hormone: An autocrine hormone that promotes lipogenesis in human sebocytes. *Proc Natl Acad Sci U S A*. 2002;99(10):7148-7153. doi:10.1073/pnas.102180999

104. Krause K, Schnitger A, Fimmel S, Glass E, Zouboulis CC. Corticotropin-Releasing Hormone Skin Signaling is Receptor-Mediated and is Predominant in the Sebaceous Glands. *Horm Metab Res*. 2007;39(2):166-170. doi:10.1055/s-2007-961811

105. Böhm M, Schiller M, Ständer S, et al. Evidence for Expression of Melanocortin-1 Receptor in Human Sebocytes In Vitro and In Situ. *J Invest Dermatol*. 2002;118(3):533-539. doi:10.1046/j.0022-202x.2001.01704.x

106. Zhang L, Li WH, Anthonavage M, Eisinger M. Melanocortin-5 receptor: A marker of human sebocyte differentiation. *Peptides*. 2006;27(2):413-420. doi:10.1016/j.peptides.2005.05.030

107. Ganceviciene R, Graziene V, Böhm M, Zouboulis CC. Increased in situ expression of melanocortin-1 receptor in sebaceous glands of lesional skin of patients with acne vulgaris. *Exp Dermatol*. 2007;16(7):547-552. doi:10.1111/j.1600-0625.2007.00565.x

108. Ständer S, Schmelz M, Metze D, Luger T, Rukwied R. Distribution of cannabinoid receptor 1 (CB1) and 2 (CB2) on sensory nerve fibers and adnexal structures in human skin. *J Dermatol Sci*. 2005;38(3):177-188. doi:10.1016/j.jdermsci.2005.01.007

109. Dobrosi N, Tóth BI, Nagy G, et al. Endocannabinoids enhance lipid synthesis and apoptosis of human sebocytes via cannabinoid receptor-2-mediated signaling. *FASEB J*. 2008;22(10):3685-3695. doi:10.1096/fj.07-104877

110. Thielitz A, Reinhold D, Vetter R, et al. Inhibitors of dipeptidyl peptidase IV and aminopeptidase N target major pathogenetic steps in acne initiation. *J Invest Dermatol*. 2007;127(5):1042-1051. doi:10.1038/sj.jid.5700439

111. Landthaler M, Kummermehr J, Wagner A, Plewig G. Inhibitory effects of 13-cis-retinoic acid on human sebaceous glands. *Arch Dermatol Res*. 1980;269(3):297-309. doi:10.1007/BF00406424

112. Dalziel K, Barton S, Marks R. The effects of isotretinoin on follicular and sebaceous gland differentiation. *Br J Dermatol*. 1987;117(3):317-323. doi:10.1111/j.1365-2133.1987.tb04138.x

113. Geißler SE, Michelsen S, Plewig G. Very low dose isotretinoin is effective in controlling seborrhea. *JDDG J Dtsch Dermatol Ges*. 2003;1(12):952-958. doi:10.1046/j.1365-2303.2003.00108.x-i1

114. de Souza Leão Kamamoto C, Sanudo A, Hassun KM, Bagatin E. Low-dose oral isotretinoin for moderate to severe seborrhea and seborrheic dermatitis: a randomized comparative trial. *Int J Dermatol*. 2017;56(1):80-85. doi:10.1111/ijd.13408

115. Reichrath J, Mittmann M, Kamradt J, Muller SM. Expression of retinoid-X receptors (-· ,-· ,-·) and retinoic acid receptors (-· ,-· ,-·) in normal human skin: an immunohistological evaluation. *Histochem J*. 1997;29(2):127-133. doi:10.1023/A:1026481205135

116. Zouboulis CC, Korge Bernhard, Akamatsu Hirohiko, et al. Effects of 13-Cis-Retinoic Acid, All-Trans-Retinoic Acid, and Acitretin on the Proliferation, Lipid Synthesis and Keratin Expression of Cultured Human Sebocytes In Vitro. *J Invest Dermatol*. 1991;96(5):792-797. doi:10.1111/1523-1747.ep12471782

117. Tsukada M, Schröder M, Orfanos CE, et al. 13-cis Retinoic Acid Exerts its Specific Activity on Human Sebocytes through Selective Intracellular Isomerization to All-trans Retinoic Acid and Binding to Retinoid Acid Receptors. *J Invest Dermatol*. 2000;115(2):321-327. doi:10.1046/j.1523-1747.2000.00066.x

118. Nelson AM, Gilliland KL, Cong Z, Thiboutot DM. 13-cis Retinoic Acid Induces Apoptosis and Cell Cycle Arrest in Human SEB-1 Sebocytes. *J Invest Dermatol*. 2006;126(10):2178-2189. doi:10.1038/sj.jid.5700289

119. Guy R, Ridden C, Kealey T. The Improved Organ Maintenance of the Human Sebaceous Gland: Modeling in Vitro the Effects of Epidermal Growth Factor, Androgens, Estrogens, 13-cis Retinoic Acid, and Phenol Red. *J Invest Dermatol*. 1996;106(3):454-460. doi:10.1111/1523-1747.ep12343608

120. Zouboulis CC, Korge BP, Mischke D, Orfanos CE. Altered Proliferation, Synthetic Activity, and Differentiation of Cultured Human sebocytes in the Absence of Vitamin A and Their Modulation by Synthetic Retinoids. *J Invest Dermatol*. 1993;101(4):628-633. doi:10.1111/1523-1747.ep12366092

121. He L, Wu WJ, Yang JK, et al. Two new susceptibility loci 1q24.2 and 11p11.2 confer risk to severe acne. *Nat Commun*. 2014;5(1):2870. doi:10.1038/ncomms3870

122. Zhang M, Qureshi AA, Hunter DJ, Han J. A genome-wide association study of severe teenage acne in European Americans. *Hum Genet*. 2014;133(3):259-264. doi:10.1007/s00439-013-1374-4

123. Lo Celso C, Berta M a, Braun KM, et al. Characterization of bipotential epidermal progenitors derived from human sebaceous gland: contrasting roles of c-Myc and beta-catenin. *Stem Cells*. 2008;26(5):1241-1252. doi:10.1634/stemcells.2007-0651

124. McNairn AJ, Doucet Y, Demaude J, et al. TGFβ signaling regulates lipogenesis in human sebaceous glands cells. *BMC Dermatol*. 2013;13:2. doi:10.1186/1471-5945-13-2

125. Snippert HJ, Haegebarth A, Kasper M, et al. Lgr6 marks stem cells in the hair follicle that generate all cell lineages of the skin. *Science*. 2010;327(5971):1385-1389. doi:10.1126/science.1184733

126. Lim X, Nusse R. Wnt Signaling in Skin Development, Homeostasis, and Disease. *Cold Spring Harb Perspect Biol*. 2013;5(2). doi:10.1101/cshperspect.a008029

127. Lim X, Tan SH, Koh WLC, et al. Interfollicular Epidermal Stem Cells Self-Renew via Autocrine Wnt Signaling. *Science*. 2013;342(6163):1226-1230. doi:10.1126/science.1239730

128. Lim X, Tan SH, Yu KL, Lim SBH, Nusse R. Axin2 marks quiescent hair follicle bulge stem cells that are maintained by autocrine Wnt/β-catenin signaling. *Proc Natl Acad Sci*. 2016;113(11):E1498-E1505. doi:10.1073/pnas.1601599113

129. Merrill BJ, Gat U, DasGupta R, Fuchs E. Tcf3 and Lef1 regulate lineage differentiation of multipotent stem cells in skin. *Genes Dev*. 2001;15(13):1688-1705. doi:10.1101/gad.891401

130. Nguyen H, Rendl M, Fuchs E. Tcf3 Governs Stem Cell Features and Represses Cell Fate Determination in Skin. *Cell*. 2006;127(1):171-183. doi:10.1016/j.cell.2006.07.036

131. Petersson M, Brylka H, Kraus A, et al. TCF/Lef1 activity controls establishment of diverse stem and progenitor cell compartments in mouse epidermis. *EMBO J*. 2011;30(15):3004-3018. doi:10.1038/emboj.2011.199

132. Niemann C, Owens DM, Hülsken J, Birchmeier W, Wat FM. Expression of ΔNLef1 in mouse epidermis results in differentiation of hair follicles into squamous epidermal cysts and formation of skin tumours. *Development*. 2002;129(1):95-109.

133. Xu M, Horrell J, Snitow M, et al. WNT10A mutation causes ectodermal dysplasia by impairing progenitor cell proliferation and KLF4-mediated differentiation. *Nat Commun*. 2017;8(1):15397. doi:10.1038/ncomms15397

134. Araviiskaia E, Berardesca E, Bieber T, et al. The impact of airborne pollution on skin. *J Eur Acad Dermatol Venereol*. 2019;33(8):1496-1505. doi:10.1111/jdv.15583

135. Liu W, Pan X, Vierkötter A, et al. A Time-Series Study of the Effect of Air Pollution on Outpatient Visits for Acne Vulgaris in Beijing. *Skin Pharmacol Physiol*. 2018;31(2):107-113. doi:10.1159/000484482

136. Kardeh S, Moein SA, Namazi MR, Kardeh B. Evidence for the Important Role of Oxidative Stress in the Pathogenesis of Acne. *Galen Med J*. 2019;8(0):1291. doi:10.31661/gmj.v8i0.1291

137. Ju Q, Zouboulis CC, Xia L. Environmental pollution and acne: Chloracne. *Dermatoendocrinol*. 2009;1(3):125-128.

138. Ju Q, Yang K, Zouboulis CC, Ring J, Chen W. Chloracne: From clinic to research. *Dermatol Sin*. 2012;30(1):2-6. doi:10.1016/j.dsi.2012.01.007

139. Schlessinger DI, Robinson CA, Schlessinger J. Chloracne. In: *StatPearls*. StatPearls Publishing; 2024. Accessed September 13, 2024. http://www.ncbi.nlm.nih.gov/books/NBK459189/

140. Connor KT, Harris MA, Edwards MR, et al. AH receptor agonist activity in human blood measured with a cell-based bioassay: evidence for naturally occurring AH receptor ligands in vivo. *J Expo Sci Environ Epidemiol*. 2008;18(4):369-380. doi:10.1038/sj.jes.7500607

141. Furue M, Takahara M, Nakahara T, Uchi H. Role of AhR/ARNT system in skin homeostasis. *Arch Dermatol Res*. 2014;306(9):769-779. doi:10.1007/s00403-014-1481-7

142. Fernández-Gallego N, Sánchez-Madrid F, Cibrian D. Role of AHR Ligands in Skin Homeostasis and Cutaneous Inflammation. *Cells*. 2021;10(11):3176. doi:10.3390/cells10113176

143. Grishanova AY, Perepechaeva ML. Aryl Hydrocarbon Receptor in Oxidative Stress as a Double Agent and Its Biological and Therapeutic Significance. *Int J Mol Sci*. 2022;23(12):6719. doi:10.3390/ijms23126719

144. Larigot L, Juricek L, Dairou J, Coumoul X. AhR signaling pathways and regulatory functions. *Biochim Open*. 2018;7:1-9. doi:10.1016/j.biopen.2018.05.001

145. Greenlee WF, Dold KM, Osborne R. Actions of 2,3,7,8-tetrachlorodibenzo-p-dioxin (TCDD) on human epidermal keratinocytes in culture. *In Vitro Cell Dev Biol*. 1985;21(9):509-512. doi:10.1007/BF02620843

146. Mandavia C. TCDD-induced activation of aryl hydrocarbon receptor regulates the skin stem cell population. *Med Hypotheses*. 2015;84(3):204-208. doi:10.1016/j.mehy.2014.12.023

147. Hou XX, Chen G, Hossini AM, et al. Aryl Hydrocarbon Receptor Modulates the Expression of TNF-α and IL-8 in Human Sebocytes via the MyD88-p65NF-κB/p38MAPK Signaling Pathways. *J Innate Immun*. 2018;11(1):41-51. doi:10.1159/000491029

148. Ding J, Zhong J, Yang Y, et al. Occurrence and exposure to polycyclic aromatic hydrocarbons and their derivatives in a rural Chinese home through biomass fuelled cooking. *Environ Pollut*. 2012;169:160-166. doi:10.1016/j.envpol.2011.10.008

149. Hu T, Wang D, Yu Q, et al. Aryl hydrocarbon receptor negatively regulates lipid synthesis and involves in cell differentiation of SZ95 sebocytes in vitro. *Chem Biol Interact*. 2016;258:52-58. doi:10.1016/j.cbi.2016.08.012

150. Agnew T, Furber G, Leach M, Segal L. A Comprehensive Critique and Review of Published Measures of Acne Severity. *J Clin Aesthetic Dermatol*. 2016;9(7):40-52.

151. Fulton Jr. JE, Farzad-Bakshandeh A, Bradley S. Studies on the Mechanism of Action of Topical Benzoyl Peroxide and Vitamin A Acid in Acne Vulgaris. *J Cutan Pathol*. 1974;1(5):191-200. doi:10.1111/j.1600-0560.1974.tb00628.x

152. HUGHES BR, NORRIS JFB, CUNLIFFE WJ. A double-blind evaluation of topical isotretinoin 0.05%, benzoyl peroxide gel 5% and placebo in patients with acne. *Clin Exp Dermatol*. 1992;17(3):165-168. doi:10.1111/j.1365-2230.1992.tb00196.x

153. Chien AL. Retinoids in Acne Management: Review of Current Understanding, Future Consideration and Focus on Topical Treatments. *J Drugs Dermatol*. 2018;17(12):5.

154. Simonart T, Dramaix M. Treatment of acne with topical antibiotics: lessons from clinical studies. *Br J Dermatol*. 2005;153(2):395-403. doi:https://doi.org/10.1111/j.1365-2133.2005.06614.x

155. Haider A, Shaw JC. Treatment of Acne Vulgaris. *JAMA*. 2004;292(6):726-735. doi:10.1001/jama.292.6.726

156. Vowels BR, Yang S, Leyden JJ. Induction of proinflammatory cytokines by a soluble factor of Propionibacterium acnes: implications for chronic inflammatory acne. *Infect Immun*. 1995;63(8):3158-3165. doi:10.1128/iai.63.8.3158-3165.1995

157. Golub LM, Lee HM, Ryan ME, Giannobile WV, Payne J, Sorsa T. Tetracyclines Inhibit Connective Tissue Breakdown by Multiple Non-Antimicrobial Mechanisms. *Adv Dent Res*. 1998;12(1):12-26. doi:10.1177/08959374980120010501

158. Gollnick H, Cunliffe W, Berson D, et al. Management of Acne: A Report From a Global Alliance to Improve Outcomes in Acne. *J Am Acad Dermatol*. 2003;49(1, Supplement):S1-S37. doi:10.1067/mjd.2003.618

159. Arowojolu AO, Gallo MF, Lopez LM, Grimes DA. Combined oral contraceptive pills for treatment of acne. *Cochrane Database Syst Rev*. 2012;(7). doi:10.1002/14651858.CD004425.pub6

160. Rabe T, Kowald A, Ortmann J, Rehberger-Schneider S. Inhibition of skin 5α-reductase by oral contraceptive progestins in vitro. *Gynecol Endocrinol*. 2000;14(4):223-230. doi:10.3109/09513590009167685

161. Lucky AW, Koltun W, Thiboutot D, et al. A combined oral contraceptive containing 3-mg drospirenone/ 20-microg ethinyl estradiol in the treatment of acne vulgaris: a randomized, double-blind, placebo-controlled study evaluating lesion counts and participant self-assessment. *Cutis*. 2008;82(2):143-150.

162. Maloney JM, Dietze P, Watson D, et al. A randomized controlled trial of a low-dose combined oral contraceptive containing 3 mg drospirenone plus 20 microg ethinylestradiol in the treatment of acne vulgaris: lesion counts, investigator ratings and subject self-assessment. *J Drugs Dermatol*. 2009;8(9):837-844.

163. Koltun W, Lucky AW, Thiboutot D, et al. Efficacy and safety of 3 mg drospirenone/20 mcg ethinylestradiol oral contraceptive administered in 24/4 regimen in the treatment of acne vulgaris: a randomized, double-blind, placebo-controlled trial. *Contraception*. 2008;77(4):249-256. doi:10.1016/j.contraception.2007.11.003

164. Koltun W, Maloney JM, Marr J, Kunz M. Treatment of moderate acne vulgaris using a combined oral contraceptive containing ethinylestradiol 20µg plus drospirenone 3mg administered in a 24/4 regimen: a pooled analysis. *Eur J Obstet Gynecol Reprod Biol*. 2011;155(2):171-175. doi:10.1016/j.ejogrb.2010.12.027

165. Layton AM, Knaggs H, Taylor J, Cunliffe WJ. Isotretinoin for acne vulgaris--10 years later: a safe and successful treatment. *Br J Dermatol*. 1993;129(3):292-296. doi:10.1111/j.1365-2133.1993.tb11849.x

166. Kapała J, Lewandowska J, Placek W, Owczarczyk-Saczonek A. Adverse Events in Isotretinoin Therapy: A Single-Arm Meta-Analysis. *Int J Environ Res Public Health*. 2022;19(11):6463. doi:10.3390/ijerph19116463

167. Jang H sung, Lee J eun, Myung C hwan, Park J il, Jo C song, Hwang JS. Particulate Matter-Induced Aryl Hydrocarbon Receptor Regulates Autophagy in Keratinocytes. *Biomol Ther*. 2019;27(6):570-576. doi:10.4062/biomolther.2019.025

168. Hinde E, Haslam IS, Schneider MR, et al. A practical guide for the study of human and murine sebaceous glands in situ. *Exp Dermatol*. 2013;22(10):631-637. doi:https://doi.org/10.1111/exd.12207

169. Benzo[a]pyrene represses DNA repair through altered E2F1/E2F4 function marking an early event in DNA damage-induced cellular senescence | Nucleic Acids Research | Oxford Academic. Accessed November 22, 2022. https://academic.oup.com/nar/article/48/21/12085/5964078

170. Safe S, Jin U ho, Park H, Chapkin RS, Jayaraman A. Aryl Hydrocarbon Receptor (AHR) Ligands as Selective AHR Modulators (SAhRMs). *Int J Mol Sci*. 2020;21(18):6654. doi:10.3390/ijms21186654

171. Davarinos NA, Pollenz RS. Aryl Hydrocarbon Receptor Imported into the Nucleus following Ligand Binding Is Rapidly Degraded via the Cytosplasmic Proteasome following Nuclear Export *. *J Biol Chem*. 1999;274(40):28708-28715. doi:10.1074/jbc.274.40.28708

172. Ma Q, Baldwin KT. 2,3,7,8-Tetrachlorodibenzo-p-dioxin-induced Degradation of Aryl Hydrocarbon Receptor (AhR) by the Ubiquitin-Proteasome Pathway: ROLE OF THE TRANSCRIPTION ACTIVATON AND DNA BINDING OF AhR*. *J Biol Chem*. 2000;275(12):8432-8438. doi:10.1074/jbc.275.12.8432

173. Giani Tagliabue S, Faber SC, Motta S, Denison MS, Bonati L. Modeling the binding of diverse ligands within the Ah receptor ligand binding domain. *Sci Rep*. 2019;9(1):10693. doi:10.1038/s41598-019-47138-z

174. Allmann S, Mayer L, Olma J, et al. Benzo[a]pyrene represses DNA repair through altered E2F1/E2F4 function marking an early event in DNA damage-induced cellular senescence. *Nucleic Acids Res*. 2020;48(21):12085-12101. doi:10.1093/nar/gkaa965

175. Chan CYY, Kim PM, Winn LM. TCDD Affects DNA Double Strand-Break Repair. *Toxicol Sci*. 2004;81(1):133-138. doi:10.1093/toxsci/kfh200

176. Das DN, Panda PK, Sinha N, Mukhopadhyay S, Naik PP, Bhutia SK. DNA damage by 2,3,7,8-tetrachlorodibenzo-p-dioxin-induced p53-mediated apoptosis through activation of cytochrome P450/aryl hydrocarbon receptor. *Environ Toxicol Pharmacol*. 2017;55:175-185. doi:10.1016/j.etap.2017.08.012

177. Salminen A. Aryl hydrocarbon receptor (AhR) reveals evidence of antagonistic pleiotropy in the regulation of the aging process. *Cell Mol Life Sci*. 2022;79(9):489. doi:10.1007/s00018-022-04520-x

178. Allmann S, Mayer L, Olma J, et al. Benzo[a]pyrene represses DNA repair through altered E2F1/E2F4 function marking an early event in DNA damage-induced cellular senescence. *Nucleic Acids Res*. 2020;48(21):12085-12101. doi:10.1093/nar/gkaa965

179. Fernandez-Capetillo O, Chen HT, Celeste A, et al. DNA damage-induced G2–M checkpoint activation by histone H2AX and 53BP1. *Nat Cell Biol*. 2002;4(12):993-997. doi:10.1038/ncb884

180. Toulza E, Mattiuzzo NR, Galliano MF, et al. Large-scale identification of human genes implicated in epidermal barrier function. *Genome Biol*. 2007;8(6):R107. doi:10.1186/gb-2007-8-6-r107

181. Zhao Z, Chen X, Dowbaj AM, et al. Organoids. *Nat Rev Methods Primer*. 2022;2(1):1-21. doi:10.1038/s43586-022-00174-y

182. Clevers H. Modeling Development and Disease with Organoids. *Cell*. 2016;165(7):1586-1597. doi:10.1016/j.cell.2016.05.082

183. Geueke A, Niemann C. Stem and progenitor cells in sebaceous gland development, homeostasis and pathologies. *Exp Dermatol*. 2021;30(4):588-597. doi:10.1111/exd.14303

184. Sun H, Zhang YX, Li YM. Generation of Skin Organoids: Potential Opportunities and Challenges. *Front Cell Dev Biol*. 2021;9:709824. doi:10.3389/fcell.2021.709824

185. Hong ZX, Zhu ST, Li H, et al. Bioengineered skin organoids: from development to applications. *Mil Med Res*. 2023;10(1):40. doi:10.1186/s40779-023-00475-7

186. Harrison RM, Jones AM, Lawrence RG. Major component composition of PM10 and PM2.5 from roadside and urban background sites. *Atmos Environ*. 2004;38(27):4531-4538. doi:10.1016/j.atmosenv.2004.05.022

187. Lewandowska AU, Staniszewska M, Witkowska A, Machuta M, Falkowska L. Benzo(a)pyrene parallel measurements in PM1 and PM2.5 in the coastal zone of the Gulf of Gdansk (Baltic Sea) in the heating and non-heating seasons. *Environ Sci Pollut Res Int*. 2018;25(20):19458-19469. doi:10.1007/s11356-018-2089-9

188. Eckhart L, Lippens S, Tschachler E, Declercq W. Cell death by cornification. *Biochim Biophys Acta BBA - Mol Cell Res*. 2013;1833(12):3471-3480. doi:10.1016/j.bbamcr.2013.06.010

189. Hanakawa Y, Shirakata Y, Yahata Y, et al. Differential Effects of Desmoglein 1 and Desmoglein 3 on Desmosome Formation. *J Invest Dermatol*. 2002;119(6):1231-1236. doi:10.1046/j.1523-1747.2002.19648.x

190. Candi E, Schmidt R, Melino G. The cornified envelope: a model of cell death in the skin. *Nat Rev Mol Cell Biol*. 2005;6(4):328-340. doi:10.1038/nrm1619

191. Has C. Peeling Skin Disorders: A Paradigm for Skin Desquamation. *J Invest Dermatol*. 2018;138(8):1689-1691. doi:10.1016/j.jid.2018.05.020

192. Sutter CH, Bodreddigari S, Campion C, Wible RS, Sutter TR. 2,3,7,8-Tetrachlorodibenzo-p-dioxin Increases the Expression of Genes in the Human Epidermal Differentiation Complex and Accelerates Epidermal Barrier Formation. *Toxicol Sci*. 2011;124(1):128-137. doi:10.1093/toxsci/kfr205

193. Theocharidis G, Tekkela S, Veves A, McGrath JA, Onoufriadis A. Single-cell transcriptomics in human skin research: available technologies, technical considerations and disease applications. *Exp Dermatol*. 2022;31(5):655-673. doi:10.1111/exd.14547

194. Houser AE, Kazmi A, Nair AK, Ji AL. The Use of Single-Cell RNA-Sequencing and Spatial Transcriptomics in Understanding the Pathogenesis and Treatment of Skin Diseases. *JID Innov*. 2023;3(4):100198. doi:10.1016/j.xjidi.2023.100198

195. Schepps S, Xu J, Yang H, et al. Skin in the game: a review of single-cell and spatial transcriptomics in dermatological research. *Clin Chem Lab Med CCLM*. 2024;62(10):1880-1891. doi:10.1515/cclm-2023-1245

196. Deng M, Odhiambo WO, Qin M, et al. Analysis of intracellular communication reveals consistent gene changes associated with early-stage acne skin. *Cell Commun Signal*. 2024;22(1):400. doi:10.1186/s12964-024-01725-4

Appendix

Table 1.

Gene		Sequence
MUC1	Forward	TGCCGCCGAAAGAACTACG
	Reverse	TGGGGTACTCGCTCATAGGAT
KRT7	Forward	GGACATCGAGATCGCCACCT
	Reverse	TGCCACCGCCACTGCTACT
FASN	Forward	AAGGACCTGTCTAGGTTTGATGC
	Reverse	TGGCTTCATAGGTGACTTCCA
SCD	Forward	TCTAGCTCCTATACCACCACCA
	Reverse	TCGTCTCCAACTTATCTCCTCC
PPARγ	Forward	ACCAAAGTGCAATCAAAGTGGA
	Reverse	ATGAGGGAGTTGGAAGGCTCT
LRIG1	Forward	CACAACAAGATTCGCAGCGTG
	Reverse	TGTTCCGCACTTCCGTGATG

KRT14	Forward	TGAGCCGCATTCTGAACGAG
	Reverse	GATGACTGCGATCCAGAGGA
KRT10	Forward	GTGGGCGAGTCTTCATCTAAG
	Reverse	GGCGCCACCTCTTCAATAA
MKI67	Forward	ACGCCTGGTTACTATCAAAAGG
	Reverse	CAGACCCATTTACTTGTGTTGGA
WNT10A	Forward	TTCGTGGTCTGCGAAGAGT
	Reverse	CCAAGACCGTAAGCCTCAGA
LGR6	Forward	TGGGGAACCCTCTGCTACAG
	Reverse	CAGGTACTGGAATGCCGATCT
LAMC2	Forward	GGCTCACCAAGACTTACACA
	Reverse	GAATCACTGAGCAGCTGAAC
TGFB2	Forward	CCCCGGAGGTGATTTCCATC
	Reverse	GGGCGGCATGTCTATTTTGTAAA
OVOL1	Forward	TGAACATGAGCCTTCGAGACT
	Reverse	CAAGGGTCACCTTCATCTTGG
FST	Forward	AGGCAAGATGTAAAGAGCAGC
	Reverse	CAGTAGGCATTATTGGTCTGGTC
SEMA4B	Forward	GGCGAGCTCTACACTGGAAC
	Reverse	GTAGGCTGAGGCCACAAAAG
AHR	Forward	GTCGTCTAAGGTGTCTGCTGGA
	Reverse	CGCAAACAAAGCCAACTGAGGTG
AHRR	Forward	GCGCCTCAGTGTCAGTTACC
	Reverse	GAAGCCCAGATAGTCCACGAT
CYP1A1	Forward	GATTGAGCACTGTCAGGAGAAGC
	Reverse	ATGAGGCTCCAGGAGATAGCAG
c-MYC	Forward	CCTGGTGCTCCATGAGGAGAC
	Reverse	CAGACTCTGACCTTTTGCCAGG
MSH2	Forward	ATCATTCTCCTTGGATGCCTTAT
	Reverse	CTTCTTCTGGTTCGTCAGTATAGA
MSH6	Forward	CCTTCACTCTCACTATCC
	Reverse	GAATTTAAGCCAGACACTAA
RAD51	Forward	GGGGTGATCAGTTTCTGTTGC
	Reverse	GCACAATCATCTGCAAGTGGG
CDKN1A	Forward	GCGACTGGTGATGCGCTAATG
	Reverse	CGGTGACAAAGTCGAAGTTCC
LMNB1	Forward	CGCTTGGTAGAGGTGGATTCTG
	Reverse	CCTCACTTGGGCATCATGTTG
GAPDH	Forward	TCGACAGTCAGCCGCATCTTC
	Reverse	AACAAATCCGTTGACTCCGAC

Table 1. Primer sequences used in RT-PCR and qPCR analysis.

Table 2.

Primary Antibodies	**Catelogue No.**	**Application used**
KRT14	905304	ICC, IHC
KRT10	905404	ICC, IHC
MUC1	ab151481	ICC, IHC
FASN (C20G5)	3180S	ICC, IHC
SCD1 (M38)	2438S	ICC, IHC
PPARγ (C26H12)	2435S	ICC, iHC
CD49f (ITGA6)	14-0495-85	ICC
KI67	ab16667	ICC
AhR (D5S6H)	#83200	ICC, WB
p21 Waf1/Cip1 (12D1)	#2947	WB
LMNB1	ab16048	WB
GAPDH (0411)	sc-47724	WB
Secondary Antibodies	**Catelogue No.**	**Application used**
Donkey Anti-Rabbit IgG H&L (AF568) Preadsorbed	ab175692	ICC, IHC
Donkey Anti-Mouse IgG H&L (AF488) Preadsorbed	ab150109	ICC, IHC
Donkey Anti-Rat IgG H&L (AF568) Preadsorbed	ab175475	ICC, IHC
Goat anti-Rabbit IRDye 680LT	925-68021	WB
Donkey anti-Mouse IRDye 800CW	925-32212	WB
Chemical Stains	**Catelogue No.**	**Application used**
Alexa Fluor 647 Phalloidn	A22287	ICC
HCS LipidTOX Green Neutral Lipid Stain	H34475	ICC
NucBlue Fixed Cell ReadyProbes Reagent (DAPI)	R37606	ICC, IHC

Table 2. Primary and secondary antibodies and chemical stains used in IF and WB analysis.

Supplementary Materials

Supplementary Figure 1

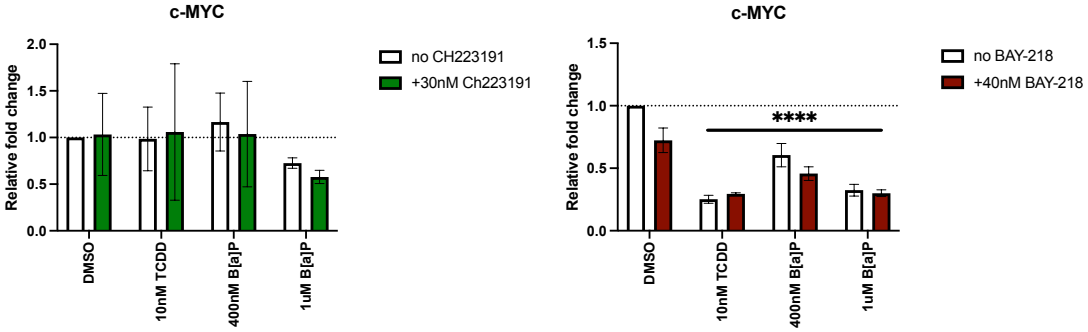

Supplementary Figure 1. qPCR analysis showed no rescue to *c-MYC* expression even when co-exposed with 30nM CH223191 or 40nM BAY-218. 1008-HFSE2 human primary sebocytes were exposed to 0.1% DMSO (Control), 400nM/1uM B[a]P and 10nM TCDD, with each exposure supplemented with 30nM CH223191 or 40nM BAY-218 for 72 hours. Two-Way ANOVA statistical analysis using Tukey multiple comparison test was applied to compare the mean relative fold change across treated groups (3 technical replicates/group) [*: <0.05, **:<0.01, ***:<0.001, ****:<0.0001]. Statistical significance represents how different the treated groups are compared to DMSO sample. *DMSO: Dimethyl sulfoxide; B[a]P: Benzo[a]pyrene; TCDD: 2,3,7,8-Tetrachlorodibenzodioxin.*

Supplementary Figure 2

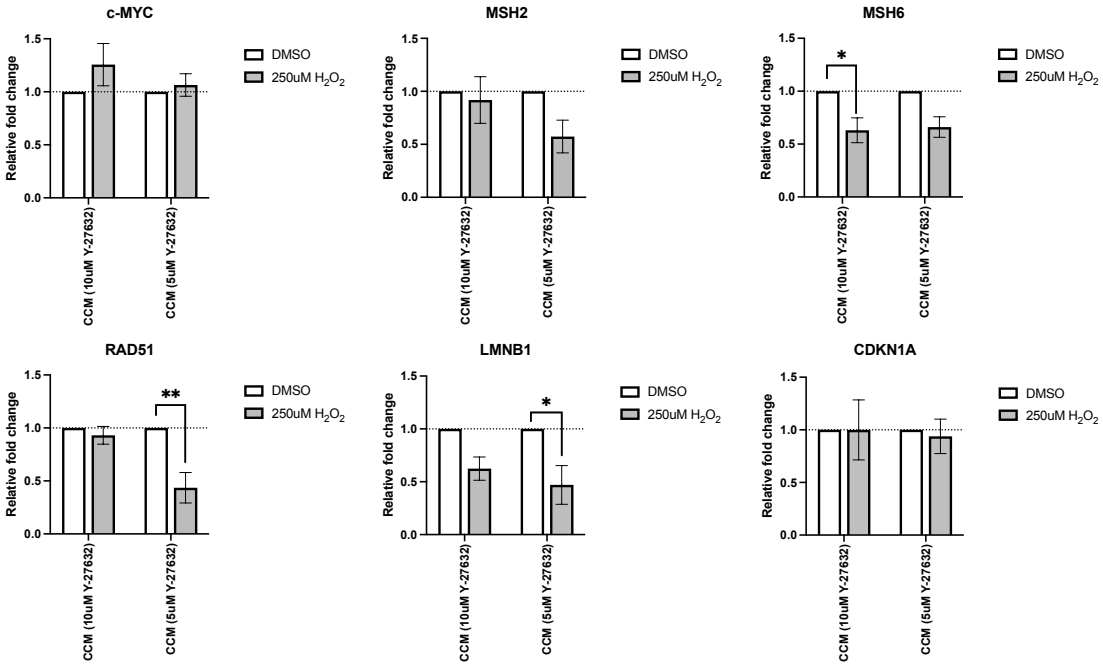

Supplementary Figure 2. CCMY cell culture media is not suitable to study DNA damage-induced cellular senescence. Proliferative marker (*c-MYC*), DNA repair genes (*MSH2/6, RAD51*) and cellular senescence markers (*LMNB1, CDKN1A*) were analyzed in 1008-HFSE2 cultured in CCM (5/10uM Y-27623) and exposed to 0.1% DMSO (Control) and a single-exposure of 250uM H_2O_2 for 72 hours. Relative fold change of gene expression was normalized to endogenous *GAPDH* and calculated based on $2^{-\Delta\Delta CT}$. One-Way ANOVA statistical analysis using Tukey multiple comparison test was applied to compare the mean relative fold change across treated groups (3 technical replicates/group) [*: <0.05, **:<0.01, ***:<0.001, ****:<0.0001]. *MSH2: DNA mismatch repair protein MutS homolog 2/6; RAD51: DNA repair protein RAD51 homolog 1; LMNB1: Lamin B1; CDKN1A: Cyclin dependent kinase inhibitor 1A; GAPDH: Glyceraldehyde 3-phosphate dehydrogenase; DMSO: Dimethyl sulfoxide; B[a]P: Benzo[a]pyrene; TCDD: 2,3,7,8-Tetrachlorodibenzodioxin.*

Supplementary Figure 3

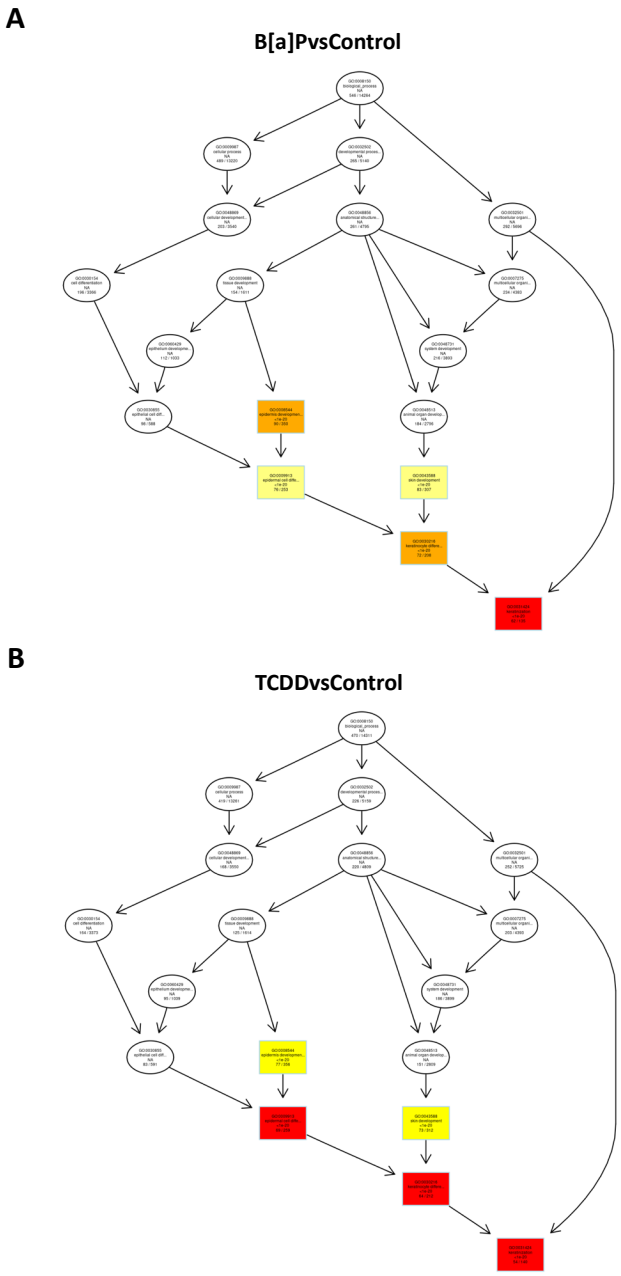

Supplementary Figure 3. GO biological processes flow chart showing biological processes significantly enriched (coloured boxes) in B[a]PvsControl (A) and TCDDvsControl (B).

Supplementary Table 1.

BaPvsControl DEGs_all			
gene_name	**log2FoldChange**	**p-value**	**padj**
HRNR	3.671142784	3.71E-120	6.72E-116
LYPD5	3.187954284	1.58E-107	1.43E-103
RPTN	2.773422094	9.02E-100	5.46E-96
TGM3	4.042785626	5.87E-97	2.66E-93
SDR9C7	2.738546739	3.26E-85	1.18E-81
CDSN	3.061641332	2.27E-82	6.88E-79
RPL22L1	-1.999625958	4.23E-77	1.10E-73
IL1B	2.33560261	3.85E-76	8.74E-73
CRCT1	3.72715267	1.16E-74	2.34E-71
PSORS1C1	2.452810737	7.07E-73	1.28E-69
PHGDH	-3.628158105	1.48E-72	2.44E-69
CNFN	3.1178611	9.95E-72	1.50E-68
ASPRV1	2.595062189	1.89E-71	2.63E-68
CYSRT1	2.791987103	2.23E-69	2.89E-66
IL36RN	1.907550719	1.18E-67	1.42E-64
DHRS9	3.089559685	2.33E-67	2.57E-64
NCCRP1	2.38868366	2.41E-67	2.57E-64
KLK6	3.835044026	1.51E-65	1.52E-62
ENDOU	3.690918049	4.77E-65	4.55E-62
CYP4F22	2.265618449	3.29E-63	2.99E-60
CYP1B1	8.141165117	4.18E-63	3.61E-60
HOPX	2.052122052	6.56E-62	5.41E-59
KRT23	2.732962345	1.52E-61	1.20E-58
TMPRSS13	2.137055411	1.20E-60	9.05E-58
PLA2G4D	2.642661292	2.26E-60	1.64E-57
LCE3E	3.519456626	8.91E-60	6.22E-57
SULT2B1	2.022301208	3.88E-59	2.61E-56
VSIG10L	2.280612959	4.36E-56	2.83E-53
ACP7	3.131991219	8.33E-56	5.21E-53
FAM43A	2.282375196	1.21E-54	7.34E-52
MAB21L4	3.008158047	1.29E-54	7.54E-52
TMEM86A	1.772117364	8.49E-54	4.82E-51
SCNN1B	2.313599921	2.51E-53	1.38E-50
SPRR2A	2.309397848	2.58E-53	1.38E-50
LCN2	3.222217306	4.51E-53	2.34E-50
KRT80	2.464008137	2.06E-52	1.04E-49
HAL	2.560666332	3.94E-52	1.93E-49
LCE1C	2.219678243	8.28E-52	3.96E-49

KRTDAP	1.509632901	1.92E-51	8.94E-49
SMPD3	2.883851635	3.21E-51	1.46E-48
CA2	2.137034441	3.85E-51	1.70E-48
SPNS2	2.428913586	1.51E-50	6.52E-48
KPRP	3.036213029	7.06E-50	2.98E-47
AC115522.1	3.560616001	7.52E-49	3.10E-46
RNF222	2.766445514	9.75E-49	3.93E-46
VASN	2.679112685	5.65E-48	2.23E-45
SPRR2G	2.752486593	1.76E-47	6.81E-45
SPRR2E	2.008084678	5.75E-47	2.17E-44
FLG2	1.977723616	9.44E-47	3.50E-44
ZNF185	1.535111251	1.95E-46	7.08E-44
RNF223	3.61848343	3.84E-46	1.37E-43
KLK7	1.876361646	8.08E-46	2.82E-43
LGALSL	1.456764494	1.03E-45	3.54E-43
SBSN	2.046714482	2.86E-45	9.59E-43
PLA2G4E	1.866990547	6.29E-45	2.08E-42
SPRR2B	3.041599168	1.73E-44	5.61E-42
TGM1	1.637902139	1.81E-44	5.75E-42
CLDN17	3.557377167	2.04E-44	6.38E-42
SPINK7	3.104465276	2.58E-44	7.94E-42
LCE1B	2.510924665	2.80E-44	8.48E-42
PNPLA1	2.423132342	1.97E-43	5.86E-41
KRT78	2.461425967	2.03E-43	5.94E-41
SYNPO	-1.885476028	3.88E-43	1.12E-40
SCEL	2.01536575	8.20E-43	2.33E-40
GDA	3.062202669	1.07E-42	2.98E-40
ATP6V1C2	2.220128755	3.78E-42	1.04E-39
LY6G6C	1.959999886	1.03E-41	2.79E-39
KRT16P2	3.049518024	3.60E-41	9.60E-39
ATP12A	2.752661905	2.09E-40	5.51E-38
AC011473.4	2.64982906	2.33E-40	6.03E-38
OVOL1	2.000379448	2.53E-40	6.47E-38
ALDH3B2	1.769788592	2.58E-40	6.49E-38
PCDH1	2.129500772	4.36E-40	1.08E-37
FLG	2.129229224	5.11E-40	1.25E-37
MAPK13	1.359602363	8.53E-40	2.06E-37
HMOX1	2.087890867	1.11E-39	2.66E-37
FRMPD1	2.644543251	1.83E-39	4.32E-37
LCE1F	2.940198284	3.79E-39	8.82E-37
GRHL1	1.777260792	5.02E-39	1.15E-36
PCK2	-2.168296025	6.39E-39	1.45E-36

ALOX12B	2.125772298	7.12E-39	1.60E-36
ADGRL2	1.887520023	8.08E-39	1.79E-36
ELMOD1	2.766436316	1.55E-38	3.37E-36
LCE2C	3.415130503	1.56E-38	3.37E-36
KLK12	2.696133019	2.22E-38	4.74E-36
GCOM1	2.407370756	3.01E-38	6.36E-36
TMPRSS11D	3.835594005	5.52E-38	1.15E-35
SLC1A4	-2.102751163	9.38E-38	1.93E-35
ALOXE3	1.780277828	1.55E-37	3.15E-35
AZGP1	2.511551722	2.19E-37	4.42E-35
SERPINB3	1.482106665	6.06E-37	1.21E-34
IVL	1.76769453	1.12E-36	2.20E-34
SPRR1A	1.59030114	2.13E-36	4.15E-34
BPIFC	2.305064967	2.84E-36	5.49E-34
SPRR1B	1.55131917	6.51E-36	1.24E-33
SPINK5	1.301848397	1.10E-35	2.08E-33
GDPD3	1.971313596	1.66E-35	3.11E-33
KRT27	4.470722368	1.74E-35	3.22E-33
USP2	2.256264986	3.54E-35	6.49E-33
ELOVL4	1.409528502	5.97E-35	1.08E-32
UGCG	1.389323334	1.46E-34	2.63E-32
CYP1A1	9.092741576	1.70E-34	3.02E-32
PSAT1	-1.632686783	2.79E-34	4.92E-32
NECTIN4	1.637135704	3.49E-34	6.09E-32
MT2A	-1.867577164	8.17E-34	1.41E-31
ESYT3	2.281547753	1.71E-33	2.93E-31
SCNN1G	2.238039939	2.62E-33	4.45E-31
HPGD	2.719823227	8.45E-33	1.42E-30
GSDMA	1.686082643	8.80E-33	1.46E-30
TGM5	3.196866201	9.52E-33	1.57E-30
TCHHL1	3.885159324	1.39E-32	2.27E-30
HAP1	2.94143992	2.81E-32	4.55E-30
PPL	1.524921496	8.63E-32	1.39E-29
OTUB2	1.534817113	1.94E-31	3.09E-29
MMP2	-2.526463301	2.52E-31	3.97E-29
NDRG4	2.183819811	2.76E-31	4.31E-29
NLRP10	1.618447984	3.07E-31	4.72E-29
SPRR2D	1.632311716	3.07E-31	4.72E-29
MT1E	-1.671934443	3.63E-31	5.53E-29
TGFBI	1.58223939	3.70E-31	5.60E-29
XKRX	2.161330781	6.06E-31	9.09E-29
DMKN	1.120494045	9.08E-31	1.35E-28

LGALS1	-2.026678742	1.15E-30	1.70E-28
MYO5B	1.43042502	1.24E-30	1.82E-28
INPP5D	1.304820819	3.98E-30	5.77E-28
ABCA12	1.56916331	6.43E-30	9.27E-28
IL1RN	1.47213992	7.62E-30	1.09E-27
CCDC3	-2.385010554	7.88E-30	1.12E-27
ALDH1A3	5.023237348	9.59E-30	1.35E-27
S1PR3	-1.294047601	1.19E-29	1.66E-27
ATP10B	2.015815523	2.18E-29	3.02E-27
C3	-1.594766221	2.99E-29	4.11E-27
ZNF750	1.499878915	6.47E-29	8.83E-27
MCM6	-1.587702975	8.81E-29	1.19E-26
FADS2	-1.735139685	1.80E-28	2.42E-26
TMEM97	-1.588207036	2.87E-28	3.83E-26
IL22RA1	1.61550845	5.95E-28	7.88E-26
A2ML1	1.358025851	1.03E-27	1.36E-25
EPN3	1.296026538	4.36E-27	5.69E-25
EPS8L1	1.414468288	4.78E-27	6.19E-25
BNIPL	1.479065557	6.41E-27	8.24E-25
MPZL3	1.330113102	7.54E-27	9.63E-25
EPHB3	1.348712592	1.39E-26	1.76E-24
SLPI	1.595848019	1.55E-26	1.95E-24
CLIC3	1.523989761	1.73E-26	2.16E-24
ADGRF1	1.418622478	2.61E-26	3.24E-24
SORT1	1.446643504	3.05E-26	3.76E-24
GPAT3	2.52872166	3.69E-26	4.52E-24
ARHGEF10L	1.207658465	4.10E-26	4.99E-24
RHCG	3.236205187	4.13E-26	5.00E-24
RORA	1.579636781	1.05E-25	1.26E-23
KLF4	1.283491555	1.70E-25	2.03E-23
ITGAX	2.7370493	1.86E-25	2.20E-23
UPK1B	1.240537465	2.14E-25	2.52E-23
KALRN	2.755299413	3.83E-25	4.48E-23
BSPRY	1.59076295	4.77E-25	5.55E-23
PI3	1.566087153	5.25E-25	6.07E-23
PLCXD1	1.269754897	5.39E-25	6.19E-23
EHF	1.299241174	9.22E-25	1.05E-22
NEU2	3.562713887	1.26E-24	1.43E-22
TNFAIP8L3	1.733068041	1.57E-24	1.77E-22
ATG9B	2.971951592	1.85E-24	2.07E-22
PIM1	1.723610556	2.07E-24	2.31E-22
WFDC5	1.967699042	2.10E-24	2.33E-22

TUBA1A	-1.273732568	2.16E-24	2.37E-22
NEFL	-1.677060008	2.17E-24	2.37E-22
TMEM184A	1.606415264	2.71E-24	2.93E-22
AL136982.5	3.089159686	2.79E-24	2.99E-22
METRNL	1.469635176	3.11E-24	3.32E-22
PEMT	-1.664201323	3.33E-24	3.53E-22
NEFM	-1.543794267	4.26E-24	4.49E-22
ABHD17B	1.234357715	5.94E-24	6.23E-22
CEACAM6	2.372476308	8.98E-24	9.37E-22
S100A12	1.709914102	1.48E-23	1.53E-21
PRSS22	3.267892706	2.36E-23	2.43E-21
SDK1	-2.124811117	2.40E-23	2.46E-21
ANKRD22	1.526267282	2.55E-23	2.60E-21
WFDC12	3.103188722	2.62E-23	2.65E-21
CDKN1A	1.159483376	3.81E-23	3.85E-21
FUT3	2.093833984	4.09E-23	4.10E-21
LCE1D	2.72480382	5.46E-23	5.45E-21
GRHL3	1.296268994	7.39E-23	7.33E-21
PADI1	2.047979065	7.69E-23	7.59E-21
DAPP1	1.127222544	1.46E-22	1.43E-20
SDK2	-1.242168147	2.07E-22	2.02E-20
SNCA	-1.313342504	2.67E-22	2.60E-20
EPB41L2	-1.179249805	2.74E-22	2.64E-20
EREG	1.390557458	3.23E-22	3.09E-20
MDM2	1.539772057	3.24E-22	3.09E-20
AC004816.1	1.79956601	5.11E-22	4.86E-20
LMO7	1.503147634	6.52E-22	6.16E-20
GLRX	1.613518133	6.83E-22	6.42E-20
MAP3K9	1.219574032	9.00E-22	8.42E-20
CASZ1	1.219667403	9.65E-22	8.98E-20
LCE1A	2.243835131	1.02E-21	9.45E-20
ST5	-1.17759133	1.12E-21	1.03E-19
KRT37	3.237540116	1.55E-21	1.42E-19
EGR3	2.154262016	2.23E-21	2.03E-19
ACSS2	-1.311387056	2.55E-21	2.31E-19
MCM5	-1.983479825	2.91E-21	2.63E-19
SLC15A1	2.190989912	3.05E-21	2.74E-19
RASAL1	2.372426606	3.29E-21	2.94E-19
LCE2D	3.284587073	4.21E-21	3.74E-19
BCAT1	-2.169985754	4.29E-21	3.80E-19
TMPRSS11E	1.444837023	4.51E-21	3.97E-19
SLC39A2	1.690600869	4.65E-21	4.07E-19

KRT24	2.167834337	4.68E-21	4.08E-19
AHRR	2.706469008	6.51E-21	5.65E-19
LCE1E	2.670340048	7.13E-21	6.16E-19
LCE3D	3.32260388	1.18E-20	1.02E-18
GLTP	1.197141333	1.30E-20	1.11E-18
MXD1	1.401003637	1.58E-20	1.35E-18
YOD1	1.164462353	1.92E-20	1.63E-18
SPRR4	2.11693375	2.10E-20	1.77E-18
CLDN4	1.831841314	2.78E-20	2.33E-18
ACER1	1.649929333	2.89E-20	2.41E-18
RPL3	-1.002666991	2.91E-20	2.43E-18
DLX3	1.299411275	3.39E-20	2.81E-18
DUOXA1	1.253108958	3.69E-20	3.04E-18
CEACAM19	1.359466386	3.75E-20	3.08E-18
DENND2C	1.280274753	3.94E-20	3.22E-18
SLC28A3	1.48371929	6.01E-20	4.88E-18
FCHSD1	1.406510462	6.02E-20	4.88E-18
GPX8	-1.44682795	6.23E-20	5.02E-18
PTPN22	1.504417735	7.73E-20	6.20E-18
KLK10	1.292081894	8.07E-20	6.45E-18
POF1B	1.220801264	8.68E-20	6.90E-18
SERPINB7	1.215298686	9.31E-20	7.38E-18
TWIST2	3.572910949	1.03E-19	8.10E-18
RAP1GAP	1.332041815	1.05E-19	8.23E-18
LIPK	2.00126052	1.05E-19	8.23E-18
KLK11	1.2423616	1.15E-19	8.95E-18
IVNS1ABP	-1.023628205	1.21E-19	9.35E-18
TTC39A	2.076449084	1.32E-19	1.02E-17
KIF26B	-1.234344668	1.34E-19	1.03E-17
OASL	1.826341107	1.63E-19	1.25E-17
PHLDB3	1.187401236	1.71E-19	1.31E-17
PGLYRP3	1.251975613	1.82E-19	1.38E-17
SCARA3	-1.781264776	1.90E-19	1.44E-17
AC103974.1	2.215621495	2.10E-19	1.58E-17
ELF3	3.807569727	2.52E-19	1.89E-17
VWF	1.937152395	2.58E-19	1.93E-17
PSAPL1	2.048011958	3.21E-19	2.39E-17
RNF225	3.008405419	3.82E-19	2.82E-17
ALDH3A1	2.797728782	4.63E-19	3.40E-17
LIPN	2.049209196	4.80E-19	3.51E-17
AL596244.1	-1.534870373	5.95E-19	4.34E-17
TIAM1	1.109763331	7.09E-19	5.14E-17

AC013268.4	2.780758126	8.05E-19	5.82E-17
ZNF426	1.064947316	8.76E-19	6.31E-17
PRKCA	-1.933914546	9.75E-19	6.99E-17
LCE3C	2.940131322	1.37E-18	9.81E-17
RAPGEF3	1.210352563	1.75E-18	1.23E-16
ABCG4	1.89678366	1.75E-18	1.23E-16
IL7R	-2.160964133	1.81E-18	1.27E-16
FAM102A	1.19051899	2.26E-18	1.59E-16
TMPRSS11F	2.063291194	2.77E-18	1.93E-16
RDH12	1.569943398	3.05E-18	2.12E-16
TRIM47	-2.181824064	3.58E-18	2.48E-16
RBMS3	-2.558243736	3.64E-18	2.51E-16
LIPM	1.961116566	3.93E-18	2.70E-16
SLC37A2	1.229447126	4.00E-18	2.74E-16
RASGEF1B	2.196926411	4.45E-18	3.03E-16
VSIR	1.4429377	5.05E-18	3.43E-16
COL5A2	-2.207832231	5.79E-18	3.92E-16
LCE6A	2.664117179	5.88E-18	3.97E-16
TMEM45B	3.285908143	6.60E-18	4.43E-16
PDPN	-1.213128824	6.83E-18	4.57E-16
KLK8	1.391967592	8.69E-18	5.79E-16
CALB2	2.033931748	8.94E-18	5.94E-16
FLVCR2	1.775132686	9.06E-18	6.00E-16
GAS7	2.019096376	9.53E-18	6.29E-16
LINC00511	1.485971415	1.03E-17	6.80E-16
MCAM	-2.28768815	1.15E-17	7.51E-16
SMIM5	2.678818441	1.60E-17	1.05E-15
SLC6A14	1.780068668	1.87E-17	1.22E-15
CDH16	1.693040257	2.14E-17	1.39E-15
PSORS1C2	1.695891142	2.29E-17	1.48E-15
JDP2	-2.07741737	2.59E-17	1.65E-15
APOL6	-1.704810945	3.37E-17	2.14E-15
TNNT2	1.908694159	3.74E-17	2.36E-15
SERPINB13	1.529503607	4.09E-17	2.58E-15
CES2	1.015687073	4.17E-17	2.62E-15
AC022075.1	-1.902483494	5.41E-17	3.38E-15
FGF19	-3.723495372	5.48E-17	3.42E-15
RNASE7	1.67193906	5.98E-17	3.72E-15
ADIRF	1.419099114	7.16E-17	4.42E-15
APOL2	-1.116261084	7.37E-17	4.53E-15
MAFB	1.002103232	7.97E-17	4.89E-15
HMMR	-2.366503038	8.19E-17	4.99E-15

COL8A1	-1.946386614	8.20E-17	4.99E-15
ANXA9	1.762040047	8.36E-17	5.07E-15
CLCF1	1.903883491	9.47E-17	5.73E-15
CEBPA	1.174712122	9.75E-17	5.88E-15
FHOD3	-1.283984365	1.06E-16	6.37E-15
OCLN	1.760344935	1.12E-16	6.72E-15
CHST2	1.204465779	1.13E-16	6.76E-15
KCNAB2	-1.813699094	1.14E-16	6.79E-15
FADS1	-1.685401465	1.25E-16	7.39E-15
DIAPH3	-1.718152733	1.48E-16	8.71E-15
ARRDC4	1.392282602	1.52E-16	8.92E-15
NRP1	-1.247515915	1.56E-16	9.14E-15
CSF2RB	1.915212065	1.65E-16	9.60E-15
CCNB2	-1.931778206	2.60E-16	1.51E-14
SLC5A1	1.436859699	3.20E-16	1.85E-14
SLC38A3	2.869425521	3.34E-16	1.92E-14
SPTSSB	1.820917278	3.52E-16	2.02E-14
DEPDC1B	-1.846644374	3.92E-16	2.25E-14
AC243829.2	4.664352491	3.99E-16	2.27E-14
CSF2RA	2.420221609	4.34E-16	2.47E-14
AC140479.7	2.473930948	4.49E-16	2.55E-14
CPEB4	1.059229605	5.07E-16	2.86E-14
SPRR3	3.372656509	5.44E-16	3.06E-14
PLEKHG1	1.415013972	6.06E-16	3.37E-14
KRT6C	1.064459685	8.24E-16	4.56E-14
HIP1	-1.274035199	8.45E-16	4.66E-14
BICDL2	1.672780533	9.76E-16	5.35E-14
PLCD1	1.281529253	1.33E-15	7.23E-14
TPRG1	1.468832191	1.37E-15	7.43E-14
HSD17B2	2.177432105	1.68E-15	9.07E-14
IGFN1	2.925393754	1.81E-15	9.73E-14
SLC26A9	2.012076558	2.43E-15	1.30E-13
SECTM1	1.365729029	2.62E-15	1.40E-13
AQP5	2.02267233	2.62E-15	1.40E-13
NEB	2.096406416	2.70E-15	1.43E-13
IFI35	-2.606120624	2.99E-15	1.58E-13
CDH4	-3.371421595	3.63E-15	1.89E-13
MYZAP	2.757413499	4.07E-15	2.12E-13
ELOVL6	-1.074259091	5.80E-15	3.00E-13
KRT13	1.153381132	6.01E-15	3.10E-13
RAB11FIP1	1.016176473	6.28E-15	3.23E-13
GAREM1	1.340030995	6.57E-15	3.37E-13

AL357033.4	1.848513126	6.90E-15	3.53E-13
LINC02560	3.266482413	8.34E-15	4.25E-13
DSC1	1.261588303	8.66E-15	4.40E-13
NFIC	-1.053580999	8.84E-15	4.48E-13
MTUS1	-1.343125694	1.00E-14	5.05E-13
GGT8P	3.37670909	1.18E-14	5.89E-13
MUC15	1.899543218	1.18E-14	5.90E-13
ACSS1	-1.623193438	1.19E-14	5.92E-13
FA2H	2.027494698	1.21E-14	6.01E-13
SYNPO2L	2.460989062	1.48E-14	7.32E-13
CARD18	1.377201302	1.59E-14	7.81E-13
CTPS2	-1.152584632	1.61E-14	7.88E-13
TTC9	1.739921482	1.80E-14	8.78E-13
AL139247.1	3.253833401	2.05E-14	9.95E-13
CST6	2.717162013	2.23E-14	1.08E-12
S100A9	1.078727208	2.43E-14	1.18E-12
RASSF5	1.262438423	2.50E-14	1.21E-12
EXPH5	1.241888673	2.88E-14	1.37E-12
CDKN3	-2.056405276	3.00E-14	1.43E-12
H6PD	-1.153072697	3.26E-14	1.55E-12
RHOF	1.565663435	4.60E-14	2.16E-12
MUCL1	1.519026004	5.18E-14	2.42E-12
Mar-03	1.752980386	5.39E-14	2.51E-12
BARX2	1.153203072	5.58E-14	2.59E-12
CALML5	1.386315782	6.14E-14	2.85E-12
ATP2C2	1.293823114	6.33E-14	2.93E-12
ARHGAP30	2.439591905	8.82E-14	4.07E-12
TROAP	-1.807035401	1.18E-13	5.40E-12
C6orf15	3.729227062	1.40E-13	6.42E-12
HCAR2	1.505534261	1.44E-13	6.56E-12
RNF39	1.470775033	1.58E-13	7.21E-12
MXRA5	-2.079452607	1.63E-13	7.39E-12
PIK3C2G	-2.263832889	1.69E-13	7.67E-12
UCP2	-1.703092911	1.70E-13	7.67E-12
RRM1	-1.045104989	1.87E-13	8.41E-12
SLC35F3	-1.033667447	1.97E-13	8.84E-12
S100P	1.618444846	2.01E-13	8.97E-12
DEGS2	1.537665821	2.10E-13	9.37E-12
DGAT2	1.003541414	2.30E-13	1.02E-11
GGT6	1.681992615	2.60E-13	1.14E-11
LRRC20	1.302273062	2.82E-13	1.24E-11
LARGE1	-1.297253373	3.02E-13	1.33E-11

TREX2	2.386040501	3.86E-13	1.69E-11
TTLL11	-1.08085494	3.93E-13	1.71E-11
CCNB1	-1.469107134	4.52E-13	1.96E-11
ABI3BP	-2.323567846	5.12E-13	2.21E-11
HIST1H1C	1.120691572	5.14E-13	2.22E-11
GLUL	-1.053683921	5.28E-13	2.27E-11
PRR11	-1.359507892	5.30E-13	2.27E-11
DPYSL2	-1.075613579	5.44E-13	2.33E-11
KLK13	1.808673638	5.84E-13	2.49E-11
DSCC1	-2.106393601	8.47E-13	3.58E-11
MCM7	-1.28638478	9.98E-13	4.21E-11
COL5A3	-1.141214903	1.14E-12	4.82E-11
KIAA0513	1.11373447	1.28E-12	5.35E-11
C16orf45	-1.63112332	1.34E-12	5.60E-11
COL4A1	-1.445411097	1.40E-12	5.82E-11
SPRR5	3.353358115	1.43E-12	5.94E-11
FRY	2.026589402	1.79E-12	7.42E-11
AL138916.1	3.38633164	2.25E-12	9.32E-11
TRPV3	1.115515383	2.70E-12	1.11E-10
TPM2	-1.175455429	2.83E-12	1.16E-10
TSHZ3	-1.135353648	3.29E-12	1.34E-10
LCE2A	2.405693297	3.32E-12	1.35E-10
AQP3	1.246445286	3.33E-12	1.35E-10
CARD9	2.293954565	3.59E-12	1.45E-10
NPR2	2.503885987	3.69E-12	1.49E-10
SMOX	1.123070287	4.08E-12	1.64E-10
SCMH1	-1.077863565	4.12E-12	1.65E-10
CGN	1.485503279	4.23E-12	1.69E-10
TSHZ2	-2.204023268	4.28E-12	1.70E-10
LFNG	-1.278016	4.50E-12	1.79E-10
PGLYRP4	1.068523469	4.86E-12	1.93E-10
CLCA4	1.192564707	5.46E-12	2.15E-10
SOWAHB	1.454855973	5.80E-12	2.27E-10
ERBB3	1.092199889	5.87E-12	2.29E-10
AURKB	-1.994472307	6.15E-12	2.40E-10
PTPN18	-1.027409541	6.86E-12	2.66E-10
SAMD9	1.139376729	7.06E-12	2.73E-10
GRB7	1.34883798	7.24E-12	2.79E-10
CTSH	1.654871258	7.61E-12	2.93E-10
PLA2G2F	1.810578613	7.91E-12	3.03E-10
EXO1	-1.773657598	8.37E-12	3.20E-10
WNT10A	-1.333485894	8.65E-12	3.30E-10

CRNN	1.79790921	8.74E-12	3.33E-10
CRISPLD2	1.565312027	9.09E-12	3.46E-10
CEACAM5	2.282377735	1.05E-11	3.98E-10
EMP3	-1.366448956	1.05E-11	3.98E-10
S100A7	2.672434878	1.12E-11	4.21E-10
PCED1B	-1.432403163	1.28E-11	4.79E-10
GDF15	1.907668807	1.35E-11	5.02E-10
SLC39A11	-1.037877556	1.44E-11	5.36E-10
PHF19	-1.386946771	1.48E-11	5.49E-10
ORC6	-1.118542735	1.50E-11	5.56E-10
IL36B	2.478178439	1.52E-11	5.63E-10
PRSS23	-1.002819051	1.56E-11	5.76E-10
ABHD4	1.08987621	1.56E-11	5.76E-10
EPB41L3	1.516420126	1.63E-11	5.98E-10
NRCAM	-1.29784031	1.77E-11	6.48E-10
CBLB	-1.002908291	1.80E-11	6.54E-10
IL1RL1	3.885758116	2.00E-11	7.24E-10
CKS1B	-1.143418462	2.03E-11	7.36E-10
PLK4	-1.360923696	2.35E-11	8.51E-10
CDC45	-1.704053661	2.43E-11	8.77E-10
SMC4	-1.026781216	2.46E-11	8.86E-10
SCNN1D	1.899147545	2.63E-11	9.44E-10
DTL	-1.93510712	2.70E-11	9.64E-10
ZNF662	1.701585465	3.00E-11	1.07E-09
HMGB2	-1.655107425	3.08E-11	1.10E-09
PLA2G4F	1.242554752	3.23E-11	1.14E-09
PARP14	-1.033562707	3.23E-11	1.14E-09
PLEKHA7	1.216814221	3.45E-11	1.22E-09
EFR3B	1.248175702	4.00E-11	1.41E-09
TCF4	-1.366289158	4.51E-11	1.58E-09
AC004233.2	2.328708354	4.63E-11	1.62E-09
IL37	3.493441382	4.91E-11	1.71E-09
GRIA3	-1.758571499	4.95E-11	1.72E-09
CEP128	-1.870835164	5.95E-11	2.06E-09
AL139385.1	1.191997305	6.61E-11	2.28E-09
POU2F3	1.782100565	7.52E-11	2.57E-09
APCDD1L-DT	1.970661491	7.90E-11	2.70E-09
AL512274.1	1.426277729	8.89E-11	3.03E-09
TENM4	-1.696566579	9.30E-11	3.15E-09
PAQR5	1.265684166	9.37E-11	3.17E-09
TCF7L1	-1.067065921	9.68E-11	3.27E-09
AL357060.1	1.520112404	1.11E-10	3.72E-09

H2AFZ	-1.097760398	1.17E-10	3.91E-09
KIF4A	-1.834098323	1.18E-10	3.94E-09
STMN1	-1.322783403	1.20E-10	4.00E-09
SERPINA12	1.43518146	1.25E-10	4.15E-09
TXNIP	-1.229150534	1.29E-10	4.26E-09
POLA1	-1.035935294	1.34E-10	4.40E-09
CYP1B1-AS1	7.068510417	1.35E-10	4.44E-09
MT1X	-1.487826574	1.48E-10	4.83E-09
TMEM255A	2.663241226	1.62E-10	5.25E-09
GCNT3	1.439415323	1.77E-10	5.71E-09
PARD3B	-2.750113837	1.82E-10	5.85E-09
CHST1	-1.715959116	1.82E-10	5.85E-09
ASIC1	-1.122608326	1.93E-10	6.17E-09
CNTRL	-1.001618591	1.95E-10	6.22E-09
HFE	-1.09302452	1.96E-10	6.25E-09
IL1F10	1.745776109	2.01E-10	6.38E-09
FAM111B	-1.915391657	2.08E-10	6.57E-09
OLFML2A	-1.41555791	2.34E-10	7.32E-09
RBBP8NL	2.014130253	2.37E-10	7.39E-09
INHBA	-1.076655863	2.42E-10	7.52E-09
GRAMD1C	1.304869625	2.44E-10	7.57E-09
NRIP1	1.031179623	2.49E-10	7.72E-09
FETUB	1.350575368	2.97E-10	9.16E-09
KCNN4	1.339411158	3.10E-10	9.51E-09
C15orf62	2.474614523	3.13E-10	9.60E-09
TMEM125	1.303596491	3.28E-10	1.00E-08
CDK14	-1.086853869	3.50E-10	1.07E-08
CDCA3	-1.635591326	3.55E-10	1.08E-08
DPYD	-2.336030506	3.65E-10	1.11E-08
LTBP1	-1.124416277	3.76E-10	1.14E-08
PTGS2	1.008700242	3.78E-10	1.14E-08
SAA1	-1.255463321	4.31E-10	1.30E-08
SLC43A2	-1.01430803	4.63E-10	1.39E-08
PCSK9	-1.044449156	4.89E-10	1.46E-08
CCDC9B	1.053545426	5.14E-10	1.53E-08
MAD2L1	-1.485519664	5.52E-10	1.64E-08
MYBPHL	1.872463535	5.97E-10	1.77E-08
KCTD17	-1.029176617	6.33E-10	1.87E-08
CRTAM	1.949680646	7.07E-10	2.08E-08
GINS4	-1.240296777	7.15E-10	2.09E-08
SNX10	-1.214168038	7.19E-10	2.10E-08
SGK2	3.992648431	7.48E-10	2.18E-08

CHAF1B	-1.39076278	7.51E-10	2.19E-08
SH3PXD2A-AS1	1.052808412	7.83E-10	2.27E-08
CNTNAP1	-1.82125199	8.52E-10	2.47E-08
CDCA7	-1.164310118	9.15E-10	2.64E-08
AP001972.5	1.551177426	9.81E-10	2.80E-08
HSPB8	1.328775662	1.09E-09	3.10E-08
MCM2	-1.179179045	1.11E-09	3.16E-08
NMI	-1.426771711	1.32E-09	3.73E-08
IGHM	1.326320205	1.35E-09	3.81E-08
MYH14	1.030038115	1.39E-09	3.92E-08
UBE2L6	-1.169309829	1.40E-09	3.95E-08
UCA1	2.143242726	1.45E-09	4.08E-08
AC092306.1	1.095470776	1.52E-09	4.23E-08
PRMT8	1.093244081	1.53E-09	4.26E-08
NRARP	1.177870311	1.70E-09	4.68E-08
GSDMD	-1.557941915	1.73E-09	4.77E-08
TENM3	-1.079337326	1.76E-09	4.83E-08
PPP1R15A	1.07613395	1.77E-09	4.88E-08
CYP1A2	7.900571286	1.78E-09	4.88E-08
FANCD2	-1.411491369	1.83E-09	5.00E-08
NUF2	-1.577240095	1.85E-09	5.05E-08
APOBEC3A	2.856259808	2.02E-09	5.46E-08
ADAMTS14	2.080309838	2.13E-09	5.74E-08
NEDD9	-2.047177269	2.16E-09	5.82E-08
GPR78	1.75471719	2.18E-09	5.88E-08
TACC3	-1.342842169	2.27E-09	6.11E-08
MAP3K8	1.372776591	2.80E-09	7.46E-08
C1orf68	3.146208969	2.95E-09	7.81E-08
KIF18B	-1.865017642	3.15E-09	8.30E-08
PLA2G3	1.53212244	3.18E-09	8.34E-08
CIDEA	2.31929585	3.18E-09	8.34E-08
CIT	-1.450373901	3.19E-09	8.35E-08
BTN3A1	-1.415376934	3.51E-09	9.15E-08
RNF224	4.185398359	3.99E-09	1.04E-07
LURAP1	-1.344903329	4.14E-09	1.07E-07
FOSB	1.47997437	4.30E-09	1.11E-07
SH3D21	1.007074109	4.44E-09	1.15E-07
PSIP1	-1.164274847	4.77E-09	1.23E-07
FCHO1	1.593113805	4.93E-09	1.26E-07
CDCA8	-1.359735567	5.01E-09	1.28E-07
LINC02158	3.215471067	5.67E-09	1.43E-07
SPC25	-2.313353534	5.69E-09	1.44E-07

METTL7A	-1.69356798	5.72E-09	1.44E-07
DHTKD1	-1.0566738	5.88E-09	1.47E-07
HJURP	-1.848321342	6.28E-09	1.57E-07
EXTL2	-1.033178983	6.57E-09	1.64E-07
CNTLN	-1.057681043	6.76E-09	1.69E-07
CDH11	2.503383078	6.97E-09	1.73E-07
AC105233.5	1.447796012	7.03E-09	1.75E-07
AC137936.2	1.553085808	7.23E-09	1.79E-07
AL034376.1	2.266985015	7.27E-09	1.80E-07
CENPI	-1.66332984	7.43E-09	1.83E-07
SKA1	-2.032722792	7.44E-09	1.83E-07
BLM	-1.915690289	7.87E-09	1.93E-07
ZEB2	2.538508076	8.12E-09	1.98E-07
AL157829.1	1.613018197	8.14E-09	1.98E-07
UNC13D	1.463042757	8.44E-09	2.05E-07
CSPG4	-1.286366169	8.49E-09	2.06E-07
TMPRSS4	1.269365783	9.40E-09	2.27E-07
MEFV	1.769226459	1.06E-08	2.54E-07
CARD14	1.459127478	1.18E-08	2.82E-07
TRIP13	-1.089213028	1.24E-08	2.96E-07
CBS	-2.512285983	1.30E-08	3.08E-07
HASPIN	-1.469108195	1.46E-08	3.46E-07
AL357033.1	2.632153972	1.80E-08	4.21E-07
IGHE	2.197841593	1.82E-08	4.26E-07
ABCC2	1.008984097	1.92E-08	4.47E-07
FOXQ1	1.157804865	1.99E-08	4.63E-07
RAD51AP1	-1.734064168	2.19E-08	5.06E-07
PYCR3	-1.233254779	2.23E-08	5.14E-07
AF165147.1	1.205129949	2.38E-08	5.47E-07
TMEM51-AS1	1.467306847	2.40E-08	5.50E-07
LNX1	1.353644866	2.56E-08	5.83E-07
SEMA4D	1.557581542	2.64E-08	5.98E-07
NEIL3	-1.617312707	2.67E-08	6.05E-07
AC015712.2	1.371086938	2.70E-08	6.09E-07
BRCA1	-1.303215107	2.70E-08	6.09E-07
MELK	-1.030446168	2.71E-08	6.09E-07
CDC6	-1.128802016	2.72E-08	6.11E-07
ERVE-1	1.442009034	2.77E-08	6.22E-07
MOXD1	-2.334766592	2.84E-08	6.37E-07
NRM	-1.098163477	2.93E-08	6.56E-07
ZNF704	-1.490075599	3.00E-08	6.70E-07
LINC01269	2.773018401	3.06E-08	6.83E-07

NRN1	3.499230201	3.08E-08	6.85E-07
MAN1A1	-1.0934648	3.09E-08	6.87E-07
IFIT5	-1.169010481	3.21E-08	7.13E-07
AURKA	-1.204222315	3.73E-08	8.23E-07
ADM2	-1.80231643	3.78E-08	8.32E-07
LINC01559	2.053411959	3.78E-08	8.32E-07
GBAP1	1.330153656	3.83E-08	8.42E-07
TMEM170B	2.288596912	3.88E-08	8.50E-07
NR1D1	1.146006303	4.08E-08	8.94E-07
RASEF	1.10394998	4.26E-08	9.29E-07
AC099521.2	2.674067108	4.60E-08	1.00E-06
CGNL1	2.326343396	4.92E-08	1.06E-06
AL357033.3	2.317243042	5.26E-08	1.13E-06
OTOP2	2.037836583	5.37E-08	1.15E-06
CENPH	-1.212526948	5.46E-08	1.17E-06
ZGRF1	-1.431174658	5.49E-08	1.17E-06
SLC47A1	-1.218739622	5.53E-08	1.17E-06
DUOX2	1.339725028	5.57E-08	1.18E-06
IGFBP3	2.68872997	5.81E-08	1.23E-06
ARC	2.367304583	6.01E-08	1.26E-06
MUC16	1.919171803	6.02E-08	1.26E-06
HSPA2	-1.063452617	6.04E-08	1.26E-06
LINC01094	1.185823251	6.18E-08	1.29E-06
DLX5	1.04914114	6.49E-08	1.35E-06
ANOS1	-1.76068766	6.56E-08	1.36E-06
OAS2	-1.021783237	6.79E-08	1.40E-06
LINC02437	2.38586431	6.85E-08	1.41E-06
SLC6A17	-1.684064287	6.96E-08	1.43E-06
MEIS3	-1.505985037	7.45E-08	1.52E-06
AC022217.1	7.833936863	7.69E-08	1.57E-06
LOXL2	-1.559695343	7.94E-08	1.62E-06
LHPP	-1.169735906	8.01E-08	1.63E-06
CENPW	-1.236486628	8.21E-08	1.67E-06
LINC01527	2.062755161	8.23E-08	1.67E-06
TTK	-1.491960456	8.51E-08	1.72E-06
SYT8	1.32528457	8.53E-08	1.72E-06
SCCPDH	-1.000998561	9.36E-08	1.88E-06
PARPBP	-1.017162704	1.08E-07	2.16E-06
TICRR	-1.004262017	1.09E-07	2.16E-06
PRSS27	1.98864579	1.10E-07	2.18E-06
LCE3A	3.440239726	1.12E-07	2.23E-06
AC011483.2	1.184178474	1.13E-07	2.25E-06

KRT84	2.067722048	1.15E-07	2.28E-06
DSG4	1.821291518	1.32E-07	2.60E-06
ORC1	-1.905355286	1.32E-07	2.60E-06
FAM129A	-1.010686826	1.33E-07	2.61E-06
CENPA	-1.81508274	1.39E-07	2.73E-06
ELF5	1.937948185	1.52E-07	2.98E-06
FAM198B	1.457828157	1.57E-07	3.06E-06
STRA6	4.628568942	1.57E-07	3.07E-06
ITGB7	1.945554109	1.58E-07	3.07E-06
AF127577.4	1.125470133	1.63E-07	3.16E-06
ZWINT	-1.343268955	1.64E-07	3.17E-06
AC019349.1	1.673716179	1.72E-07	3.33E-06
KDM7A-DT	1.093899415	1.79E-07	3.45E-06
PEG10	-4.234323385	1.86E-07	3.59E-06
IGFBP4	1.268224434	1.91E-07	3.68E-06
LRRCC1	-1.474318229	1.93E-07	3.71E-06
ARHGAP31	-1.229113523	1.94E-07	3.72E-06
SHCBP1	-1.655094217	2.00E-07	3.81E-06
BLNK	1.335001838	2.03E-07	3.87E-06
CHRNA9	1.68565509	2.08E-07	3.95E-06
HCAR3	1.341460266	2.15E-07	4.07E-06
SLC7A2	-1.221775216	2.17E-07	4.11E-06
AL158206.1	1.093834046	2.19E-07	4.14E-06
KIF21B	-2.165321834	2.29E-07	4.32E-06
KLHL13	-1.652089327	2.44E-07	4.59E-06
C4orf19	2.752125126	2.83E-07	5.27E-06
HOXC4	-1.079593648	2.88E-07	5.35E-06
SLC2A3	-1.377240974	3.01E-07	5.58E-06
KCTD4	3.934748459	3.04E-07	5.63E-06
AC009084.3	1.139635988	3.06E-07	5.66E-06
IFIT3	-1.836667562	3.10E-07	5.73E-06
ARID5A	-1.13713134	3.62E-07	6.64E-06
VILL	1.121392877	3.88E-07	7.07E-06
DIO2	3.251605373	4.16E-07	7.56E-06
ADAMTS6	-1.180030891	4.30E-07	7.79E-06
CDCA5	-1.474315299	4.44E-07	8.01E-06
AC105219.1	1.79283187	4.54E-07	8.18E-06
LIPE-AS1	1.383800717	4.73E-07	8.50E-06
VGLL1	1.032030306	5.36E-07	9.56E-06
RHOBTB1	-1.043087408	5.46E-07	9.70E-06
LXN	-1.451385609	5.51E-07	9.76E-06
TDRD9	2.207995836	5.62E-07	9.93E-06

FBXL16	-1.128329419	6.02E-07	1.05E-05
WDR76	-1.875277512	6.11E-07	1.07E-05
STX19	1.360266118	6.35E-07	1.11E-05
AC004943.2	-1.177912424	6.36E-07	1.11E-05
SLC6A2	-2.277737027	6.38E-07	1.11E-05
CEACAM1	1.184300267	6.60E-07	1.15E-05
CENPK	-1.258869472	6.72E-07	1.17E-05
IFITM10	1.579797626	6.74E-07	1.17E-05
FER1L6	2.780688072	7.38E-07	1.28E-05
MCOLN3	-1.013409035	7.43E-07	1.28E-05
AC011473.2	1.27119047	7.74E-07	1.33E-05
CYP4F3	2.227227077	7.74E-07	1.33E-05
GNAO1	1.013943792	8.02E-07	1.37E-05
AC055811.4	1.20308526	8.04E-07	1.37E-05
HS3ST6	2.13598011	8.24E-07	1.41E-05
FGD2	2.930345348	8.47E-07	1.44E-05
NUDT1	-1.026951141	8.52E-07	1.45E-05
AQP9	1.07120956	8.58E-07	1.46E-05
LYNX1	1.190511681	8.68E-07	1.47E-05
SLC22A20P	1.50538261	8.73E-07	1.48E-05
MYH15	-1.889494846	9.00E-07	1.52E-05
TNFSF18	-1.579016899	9.37E-07	1.57E-05
BDNF	1.614540378	9.37E-07	1.57E-05
CORO2B	-2.081955094	9.43E-07	1.58E-05
SERPINB2	1.811674081	9.77E-07	1.64E-05
COL6A2	2.439330209	1.00E-06	1.67E-05
LINC00589	1.360311373	1.08E-06	1.78E-05
LINC01405	2.950264213	1.09E-06	1.81E-05
AADACL2	1.56711631	1.10E-06	1.82E-05
TEC	1.44422909	1.22E-06	2.00E-05
KRT77	1.326487068	1.23E-06	2.01E-05
PROC	-2.522101097	1.25E-06	2.05E-05
C5	-1.705216191	1.28E-06	2.08E-05
SLURP1	1.785134509	1.34E-06	2.18E-05
FAM198B-AS1	1.290733545	1.46E-06	2.36E-05
ADAM11	2.660843719	1.53E-06	2.46E-05
AC055854.1	2.427457796	1.56E-06	2.50E-05
IL32	-1.239526683	1.60E-06	2.56E-05
THBD	1.045472204	1.61E-06	2.57E-05
CES3	1.128285519	1.74E-06	2.75E-05
SKA3	-1.379502797	1.80E-06	2.83E-05
AL139423.1	1.472726212	1.90E-06	2.98E-05

SLC25A25-AS1	1.177922989	2.06E-06	3.19E-05
AL033397.1	-1.059282656	2.07E-06	3.21E-05
FAM20C	-1.425864337	2.19E-06	3.38E-05
LINC01348	1.477772239	2.27E-06	3.48E-05
SPAG5	-1.150589584	2.31E-06	3.54E-05
SLIT3	-3.159784853	2.37E-06	3.63E-05
AC117386.1	6.828898309	2.44E-06	3.72E-05
PKIB	1.235356697	2.49E-06	3.78E-05
QRFPR	-2.460978899	2.50E-06	3.79E-05
LINC00504	1.33479367	2.55E-06	3.86E-05
IGSF22	2.39634193	2.58E-06	3.90E-05
NINL	-1.247054843	2.65E-06	4.00E-05
LINC01792	2.541618473	2.68E-06	4.03E-05
CLSPN	-1.423000055	2.76E-06	4.15E-05
ITGB2	-1.236166356	2.82E-06	4.22E-05
AC007182.1	1.953942706	2.84E-06	4.25E-05
ZIK1	1.256904997	2.86E-06	4.27E-05
TCF19	-1.295658353	3.01E-06	4.47E-05
KCNS3	-1.171393142	3.03E-06	4.49E-05
C5orf46	1.187047953	3.16E-06	4.65E-05
UNC5B	1.052959869	3.19E-06	4.68E-05
STX11	1.6798543	3.23E-06	4.74E-05
STMN3	-1.110167251	3.36E-06	4.93E-05
AC004231.1	3.20059078	3.38E-06	4.94E-05
RECQL4	-1.17198099	3.48E-06	5.08E-05
MERTK	1.32816314	3.56E-06	5.20E-05
MPIG6B	1.538432904	3.57E-06	5.20E-05
BTN3A3	-1.306248683	3.61E-06	5.26E-05
GCNT1	-1.000577655	3.71E-06	5.36E-05
PARD6B	1.112025379	3.72E-06	5.37E-05
SLC34A3	3.31507072	3.82E-06	5.50E-05
KRT42P	1.153433809	3.95E-06	5.67E-05
CDC25C	-1.749506676	4.00E-06	5.74E-05
SULT1E1	-1.232547699	4.02E-06	5.75E-05
KIF15	-1.481425229	4.16E-06	5.95E-05
NKPD1	1.026113846	4.25E-06	6.06E-05
CHEK1	-1.131456409	4.58E-06	6.47E-05
KIF24	-1.186516161	4.66E-06	6.58E-05
LZTS1	-1.8896418	4.70E-06	6.63E-05
LCE2B	2.646464655	4.77E-06	6.70E-05
HLA-B	-1.354672708	4.84E-06	6.79E-05
FUOM	-1.037561054	4.85E-06	6.79E-05

CAMKV	2.563437139	5.04E-06	7.03E-05
ZBTB16	-1.336006915	5.06E-06	7.05E-05
SPANXN5	5.541110133	5.09E-06	7.08E-05
AC093904.3	2.671102695	5.11E-06	7.11E-05
RAD54L	-1.649891403	5.32E-06	7.36E-05
RFC3	-1.172600467	5.33E-06	7.37E-05
FKBP9P1	-1.019869207	5.44E-06	7.50E-05
PKMYT1	-1.31456307	5.71E-06	7.86E-05
PRR9	2.385019036	5.82E-06	8.00E-05
FAM107B	-1.061598369	5.88E-06	8.07E-05
SLC41A2	-1.052651326	5.93E-06	8.12E-05
ITGA4	-1.421656606	5.93E-06	8.12E-05
BARD1	-1.234588604	5.96E-06	8.13E-05
SH3BGRL2	1.002770277	6.13E-06	8.33E-05
MLXIPL	-2.802280995	6.33E-06	8.56E-05
TTLL11-IT1	-1.491875081	6.98E-06	9.35E-05
AC108215.1	2.635656034	7.06E-06	9.43E-05
TEDC1	-1.059874523	7.24E-06	9.66E-05
BEGAIN	-2.995743172	7.33E-06	9.75E-05
DIP2C	-1.584575644	7.33E-06	9.75E-05
BTN3A2	-1.025175999	7.58E-06	0.0001
ARG1	1.237320182	7.72E-06	0.000102
SRGAP2D	-1.343154638	7.74E-06	0.000102
SEMA3B	1.231696718	7.90E-06	0.000104
HAUS1	-1.011283076	8.12E-06	0.000106
AC011503.1	3.412978099	8.35E-06	0.000109
DHX58	-1.335571546	8.60E-06	0.000112
TGM2	-2.196011804	9.10E-06	0.000118
GTSE1	-1.396991376	9.17E-06	0.000119
GAST	2.295389362	9.36E-06	0.000121
GCKR	4.803013726	9.70E-06	0.000125
RMDN2-AS1	6.61447883	9.85E-06	0.000127
FBXO17	-1.094297062	1.02E-05	0.00013
TJP3	1.219332305	1.07E-05	0.000136
PRDM1	1.640143912	1.07E-05	0.000136
RBL1	-1.144079725	1.07E-05	0.000136
PTPRH	2.294164098	1.08E-05	0.000138
AC011473.3	4.12030202	1.08E-05	0.000138
SLAMF9	1.571010353	1.10E-05	0.00014
ID2	1.530779964	1.11E-05	0.000141
ABCB11	2.688736778	1.14E-05	0.000144
RTN4R	-1.032338334	1.17E-05	0.000147

ASIC3	1.286826816	1.23E-05	0.000154
ADAMTS7	1.595593649	1.23E-05	0.000154
RAD51B	-1.226216473	1.23E-05	0.000154
NPHP1	-1.40677143	1.27E-05	0.000158
MSC	-2.205068162	1.31E-05	0.000163
NOVA1	3.170541314	1.35E-05	0.000167
RASA4CP	1.570670675	1.38E-05	0.000171
HAUS8	-1.184372158	1.39E-05	0.000171
AC129492.1	1.6150943	1.39E-05	0.000172
WNT5B	-1.599329107	1.42E-05	0.000175
PSMB9	-1.799456339	1.42E-05	0.000175
PLA2G4B	2.175343917	1.46E-05	0.00018
FGD3	1.363629402	1.49E-05	0.000183
MAP6	-1.517566709	1.50E-05	0.000184
MTX1P1	3.28219991	1.52E-05	0.000186
SPARC	-1.718581621	1.55E-05	0.000189
DHRS13	-1.134645595	1.56E-05	0.00019
STC2	-1.238952281	1.57E-05	0.000191
LINC01705	2.781163914	1.71E-05	0.000207
ECM2	-2.125054614	1.71E-05	0.000207
ISYNA1	1.012007214	1.76E-05	0.000213
NLRC5	-1.535568122	1.81E-05	0.000217
AC084262.2	2.452407966	1.86E-05	0.000223
NR2F1	2.281782337	1.98E-05	0.000236
MEGF6	-1.464348851	2.04E-05	0.000243
ST6GALNAC5	1.291179885	2.10E-05	0.000249
EFNB3	-1.064595881	2.15E-05	0.000255
AC074033.1	6.452741703	2.16E-05	0.000256
TNIP3	-2.577563154	2.20E-05	0.00026
LYPD6	-1.217008437	2.20E-05	0.00026
AC087783.2	2.244795646	2.34E-05	0.000274
ZNF367	-1.467506176	2.41E-05	0.000281
SPRR2F	1.708614838	2.42E-05	0.000282
RHOBTB3	-1.450010989	2.44E-05	0.000285
ROS1	-1.495599702	2.46E-05	0.000287
HHIPL1	-1.898856743	2.51E-05	0.000291
C14orf132	-1.066789658	2.51E-05	0.000291
AP003068.4	1.202806006	2.57E-05	0.000298
AC093904.2	4.229198301	2.67E-05	0.000308
PTGER3	2.477175443	2.67E-05	0.000308
CHAC1	-1.322784724	2.76E-05	0.000317
DOCK3	1.282191569	2.76E-05	0.000317

MAPK4	-6.246090493	2.79E-05	0.00032
ATP8A2	-1.948266827	2.89E-05	0.00033
SGCE	-1.431857128	2.91E-05	0.000332
HNRNPA1P27	2.803221666	3.01E-05	0.000342
OGDHL	-1.375776305	3.02E-05	0.000343
RMI2	-1.129990703	3.10E-05	0.000352
AGAP11	3.476066468	3.12E-05	0.000354
DSG1-AS1	1.311086903	3.13E-05	0.000355
FAM25C	1.369556634	3.17E-05	0.000359
BUB1B	-1.959732209	3.26E-05	0.000368
SYTL2	1.055237013	3.39E-05	0.000382
REPS2	-1.825038425	3.40E-05	0.000382
SUSD1	1.265662052	3.42E-05	0.000385
LRRC37A6P	-1.367329185	3.56E-05	0.000398
TMC8	-1.530134488	3.64E-05	0.000407
GLI1	-2.746333029	3.70E-05	0.000413
NCF1	1.405531252	3.71E-05	0.000414
LINC02487	6.53274389	3.82E-05	0.000425
TRIB3	-1.552246274	3.83E-05	0.000425
AC004233.3	1.961501836	3.93E-05	0.000436
TCHH	1.011266101	3.96E-05	0.000439
CCDC150	-2.398965854	3.97E-05	0.000439
VIM	-1.9356096	4.15E-05	0.000458
ESCO2	-1.567855574	4.22E-05	0.000465
PCLAF	-1.204334521	4.33E-05	0.000476
EEF1A2	1.418603131	4.34E-05	0.000476
CXCR2	1.121222037	4.43E-05	0.000485
AKAP7	-1.451184879	4.47E-05	0.000489
TLL2	-1.572029015	4.50E-05	0.000492
CREB3L4	-1.229913575	4.52E-05	0.000494
TRAPPC6A	-1.226794625	4.64E-05	0.000505
NT5M	-2.327274862	4.65E-05	0.000505
RHBG	1.853243176	4.73E-05	0.000514
ARHGEF40	-1.091990033	4.77E-05	0.000517
KHDRBS3	-1.663568466	5.05E-05	0.000543
KANK4	-5.042564395	5.05E-05	0.000543
SLC12A7	-1.826010363	5.16E-05	0.000553
ABCA4	-2.026529003	5.21E-05	0.000557
CCNE2	-1.230576128	5.33E-05	0.000567
RGS17	2.611193731	5.40E-05	0.000573
KRT82	3.439583986	5.48E-05	0.000581
PSRC1	-1.016155062	5.51E-05	0.000584

KIAA0319	2.390465989	5.60E-05	0.000592
AC105046.1	2.304340294	5.69E-05	0.000599
MSC-AS1	-1.795164554	5.76E-05	0.000606
ERCC6L	-1.258793538	5.80E-05	0.000609
COL4A2	-1.742842024	5.83E-05	0.000611
AC093904.4	2.397666768	6.24E-05	0.000649
PLEKHA4	-1.464580664	6.37E-05	0.000662
AADAC	1.315680674	6.42E-05	0.000666
AC068831.7	-2.530304252	6.43E-05	0.000667
SHANK1	1.875406362	6.46E-05	0.000669
CDH10	2.148930791	6.53E-05	0.000674
SLC24A3	-1.356975927	6.61E-05	0.000681
IRAK3	-1.884333914	6.68E-05	0.000688
AC008663.1	2.071849046	6.69E-05	0.000688
LMCD1	-2.636582966	6.93E-05	0.00071
FAIM2	2.594827001	7.16E-05	0.000731
MYOM3	-1.448577496	7.44E-05	0.000757
KCNK10	-1.552083692	7.44E-05	0.000757
PAQR8	-1.466526369	7.45E-05	0.000757
AL049767.1	3.472011852	7.50E-05	0.000761
AC027612.1	5.771835061	7.52E-05	0.000762
SYNE3	-1.134133737	7.75E-05	0.000785
PAEP	1.676545994	8.02E-05	0.000809
SPATA6L	1.668591187	8.13E-05	0.00082
OTP	2.454989603	8.37E-05	0.000841
LUCAT1	1.05258631	8.51E-05	0.000854
C9orf131	3.153739527	8.58E-05	0.00086
MANEAL	-1.275583085	8.90E-05	0.000889
AL356056.1	-2.604153701	9.07E-05	0.000905
KIF20A	-1.859214379	9.39E-05	0.000931
CCNJL	-5.538172444	9.55E-05	0.000945
RGS5	-2.05511396	9.64E-05	0.000953
CCDC15	-1.211935462	9.94E-05	0.00098
FAM25BP	2.175305156	1.08E-04	0.001055
GDF7	4.112017549	1.10E-04	0.001074
TESK2	-1.128628681	1.16E-04	0.001131
AP000944.2	1.866244074	1.18E-04	0.001146
MYCBPAP	1.750958106	1.24E-04	0.001196
TNFAIP8L1	-1.008097954	1.25E-04	0.001205
SYT12	-1.359637175	1.26E-04	0.001206
PNMA5	6.318904693	1.28E-04	0.001226
THRB	1.12084815	1.28E-04	0.001229

ATP13A4	1.583007298	1.29E-04	0.001237
GNA14	2.142954988	1.30E-04	0.001242
C15orf48	1.794314891	1.38E-04	0.001307
CLIC5	2.379981687	1.39E-04	0.001323
CDC20	-1.858967769	1.42E-04	0.001342
GFPT2	2.735529965	1.42E-04	0.001345
CRISP3	4.038243886	1.43E-04	0.00135
POLE2	-1.285545725	1.46E-04	0.001374
LMNB1	-1.939276061	1.47E-04	0.00138
PKN3	-1.530859239	1.51E-04	0.001412
MUC19	1.474145685	1.51E-04	0.001412
AP000812.3	3.621357452	1.51E-04	0.001412
KLK14	1.682627278	1.54E-04	0.001435
ANKRD36C	-1.151338728	1.58E-04	0.001467
PART1	1.419122691	1.59E-04	0.001475
CEP55	-1.959645241	1.61E-04	0.001485
KANK3	1.559314365	1.66E-04	0.001528
HID1	1.034448744	1.69E-04	0.001554
GREB1L	-1.027607816	1.70E-04	0.001561
FAM86EP	-1.111352123	1.71E-04	0.001564
DGCR5	-1.088833934	1.75E-04	0.001599
AC010186.3	-1.416880281	1.76E-04	0.00161
LY6D	1.433114718	1.80E-04	0.001634
LRRIQ1	-1.391755331	1.81E-04	0.001642
HRASLS2	1.572878645	1.87E-04	0.001693
ARHGEF19	-1.298556996	1.90E-04	0.001713
UNC93A	1.468393024	1.92E-04	0.00173
FES	2.136950434	1.92E-04	0.00173
FANCB	-1.293766647	1.93E-04	0.001738
SLC13A4	2.222987331	1.98E-04	0.001776
NUSAP1	-1.698711604	1.99E-04	0.001781
SCN4B	-1.006520675	2.00E-04	0.00179
AL513497.1	1.322997125	2.02E-04	0.001804
MKI67	-1.955389351	2.03E-04	0.001807
CBSL	-3.786529028	2.03E-04	0.001812
KIF12	-1.588708897	2.04E-04	0.001816
SOX2	2.522315339	2.07E-04	0.001843
FAM174B	-1.599179316	2.11E-04	0.001869
IGFL2-AS1	1.075606845	2.11E-04	0.001872
AC011497.2	1.626817552	2.17E-04	0.001919
LGI2	3.446359568	2.17E-04	0.00192
AC009133.4	-2.620596732	2.23E-04	0.00196

EGR2	1.869376033	2.24E-04	0.001969
AC008738.5	1.149792765	2.29E-04	0.002013
ATAD5	-1.158304791	2.34E-04	0.002048
CACNB1	-1.095383787	2.40E-04	0.0021
SERPINB9	1.917910827	2.48E-04	0.002165
KLHL23	-1.03931036	2.49E-04	0.00217
DNAH17	-1.932492924	2.50E-04	0.002182
MT-TY	1.016647442	2.64E-04	0.002294
GALM	-1.156064261	2.76E-04	0.002386
UBE2FP1	1.492251127	2.81E-04	0.00243
TRAF5	-1.03835406	2.82E-04	0.002436
SMO	-1.273016062	2.92E-04	0.002507
CYP4X1	-1.49819145	2.92E-04	0.00251
AC245297.3	-1.193476206	2.97E-04	0.002542
DUOXA2	1.814886822	2.98E-04	0.002543
TPX2	-1.308460331	3.02E-04	0.002571
CSGALNACT1	1.557997055	3.05E-04	0.002591
SAMD9L	-1.728937304	3.05E-04	0.002591
DAGLA	-4.085838327	3.10E-04	0.002622
EDA2R	1.12024321	3.12E-04	0.002635
C14orf28	-1.040829341	3.16E-04	0.002665
OIP5	-1.745649489	3.23E-04	0.002714
ANKFN1	1.37807212	3.29E-04	0.002757
Sep-05	1.817820151	3.33E-04	0.002788
DDIAS	-1.12469028	3.42E-04	0.002856
FAM222A	1.391987389	3.47E-04	0.002892
TREML3P	1.318461546	3.50E-04	0.002913
KIF2C	-1.815002379	3.54E-04	0.002939
TNFRSF13C	2.471396653	3.60E-04	0.002976
MSLNL	3.190580918	3.61E-04	0.002982
MYRF	1.308583857	3.76E-04	0.003103
MPL	1.756791553	3.78E-04	0.003117
AL161431.1	1.217496883	3.80E-04	0.003129
KIF11	-1.510242136	3.90E-04	0.003201
ACSBG1	1.20077916	3.91E-04	0.00321
TLR1	-1.698063172	3.97E-04	0.003252
IQGAP3	-1.740027088	4.06E-04	0.003312
LINC02448	2.466544185	4.08E-04	0.003326
SLC22A14	1.241422195	4.08E-04	0.00333
SERPIND1	4.249459398	4.11E-04	0.003352
PPP1R3C	-1.169183266	4.12E-04	0.003361
SALL2	-1.534208401	4.17E-04	0.003391

AP001266.1	1.813061314	4.20E-04	0.003419
HIVEP3	-1.189187143	4.30E-04	0.003486
ASPM	-1.552319699	4.44E-04	0.003594
PLK1	-1.749804701	4.53E-04	0.003667
NFAM1	-3.525498114	4.59E-04	0.003704
LINC00475	4.778424262	4.61E-04	0.003718
MCF2L2	1.413737073	4.62E-04	0.003729
MATN2	-1.125261399	4.64E-04	0.003734
FAAHP1	2.145708983	4.67E-04	0.003752
AC025423.4	1.896125813	4.75E-04	0.003802
LINC02029	1.156511865	4.93E-04	0.003936
MYO16	1.695960743	4.96E-04	0.003951
AL121761.1	1.409050973	4.96E-04	0.003951
PIF1	-1.91054454	5.01E-04	0.003988
AC005392.2	2.2198962	5.10E-04	0.004046
SFMBT2	-3.164968577	5.19E-04	0.004112
AC015912.3	1.556998097	5.21E-04	0.004121
DLGAP5	-1.781126897	5.21E-04	0.004123
PDE6G	3.978699553	5.25E-04	0.00415
GDPD5	-1.539883714	5.35E-04	0.004221
AC131212.3	1.043710669	5.37E-04	0.004233
POLQ	-1.075505634	5.46E-04	0.0043
GLT8D2	-2.096862701	5.49E-04	0.004319
MFSD2B	3.164345658	5.58E-04	0.004382
BUB1	-1.922657296	5.59E-04	0.004392
LINC01515	-1.413049679	5.65E-04	0.004434
AC007342.5	1.819611329	5.91E-04	0.004615
NCAPG	-1.846792827	5.97E-04	0.004654
OLFML3	1.351298054	5.99E-04	0.004666
APOL4	1.830506052	6.13E-04	0.004756
PLBD1	1.111742051	6.23E-04	0.004828
LINC00514	3.514822074	6.31E-04	0.004884
PRUNE2	-2.215103549	6.37E-04	0.004924
AL031058.1	1.121793009	6.44E-04	0.004969
RTEL1-TNFRSF6B	-2.325388275	6.47E-04	0.004991
DRD5	2.430367501	6.60E-04	0.005072
HIST1H1E	1.468413432	6.66E-04	0.005113
ESR1	-1.066983552	6.81E-04	0.005205
FAM86B2	-1.193237849	6.88E-04	0.005256
BCL11A	-1.441736449	6.96E-04	0.005314
FOXM1	-1.784531338	7.08E-04	0.00539
ASS1	-1.988720689	7.16E-04	0.005446

CCNA2	-1.506589184	7.39E-04	0.005597
AP003396.3	3.140748333	7.53E-04	0.0057
STON1	-1.203269895	7.54E-04	0.005707
KRT4	1.889628551	7.64E-04	0.005777
SMIM11A	3.97657868	7.83E-04	0.005901
AC092017.1	2.044316584	7.95E-04	0.005974
MEG3	1.015423294	8.03E-04	0.006029
MAMLD1	-1.380395802	8.27E-04	0.00618
FFAR2	4.557415881	8.30E-04	0.006198
GPLD1	1.484488334	8.39E-04	0.006256
MT2P1	-1.755192299	8.43E-04	0.006288
MAP1B	-1.481454344	8.45E-04	0.006292
NEK10	1.045007888	8.52E-04	0.006339
MT4	-1.79043921	8.73E-04	0.006491
AC129492.6	3.734710142	8.76E-04	0.006511
FOLR1	2.730039055	8.83E-04	0.006554
TNXB	1.148084519	9.02E-04	0.006666
RGS16	1.516370019	9.05E-04	0.006681
FAM3D	1.560365008	9.10E-04	0.006712
CBR3	-1.198274854	9.11E-04	0.006716
RPH3AL	-2.112314453	9.30E-04	0.006842
TNK2-AS1	1.073910202	9.34E-04	0.006865
CD22	2.834525032	9.40E-04	0.006908
SEMA6B	-3.331334395	9.65E-04	0.007054
LINC01932	1.232225592	9.66E-04	0.007063
ENOX1	-1.299118518	9.71E-04	0.007092
AZIN2	-1.102725008	1.01E-03	0.007309
MRAP2	-1.54405574	1.04E-03	0.007502
AADAT	-1.04476784	1.05E-03	0.007577
FAM171A2	-1.243274546	1.07E-03	0.007661
TOP2A	-1.796294087	1.07E-03	0.007668
NUPR1	-1.057789416	1.09E-03	0.007812
ASNS	-1.982559197	1.11E-03	0.007906
ARHGAP11A	-1.501206435	1.11E-03	0.007928
FAM72D	-1.560000355	1.14E-03	0.008096
TET1	-1.780328198	1.16E-03	0.008189
ERVW-1	2.606166827	1.17E-03	0.008259
SNCB	1.467599513	1.17E-03	0.008263
NFATC2	1.652368566	1.18E-03	0.008269
DEPTOR	-1.490934521	1.19E-03	0.008379
CACNA1D	1.986459921	1.20E-03	0.008414
CALCRL	-1.348595999	1.25E-03	0.008709

SLC47A2	1.123196869	1.25E-03	0.008728
MACROD2	-1.726520792	1.25E-03	0.008737
P2RY6	2.188900752	1.26E-03	0.008786
LINC01140	1.901275195	1.28E-03	0.008899
TIE1	3.691342607	1.29E-03	0.008971
AP001962.1	2.058786224	1.31E-03	0.009064
PKNOX2	1.652884848	1.32E-03	0.00908
SCEL-AS1	2.060744615	1.32E-03	0.009083
AC022239.1	1.469705646	1.34E-03	0.009214
LUARIS	-1.278283458	1.35E-03	0.009243
PPP1R16B	2.317152281	1.36E-03	0.009322
AC092123.1	1.201683906	1.38E-03	0.009426
IL15RA	-2.25867904	1.38E-03	0.009444
MYLIP	-1.012153503	1.41E-03	0.009591
NPTXR	-1.775667396	1.45E-03	0.009854
CYP4F2	1.400662878	1.47E-03	0.010003
NDC80	-1.77074394	1.48E-03	0.010003
KIFC1	-1.737507406	1.48E-03	0.010039
VIM-AS1	-2.104684831	1.50E-03	0.010119
MAL	2.919975173	1.50E-03	0.010128
TMEM191C	1.379968776	1.54E-03	0.010386
AZGP1P1	2.211948667	1.55E-03	0.010432
PRRX1	2.649070925	1.56E-03	0.010466
NHLH2	1.540700328	1.56E-03	0.010496
CES1	1.261376517	1.59E-03	0.010635
LINC00592	1.976256771	1.61E-03	0.010741
AC012645.4	2.002135166	1.61E-03	0.010741
ZBED3	-1.122207757	1.61E-03	0.010741
PID1	-1.21974377	1.67E-03	0.011078
LINC01336	1.299073721	1.68E-03	0.011124
KCNJ5	-2.583398752	1.69E-03	0.011176
PRIM1	-1.762074343	1.70E-03	0.011256
EML6	-1.014242122	1.71E-03	0.011291
DEPDC1	-1.917136953	1.72E-03	0.011346
CKS2	-1.319752441	1.73E-03	0.011413
EPSTI1	-1.43884857	1.76E-03	0.01162
AC108134.1	1.81159549	1.81E-03	0.011874
DLEU2	-1.123739743	1.83E-03	0.01203
AL356056.2	-1.987714012	1.86E-03	0.012146
CCL20	-1.157377214	1.87E-03	0.012196
RGS2	1.08199233	1.94E-03	0.012583
MIR4537	3.49754025	1.97E-03	0.012806

CHN1	-3.793179109	2.00E-03	0.01295
PDE6A	-2.632599725	2.02E-03	0.013042
ERP27	1.571224848	2.04E-03	0.013146
TOB1-AS1	1.486342622	2.06E-03	0.0133
EMILIN3	1.593391547	2.07E-03	0.013336
NWD1	-1.043340103	2.07E-03	0.013365
ITGB2-AS1	-1.885684482	2.09E-03	0.013457
PLEKHO1	-1.112567794	2.12E-03	0.013601
IL1R2	1.604707211	2.19E-03	0.013984
AC004990.1	2.46862641	2.19E-03	0.013986
ACTL10	-1.665893923	2.20E-03	0.014025
ARHGAP33	-1.393835373	2.22E-03	0.014156
CENPM	-1.204693828	2.23E-03	0.01423
AC016205.1	-1.997081487	2.26E-03	0.014409
EME1	-1.011123219	2.34E-03	0.01483
PSCA	1.382282803	2.37E-03	0.014971
KRT33A	3.558345196	2.41E-03	0.015162
AC004840.1	3.872604282	2.42E-03	0.015233
ISM2	-1.631234959	2.42E-03	0.015257
UBE2C	-1.742345196	2.43E-03	0.015269
SPINK13	1.88120706	2.48E-03	0.01556
B4GALNT1	-1.539123145	2.48E-03	0.015565
SERPINB11	1.122930062	2.49E-03	0.015581
SLC8A1	-2.306089698	2.62E-03	0.016332
WNT4	-2.473746831	2.69E-03	0.016638
PRSS35	1.572868946	2.72E-03	0.016763
WNT3A	-1.735105283	2.72E-03	0.016764
GNRHR	1.335150412	2.75E-03	0.016961
KLKP1	3.01667726	2.78E-03	0.01707
NDST1-AS1	1.228907803	2.79E-03	0.01712
ANKRD65	1.033496249	2.84E-03	0.017387
AC128657.1	-1.072667376	2.88E-03	0.017597
AC004241.5	2.180863314	2.90E-03	0.01771
GINS2	-1.60568091	2.92E-03	0.017805
FANCI	-1.169216908	2.92E-03	0.017846
HPX	1.232097087	2.95E-03	0.017963
CLEC18B	1.387699247	2.97E-03	0.018067
CXCL14	-1.718102771	3.00E-03	0.018163
FZD4	-1.196621268	3.03E-03	0.018328
AC234582.2	1.672886434	3.07E-03	0.01854
CCDC146	-1.440607322	3.07E-03	0.018566
NXPH4	-1.398618857	3.21E-03	0.019235

CENPF	-1.619912965	3.25E-03	0.019458
AC083841.2	3.379190964	3.26E-03	0.019541
AC007325.4	-1.566543283	3.30E-03	0.019711
SCN8A	-1.589568401	3.31E-03	0.019757
TRIML1	3.13078665	3.34E-03	0.01991
TRAIP	-1.083090648	3.35E-03	0.019952
AC018557.1	1.766827632	3.36E-03	0.020027
ALDH1L1	-1.228119441	3.40E-03	0.020217
FAM72C	-2.12383601	3.40E-03	0.020222
MYBL2	-1.95603621	3.40E-03	0.020225
DTNA	-1.921020607	3.43E-03	0.020348
SYNPO2	-1.758301349	3.47E-03	0.02055
NCAPH	-1.708578535	3.48E-03	0.020594
PPP2R2B	-1.297336615	3.50E-03	0.020649
PTPRG-AS1	-1.24287539	3.51E-03	0.020726
CLDN7	1.909308158	3.55E-03	0.020926
VWCE	1.100592278	3.57E-03	0.021031
AP002770.1	1.004623388	3.57E-03	0.021042
EDAR	1.173673308	3.58E-03	0.021093
ENPP2	2.32115865	3.62E-03	0.021288
AC121338.1	2.945387633	3.63E-03	0.021336
SLC46A2	2.114776442	3.82E-03	0.022275
AC009088.3	1.283176234	3.83E-03	0.022301
FAM25A	2.923968462	3.83E-03	0.022316
BIRC5	-1.772003606	3.87E-03	0.022428
ZFHX4	1.440592446	3.87E-03	0.022428
KRT2	1.845352046	3.90E-03	0.022581
HMGB1P10	-1.317746509	3.92E-03	0.022675
INCA1	1.325945294	3.96E-03	0.022856
KCNE4	1.188792618	4.11E-03	0.023603
FMO5	-1.083747776	4.14E-03	0.023716
LINC02273	1.162487201	4.16E-03	0.023829
LINC00482	2.023066638	4.16E-03	0.023829
AC010186.2	-1.995462282	4.17E-03	0.023829
LRRC74B	2.002940678	4.18E-03	0.023862
C9orf84	1.444221389	4.20E-03	0.024006
AC025280.3	3.129244922	4.21E-03	0.024032
PKD1P1	-2.909465871	4.22E-03	0.024035
MYO1H	1.617947887	4.25E-03	0.024181
ANKRD36BP2	1.419763866	4.26E-03	0.024233
HTR1B	-1.440665992	4.48E-03	0.025276
CXCL2	-1.195920824	4.55E-03	0.025571

AL158801.5	1.563171335	4.56E-03	0.025601
CLCA3P	1.186932008	4.58E-03	0.025691
AP003096.1	1.469035546	4.62E-03	0.025862
CENPE	-1.237203779	4.64E-03	0.025984
CREG2	1.406896982	4.67E-03	0.026076
COL13A1	-4.062472518	4.69E-03	0.026197
AC000095.1	2.456836914	4.72E-03	0.026373
SLC23A1	1.731738778	4.74E-03	0.026469
UBL7-AS1	-1.146878586	4.77E-03	0.02659
EIF1P6	3.457227865	4.79E-03	0.026672
AC113404.3	1.036399556	4.85E-03	0.026959
ANLN	-1.305772317	4.86E-03	0.027015
AL160408.3	1.679895308	4.90E-03	0.02718
NBEA	-2.245696464	5.00E-03	0.027679
HYAL4	1.792446819	5.02E-03	0.027768
MBOAT1	-1.277764707	5.03E-03	0.027819
ZNF792	-1.089455573	5.03E-03	0.027819
RNU6-1161P	1.641081994	5.05E-03	0.027891
AC093908.1	-1.131886602	5.12E-03	0.028185
KLK4	2.455241349	5.22E-03	0.028634
AC021491.2	1.249039461	5.26E-03	0.028792
CRYBB2	2.77890742	5.27E-03	0.028841
TNC	-1.403111569	5.29E-03	0.028933
CDKN2C	-1.45922225	5.30E-03	0.02896
NSD2	-1.203729978	5.40E-03	0.029447
ARMC12	1.148093523	5.42E-03	0.029529
TPK1	-1.509902237	5.49E-03	0.029829
MLPH	1.218818395	5.52E-03	0.029987
RNF208	1.057101061	5.56E-03	0.030101
EGFL6	-2.501824233	5.58E-03	0.030175
AC007292.2	1.823786583	5.61E-03	0.030281
AC097460.1	-1.28446731	5.71E-03	0.030719
NDST2	1.050848618	5.73E-03	0.030835
RRAD	1.52655873	5.74E-03	0.030847
AC145138.1	-3.124018576	5.78E-03	0.031053
HBEGF	1.01091036	5.84E-03	0.031277
TNF	-1.392112768	5.88E-03	0.031455
AC091057.1	-1.203884937	5.89E-03	0.031492
CACNA1S	2.096190104	5.94E-03	0.031684
HRAT92	1.026550436	6.00E-03	0.031922
AC138969.1	-1.582200585	6.01E-03	0.031976
TK1	-1.767441528	6.11E-03	0.032384

AC124944.1	2.90511722	6.11E-03	0.032384
TLR2	-1.539448485	6.23E-03	0.032865
AC026740.1	1.130026266	6.38E-03	0.033558
GPRC5A	1.572219738	6.39E-03	0.033586
RSAD2	-3.182135326	6.42E-03	0.033747
AC135050.3	2.219907247	6.43E-03	0.033801
CNTNAP4	1.476164225	6.49E-03	0.034011
LINC01206	1.806358021	6.53E-03	0.034165
AC009078.3	1.026936783	6.53E-03	0.034165
MAP1A	-1.93179637	6.53E-03	0.034165
RAMP1	-1.277032519	6.57E-03	0.034353
LINC02137	2.362822548	6.62E-03	0.03455
CD7	2.320222539	6.68E-03	0.034828
AC144831.1	1.633435726	6.69E-03	0.03486
CPXCR1	2.300823834	6.71E-03	0.03497
PCYT1B	-2.418972052	6.76E-03	0.035198
TNNI2	1.949307453	6.80E-03	0.035316
CALB1	2.53600808	6.83E-03	0.035409
CKAP2L	-1.557670424	6.95E-03	0.035901
AC097478.1	1.031189124	7.02E-03	0.036179
LINC00173	-3.26696308	7.16E-03	0.036726
NRXN3	-3.374453355	7.17E-03	0.036734
LINC01554	2.744450928	7.22E-03	0.036925
UGT1A7	1.888613508	7.25E-03	0.037038
FZD2	-1.087210386	7.37E-03	0.037572
FYB1	1.231591077	7.45E-03	0.037908
JPH4	1.86455134	7.49E-03	0.038035
AC068057.1	1.327887335	7.51E-03	0.038131
SFTPD	2.206201003	7.51E-03	0.038145
AL122023.1	1.175825908	7.53E-03	0.038214
BACH2	-1.877443211	7.56E-03	0.038349
NCAPG2	-1.281884	7.59E-03	0.038458
LINC01764	2.422897808	7.64E-03	0.038634
KPNA7	1.443320954	7.72E-03	0.038963
TBX19	1.086687395	7.78E-03	0.039191
DEPP1	-1.193529572	7.80E-03	0.039216
AC017101.1	-1.780074341	7.80E-03	0.039228
NKILA	-1.913489661	7.81E-03	0.03928
GPC4	-1.381154304	7.86E-03	0.039488
AC130304.1	1.424888899	7.98E-03	0.040017
HIST2H4B	1.9472636	7.99E-03	0.040048
LSMEM1	1.180276546	8.00E-03	0.040062

TXK	1.720506239	8.00E-03	0.040081
CGA	2.006092246	8.01E-03	0.040081
AC006262.1	1.026958909	8.04E-03	0.040222
NEK2	-1.583292517	8.06E-03	0.040285
SIGIRR	-1.342406053	8.23E-03	0.04104
MYH16	1.068565975	8.44E-03	0.041936
FIBCD1	-2.031857611	8.44E-03	0.041936
FAM83D	-1.374837745	8.57E-03	0.042448
CCL22	2.397467793	8.64E-03	0.042708
AC025048.2	-1.061124858	8.72E-03	0.043033
DUX4L50	1.131951223	8.86E-03	0.043604
AC093159.1	-1.774361429	8.88E-03	0.043687
APOB	1.52143081	9.08E-03	0.044466
HAS2	2.514468167	9.15E-03	0.044681
FAM72B	-1.060222087	9.17E-03	0.044773
GLRA4	-1.124030572	9.49E-03	0.046073
EAF1-AS1	1.199035734	9.59E-03	0.046496
STOX1	-1.61276047	9.65E-03	0.046687
AL365356.3	1.932410818	9.70E-03	0.046889
ABCB6	1.538120864	9.79E-03	0.047253
AP001615.1	1.117559777	9.79E-03	0.047265
LINC01805	1.35498779	9.80E-03	0.047267
SMAD9	-1.474135056	9.85E-03	0.047424
APOBEC3G	-2.867841623	9.87E-03	0.047475
PAMR1	-2.431106936	9.88E-03	0.047501
AC009831.1	1.033110215	9.90E-03	0.047541
AC098934.1	2.835561457	1.00E-02	0.048053
EMBP1	-1.495820671	1.00E-02	0.048059
ALPP	2.414652629	1.00E-02	0.048059
EN2	2.711465819	1.01E-02	0.048507
MSANTD1	1.664928431	1.02E-02	0.048755
WDFY4	1.912919734	1.04E-02	0.049622

Supplementary Table 1. DEGs list for all significantly upregulated and downregulated genes in BaPvsControl Group.

Supplementary Table 2.

TCDDvsControl DEGs_all			
gene_name	**log2FoldChange**	**pvalue**	**padj**
LCE3E	4.259215017	6.58E-166	1.20E-161
LYPD5	3.435431317	7.64E-151	7.00E-147
CYP1B1	9.832144977	1.11E-147	6.76E-144
SPRR2G	3.265672903	1.66E-142	7.58E-139
LCE3D	3.896184331	1.02E-141	3.73E-138
CDSN	3.54803508	9.10E-139	2.78E-135
CNFN	3.446890965	3.72E-120	9.74E-117
SPRR2A	3.334577105	3.64E-116	8.33E-113
LCN2	3.866271268	6.73E-114	1.37E-110
IL1B	2.727575505	1.42E-106	2.61E-103
SPRR5	4.145521642	3.69E-105	6.14E-102
CRCT1	3.954612265	1.87E-92	2.86E-89
ADGRF1	2.445723425	4.69E-92	6.61E-89
TGM3	3.777266303	4.15E-91	5.43E-88
CYP1A1	11.66091231	1.00E-90	1.23E-87
UPK1B	2.216981333	3.23E-90	3.70E-87
SPRR3	3.386791292	5.06E-88	5.45E-85
PSORS1C1	2.882615492	2.05E-81	2.08E-78
ACP7	3.258079458	6.03E-77	5.81E-74
SPINK7	3.127289766	3.65E-73	3.35E-70
RNASE7	2.766697432	2.40E-70	2.09E-67
PSAT1	-2.097628618	5.20E-70	4.32E-67
SPRR2E	2.197227181	6.00E-70	4.78E-67
IL36RN	1.964179489	9.10E-69	6.94E-66
LCE3C	3.928998817	5.44E-68	3.98E-65
ADIRF	2.30595451	2.39E-66	1.68E-63
SPRR2B	3.187401173	2.26E-65	1.53E-62
KRT37	4.124091431	6.45E-64	4.22E-61
CLDN17	3.692499017	6.88E-62	4.35E-59
FA2H	3.094904195	1.54E-61	9.39E-59
SPRR2D	2.041229035	7.13E-61	4.21E-58
AC115522.1	3.701822091	2.86E-60	1.64E-57
FNDC4	2.570143567	5.24E-60	2.91E-57
GPAT3	3.462783481	5.33E-59	2.87E-56
HRNR	2.881987191	2.19E-56	1.15E-53
HSD17B2	3.355714048	4.40E-56	2.24E-53
KPRP	2.778765763	8.42E-56	4.16E-53

NEFL	-2.34574714	2.89E-55	1.39E-52
GDA	3.092414499	1.96E-52	9.20E-50
PHGDH	-2.563510067	6.96E-48	3.18E-45
SULT2B1	1.808854613	1.32E-47	5.91E-45
LGALSL	1.529110369	2.20E-47	9.60E-45
HOPX	1.989835166	2.32E-47	9.86E-45
TMPRSS13	1.879682875	1.01E-46	4.22E-44
HMOX1	2.158022082	1.55E-46	6.21E-44
ADGRE2	1.640517068	1.56E-46	6.21E-44
EPN3	1.55460249	3.52E-45	1.37E-42
KRT34	2.162617943	4.27E-45	1.63E-42
KLK10	1.903697913	4.80E-45	1.79E-42
FCHSD1	1.588715	5.99E-45	2.19E-42
MYO5B	1.699857459	7.12E-45	2.56E-42
NCCRP1	2.022007307	7.80E-45	2.75E-42
SCEL	1.990816123	1.36E-44	4.70E-42
ALDH1A3	5.341034717	2.00E-44	6.78E-42
NID1	-3.152255946	2.40E-44	7.99E-42
ESYT3	2.341821853	5.99E-44	1.96E-41
CEMIP2	1.727201687	6.28E-44	2.02E-41
AC007325.2	1.740340552	7.74E-44	2.44E-41
DAPP1	1.409281425	1.23E-43	3.81E-41
SLPI	2.009716703	1.30E-43	3.97E-41
BCAT1	-1.853848316	1.48E-43	4.43E-41
AC004816.1	2.136418512	2.61E-43	7.70E-41
SPNS2	2.255369594	3.06E-43	8.90E-41
AHRR	3.378001513	7.91E-43	2.26E-40
ZNF185	1.336521372	9.38E-43	2.64E-40
UCA1	3.314524043	3.06E-42	8.50E-40
CTSV	1.595406942	6.47E-42	1.77E-39
NQO1	1.381004549	8.93E-42	2.41E-39
RNF222	2.412976243	1.37E-41	3.63E-39
IL1RN	1.630741675	3.61E-41	9.45E-39
KRT16P2	3.163815781	3.92E-41	1.01E-38
DHRS9	2.49312861	1.04E-40	2.65E-38
LMO7	1.956152529	1.14E-40	2.87E-38
HS3ST2	2.725524809	4.70E-40	1.16E-37
LCE2D	3.649893249	5.01E-40	1.22E-37
TGFBI	1.850195133	1.53E-39	3.68E-37
ITM2A	-2.267554841	2.06E-39	4.89E-37
GLRX	2.272323318	2.98E-39	7.00E-37
SPRR1B	1.331887723	5.19E-39	1.20E-36

NLRP10	1.749896656	5.66E-39	1.30E-36
ENDOU	2.759966839	1.93E-38	4.35E-36
KRT80	2.115600859	2.35E-38	5.26E-36
MFAP5	1.395203866	6.40E-38	1.41E-35
GSDMA	1.587968439	9.21E-38	2.01E-35
SDR9C7	1.925868047	2.05E-37	4.41E-35
MYO16	4.096332909	4.57E-37	9.74E-35
THBS2	-1.240894801	9.24E-37	1.94E-34
AL136982.5	3.122875606	1.02E-36	2.12E-34
SPRR4	2.354731048	2.60E-36	5.35E-34
FAM167A	1.361511106	4.52E-36	9.21E-34
A2ML1	1.624901352	9.93E-36	2.00E-33
VSNL1	-1.638063925	1.28E-35	2.54E-33
SYNPO2L	3.253344026	1.86E-35	3.66E-33
PALMD	-1.939037042	5.58E-35	1.09E-32
FUT3	1.994271342	1.41E-34	2.72E-32
GCOM1	2.097402859	2.01E-34	3.83E-32
TCHHL1	3.460852278	2.30E-34	4.34E-32
EPGN	1.342399292	4.31E-34	8.05E-32
C1orf116	1.305167962	5.65E-34	1.05E-31
IGFN1	3.267552447	8.06E-34	1.48E-31
UGCG	1.363894222	9.26E-34	1.68E-31
IER3	1.724665052	1.36E-33	2.44E-31
KRT24	2.081791864	2.15E-33	3.83E-31
ADGRL2	1.465151056	4.00E-33	7.04E-31
FOLR3	1.467368214	7.05E-33	1.23E-30
PCDH1	1.950433729	1.27E-32	2.19E-30
ECM1	1.584023221	1.79E-32	3.06E-30
METTL7A	-3.659923288	2.01E-32	3.41E-30
AC022075.1	-2.622314734	5.59E-32	9.38E-30
VSIG10L	1.725725813	5.89E-32	9.81E-30
IGFBP3	4.111017642	6.17E-32	1.02E-29
EREG	1.736244396	7.25E-32	1.18E-29
S100A7A	4.963306277	9.74E-32	1.58E-29
RNF223	2.991031	1.05E-31	1.69E-29
AC004233.2	3.488724688	1.74E-31	2.77E-29
PLCXD1	1.380014222	1.95E-31	3.08E-29
SLC7A5	1.292851269	3.56E-31	5.57E-29
ELMOD1	2.427120483	3.68E-31	5.71E-29
MUC16	2.782289061	9.47E-31	1.46E-28
KLK6	2.714727729	1.14E-30	1.74E-28
MCAM	-2.523486108	1.89E-30	2.87E-28

S100A12	1.649841927	5.95E-30	8.93E-28
CAMK2N1	2.219621164	6.17E-30	9.18E-28
FAM25C	2.276483273	1.12E-29	1.65E-27
TTC9	2.365543969	1.63E-29	2.39E-27
LCE1F	2.532470344	2.17E-29	3.16E-27
USP2	1.940943577	2.40E-29	3.46E-27
PRSS23	-1.54137981	2.62E-29	3.74E-27
GSR	-1.246363569	2.75E-29	3.90E-27
PLA2G4E	1.655577439	2.97E-29	4.18E-27
MXD1	1.365962284	1.02E-28	1.43E-26
AC011473.4	2.420280075	1.17E-28	1.62E-26
LCE1A	2.517784174	1.26E-28	1.73E-26
SECTM1	1.934258285	1.61E-28	2.20E-26
KLK5	1.158764546	2.06E-28	2.79E-26
LCE6A	2.983491763	2.10E-28	2.83E-26
AC004233.3	3.616430442	2.43E-28	3.25E-26
RAP1GAP	1.540299472	3.35E-28	4.45E-26
SULT1E1	-3.049470992	4.76E-28	6.27E-26
SCNN1B	1.693438812	5.71E-28	7.47E-26
MAP3K9	1.434471939	5.93E-28	7.70E-26
CDH16	1.769780742	8.41E-28	1.08E-25
LTBP1	-1.449537964	1.10E-27	1.41E-25
TMEM86A	1.353045251	1.28E-27	1.63E-25
TDRD9	3.465775881	1.56E-27	1.97E-25
CYFIP2	-2.069289925	2.00E-27	2.51E-25
MUCL1	2.132702333	2.41E-27	3.00E-25
NTN4	1.603461272	2.53E-27	3.13E-25
KCNN4	1.923780836	3.30E-27	4.05E-25
FAM84B	1.266542678	3.99E-27	4.87E-25
PALM	-2.828724724	1.15E-26	1.40E-24
ABCG2	1.187044466	1.29E-26	1.55E-24
SCNN1D	2.485765141	2.17E-26	2.59E-24
CLCF1	2.16345519	3.43E-26	4.07E-24
MYCBPAP	2.831614164	3.47E-26	4.10E-24
CCDC3	-2.228530096	3.67E-26	4.31E-24
ARRDC4	1.812778644	3.86E-26	4.50E-24
ATG9B	2.625626703	4.64E-26	5.38E-24
TMPRSS11E	1.638641467	5.03E-26	5.80E-24
COL5A2	-2.410215656	5.23E-26	5.99E-24
LOR	-3.494984637	5.93E-26	6.74E-24
ABCA12	1.206714173	7.85E-26	8.88E-24
IL1A	1.537920149	9.96E-26	1.12E-23

NDRG4	1.999451644	1.12E-25	1.25E-23
CLMN	1.448724332	3.56E-25	3.95E-23
KRT23	1.979453067	6.17E-25	6.81E-23
CCDC9B	1.381148615	6.76E-25	7.41E-23
TYMS	-1.318986012	8.35E-25	9.11E-23
DENND2C	1.196097239	1.49E-24	1.61E-22
ELOVL4	1.129126088	1.88E-24	2.02E-22
LCE2C	2.674800164	2.56E-24	2.74E-22
CDCA7	-1.413820276	5.79E-24	6.17E-22
WFDC12	2.890680613	7.74E-24	8.19E-22
HCAR2	1.847638988	9.13E-24	9.61E-22
ATP12A	2.734052259	1.44E-23	1.50E-21
SERPINB6	1.216861056	1.89E-23	1.96E-21
PADI1	2.089869723	2.05E-23	2.12E-21
AL139247.1	3.439253372	2.96E-23	3.05E-21
NEFM	-1.405201783	5.16E-23	5.28E-21
TMEM45B	3.483367383	9.44E-23	9.60E-21
F3	1.161920025	9.92E-23	1.00E-20
LCE3A	4.837716839	1.11E-22	1.11E-20
CRTAM	2.635443434	2.07E-22	2.06E-20
HES2	1.11338848	3.09E-22	3.05E-20
LINC01705	4.051578238	3.09E-22	3.05E-20
C4orf19	4.050228836	3.19E-22	3.13E-20
GRIA3	-3.020027731	3.65E-22	3.56E-20
RNF39	1.390353648	3.80E-22	3.68E-20
PTGS2	1.539687344	4.34E-22	4.18E-20
OLFML3	2.624790571	4.66E-22	4.47E-20
ADRB2	1.298213672	5.10E-22	4.86E-20
SLC43A2	-2.064290544	5.15E-22	4.89E-20
GBA	1.007527902	6.51E-22	6.14E-20
GRHL1	1.137008808	7.63E-22	7.17E-20
KLK12	1.872519719	7.67E-22	7.17E-20
ALOXE3	1.307438324	9.32E-22	8.66E-20
EHF	1.167339896	9.51E-22	8.80E-20
SLC44A2	1.315881864	1.08E-21	9.98E-20
EFEMP1	-1.049718561	1.38E-21	1.27E-19
SAA1	-1.596257496	1.80E-21	1.64E-19
PCK2	-1.424782004	2.04E-21	1.85E-19
ACSS1	-2.037060078	2.57E-21	2.32E-19
RPTN	1.460531494	3.37E-21	3.02E-19
BSPRY	1.413515906	3.50E-21	3.12E-19
ZBTB16	-2.878740546	4.03E-21	3.58E-19

ANXA9	1.814655461	4.33E-21	3.83E-19
ANKRD22	1.347986052	4.86E-21	4.28E-19
LMNB1	-1.65794636	5.68E-21	4.98E-19
NCF2	1.213152373	6.68E-21	5.82E-19
OVOL1	1.447036414	8.68E-21	7.53E-19
MPZL3	1.121126744	1.04E-20	8.97E-19
NUPR1	-2.745938272	1.19E-20	1.02E-18
SPARC	-1.578375823	1.31E-20	1.12E-18
AC243829.2	4.862691221	1.31E-20	1.12E-18
KRT78	1.680845995	1.32E-20	1.12E-18
PPL	1.286546502	1.32E-20	1.12E-18
OCLN	1.801180321	1.48E-20	1.25E-18
WNT10A	-1.735041816	1.81E-20	1.52E-18
PIK3C2G	-2.973253361	1.98E-20	1.65E-18
DSCAM	1.894575933	2.27E-20	1.88E-18
AC137936.2	2.140272715	2.30E-20	1.90E-18
MAB21L4	2.161482388	2.48E-20	2.04E-18
LCE2A	2.459551097	2.94E-20	2.41E-18
TMPRSS11F	1.646797641	2.96E-20	2.41E-18
KALRN	2.332033846	3.98E-20	3.22E-18
TCF4	-1.550325655	4.09E-20	3.29E-18
FN1	1.71218132	4.09E-20	3.29E-18
TYMP	-1.639515749	4.80E-20	3.83E-18
SBSN	1.293910808	5.00E-20	3.98E-18
AC011473.2	2.060071416	5.31E-20	4.21E-18
AC126696.2	1.495858063	5.37E-20	4.24E-18
TGM1	1.38612709	5.69E-20	4.47E-18
NRP1	-1.40400225	6.00E-20	4.69E-18
DEPDC1B	-1.417060662	6.49E-20	5.06E-18
EXPH5	1.31813711	7.22E-20	5.60E-18
OLFML2A	-2.169043604	7.26E-20	5.61E-18
DSC2	1.064277325	7.46E-20	5.74E-18
AL596244.1	-1.480628786	8.42E-20	6.45E-18
EMP1	1.532171474	8.47E-20	6.46E-18
ALOX12B	1.518266315	1.40E-19	1.06E-17
RAB11FIP1	1.167186544	2.14E-19	1.62E-17
VASN	2.169085178	2.15E-19	1.62E-17
NECTIN4	1.231176341	3.33E-19	2.50E-17
TMEM51-AS1	1.990362838	3.43E-19	2.57E-17
EFR3B	1.59519315	5.70E-19	4.24E-17
SLC39A2	1.633835955	5.83E-19	4.33E-17
LINC02029	2.235051692	6.31E-19	4.66E-17

CAB39	1.158247825	8.09E-19	5.95E-17
SERPINB7	1.011359906	8.37E-19	6.13E-17
RALGPS2	1.223687401	8.40E-19	6.13E-17
TOP2A	-1.38352868	8.96E-19	6.51E-17
LCE1D	2.468596781	9.17E-19	6.64E-17
DLG1	1.059845132	9.26E-19	6.68E-17
DHFR	-1.074176689	1.06E-18	7.61E-17
FSTL4	-3.253399409	1.19E-18	8.49E-17
MBOAT2	1.468880717	1.62E-18	1.15E-16
STRIP2	1.151855964	2.11E-18	1.50E-16
CSPG4	-1.982045892	2.50E-18	1.77E-16
AL138916.1	3.63245979	3.01E-18	2.12E-16
BLMH	-1.002026754	4.79E-18	3.36E-16
TRPV3	1.233346136	4.89E-18	3.42E-16
HS3ST1	1.506425983	5.63E-18	3.92E-16
NINJ1	-1.913752101	5.65E-18	3.92E-16
LINC01559	2.663492459	5.88E-18	4.06E-16
EPS8L1	1.169557809	6.23E-18	4.27E-16
REEP1	1.828237248	7.36E-18	5.01E-16
GGT1	-1.501560122	7.39E-18	5.02E-16
SLC28A3	1.251352893	8.24E-18	5.56E-16
LCE1E	2.326182467	9.99E-18	6.72E-16
TMPRSS11D	3.019915071	1.14E-17	7.67E-16
IL36B	2.574332832	1.31E-17	8.77E-16
LINC00511	1.55648418	1.35E-17	8.99E-16
MMP15	1.130774639	1.44E-17	9.54E-16
PIK3IP1	-1.261058516	1.58E-17	1.04E-15
MAPRE2	1.026989676	1.63E-17	1.07E-15
TSC22D2	1.129391962	1.65E-17	1.08E-15
TK1	-1.565439689	1.88E-17	1.22E-15
SMPD3	1.692159204	1.90E-17	1.24E-15
RAB7B	-1.493864834	2.34E-17	1.51E-15
MYLK	-1.35657191	2.44E-17	1.57E-15
TCN1	-1.469247483	2.49E-17	1.59E-15
APCDD1L-DT	2.25033004	2.71E-17	1.72E-15
IVL	1.279898108	2.75E-17	1.74E-15
SPRR1A	1.440688655	3.16E-17	2.00E-15
MAFB	1.172686507	4.52E-17	2.83E-15
AKR1B10	-1.131899909	4.55E-17	2.83E-15
TMEM200A	1.316358721	4.76E-17	2.95E-15
BPIFC	1.42537129	4.79E-17	2.96E-15
FRMPD1	1.852447072	5.62E-17	3.46E-15

GSTA4	-1.119982936	6.27E-17	3.85E-15
HMGB2	-1.354113064	6.86E-17	4.20E-15
OTUB2	1.127634889	7.21E-17	4.40E-15
METRNL	1.266417561	7.56E-17	4.60E-15
TNFAIP8L3	1.425783887	7.69E-17	4.66E-15
DLGAP5	-1.61386927	8.00E-17	4.82E-15
AC013268.4	2.400765782	1.11E-16	6.65E-15
AIF1L	1.123861201	1.45E-16	8.67E-15
SYNPO	-1.18248694	1.58E-16	9.40E-15
BNIP3L	1.074022375	1.68E-16	9.97E-15
AP000812.2	3.305887243	1.83E-16	1.08E-14
YOD1	1.140031029	1.90E-16	1.12E-14
FOXM1	-1.590502582	1.99E-16	1.17E-14
VGLL3	1.279974109	2.34E-16	1.37E-14
SLC1A4	-1.227557542	2.55E-16	1.48E-14
OAS2	-1.002814864	2.58E-16	1.50E-14
GPSM1	1.0536274	2.69E-16	1.56E-14
TP53INP2	1.193923184	2.89E-16	1.65E-14
SLC37A2	1.2646037	3.13E-16	1.78E-14
CEACAM6	3.18313284	4.64E-16	2.62E-14
AL512274.1	1.661585699	4.94E-16	2.78E-14
MKI67	-1.394022375	5.03E-16	2.82E-14
ST5	-1.041031917	5.54E-16	3.09E-14
S100P	1.657924441	6.17E-16	3.43E-14
PI3	1.344684918	6.31E-16	3.50E-14
UCP2	-1.835970467	6.47E-16	3.58E-14
AC011483.2	1.475993369	6.76E-16	3.73E-14
SLC38A3	2.758223876	7.14E-16	3.92E-14
CYSRT1	2.019938345	7.23E-16	3.94E-14
CCNB1	-1.181935571	7.34E-16	3.99E-14
CLDN4	1.628716034	9.02E-16	4.86E-14
PLCD1	1.201000226	9.15E-16	4.91E-14
LCE1C	1.326388248	9.46E-16	5.07E-14
ADAMTS14	2.373463343	1.00E-15	5.34E-14
PLEKHA6	1.057737655	1.05E-15	5.56E-14
VSIR	1.082740318	1.09E-15	5.79E-14
AP000944.2	2.954979485	1.15E-15	6.08E-14
PGLYRP3	1.061028237	1.17E-15	6.14E-14
MTUS1	-1.457151602	1.20E-15	6.27E-14
TGM5	2.293588412	1.29E-15	6.72E-14
SDK1	-1.594137385	1.90E-15	9.82E-14
RASSF5	1.13959511	1.97E-15	1.02E-13

CTNS	1.065069615	2.02E-15	1.04E-13
BIRC5	-1.557743353	2.05E-15	1.05E-13
ST6GALNAC5	2.034455712	2.20E-15	1.12E-13
LIG1	-1.155408437	2.21E-15	1.13E-13
GGT8P	3.461003213	2.43E-15	1.24E-13
LINC01527	2.605649414	2.84E-15	1.44E-13
SCPEP1	-1.022403614	2.93E-15	1.48E-13
LIPK	1.638582865	3.55E-15	1.78E-13
GCKR	6.962444177	4.34E-15	2.16E-13
S100A7	3.150516425	4.50E-15	2.23E-13
MRC2	-1.523448453	4.52E-15	2.24E-13
RASGEF1B	2.103321856	5.03E-15	2.48E-13
ELFN2	-1.604454761	6.30E-15	3.10E-13
SCARA3	-1.56946269	6.71E-15	3.29E-13
LY6K	1.323099906	7.67E-15	3.75E-13
MMP17	1.318642671	7.68E-15	3.75E-13
LCP1	1.872112325	7.94E-15	3.87E-13
LINC00504	1.89832781	1.08E-14	5.24E-13
GRB7	1.223377239	1.14E-14	5.50E-13
SNRK	1.001581316	1.29E-14	6.20E-13
SNHG4	-1.748201723	1.32E-14	6.34E-13
IER3-AS1	1.997703712	1.43E-14	6.85E-13
AC087783.2	3.158334623	1.45E-14	6.93E-13
NPR2	2.61621227	1.47E-14	6.98E-13
LNX1	1.636352804	1.47E-14	6.98E-13
KIF20A	-1.478647279	1.67E-14	7.88E-13
PIM1	1.318101289	1.68E-14	7.93E-13
MAF	-1.598129332	1.88E-14	8.82E-13
UBE2L6	-1.596015994	2.07E-14	9.71E-13
SH3KBP1	1.212939935	2.25E-14	1.05E-12
BMP2	1.534286767	2.30E-14	1.07E-12
COL7A1	-1.376212605	2.68E-14	1.24E-12
ALDH7A1	-1.053708925	3.16E-14	1.46E-12
FAM198B	-2.811399273	4.36E-14	2.00E-12
CENPF	-1.361251105	4.91E-14	2.25E-12
IL36G	1.254547555	4.92E-14	2.25E-12
SAMD9	1.000872524	5.10E-14	2.32E-12
WNT7A	1.151094751	5.27E-14	2.39E-12
SERPINB2	2.713476883	5.34E-14	2.42E-12
S1PR3	-1.087768409	5.35E-14	2.42E-12
OTOP2	2.445009033	5.57E-14	2.51E-12
MOCOS	-1.039397521	5.68E-14	2.56E-12

GSTM1	-1.624263881	7.07E-14	3.15E-12
AL161431.1	1.313401172	7.16E-14	3.18E-12
TROAP	-1.586618545	7.52E-14	3.33E-12
CYP1A2	9.233557744	7.58E-14	3.35E-12
CALML3-AS1	-2.363912263	8.94E-14	3.94E-12
C15orf62	2.48680354	9.53E-14	4.17E-12
CDC20	-1.382274564	9.69E-14	4.24E-12
MAFF	1.185848418	9.96E-14	4.34E-12
AC022150.4	1.420332417	1.02E-13	4.42E-12
HMMR	-1.407323206	1.06E-13	4.58E-12
MXRA5	-2.208864977	1.20E-13	5.21E-12
GCLC	-1.067067641	1.33E-13	5.73E-12
LY6G6C	1.122961639	1.52E-13	6.50E-12
ARHGEF19	-2.772076417	2.19E-13	9.30E-12
SLCO2A1	2.259110329	2.22E-13	9.42E-12
CYP1B1-AS1	8.821113451	3.14E-13	1.31E-11
GALNT5	1.270023748	3.20E-13	1.33E-11
ENPP1	1.893783653	3.51E-13	1.45E-11
PKIB	1.719922225	3.59E-13	1.48E-11
SLC22A3	-1.346242928	3.85E-13	1.58E-11
TMEM125	1.4372176	4.12E-13	1.68E-11
FILIP1L	-1.240397306	4.51E-13	1.83E-11
KIF26A	2.318384207	4.70E-13	1.91E-11
BUB1	-1.235879179	5.10E-13	2.06E-11
AC140479.7	2.406602155	5.12E-13	2.06E-11
TPM2	-1.472547863	5.50E-13	2.21E-11
NPNT	-1.050565333	5.65E-13	2.26E-11
ANXA1	1.297415167	6.27E-13	2.50E-11
MAP2	1.150023594	6.61E-13	2.63E-11
B3GNT3	1.411670837	6.62E-13	2.63E-11
FAM198B-AS1	-2.419032192	7.77E-13	3.07E-11
PGBD5	-1.06974213	8.46E-13	3.33E-11
MYO5C	1.957159614	8.47E-13	3.33E-11
CDCA3	-1.510901409	8.77E-13	3.45E-11
ATP6V1C2	1.259491374	8.97E-13	3.52E-11
CLEC2B	-1.044569767	9.03E-13	3.53E-11
CEP55	-1.446403865	1.17E-12	4.54E-11
CCL22	3.87910885	1.22E-12	4.74E-11
LGI2	6.660779829	1.33E-12	5.16E-11
FLNB	1.184862978	1.38E-12	5.35E-11
CLIC3	1.278273775	1.45E-12	5.61E-11

MYO3B	-1.35225985	1.58E-12	6.07E-11
NUAK1	-1.03124089	1.63E-12	6.28E-11
PLA2G4D	1.403004868	1.63E-12	6.28E-11
EGLN3	-1.611169659	1.69E-12	6.45E-11
AC005392.2	3.164583516	1.81E-12	6.90E-11
LINC01269	3.068572773	2.10E-12	7.95E-11
ADAMTS17	2.713117457	2.38E-12	8.98E-11
IL7R	-1.685901243	2.52E-12	9.46E-11
AL732437.1	-2.70764756	2.77E-12	1.04E-10
MAD2L1	-1.028198924	3.14E-12	1.17E-10
IQGAP3	-1.404882581	3.27E-12	1.21E-10
GLI3	-1.001219378	3.28E-12	1.21E-10
IDS	1.0540585	3.41E-12	1.26E-10
LCE1B	1.547705795	3.49E-12	1.29E-10
CCNA2	-1.232656277	3.64E-12	1.34E-10
SHANK1	2.506515608	4.10E-12	1.50E-10
CWH43	1.256525057	4.14E-12	1.51E-10
OAS1	-1.008588709	4.23E-12	1.54E-10
ARNTL2	1.29548893	4.64E-12	1.68E-10
SDK2	-1.022010578	4.80E-12	1.74E-10
PNPLA1	1.403587721	5.35E-12	1.92E-10
FOXQ1	1.226135579	5.36E-12	1.92E-10
ADAM23	-1.38812439	5.58E-12	2.00E-10
CIT	-1.256088369	5.78E-12	2.07E-10
PPP1R15A	1.125558849	6.02E-12	2.15E-10
TMEM255A	2.608675072	6.17E-12	2.19E-10
FANCD2	-1.12167486	6.18E-12	2.19E-10
INPP5D	-1.117130851	6.29E-12	2.23E-10
CLCA4	-1.5003793	6.55E-12	2.31E-10
NR1D2	1.308472174	6.82E-12	2.40E-10
TNFSF10	-1.161586776	7.38E-12	2.59E-10
FADS1	-1.269472057	7.46E-12	2.61E-10
PRSS22	2.454667393	8.25E-12	2.88E-10
IL1R2	4.263221961	9.41E-12	3.28E-10
VWF	1.679008546	9.84E-12	3.42E-10
FBXO17	-1.343379078	9.99E-12	3.46E-10
SNCB	2.353899675	1.02E-11	3.54E-10
KIF18B	-1.374555701	1.11E-11	3.81E-10
EGR1	-1.279688381	1.19E-11	4.08E-10
PPARD	1.062982045	1.31E-11	4.45E-10
MCM5	-1.006564706	1.37E-11	4.68E-10
AC015712.2	1.69056957	1.41E-11	4.78E-10

DAPL1	-1.641936766	1.63E-11	5.47E-10
AC139769.2	2.518327581	1.64E-11	5.50E-10
FAM25BP	3.057583167	1.69E-11	5.65E-10
GAL3ST4	-1.526539455	1.83E-11	6.09E-10
KIF14	-1.165954121	1.95E-11	6.48E-10
IL22RA1	1.110117183	2.08E-11	6.91E-10
TIMP2	1.201586521	2.21E-11	7.32E-10
JDP2	-1.623624136	2.28E-11	7.51E-10
SLAMF9	2.104173464	2.47E-11	8.12E-10
PLCD4	-1.09085554	2.58E-11	8.47E-10
KIFC1	-1.407153465	2.64E-11	8.64E-10
DEPDC1	-1.269607407	2.75E-11	8.99E-10
UCN2	-1.473169663	2.88E-11	9.38E-10
C11orf87	-2.691370339	2.99E-11	9.70E-10
COL4A2	-1.091263983	3.02E-11	9.79E-10
CCNB2	-1.22557111	3.42E-11	1.10E-09
UPP1	1.227950444	3.55E-11	1.14E-09
DDX11	-1.025456654	4.01E-11	1.28E-09
BHLHE41	-2.362291193	4.12E-11	1.31E-09
HCAR3	1.629768036	4.62E-11	1.46E-09
TREML3P	1.943027118	4.67E-11	1.48E-09
AL139158.2	-2.278967916	5.30E-11	1.67E-09
PITPNC1	1.020288931	5.57E-11	1.75E-09
CSF2RB	1.670827334	5.75E-11	1.80E-09
CALML3	-2.675508015	5.95E-11	1.86E-09
GULP1	3.104106928	6.24E-11	1.94E-09
NPTX1	2.891398137	6.38E-11	1.98E-09
CABLES1	-1.728093557	6.87E-11	2.13E-09
CENPH	-1.162154252	7.00E-11	2.16E-09
KRT27	2.775790613	9.29E-11	2.85E-09
KIF2C	-1.384701235	9.43E-11	2.89E-09
PLK1	-1.264174308	1.00E-10	3.06E-09
CENPW	-1.319345751	1.07E-10	3.28E-09
SERPINB13	1.053998396	1.10E-10	3.36E-09
ITGAX	1.555915183	1.12E-10	3.40E-09
NFIC	-1.009448354	1.16E-10	3.51E-09
MAP7D2	-1.242093999	1.19E-10	3.59E-09
ASPM	-1.143904806	1.30E-10	3.94E-09
GCSAM	-1.901001629	1.35E-10	4.08E-09
PPP1R3C	-1.927906739	1.47E-10	4.40E-09
KCNAB2	-1.368229042	1.47E-10	4.40E-09
GINS4	-1.303478188	1.57E-10	4.65E-09

MAP3K8	1.35703568	1.63E-10	4.84E-09
LINC02158	3.423954297	1.99E-10	5.85E-09
FRY	1.758949223	2.00E-10	5.86E-09
PSMB8	-1.058494856	2.02E-10	5.91E-09
AL121772.1	1.256457508	2.03E-10	5.95E-09
NEU2	2.570817091	2.10E-10	6.13E-09
TTC39A	1.494774266	2.19E-10	6.38E-09
MANCR	1.395600365	2.21E-10	6.43E-09
GJB4	1.09436582	2.24E-10	6.49E-09
ABI3BP	-1.818916946	2.52E-10	7.26E-09
CKS2	-1.081524913	2.56E-10	7.35E-09
KLK14	2.339339578	2.65E-10	7.59E-09
BTN3A3	-1.631987863	2.68E-10	7.66E-09
AC008011.2	1.061244558	2.79E-10	7.96E-09
PRR15	1.014370474	3.20E-10	9.08E-09
FAM83D	-1.206050877	3.28E-10	9.31E-09
MMP2	-1.140196093	3.77E-10	1.05E-08
LRRC20	1.132919626	4.30E-10	1.20E-08
LINC01792	2.956996751	4.53E-10	1.26E-08
VLDLR	-1.207245932	4.56E-10	1.27E-08
PLA2G3	1.695238867	5.01E-10	1.39E-08
LIPE-AS1	1.515785349	5.09E-10	1.40E-08
CDK1	-1.177089201	5.10E-10	1.41E-08
C15orf48	2.323803536	5.18E-10	1.43E-08
LAMP3	-2.140954675	5.20E-10	1.43E-08
CENPM	-2.113271251	5.64E-10	1.54E-08
NEURL1B	-5.314665836	5.83E-10	1.59E-08
SPAG5	-1.203021088	5.94E-10	1.62E-08
AF165147.1	1.389804426	6.15E-10	1.67E-08
IL1RL1	5.455777029	6.37E-10	1.73E-08
TPRG1	1.311170117	6.49E-10	1.76E-08
DEFB4A	4.790109148	7.00E-10	1.88E-08
NDRG2	1.258659839	7.11E-10	1.91E-08
PSORS1C2	1.757271869	7.32E-10	1.96E-08
KRT10	-1.927581638	7.46E-10	2.00E-08
CDKN3	-1.588762282	8.06E-10	2.15E-08
LAMA1	-1.16751912	8.90E-10	2.36E-08
LGALS7B	-1.936058566	9.07E-10	2.40E-08
LINC02541	-1.285549165	9.78E-10	2.58E-08
MYBL2	-1.290095503	9.98E-10	2.63E-08
ASPRV1	1.128756575	1.24E-09	3.26E-08
CXCL14	-3.638191263	1.27E-09	3.32E-08

NRARP	1.108363907	1.42E-09	3.72E-08
SPANXN3	7.815330307	1.47E-09	3.82E-08
KCTD17	-1.040527933	1.48E-09	3.86E-08
KIF4A	-1.31717006	1.51E-09	3.92E-08
TRIM22	-1.294449191	1.53E-09	3.95E-08
PAPLN	-1.556244197	1.67E-09	4.30E-08
ITGA4	-1.794606207	1.91E-09	4.89E-08
TSHZ2	-1.597831033	1.93E-09	4.91E-08
NEDD9	-1.880016497	2.03E-09	5.16E-08
CDCA8	-1.05334988	2.11E-09	5.34E-08
SYT12	-1.958844485	2.30E-09	5.81E-08
LINC02009	2.21331539	2.32E-09	5.84E-08
CXCR1	1.195844996	2.32E-09	5.84E-08
CERNA2	-1.101140285	2.47E-09	6.21E-08
C6orf15	3.11824303	2.61E-09	6.55E-08
KIF13B	1.067472069	2.77E-09	6.93E-08
COL18A1	-1.044779766	3.06E-09	7.62E-08
HYAL1	1.276644115	3.14E-09	7.78E-08
FAM45BP	1.022572185	3.37E-09	8.32E-08
MOXD1	-2.409746225	4.10E-09	9.97E-08
MAML2	-1.042516577	4.15E-09	1.01E-07
IFIT3	-2.038677536	4.16E-09	1.01E-07
CHCHD10	-1.151962903	4.20E-09	1.02E-07
P2RY6	3.135460067	4.48E-09	1.08E-07
NEK2	-1.455507261	4.51E-09	1.08E-07
ARHGAP19	-1.016107454	4.51E-09	1.08E-07
GBP1	-1.191264283	4.72E-09	1.13E-07
ALDH4A1	-1.13925649	4.85E-09	1.16E-07
PGF	-1.105950202	5.26E-09	1.25E-07
MMP9	1.389803966	5.34E-09	1.27E-07
ADM2	-1.574499209	6.14E-09	1.45E-07
C2orf16	3.276684826	6.20E-09	1.46E-07
TLR3	-1.294233564	6.32E-09	1.49E-07
BUB1B	-1.133291606	6.46E-09	1.52E-07
ACTBP13	1.264604277	6.57E-09	1.54E-07
CKAP2L	-1.192366858	7.24E-09	1.69E-07
AL033397.1	-1.170578522	7.26E-09	1.69E-07
AURKB	-1.232334953	7.30E-09	1.69E-07
ZNF812P	-1.100784286	8.05E-09	1.85E-07
MATN2	-1.52910543	9.02E-09	2.07E-07
CLIC2	1.563398511	9.75E-09	2.23E-07
PLA2G2F	1.632912936	1.01E-08	2.31E-07

MRAS	-1.28299495	1.07E-08	2.44E-07
BTN3A1	-1.055653488	1.07E-08	2.44E-07
IL33	-3.215264847	1.21E-08	2.74E-07
DLX2	1.072027225	1.25E-08	2.83E-07
TSC22D3	-1.040439612	1.31E-08	2.95E-07
PARD6B	1.26252211	1.53E-08	3.43E-07
FOSB	1.365591256	1.55E-08	3.47E-07
NR1D1	1.067126359	1.64E-08	3.67E-07
DIO2	3.435688405	1.66E-08	3.71E-07
IGHE	2.042985892	1.75E-08	3.90E-07
SHCBP1	-1.187474326	1.86E-08	4.12E-07
PBK	-1.049544545	1.90E-08	4.20E-07
IRF7	1.105360312	1.93E-08	4.27E-07
RRM2	-1.012920628	2.00E-08	4.41E-07
SERPINB4	-1.814271623	2.08E-08	4.58E-07
BLACAT1	1.100687426	2.11E-08	4.63E-07
PIMREG	-1.947282222	2.18E-08	4.77E-07
GLRA4	-2.653977459	2.48E-08	5.38E-07
LARGE2	-1.211837648	2.56E-08	5.53E-07
AZGP1	1.171373827	2.57E-08	5.55E-07
GINS2	-1.07005188	2.69E-08	5.79E-07
NDC80	-1.293142746	2.78E-08	5.98E-07
TLR6	-1.29300736	2.80E-08	6.00E-07
RAD54L	-1.276421545	2.96E-08	6.31E-07
MLLT11	-1.072699034	3.15E-08	6.70E-07
LUARIS	-2.304253757	3.18E-08	6.75E-07
CDT1	-1.233018099	3.49E-08	7.36E-07
TRAF1	-1.055959139	3.54E-08	7.43E-07
FAM43A	1.249088998	3.65E-08	7.65E-07
AC241952.1	-1.106057555	3.88E-08	8.12E-07
SESN1	-1.002318469	3.97E-08	8.29E-07
RNF225	2.236120547	4.01E-08	8.36E-07
LINC02560	2.390196027	4.07E-08	8.48E-07
ZBTB7C	-1.827267614	4.33E-08	8.99E-07
GSDMD	-1.1528069	4.38E-08	9.06E-07
PADI2	2.777793065	4.51E-08	9.33E-07
AC093904.3	2.78001496	4.62E-08	9.53E-07
SMIM10L2A	-2.09181717	5.11E-08	1.05E-06
LINC00589	1.441043352	5.20E-08	1.07E-06
TTLL11-IT1	-1.712253418	5.55E-08	1.13E-06
TXNIP	-1.032034384	5.60E-08	1.14E-06
ELF3	2.486575355	5.60E-08	1.14E-06

GRTP1	-1.50338344	5.96E-08	1.21E-06
LINC02487	7.311261204	6.27E-08	1.26E-06
TNFSF18	-1.668252449	6.52E-08	1.31E-06
SKA1	-1.165193996	6.53E-08	1.31E-06
CBS	-1.627616423	6.73E-08	1.35E-06
PSTPIP1	-1.305705173	6.74E-08	1.35E-06
SPANXN5	6.117739888	7.19E-08	1.43E-06
TMEM156	2.330343876	7.64E-08	1.52E-06
COL8A1	-1.178706064	7.99E-08	1.59E-06
AC011503.1	3.648978585	8.09E-08	1.60E-06
ATP10B	1.073358413	8.19E-08	1.62E-06
MYCT1	3.539664277	8.60E-08	1.69E-06
HID1	1.206255265	8.67E-08	1.71E-06
CDCA5	-1.007971687	8.74E-08	1.72E-06
C9orf131	3.65149291	8.93E-08	1.75E-06
CSF2RA	1.68429439	1.00E-07	1.94E-06
GAS1	-2.082173064	1.03E-07	2.00E-06
SALL2	-2.546915155	1.04E-07	2.01E-06
POLQ	-1.136244464	1.04E-07	2.02E-06
ARG1	-1.938832501	1.05E-07	2.03E-06
LRRK2	-1.479025942	1.05E-07	2.03E-06
SFXN2	-1.027049239	1.09E-07	2.08E-06
TP73	-2.261276508	1.10E-07	2.10E-06
RECQL4	-1.03974126	1.15E-07	2.19E-06
ALDH3A1	1.729756727	1.22E-07	2.33E-06
BLM	-1.236479545	1.27E-07	2.42E-06
EDA2R	-1.746062891	1.38E-07	2.58E-06
ASF1B	-1.327257107	1.42E-07	2.65E-06
APOBEC3A	2.477351948	1.49E-07	2.76E-06
TRIM63	6.933902533	1.51E-07	2.80E-06
STON1	-1.95893883	1.63E-07	3.00E-06
OIP5	-1.67409139	1.66E-07	3.05E-06
XKRX	1.148457345	1.73E-07	3.17E-06
ARHGAP30	1.768165482	1.76E-07	3.21E-06
RBMS3	-1.412575138	1.76E-07	3.22E-06
SESN3	-1.680481068	2.00E-07	3.61E-06
NCAPG	-1.021365172	2.00E-07	3.62E-06
MT4	-3.08965617	2.11E-07	3.80E-06
ZNF774	-1.402952442	2.15E-07	3.87E-06
CA11	-2.437411979	2.20E-07	3.95E-06
HAPLN3	-1.388261558	2.24E-07	4.01E-06
POU3F1	-1.451656859	2.30E-07	4.10E-06

LINC01795	7.061352282	2.36E-07	4.19E-06
SCN4B	-1.456147453	2.56E-07	4.51E-06
TTYH2	-1.371832785	2.64E-07	4.63E-06
LINC00520	1.391258899	2.66E-07	4.66E-06
STMN3	-1.241809583	2.83E-07	4.94E-06
C5	-1.41236487	2.89E-07	5.03E-06
CRIP2	-1.029321398	3.00E-07	5.21E-06
AL357060.1	1.080201254	3.30E-07	5.70E-06
FAM171B	-1.041348816	3.46E-07	5.94E-06
ABLIM2	1.06407614	3.46E-07	5.94E-06
RAD51AP1	-1.124360989	3.49E-07	5.96E-06
STXBP6	2.863289519	3.60E-07	6.14E-06
STAR	-1.389647208	3.69E-07	6.30E-06
BDH2	-1.006440275	3.81E-07	6.48E-06
AC006262.2	-1.564327936	4.04E-07	6.84E-06
PRR9	2.376167153	4.12E-07	6.97E-06
GPRC5A	3.046966603	4.75E-07	7.99E-06
PLIN4	-1.405198487	4.90E-07	8.21E-06
SELPLG	1.180387845	5.03E-07	8.41E-06
NPL	-1.144566413	5.12E-07	8.54E-06
CYP39A1	-1.417818313	5.19E-07	8.64E-06
CR1	-3.086494283	5.91E-07	9.77E-06
CARD11	1.206426462	6.39E-07	1.05E-05
ASS1	-2.042666354	6.48E-07	1.06E-05
AC103974.1	1.267825827	6.74E-07	1.10E-05
MAP1B	-1.021292718	7.05E-07	1.15E-05
IL37	2.6547476	7.08E-07	1.15E-05
PLCE1	3.807616909	7.62E-07	1.24E-05
SLC16A3	1.228579858	7.66E-07	1.24E-05
TNFRSF14	-1.418272744	7.72E-07	1.25E-05
TP53AIP1	-1.979170335	8.13E-07	1.31E-05
OSBPL7	-1.36959652	8.64E-07	1.39E-05
HPGD	1.202371395	9.00E-07	1.44E-05
EPHB6	-1.226002686	9.05E-07	1.45E-05
MRGPRX4	-6.771061993	9.26E-07	1.48E-05
PRELP	3.477957088	9.50E-07	1.52E-05
IFIT5	-1.035988004	1.00E-06	1.60E-05
THEM5	-1.419248868	1.16E-06	1.82E-05
FLVCR2	1.031083705	1.19E-06	1.86E-05
TMPRSS11B	4.415266955	1.19E-06	1.87E-05
RAMP1	-2.392709222	1.20E-06	1.88E-05
AC090017.1	3.00907494	1.21E-06	1.90E-05

MAMDC4	-1.583094307	1.29E-06	2.01E-05
NPTXR	-2.864034121	1.29E-06	2.01E-05
AATBC	-2.030140115	1.31E-06	2.04E-05
NCAPH	-1.048706016	1.38E-06	2.13E-05
SGK2	3.383845846	1.45E-06	2.23E-05
RHCG	1.766039014	1.58E-06	2.42E-05
SLC25A42	-1.308825281	1.61E-06	2.46E-05
IFI6	-2.095965611	1.62E-06	2.46E-05
KIF15	-1.128006905	1.63E-06	2.48E-05
ISG20	1.268176965	1.68E-06	2.54E-05
UBE2C	-1.091132761	1.78E-06	2.69E-05
CGN	1.051705799	1.79E-06	2.69E-05
IL17RB	3.694139835	1.82E-06	2.74E-05
SYT14	1.632455425	1.94E-06	2.89E-05
AC128657.1	-1.370441823	1.96E-06	2.92E-05
HLA-F-AS1	1.206657193	1.98E-06	2.94E-05
FOXP2	-2.35021807	2.18E-06	3.22E-05
FER1L6	2.580877655	2.20E-06	3.25E-05
ARRDC1-AS1	-1.082046429	2.21E-06	3.26E-05
KIF18A	-1.085411243	2.30E-06	3.37E-05
CACNA1S	2.736903596	2.44E-06	3.54E-05
SUSD1	1.349192759	2.45E-06	3.56E-05
CDC25C	-1.334607834	2.65E-06	3.83E-05
NLRP3	1.190851979	2.69E-06	3.88E-05
MLIP	3.030018918	2.73E-06	3.92E-05
FOXA2	-1.160410606	3.02E-06	4.32E-05
INSYN2B	3.226507187	3.07E-06	4.39E-05
PLEKHA4	-1.401982186	3.11E-06	4.44E-05
CALB2	1.072712754	3.31E-06	4.70E-05
CYP2C18	-1.868377654	3.38E-06	4.79E-05
UNC13D	1.135128745	3.43E-06	4.84E-05
AC008897.2	6.642055105	3.48E-06	4.91E-05
HAS2	3.41827727	3.71E-06	5.20E-05
GIPR	1.004740123	3.75E-06	5.25E-05
ITGA1	1.072694222	3.82E-06	5.33E-05
BCO2	-1.241839101	4.00E-06	5.56E-05
CREG2	2.009325603	4.40E-06	6.07E-05
STX11	1.50453398	4.57E-06	6.28E-05
SCEL-AS1	2.536211203	4.78E-06	6.54E-05
C12orf56	6.221819266	4.83E-06	6.60E-05
RMDN2-AS1	6.671927645	4.86E-06	6.63E-05
FAM222A	1.53368426	4.98E-06	6.78E-05

AL606519.1	6.188031266	5.03E-06	6.83E-05
EEPD1	1.250979267	5.08E-06	6.89E-05
ARC	1.970759792	5.19E-06	7.02E-05
UGT1A7	2.34499642	5.20E-06	7.03E-05
AC027612.1	6.181763798	5.21E-06	7.03E-05
TGFA	1.465417603	5.22E-06	7.04E-05
SLC6A14	1.60506098	5.29E-06	7.14E-05
CEP128	-1.10727734	5.56E-06	7.44E-05
LINC00514	4.080068258	5.71E-06	7.63E-05
NEIL3	-1.076952362	6.18E-06	8.18E-05
PID1	-1.749327206	6.25E-06	8.25E-05
LINC02448	2.80147789	6.77E-06	8.90E-05
TLR1	-2.149994082	6.93E-06	9.10E-05
DPYD	-1.186901009	6.96E-06	9.12E-05
TM4SF19	1.088796534	7.42E-06	9.66E-05
PBX1	-1.173615717	7.77E-06	0.00010074
AC097059.1	5.420714851	7.80E-06	0.00010102
SAMD9L	-2.409452373	8.12E-06	0.00010465
KLK8	1.001436099	8.22E-06	0.00010584
NPHP1	-1.15477472	8.51E-06	0.00010932
PTPRH	2.026093342	8.59E-06	0.00011009
CYP4X1	-1.680089578	8.61E-06	0.00011028
AL121988.1	1.278769022	8.63E-06	0.00011054
PCLAF	-1.195584225	8.88E-06	0.00011342
FAM25A	3.585634051	9.13E-06	0.00011629
CD86	2.529812523	9.38E-06	0.00011932
AC130360.1	6.488066618	9.44E-06	0.00011977
RASGRP1	-2.191639034	9.88E-06	0.00012461
AADAT	-1.38419845	9.89E-06	0.00012464
AL033384.1	1.23153882	1.01E-05	0.0001273
LINC02137	3.136254388	1.05E-05	0.00013126
AL354813.1	-1.020629673	1.05E-05	0.00013205
HERC5	-1.684517488	1.07E-05	0.00013402
SPRY1	-1.188288567	1.13E-05	0.00013967
TEC	1.141392853	1.14E-05	0.00014128
ORC1	-1.042512176	1.14E-05	0.00014143
NEB	1.082666852	1.19E-05	0.00014636
MAL	3.820526551	1.20E-05	0.00014652
CBR3	-1.27022982	1.21E-05	0.00014751
SMO	-1.634166399	1.25E-05	0.00015314
ZP4	2.105983366	1.29E-05	0.00015693
TBC1D30	1.207559265	1.33E-05	0.00016094

AP000812.3	3.803059773	1.33E-05	0.00016131
ZNF704	-1.085076576	1.35E-05	0.00016333
TRPM6	-1.811762747	1.36E-05	0.00016483
CLEC7A	-2.5198643	1.38E-05	0.00016704
DLGAP3	-2.335358024	1.43E-05	0.00017186
HTR1D	2.171697287	1.43E-05	0.00017208
ITGB2	-1.028173737	1.45E-05	0.00017349
GSTM2	-2.001236058	1.45E-05	0.00017365
DDX12P	-1.136336619	1.48E-05	0.00017685
KLHL13	-1.281603659	1.65E-05	0.00019574
MYH15	-1.465901325	1.66E-05	0.00019698
TMC4	-1.191682266	1.72E-05	0.00020347
IL20RA	-1.117368289	1.72E-05	0.00020362
AADAC	-2.332903711	1.75E-05	0.00020676
CGNL1	1.889784364	1.79E-05	0.00021077
CHDH	4.115992955	1.80E-05	0.00021209
SIDT1	-2.117782817	1.81E-05	0.00021322
RAB3B	1.165650799	1.86E-05	0.00021824
TRAF5	-1.180014931	1.89E-05	0.00022131
IFI44	-2.381007338	2.03E-05	0.00023666
NT5M	-2.103922717	2.04E-05	0.00023745
HNMT	-1.744934495	2.12E-05	0.00024603
ZNF385B	5.220102902	2.15E-05	0.00024888
PIF1	-1.480913184	2.19E-05	0.00025206
RHBDL1	-1.204838317	2.21E-05	0.00025446
GAMT	-1.426951617	2.47E-05	0.00028152
IFI44L	-6.364130955	2.54E-05	0.0002883
LINC01315	-2.59706635	2.65E-05	0.00029949
CXCL10	-3.293448205	2.67E-05	0.00030097
MND1	-1.393668833	2.68E-05	0.00030138
ABCB11	2.503274128	2.76E-05	0.00030988
RNF128	-1.109797332	2.79E-05	0.00031278
PEG10	-2.260558671	2.87E-05	0.00032003
PRDM1	1.550591344	2.92E-05	0.00032544
LUCAT1	1.047683246	2.93E-05	0.00032572
FZD10	2.07967247	2.97E-05	0.00033022
OGDHL	-1.668076003	2.98E-05	0.00033076
PSMB9	-1.703566544	3.03E-05	0.000335
GAST	2.052785716	3.03E-05	0.00033517
AC021491.2	1.552305572	3.04E-05	0.00033577
KCTD4	3.26907434	3.05E-05	0.00033651
QRFPR	-1.890164661	3.28E-05	0.00035923

AC005863.1	1.309154251	3.36E-05	0.00036602
PAQR8	-1.1959274	3.42E-05	0.00037212
NAP1L2	-1.494442633	3.53E-05	0.0003834
KIAA0319	2.236111013	3.61E-05	0.00039094
SDSL	-1.371692339	3.72E-05	0.00040069
SPRR2F	1.987456894	3.82E-05	0.00041073
TJP3	1.091885253	3.91E-05	0.0004188
NUSAP1	-1.470162784	4.04E-05	0.0004309
MYH16	1.48048002	4.05E-05	0.00043247
FGD2	2.599823936	4.06E-05	0.00043321
SLC2A5	-1.101134206	4.48E-05	0.00047287
C10orf67	-1.910153143	4.67E-05	0.00048908
MYZAP	1.839572114	4.70E-05	0.00049275
P2RX6	-1.227694867	4.84E-05	0.00050452
WNT4	-2.802137644	4.86E-05	0.00050581
RASAL1	1.232357179	4.99E-05	0.00051872
SOST	2.573930201	5.39E-05	0.00055663
KLHDC7B	-2.997081677	5.44E-05	0.0005609
TLL2	-1.323339464	5.70E-05	0.00058573
NAV3	1.573969386	5.97E-05	0.00061003
TMEM170B	1.732036946	6.13E-05	0.00062336
VIPR1	1.139433099	6.30E-05	0.00063881
PCP4L1	-1.227120867	6.41E-05	0.00064726
EPHB2	-1.828035842	6.48E-05	0.00065443
KCNJ5	-3.872153314	6.52E-05	0.00065742
ZBED3	-1.357757606	6.52E-05	0.00065742
ZNF460	1.046303146	6.63E-05	0.00066739
KLK13	1.042926274	6.63E-05	0.00066755
GPM6B	-1.611421433	6.68E-05	0.00067207
AF106564.1	-1.646282287	7.19E-05	0.00071769
MICALL2	-1.625658419	7.29E-05	0.00072704
FOLR1	2.992340957	7.43E-05	0.00074095
KPNA7	1.926707284	7.79E-05	0.00077384
ASCL2	-1.551813399	8.14E-05	0.00080514
KLHL4	-1.214794203	8.16E-05	0.00080661
AL357033.1	2.047413334	8.39E-05	0.00082618
MICE	1.064785569	8.63E-05	0.00084694
AC108215.1	2.243052377	8.73E-05	0.00085627
PRAF2	-1.27625649	8.78E-05	0.0008591
CCL5	-1.283508952	9.09E-05	0.00088541
CD244	1.395027996	9.28E-05	0.00090089
LOXHD1	4.322850326	9.44E-05	0.0009151

TGFB2	-1.568252001	9.69E-05	0.00093722
ANKRD31	1.372899116	9.73E-05	0.00093914
EGFL6	-4.833831575	9.73E-05	0.00093914
GLI1	-1.983544794	0.00010177	0.00097881
GBP2	-2.015937898	0.00010347	0.00098939
KLRC1	-1.732014501	0.00010496	0.00100161
CIDEA	1.542843058	0.00010774	0.00102545
CACNA1D	2.182017348	0.00010816	0.00102783
CHP2	-1.839945385	0.00010952	0.00103917
TMEM158	-1.174435896	0.00011272	0.0010656
FAM229B	-1.346718886	0.00011669	0.00109864
SLC25A27	-1.292413025	0.00011796	0.00110948
ABCA4	-1.441938958	0.00012168	0.00113803
AC011374.1	-1.551656532	0.00012311	0.00115073
LINC00243	2.085896201	0.00012354	0.00115363
AC004803.1	-1.473449603	0.00012592	0.00117468
B3GALT4	1.329788719	0.00012648	0.00117863
SLC38A4	-1.37897924	0.00012928	0.00120231
CTAGE15	1.249083469	0.00013389	0.00124082
GALM	-1.023568786	0.00013515	0.00125116
AL356056.2	-2.320785084	0.00013737	0.00126725
KCNK7	-2.384047578	0.00013808	0.00127315
SPC25	-1.300664684	0.00013867	0.00127731
KRT2	2.068426654	0.00013972	0.00128376
SEMA3D	-1.216776006	0.0001416	0.00129913
AC093904.2	3.889899385	0.00014575	0.00133246
IRAK3	-1.490749424	0.00015054	0.00137079
TLR10	3.894303414	0.00015085	0.00137295
HYPK	-1.904862511	0.00015215	0.00138411
GLS2	-1.388634234	0.00015747	0.0014282
SLC15A2	-1.027167704	0.00015785	0.00143022
PLAUR	1.452563935	0.00016026	0.00144494
ADGRB2	-1.117681721	0.000161	0.00145086
AC040173.1	2.41140733	0.00016407	0.00147496
RAB20	-1.000573625	0.00016473	0.00147941
GREB1	-1.574949164	0.00016782	0.0015003
LINC02188	-2.226319023	0.00016871	0.00150675
AC092115.2	1.87022413	0.00016884	0.00150675
NFATC2	1.527133857	0.00017122	0.00152496
ADAM11	2.117705389	0.00017197	0.00153092
LINC02437	1.561107268	0.00017597	0.00156423
TRAPPC6A	-1.042804686	0.00017698	0.00157093

ITGB2-AS1	-1.457210362	0.0001818	0.0016106
FAM83A	1.223738686	0.00018512	0.00163446
CAVIN4	1.691057361	0.00019173	0.00168554
REXO5	-1.094473539	0.00019346	0.0016999
HMGB3P32	3.118542518	0.00019908	0.00174176
RASD1	1.751360647	0.00019971	0.00174649
SLC52A1	-3.349451672	0.00020128	0.00175851
SMIM5	1.490387396	0.00020241	0.00176585
AL359692.1	3.339249279	0.0002046	0.0017799
NCALD	1.123758846	0.00020491	0.00178168
AL157829.1	1.089384695	0.00020655	0.00179341
MCF2L2	1.373759046	0.00022634	0.00194244
SLC6A2	-1.276572768	0.00022812	0.00195477
GCHFR	2.310193226	0.00023506	0.00200286
KANK4	-2.620431822	0.00023588	0.00200721
FAM25G	3.05464603	0.00024035	0.00203857
SMARCD3	-1.154920462	0.00024052	0.00203905
FKBP7	-1.419673302	0.00024409	0.00206621
LYRM9	-1.355288798	0.00024733	0.00209006
ARHGEF6	-1.272253593	0.00026542	0.00222439
NXPE2	4.117776151	0.00027008	0.00225523
AL034376.1	1.45951552	0.00027305	0.0022769
ZNF488	-1.169225261	0.00027326	0.00227764
STRA6	3.42590788	0.00027739	0.00230473
AC010186.3	-1.087747291	0.00029073	0.00240428
NEURL1	2.551029732	0.00029823	0.0024567
LAYN	-2.658188882	0.00029959	0.00246345
UBA7	-2.83156718	0.00030456	0.00250091
GUCY1B1	4.67915618	0.00031609	0.00258862
IL9R	1.836830338	0.00032384	0.00264266
KRT16P3	1.008499842	0.00032673	0.00266029
IL24	2.9574337	0.00032793	0.00266775
SLC22A14	1.18148381	0.00033552	0.00272162
AL139423.1	1.010696566	0.00034074	0.0027572
NGFR	-1.586951721	0.00034303	0.00277085
ASNS	-1.752996604	0.00035803	0.00288697
BBC3	-1.612853638	0.0003611	0.00290401
AC092279.1	1.00381779	0.00037968	0.00303349
AL031316.1	2.804208726	0.00038797	0.00308802
AL122023.1	1.32746687	0.00040168	0.00318148
STOX2	-1.0449192	0.00040335	0.00319332
AC124944.3	-1.044734813	0.00040845	0.00322396

UBE2D3P1	1.127667704	0.0004137	0.00325692
ELFN1	-5.177890325	0.00043155	0.00337427
MFSD2B	3.045485315	0.00043433	0.00339314
AC130466.1	1.501939249	0.00044107	0.00343551
BMF	1.323314406	0.00044676	0.00346948
PROC	-1.473732911	0.00044823	0.00347794
AL138789.1	3.632700291	0.00045786	0.0035377
SCG5	1.120293168	0.00045826	0.0035393
ZNF239	-1.139779504	0.00046865	0.00360436
CALB1	2.577765628	0.00048061	0.00368855
CDHR4	-4.034760822	0.0004834	0.00370688
RAD51AP2	-2.18216049	0.0004867	0.00373058
AL353586.1	-4.442692949	0.0004971	0.00380077
EFCAB12	1.537896987	0.00050769	0.00387045
FAM155B	2.068506929	0.00051638	0.00392526
AP005264.1	2.288766542	0.00051819	0.00393735
TMOD1	2.053130816	0.00052513	0.00398352
AKAP12	3.089997216	0.00054243	0.00410285
STX1B	-1.362967064	0.00055435	0.0041861
LIF	-1.320314024	0.00058636	0.0044114
AC093904.4	2.026476229	0.00058963	0.00442879
DLEU2	-1.091221362	0.00060089	0.0045004
DPYSL3	-1.579935074	0.00061338	0.00458458
NDUFA4L2	-2.610522493	0.00062866	0.00467586
TMEFF1	3.431726536	0.0006394	0.0047461
EPSTI1	-1.283973316	0.00064269	0.00476669
RSPH1	-1.476720611	0.00065115	0.00481575
AL049767.1	3.039213989	0.00065682	0.00484593
BRSK2	-1.17497929	0.00067807	0.00498469
GREM1	3.704029953	0.00070637	0.00516577
EME1	-1.004830677	0.00073054	0.00531204
USP17L8	3.1372612	0.00073072	0.00531204
AC024597.1	2.217678652	0.00075454	0.00546128
LINC01127	2.050256729	0.00075647	0.00547096
WNT9A	2.054854324	0.00077097	0.00556703
ECM2	-1.454777928	0.00080996	0.0058142
LGALS7	-1.161519107	0.00081959	0.00586489
AC084262.2	1.976074859	0.00083754	0.00597466
IFIT2	-2.310984285	0.00084052	0.00599363
SHROOM4	-2.362919734	0.00084095	0.00599432
HIST2H2BF	-1.316181945	0.00084709	0.00603338
NXF3	2.976962555	0.00085398	0.00607302

DUSP4	1.344742657	0.00086473	0.00614473
PDPK2P	2.368083112	0.00086916	0.00617144
FAM149A	-2.158138588	0.00087299	0.0061962
HOTAIR	-1.002716523	0.00087848	0.00622073
LINC02273	1.04570466	0.00088568	0.00626198
ACTG1P17	-2.896348285	0.00089386	0.00631008
AC026333.3	3.548238364	0.00089958	0.00634558
MSC	-1.511223758	0.00093917	0.00658425
PSCA	1.243246152	0.0009486	0.00664022
AC138969.1	-1.741173906	0.00095385	0.00667442
TMC1	1.636072673	0.00095875	0.00669622
LINC01451	-1.175598747	0.00096412	0.00672829
MGAM	-1.14064672	0.00096892	0.0067588
ECHDC3	-1.682516334	0.00098615	0.00686109
AC068985.1	2.027751189	0.00102132	0.00706283
RNF224	2.84807615	0.00103325	0.00712916
APOL1	-2.42688676	0.00105106	0.00723573
CALCRL	-1.040455246	0.00106089	0.00728694
EN1	-2.0916087	0.00108935	0.00744889
HENMT1	-1.783042409	0.0011092	0.00755923
AL391425.1	2.626945435	0.0011147	0.00759107
HIST1H2AI	-1.560153924	0.00112012	0.00762516
KCNK10	-1.032151623	0.00115459	0.00783359
DPEP2NB	2.540716667	0.00115701	0.00784421
AADACL3	2.959694993	0.00118135	0.00799149
DAB2	1.031656281	0.00119364	0.0080597
CST6	1.406127763	0.00120277	0.00810941
AC084033.3	-2.296006815	0.00120849	0.00813688
TMC8	-1.456424338	0.00121716	0.00818231
SAA2	-1.159679317	0.00123983	0.00831338
RPL39L	-1.043824667	0.00124097	0.00831792
AL050404.1	1.806998349	0.00125737	0.00841558
AC126768.1	-2.118909255	0.00126565	0.00846482
KRTAP2-3	2.098455908	0.00126941	0.00848682
ALDH1L1	-1.29017448	0.00129426	0.00863089
NELL2	-1.484445111	0.00132795	0.00880092
AL445253.1	-2.098993366	0.00133372	0.00883297
ANKRD1	4.275932923	0.00135746	0.00896743
PRR15L	1.517825403	0.0013614	0.00898377
SCN2A	-3.389935112	0.00136658	0.00901144
IGFBP5	-4.273305417	0.00137141	0.00903677
AC022497.1	3.616656309	0.00137981	0.00908885

FAM13C	-2.141093427	0.0013946	0.00917637
FLNB-AS1	1.365444636	0.0014052	0.00923952
AC092811.2	3.11706693	0.0014107	0.00926571
MSC-AS1	-1.177342054	0.00149557	0.00973236
IGSF22	1.736940141	0.00150434	0.00977205
FERMT1	1.233912431	0.00151751	0.00983539
FGF14-AS2	-2.240166811	0.00151785	0.00983539
ID2	1.190248181	0.00151963	0.00983545
U62317.1	-1.351420406	0.00153587	0.00991356
AC011473.3	3.18208742	0.0015433	0.00994751
NPIPP1	-1.270060225	0.00155615	0.01002329
PRIM1	-1.245571572	0.00158653	0.01018315
SOD3	1.799837859	0.00160751	0.01029616
AC133785.1	1.59386633	0.00162459	0.01039104
ITGB7	1.033384942	0.00163858	0.01045982
RBBP8NL	1.228243746	0.00164312	0.0104766
RGPD5	1.474215418	0.00164468	0.01048293
LINC02031	-4.2237616	0.00167291	0.01063693
GPC4	-1.291040002	0.00168492	0.01070849
LZTS1	-1.10581342	0.00168826	0.01072333
CPE	-1.213022546	0.00170042	0.01077068
AC003958.2	1.618151744	0.00171492	0.01085101
IFIT1	-2.819357415	0.00171547	0.01085101
BCL11A	-1.01943678	0.00173542	0.01096853
CLDN9	2.741604433	0.0017543	0.01106239
MUC19	-1.314429513	0.00181776	0.01141521
AKR1B15	-1.193542902	0.00182287	0.01143554
HNRNPA1P27	2.078731311	0.00184079	0.01153615
DEPTOR	-1.264540302	0.00189302	0.01181896
TMEM132B	1.736010483	0.00189857	0.01184552
AC093535.2	1.330502979	0.0019066	0.01187947
UNC13A	-1.598399698	0.00193192	0.01202899
ALDH1A1	-2.510137799	0.00194468	0.01208794
RYR2	1.173148671	0.00196356	0.01219285
NTN1	-1.406304704	0.00198239	0.01228893
FAM83E	2.188691457	0.00199444	0.01234273
SP2-AS1	-1.195497601	0.00200569	0.01239563
CHRNA6	-1.387427598	0.0020111	0.01242487
AC104986.2	-2.003614753	0.00201888	0.01245192
AC009229.2	4.267802807	0.00204908	0.01260422
NHLH2	-3.134218302	0.00213628	0.01306165
BACH1-IT1	1.601179905	0.00214366	0.01308488

POU2AF1	-1.91593738	0.00218957	0.01332958
BEGAIN	-1.755350186	0.00219367	0.01335013
ADAMTSL1	-2.889003573	0.00220202	0.01338213
FAM72D	-1.257523267	0.00220206	0.01338213
AC022239.1	1.41323603	0.00220321	0.01338213
AC018553.2	-1.122619154	0.00226743	0.01370788
AC092279.2	2.242236238	0.00228963	0.01382843
LCE2B	1.933285604	0.00229556	0.01385963
ZNF436-AS1	-1.13714685	0.00230774	0.01392861
CHRNB2	1.982461099	0.00234057	0.01409888
KCNS2	-2.377106485	0.00235374	0.01416566
AL118508.1	-1.616767072	0.00239386	0.01438202
EIF3C	-1.12311053	0.00241397	0.01447905
KCNQ3	1.241254878	0.00247458	0.01478451
AC099521.2	1.623518927	0.00249613	0.01489381
RSAD2	-2.705012653	0.00252914	0.01506135
AC006978.1	-1.052215185	0.00254692	0.01515242
AKNAD1	1.097080741	0.00258905	0.01535321
PCSK1	-1.945023705	0.00259699	0.01538532
TNFSF12	1.343826676	0.00267982	0.01575878
AOC1	3.068705898	0.0027157	0.01593395
ZNF546	-1.738310245	0.00275698	0.01615239
HRASLS2	1.054085972	0.00275998	0.01615239
PDE6A	-1.955551615	0.0027857	0.01627166
LYPD2	-2.01628191	0.00280263	0.01634969
CD36	-1.461912739	0.00282834	0.01647348
AL049875.1	2.427669931	0.00287112	0.01668923
PDE4A	-1.26745145	0.0029102	0.01688578
AL449106.1	2.558058528	0.00292582	0.0169657
AC009088.3	1.259528625	0.00300192	0.01731376
AATK	-1.644897927	0.003028	0.01742976
SLC16A6	-1.694245278	0.00304721	0.0175088
AC080038.1	-2.764205292	0.0030819	0.01769703
MAPK4	-2.954835701	0.00314887	0.01800935
AL049629.2	1.969392851	0.00323835	0.01836501
DNAH17	-1.023984712	0.00327845	0.01856125
IGSF11	1.514519646	0.00332556	0.01879559
ESM1	4.189019395	0.00335737	0.01894031
SV2B	3.013811058	0.00339928	0.01912367
ANKRD36BP2	1.328381333	0.00343095	0.01928408
SSPN	-1.34658798	0.00343528	0.01929657
MYO7B	2.712063968	0.00343974	0.01931568

CASC2	-1.262477263	0.00345872	0.01938662
LINC02076	-2.574307108	0.00347131	0.01941556
AC141557.1	-4.0095961	0.0035182	0.01961956
CALML6	-1.72274051	0.00356242	0.01982828
GASAL1	-1.064323369	0.00356574	0.01983764
AL356515.1	-2.523988436	0.00357182	0.01986247
AC087491.1	-2.046210247	0.00358081	0.01989433
PSG6	1.908447601	0.00364499	0.02015916
CLYBL	-1.211240294	0.00368061	0.0203247
NFAM1	-2.127011345	0.00368158	0.0203247
RGS9	1.203622176	0.00369251	0.02037894
AP001266.1	1.472220336	0.00378675	0.02078003
LINC01415	-2.187738925	0.003807	0.02088059
ACOX2	-1.191688606	0.00385195	0.02108096
AC132192.2	-1.674345999	0.00386448	0.0211432
SERPIND1	3.573395278	0.00393693	0.02142438
AC026740.1	1.13231919	0.00394803	0.02146565
AL049629.1	1.158352354	0.00395301	0.02147997
KCTD8	1.378082651	0.00395593	0.02148311
SORCS1	3.018520254	0.00398985	0.02165444
FAM83A-AS1	1.83549307	0.00401501	0.02175879
ERVW-1	2.257902156	0.00402843	0.02181039
SMG1P6	1.259228489	0.0040591	0.02193927
FIBCD1	-1.930472682	0.00413763	0.02229132
FABP4	3.272934844	0.00414673	0.02233382
SEMA3G	-1.624588821	0.00415536	0.022354
SLC34A3	2.27495131	0.00416379	0.02237959
LINC01505	1.684006689	0.00420452	0.02255878
AC009229.4	3.257586446	0.00422186	0.02263194
PLA2G4E-AS1	1.570293388	0.004261	0.02277507
AC090971.1	1.072755585	0.00430947	0.02298524
ANPEP	2.426804179	0.00435261	0.0231566
GOLGA8N	-1.139258868	0.00440629	0.02338104
SEMA6D	-2.022973926	0.00440981	0.02339296
ACTL10	-1.773128373	0.00442064	0.02343005
ANKS1B	3.267868577	0.00444392	0.02352616
RTL5	-1.347644397	0.00447977	0.0236432
AL358472.2	-2.25841247	0.00458639	0.02409234
CDH10	-2.515956442	0.00459117	0.02409674
AC006449.3	-1.193236108	0.00467974	0.02449838
IL15RA	-1.434672108	0.00473709	0.02474909
PAEP	1.318402191	0.00482128	0.02513157

PAXIP1-AS1	-1.034959802	0.00485327	0.02529112
AC013652.1	1.084477704	0.00485894	0.02530631
AC012653.2	-1.571139614	0.00494048	0.02569441
TYMSOS	-1.034757866	0.00498238	0.02585165
LINC01562	2.434628284	0.00506604	0.02619869
DERL3	-2.775621936	0.00506605	0.02619869
AL645608.7	-2.377125462	0.00507637	0.02623722
TMEM240	-1.73862298	0.00508791	0.02628944
AL139384.1	-1.577405696	0.00518483	0.02669234
SERPINB1	1.09093656	0.00520292	0.02675538
NYAP1	-1.184236517	0.00523301	0.02688744
CICP14	-2.455677089	0.00527274	0.02703849
ICAM5	-1.613887995	0.00528161	0.02707637
AL035696.3	3.248011686	0.00532482	0.02724451
DUSP13	-2.775497678	0.00533195	0.02725127
AP001962.1	1.775136834	0.00533358	0.02725127
MPL	1.426746372	0.00533535	0.02725271
LINC00887	1.264098975	0.00544564	0.0276771
CLIC5	1.778146436	0.00545096	0.02769646
PCDHB16	-1.418900001	0.00560501	0.02827153
AC022034.1	-2.898561238	0.00561596	0.02829926
NCF1	1.006898275	0.00566208	0.02847681
LINC01152	-2.044297623	0.00568204	0.02856935
LINC02154	1.455702864	0.00570197	0.02864595
Sep-04	-3.078432874	0.00576024	0.02885953
LRTOMT	-1.033023061	0.0057965	0.02900861
MIR5188	2.365926289	0.00588326	0.02934009
RBMS2P1	2.884457991	0.00588938	0.0293421
MYO1G	1.646722941	0.00591008	0.02941287
AC129492.1	1.02595385	0.0059547	0.02960697
AL391427.1	1.42140616	0.00595683	0.02960952
USP32P3	-1.141105957	0.0060139	0.02985269
KRT82	2.554075504	0.0061701	0.0304958
SARDH	-2.722301467	0.0061749	0.03051126
AC004771.3	-1.038138374	0.00624037	0.03076007
TMPRSS11GP	1.41367741	0.00632344	0.03107298
TLE2	-1.495462707	0.00634735	0.03112817
EOMES	-1.79472506	0.0063572	0.03115758
TBX2	2.759780687	0.0063789	0.03124109
ISM2	-1.663689312	0.00639859	0.03132076
AL359182.1	2.675596629	0.00647246	0.03162317
NUDT10	-2.129919355	0.00650799	0.03174663

AC008105.3	-1.623014502	0.00655679	0.03191597
TWIST2	1.448701882	0.00657858	0.03198806
AC009148.1	-3.328574809	0.00668652	0.032434
MKNK1-AS1	1.007734378	0.00668801	0.032434
AL133325.3	-1.206086515	0.00672661	0.03256944
PLXNC1	-1.968129932	0.00687153	0.03314784
UBE2FP1	1.116522811	0.00688524	0.03319709
MLXIPL	-1.286495397	0.00689468	0.03323385
PKD1L2	2.021102627	0.00695746	0.03347478
XCR1	1.664088016	0.00703246	0.03376548
NXPH4	-1.039408112	0.00732125	0.03489484
LINC02015	-1.971995315	0.00732311	0.03489484
CXCL11	-3.46359058	0.00735207	0.03500546
S100A15A	2.796068635	0.00735743	0.03502192
ZNF878	1.28464121	0.00742048	0.0352476
KIAA1024	1.609925344	0.00742459	0.0352476
PROB1	-1.019979572	0.00744991	0.03533329
BX537318.1	-1.53044093	0.00757091	0.03576844
AL033397.2	-1.071749215	0.0076618	0.03611661
AL133367.1	-1.442536636	0.00767391	0.03616175
ETV2	-1.010997513	0.0077633	0.03644187
AC009229.1	2.547934176	0.00798202	0.03724942
AC025171.2	-1.306401421	0.00808289	0.03766257
KRT33A	3.206912465	0.00813048	0.03781694
CARD17	-1.362078571	0.00813262	0.0378173
RPL3L	-1.099808095	0.00817403	0.03796165
AC034102.5	-2.019118702	0.00819064	0.03801953
LINC01410	-1.067832125	0.00835959	0.03867628
SNORA33	-1.029569434	0.00840288	0.03883735
AC114730.1	-1.82708709	0.00846319	0.03905692
AL365181.3	-1.815095751	0.0085081	0.0392444
PSG5	1.338703013	0.00853473	0.03932573
PHYHIPL	2.597727297	0.00853872	0.03932573
LINC02303	-1.963725343	0.0086268	0.03964215
AL121658.1	-3.041999818	0.0087155	0.0399395
IQCD	1.566208681	0.00880999	0.04033213
LIFR	-1.143378868	0.00882978	0.04040255
PTCHD4	-1.122832342	0.00887723	0.04057909
AL355488.1	-2.276074736	0.00892071	0.04074734
DPP4	-1.389533149	0.00899474	0.04106499
AGAP11	2.44505098	0.00910137	0.04145877
CPXM2	3.439314845	0.00914298	0.04160226

AC011477.1	-1.18462631	0.00936531	0.04238692
CU634019.1	1.097974968	0.00943258	0.04265102
AC112497.1	1.385280047	0.00943297	0.04265102
AC130304.1	1.354019071	0.00951254	0.04293657
WNT6	-2.732869594	0.00953012	0.04299749
AP003096.1	1.256584551	0.00953074	0.04299749
DIRAS1	-1.365371577	0.00968472	0.04354199
AC004951.2	-1.421597579	0.00977995	0.04391626
RET	-1.535683785	0.0098313	0.04406038
GRAMD1B	1.992504736	0.0098552	0.04413509
TRAF3IP3	1.086670745	0.010043	0.04485546
AC019127.1	-1.080153716	0.01013697	0.04518493
AC099066.2	-2.979617633	0.01014106	0.04518493
AC006449.6	-1.317057568	0.01014391	0.04518493
LINC02159	-1.004818515	0.01021663	0.04546462
LFNG	-1.135318939	0.01023119	0.0455073
LOX	-1.051263421	0.01030045	0.04574867
AP002383.2	1.046025101	0.01043084	0.04615987
FABP6	-2.514103247	0.01047312	0.04631339
GPER1	-1.894011417	0.01050953	0.04644076
AOX2P	2.741640323	0.01058574	0.04670991
CBFA2T3	-2.689624832	0.01067898	0.04705329
TMEM221	1.550376741	0.01082888	0.0475536
SPOCD1	1.437211997	0.01109591	0.04845894
MYOZ1	2.231722133	0.01113552	0.04859946
PAPPA	-1.382894957	0.01116564	0.048717
RIBC1	-1.252118045	0.01119062	0.0487911

Supplementary Table 2. DEGs list for all significantly upregulated and downregulated genes in TCDDvsControl Group.